



universität  
wien

# DISSERTATION

Titel der Dissertation

**Functional Characterisation of  
Calcium-Activated Chloride Channel 2 (CLCA2)  
in Human Tumour Cells**

angestrebter akademischer Grad

Doktorin der Naturwissenschaften (Dr. rer.nat.)

Verfasserin / Verfasser:	Mag. Daniela Kozina
Matrikel-Nummer:	9604611
Dissertationsgebiet (lt. Studienblatt):	Anthropologie
Betreuerin / Betreuer:	Univ.-Doz. Dr. Wolfgang Sommergruber

Wien, am 18. März 2009



*“Grau, teurer Freund, ist alle Theorie. Und grün des Lebens goldner Baum“*  
*Goethe, Faust I (Vers 2038) Mephistopheles*

*"Als Anwalt würde ich den Krebszellen einfach verbieten zu wachsen"*  
*Alexander Scheer, 30.07.2005*



# DANKSAGUNGEN

Besonders bedanken möchte ich mich bei Wolfgang Sommergruber (Gruppenleiter bei Boehringer Ingelheim Austria), für die Möglichkeit die Dissertation in seinem Labor durchzuführen: Lieber Wolfgang, danke für die Betreuung und die unschätzbare Hilfe bei der Fertigstellung der vorliegenden Dissertation! Ohne dich gäbe es die vorliegende Arbeit nicht!

Ich bewundere wie du nach Jahrzehnten in der Forschung immer noch mit unermüdlichem Einsatz und Enthusiasmus dabei bist, dich nie unterkriegen lässt und du auch nie damit aufgehört hast junge Menschen für die Wissenschaft zu motivieren und sie bei ihrem wissenschaftlichen Weg zu unterstützen wo du kannst.

Danke möchte ich auch meinen Laborkollegen Wigg, Sebastian, und Daniel sagen: Wigg – dem beste Ansprechpartner für technische Fragen aller Art – danke für deine Hilfsbereitschaft, von dir hab ich nie ein „jetzt nicht“, oder „weiß nicht“ gehört! Sebastian: Danke für die vielen Diskussionen zu dieser Arbeit und deine vielen Anregungen! Und ein Danke auch an Daniel, du hast das Team gut abgerundet und bist sogar mit uns Staffel beim Wien Marathon mitgelaufen! Keinesfalls unerwähnt darf an dieser Stelle Kuan-Chung bleiben – der beste Feriapraktikant den jemals jemand hatte: Danke für deine Unterstützung im Sommer 2007!

Auch bedanken möchte ich mich bei Helmut, der mir gelernt hat Spheroids zu kultivieren – ohne dich gäbe es dieses Kapitel nicht! Ein Danke auch an Christian und Andreas für die Hilfe bei der bioinformatischen Auswertung, und bei Pilar und Christina, ohne die es das IHC-Kapitel nicht gäbe.

Bei meinen Eltern möchte ich mich dafür bedanken, dass sie mir das Studium ermöglicht haben und mich darüber hinaus auch noch während des Doktorat-Studiums immer unterstützt haben wo es nur ging: Danke, dass ihr mir immer die Freiheit gelassen habt mich in dem Bereich weiterzuentwickeln, der mich am meisten interessiert hat und ihr mir alle Möglichkeiten gegeben habt, die man sich wünschen kann.

Danke möchte ich auch meinen lieben Freundinnen Bettina, Karin und Susi sagen – Gesprächspartner mit offenen Ohren – im wissenschaftlichen wie auch privaten Bereich.

Ihr seid treue Freundinnen seit vielen Jahren und ich hoffe, dass sich das auch in Zukunft nie ändern wird!

Und ein besonders liebes Danke an Alex - trotzdem! ;-)

Ohne die schöne Zeit mit dir wäre die Diss wohl eher fertig geschrieben gewesen. Aber letztlich zählt das Endergebnis, und noch viel mehr, den richtigen Menschen an seiner Seite zu haben! Danke dafür, dass du immer für mich da bist, mir Kraft, Ausgeglichenheit und Verständnis gibst, und noch viel mehr als nur das.



# TABLE OF CONTENTS

<b>DANKSAGUNGEN .....</b>	<b>5</b>
<b>TABLE OF CONTENTS .....</b>	<b>7</b>
<b>ABSTRACT .....</b>	<b>13</b>
<b>ZUSAMMENFASSUNG .....</b>	<b>15</b>
<b>INTRODUCTION .....</b>	<b>17</b>
<i>Cancer .....</i>	<i>17</i>
<i>Epithelial and Squamous Cell Carcinoma (SCC) .....</i>	<i>20</i>
<i>Identification of the Novel Tumour-Specific Gene CLCA2 .....</i>	<i>21</i>
<i>The CLCA (CaCC) Family of Putative Calcium-Activated Chloride Channels .....</i>	<i>22</i>
<i>Human CLCA2: Present Status and Rationale .....</i>	<i>23</i>
<b>RESULTS .....</b>	<b>25</b>
<i>In Silico Analysis of Expression Data .....</i>	<i>25</i>
Expression Profiling of CLCA2 in Normal Tissue Samples .....	26
Expression Profiling of CLCA2 in Tumourous Tissue Samples .....	27
Expression Profiling of CLCA2 in Tumour Cell Lines .....	39
Chromosomal Amplifications of CLCA2 Locus in Tumour Cell Lines .....	43
Identification of Differential Gene Expression Profiles .....	46
<i>Knock-Down of CLCA2 in CLCA2-Positive Tumour Cells .....</i>	<i>47</i>
siRNA Experiments in Human Head and Neck SCC Tumour Cell Line HN5.....	47
Evaluation of CLCA2 siRNAs .....	47
Proliferation Assay .....	51
Apoptosis .....	52
Cell Cycle .....	54
siRNA Experiments in Human Breast Carcinoma Cell Line MDA-MB-453 .....	55
siRNA Experiments in a Stable CLCA2-Constitutively-Expressing T47D Clone .....	59
<i>Antibody Generation .....</i>	<i>61</i>
Selection of Peptides for Generation of Antisera .....	61
Anti-CLCA2 Polyclonal Peptide Antisera and Their Use for Western Blots .....	63
<i>Immunohistochemistry .....</i>	<i>64</i>
<i>Cloning CLCA2 .....</i>	<i>65</i>
Cloning Various Tags to Expression Vector pCMV-Tag1 .....	65
Amplification of CLCA2 and TA-Cloning to pGEM T-Easy Vector .....	65

Cloning CLCA2-Tag to Expression Vector pTRE2pur .....	66
Evaluation of Tags on Western Blot.....	67
<b><i>Establishment of Stable wt-CLCA2 Clones .....</i></b>	<b>68</b>
<b><i>Proteolytic Processing .....</i></b>	<b>70</b>
Mutating Conserved Cysteines.....	72
Mutational Analysis of the Putative Hydrolase Domain .....	73
Mutational Analysis of the Putative Cleavage Site .....	74
Establishment of Stable Mutant-CLCA2 Clones .....	75
Inhibition of Post-Translational Modifications .....	77
<b><i>Integrin <math>\beta</math>4.....</i></b>	<b>79</b>
Integrin-Mediated Cell Adhesion Assay.....	80
<b><i>3D-In Vitro Carcinoma Assay: Spheroids .....</i></b>	<b>82</b>
Growth Curve of CLCA2-Expressing Clones (T47D Tet-on): 2D versus 3D.....	89
<b><i>Affymetrix Microarray Studies .....</i></b>	<b>91</b>
Sfi1 .....	95
TP53BP1 .....	96
CDIPT.....	97
MLL2 .....	98
AFF4 (MCEF) .....	100
UNC84A .....	101
DTX2 (Deltex2).....	102
C10orf118.....	103
SATB1 .....	104
EP300.....	105
LTBP1 .....	106
TSC1 .....	107
MACF1 .....	108
CHD6.....	109
RUTBC3 .....	110
P4HA2 .....	111
ASPM .....	112
Linking Profiles of Cells with Induced CLCA2 Expression to Canonical Pathways .....	114
Phospho-Proteomic Studies: Canonical Signaling Transduction Pathways ....	119



Western Blots .....	120
Antibody Arrays: Proteome Profiler.....	123
<b>DISCUSSION .....</b>	<b>125</b>
<i>Introductory Remarks: General Reflections on Targeted Therapy in Oncology</i> .....	<b>125</b>
<i>In Silico Analysis of Expression Data .....</i>	<b>128</b>
<i>Knock-Down of CLCA2 in CLCA2-Positive Tumour Cells .....</i>	<b>131</b>
<i>Antibody Generation and Immunohistochemistry .....</i>	<b>132</b>
<i>Proteolytic Processing .....</i>	<b>133</b>
Putative Hydrolase Domain .....	133
Putative Cleavage Site .....	134
Inhibition of Post-Translational Modifications .....	135
<i>Integrin <math>\beta 4</math>.....</i>	<b>135</b>
<i>3D-In Vitro Carcinoma Assay: Spheroids .....</i>	<b>136</b>
<i>Affymetrix Microarray Studies .....</i>	<b>137</b>
<i>Summary.....</i>	<b>140</b>
<b>MATERIAL AND METHODS .....</b>	<b>143</b>
<i>Molecular Biology .....</i>	<b>143</b>
Total RNA Isolation .....	143
Single Strand cDNA Synthesis (First Strand Synthesis).....	143
Real-Time Quantitative PCR (RT-qPCR) .....	144
PCR (Polymerase Chain Reaction) .....	145
PCR-Amplification.....	145
Colony Screening .....	146
Cloning PCR Products (TA-Cloning) .....	147
A-Tailing of PCR Products.....	147
Restriction Digestion.....	148
Filling 5'-Overhangs with dNTPs .....	148
Converting a 3'-Overhang to a Blunt End .....	148
<i>In Vitro</i> Site-Directed Mutagenesis .....	149
Purification of DNA .....	150
Phenol/Chloroform Extraction of DNA .....	151
Precipitation of DNA/RNA.....	151
Agarose Gel Electrophoresis .....	151

---

Recovery of DNA from Agarose Gels .....	152
Ligation of DNA .....	152
Transformation of Bacteria .....	153
Bacterial Strains.....	153
Transformation of JM109 .....	153
Transformation of JM110 .....	153
Plasmid Preparations .....	154
Miniprep .....	154
Maxiprep .....	154
Determination of DNA/RNA Concentration.....	155
DNA Sequencing .....	155
Freezing of Bacteria .....	156
<b>Cell Biology .....</b>	<b>156</b>
Cell Lines.....	156
HN5.....	156
T47D Tet-on.....	156
Thawing and Freezing of Cells .....	157
Propagation of Adherent Cells.....	157
Determination of Cell Count .....	157
Determination of Growth Curve .....	158
Transient Transfection of Plasmid DNA to Eukaryotic Cells .....	158
Generation of Stable Cell Lines .....	158
Generation of Cell Lysates from Human Tumour Cells .....	159
Inhibition of Post-Translational Modifications .....	159
Proliferation Assay (Alamar Blue).....	159
siRNA Experiments .....	160
siRNAs.....	160
siRNA Transfection in 6-Well-Plates .....	160
siRNA Transfection in 96-Well-Plates .....	161
DharmaFECT Reagents .....	161
Live-Cell High-Content Screening (HCS) with Cellomics ArrayScan® .....	161
Tissue Culture.....	162
Staining Procedure .....	162
Settings.....	162

---

Features.....	163
Integrin-Mediated Cell Adhesion Assays.....	163
Human Tissue Samples .....	163
3D- <i>In Vitro</i> Carcinoma Assay: Spheroids .....	164
Methylcellulose .....	164
Spheroid Formation .....	164
Harvesting of Spheroids.....	164
Gel Pouring Device .....	164
Collagen Gel Preparation.....	165
Matrigel .....	165
Probidium Iodide Staining .....	166
Measuring of Diameter and Volume of Spheroids .....	166
<b>Biochemistry .....</b>	<b>166</b>
Determination of Protein Concentration in Cell Lysates (Bradford Assay).....	166
SDS-PAGE.....	166
Western Blotting .....	167
Proteome Analyses with Proteome Profiler™ (R&D Systems) .....	167
MAPK-Array .....	167
RTK-Array.....	168
Immunohistochemistry.....	168
Antibody Generation.....	168
<b><i>In Silicio</i> Analyses .....</b>	<b>169</b>
Statistical and Bioinformatic Analyses .....	169
Sequence Alignment .....	169
Expression Profiling.....	169
<b>Media and Buffers .....</b>	<b>170</b>
Molecularbiology .....	170
Cell Culture.....	172
<b>Primer.....</b>	<b>174</b>
Cloning Primer.....	174
Cloning Primer for <i>In Vitro</i> Site-Directed Mutagenesis of CLCA2 .....	174
Sequencing Primers .....	176
<b>Oligomers .....</b>	<b>177</b>
<b>Plasmids .....</b>	<b>178</b>

---

TABLE OF CONTENT

---

pTRE2pur Expression Vector .....	178
pGEM-T Easy Vector.....	179
pCMV-Tag1 Expression Vector .....	179
Human Full-Length cDNA Clone of CLCA2 in pCMV6-XL4.....	180
<b><i>Antibodies</i></b> .....	<b>181</b>
<b>APPENDIX</b> .....	<b>183</b>
<b><i>Sequence of CLCA2</i></b> .....	<b>183</b>
DNA Sequence.....	183
Potein Sequence .....	184
<b><i>Abbreviations</i></b> .....	<b>188</b>
<b>REFERENCES</b> .....	<b>192</b>
<b>CURRICULUM VITAE</b> .....	<b>205</b>

## ABSTRACT

Identification of novel tumour-specific genes and pathways is a key strategy to gain additional prognostic markers and to identify molecular targets for chemical and/or immunological therapy. Combination of subtractive cDNA libraries and cDNA microarrays lead us to identify the human calcium-activated chloride channel 2 (CLCA2) as one gene being highly expressed in lung squamous cell carcinoma (lung SCC) [1]. The presence of T cell epitopes of CLCA2 and its immunological properties have also been described by our group [2]. CLCA2 is a member of the family of calcium-activated cytoplasmic trans-membrane chloride channel proteins [3]. Four human members have been identified, three of them are proteolytically processed into two subunits, whereas CLCA3 represents a truncated and secreted protein [4]. In contrast to other family members, CLCA2 displays a very restricted expression profile in normal tissues (larynx, esophagus, skin).

In the course of this PhD-Thesis a preferential overexpression of CLCA2 in human squamous cell carcinomas (SCC) of different origins, including their lymph node metastases, could be demonstrated. In addition, overexpression was also detected in mycosis fungoides, a cutaneous T cell lymphoma, and in a subset of infiltrating ductal breast cancers. Preliminary IHC analyses confirmed expression of CLCA2 in human SCC samples. *In silico* expression analyses of xenografted SCC cell lines into nude mice revealed a dramatic increase in CLCA2 expression, suggesting a role of CLCA2 in late stage tumourigenesis.

Loss-of-function studies in SCC cell lines by siRNA-mediated knock-down of CLCA2 lead to inhibition of proliferation, reduction in viability, subsequently to induction of apoptotic processes, and to an arrest in G2-phase of the cell cycle. In contrast, breast cancer cell lines stayed unaffected at least in 2D-tissue culture. Inducible expression of CLCA2 in tumour cells in combination with a detailed mutational analysis demonstrated a proteolytic (most likely autocatalytic) processing (hydrolase) activity of CLCA2 and proposed a structural metal site for  $Zn^{2+}$  coordination. Altogether, these data strongly support the presence of a zincin-like hydrolase domain in the N-terminal region of CLCA2. As predicted by bioinformatic analyses and in analogy to CLCA1 a monobasic cleavage site could be confirmed by “Alanine-walking” mutagenesis, with the predicted cleavage recognition site: P3(Tyr/Phe) – P2(X) – P1(Arg/Lys) – P1'(Tyr/Phe) – P2'(Phe/Ala).

Inhibition of glycosylation revealed that both, the stability and the proteolytic processing are impaired when glycosylation is inhibited.

For a better simulation of the situation in a tumour, CLCA2-expressing clones were also grown in multicellular tumour spheroids. In contrast to growth in 2D-cultures a > 2.5-fold increase in the relative proliferation rate in the three-dimensional culture could be identified upon induction of CLCA2 expression.

For a better understanding of the involvement of CLCA2 in signal transduction a comprehensive expression profiling study on Affymetrix GeneChips was performed followed by RT-qPCR and phospho-proteom studies with selected genes. In total ~ 150 genes were shown to be differentially regulated upon induction of CLCA2 expression. Among those genes are CDIPT, MLL2, and SFI1 which play an important role in cell cycle regulation. Utilising Ingenuity Pathways Analysis – a text- and data-mining program – several interaction-networks were identified. All of them could be linked with important canonical signal transduction cascades or interaction networks such as the TNF–IL2–IL10 interaction network or the ERK–MAPK signaling cascade. Phospho-proteom studies confirmed these findings and additionally identified a strong impact of CLCA2 on translational modulation.

Although these expression profiling data can only be regarded as preliminary they, however, offer the basis for further focused studies for the characterisation of CLCA2 as a promising target in SCC tumourigenesis.

## ZUSAMMENFASSUNG

Die Identifikation von neuen tumorspezifischen Genen und Signalwegen ist eine Schlüsselstrategie, um neue zusätzliche prognostische Marker und molekulare Targets für chemische und/oder immunologische Therapien zu finden.

Eigene Arbeiten führten mittels Kombination von subtraktiven cDNA Banken und cDNA Gen-Chips zur Identifikation des humanen Kalzium-aktivierten Chloridkanals 2 (CLCA2), als ein Gen, das im Plattenepithelkarzinom der Lunge überexprimiert wird [1]. Die Anwesenheit von T-Zell Epitopen und dessen immunologische Eigenschaften wurden ebenfalls von uns beschrieben [2].

CLCA2 ist ein Familienmitglied der Kalzium-aktivierten cytoplasmatischen transmembranen Chloridkanal Proteine [3]. Vier humane Mitglieder wurden bislang identifiziert, drei davon werden proteolytisch in zwei Untereinheiten gespalten, wobei CLCA3 ein trunkiertes segregiertes Protein ist [4]. Im Unterschied zu anderen Familienmitgliedern zeigt CLCA2 ein sehr restriktives Expressionsprofil in Normalgeweben (Larynx, Ösophagus, Haut).

Im Zuge der vorliegenden Dissertation konnte eine präferenzielle Überexpression vom CLCA2 in humanen Plattenepithelkarzinomen verschiedenen Ursprungs, wie auch deren korrespondierender Lymphknoten-Metastasen nachgewiesen werden.

Zusätzlich konnte eine Überexpression auch in Mycosis fungoides (einem T-Zell Lymphom, das vorwiegend die Haut betrifft) und in einer Untergruppe von infiltrierenden dukталen Brustkarzinomen gezeigt werden.

Präliminäre immunohistochemische Analysen bestätigten die Expression von CLCA2 in Proben von humanen Plattenepithelkarzinomen. *In silico* Transkriptionsanalysen weisen auf einen dramatischen Anstieg der CLCA2 Expression hin, wenn Plattenepithelkarzinom-Zelllinien in einem Xenograft-Nacktmaus-Modell implantiert werden, was Rückschlüsse auf eine mögliche Rolle von CLCA2 in der späten Phase der Tumorgenese zulässt.

Das Ausschalten der Funktion von CLCA2 in Plattenepithelkarzinomen mittels siRNA führte zur Inhibition der Proliferation, zur Reduktion der Viabilität, zur Induktion von apoptotischen Prozessen und zu einem Arrest in der G2-Phase des Zellzykluses. Im Vergleich dazu, blieben Brustkarzinom-Zelllinien - zumindest in 2D-Zellkulturen - davon unbeeinflusst. Induzierte Expression von CLCA2 in Tumorzellen in Kombination mit Mutationsanalyse wiesen eine proteolytische (höchstwahrscheinlich

autokatalytische) Prozessierungsaktivität (Hydrolaseaktivität) von CLCA2 nach und lassen die Präsenz einer strukturellen Metallallionen-Stelle für die Koordination von  $Zn^{2+}$  vermuten.

Zusammengefasst weisen diese Daten auf eine Zincin-ähnliche Hydrolasedomäne in der N-terminalen Region von CLCA2 hin.

Wie in bioinformatischen Analysen vorhergesagt und in Analogie zu CLCA1, konnte eine „monobasische Spaltstelle“ durch „Alanin-walking“ bestätigt werden, wobei die vorhergesagte Spaltstelle sich wie folgt präsentiert: P3(Tyr/Phe) – P2(X) – P1(Arg/Lys) – P1'(Tyr/Phe) – P2'(Phe/Ala).

Inhibition der Glykkosylierung zeigte, dass dadurch sowohl die Stabilität als auch die proteolytische Prozessierung beeinträchtigt werden.

Für eine bessere Simulation der Situation in einem Tumor wurden CLCA2-exprimierende Klone in multizellulären Tumor-Sphäroiden kultiviert. Im Vergleich zu 2D-Kulturen konnte ein über 2,5-facher Anstieg der relativen Proliferationsrate in der dreidimensionalen Kultur aufgrund von CLCA2 Expression nachgewiesen werden.

Für ein besseres Verständnis der Beteiligung von CLCA2 in der Signaktransduktion, wurde eine umfassende Transkriptionsprofilierungs-Studie mit Affymetrix Gen-Chips durchgeführt. Im Anschluss daran folgten weitere Untersuchungen durch quantitative Real-Time PCR und Phospho-Protein Studien mit ausgewählten Genen. Insgesamt konnte gezeigt werden, dass aufgrund von CLCA2-Induktion ~ 150 Gene differentiell reguliert sind. Unter anderem sind das CDIPT, MLL2 und SFI1, welche eine wichtige Rolle in der Zellzyklus-Regulation spielen. Durch die Verwendung von „Ingenuity Pathways Analysis“ – einem „text- and data-mining“ – Analysenprogramm konnten Interaktionsnetzwerke identifiziert werden, die allesamt in Verbindung mit wichtigen kanonischen Signaltransduktionskaskaden oder Interaktionsnetzwerken gebracht werden können, wie etwa das TNF–IL2–IL10 Interaktionsnetzwerk, oder die ERK–MAPK Signalkaskade. Phosphoproteom Studien bestätigten in der Folge diese Ergebnisse und konnten zusätzlich den Zusammenhang dieser Interaktionsnetzwerke mit translationaler Modulation aufzeigen.

Obwohl die Daten der Transkriptionsprofilierung nur ein vorläufiges Zwischenergebnis darstellen, dienen sie als gute Ausgangsbasis für die Planung weiterer Studien zur Charakterisierung von CLCA2 als ein vielversprechendes Target in der Plattenepithel-Tumorgenese.



# INTRODUCTION

## *Cancer*

In all industrialised countries, cancer is the second most common cause of death, exceeded only by cardiovascular diseases. To imagine, a total of 1,437,180 new cancer cases and 565,650 deaths from cancer are projected to occur in the United States in 2008 – but these cases do not even include basal cell and squamous cell cancers of the skin [5].

“Cancer” refers to over 150 diseases which have in common the characteristics of uncontrolled growth of cells and the ability to invade and damage normal tissues – locally or at distant sites in the body.

Dependent on the tissue of origin, tumours can be classified into the three major groups of carcinomas, sarcomas and leukaemias. Carcinomas are derived from epithelial cells and account for 90 % of human cancers. Sarcomas are developing from mesodermal cells; they are tumours of the connective or supportive tissue such as bone, cartilage, muscle, blood vessels, fat and of soft tissue. Leukaemias or lymphomas are originating from blood or the lymphatic system, respectively. Furthermore, there is the group of melanomas, which are malignant tumours of melanocytes, which are found predominantly in skin and gliomas, which are tumours with its origin in brain or spine (nerve tissue).

Cancer is predominately a genetic disease arising from the accumulation of mutations [6], either inherited (germline) or acquired (somatic), in critical proto-oncogenes or tumour suppressor genes. Also epigenetic changes can cause cancer [7], such as loss of imprinting [8] or hyper- or hypomethylation of 5-methylcytosine [9], as well as chromosomal instability [10] and microsatellite instability [11].

The transformation of a normal cell into a highly malignant tumour cell – the process of tumourigenesis – is a multistep process [12-14] in terms of stepwise genetic variation. The originally proposed model of Nowell [12], suggests the evolution of tumour cell populations in terms of stepwise genetic variation by an induced change in a single previously normal cell which makes it neoplastic and provides it with a selective growth advantage over adjacent normal cells. As a result of genetic instability in the expanding population, mutant cells are produced, which are nearly all eliminated due to metabolic disadvantages or immunologic destruction, but

occasionally one has an additional selective advantage and this mutation becomes the precursor of a new predominant subpopulation. Over time there is a sequential selection by an evolutionary process of sublines which are genetically and biologically increasingly abnormal. Different tumours acquire certain similarities, but divergences occur as well, as local conditions in each neoplasm differently affect the emergence of variant sublines.

Frequently, a single cancer cell contains mutations in a lot of genes, gross chromosomal abnormalities and widespread changes in its gene expression profile [15]. Hanahan and Weinberg suggest a succession of six independent steps of essential alteration in the genotype of a cell, whereby each step represents a physiological barrier that must be overcome in order for a cell to progress further toward the end point of malignancy [13;16]. These steps are:

- “*Self-sufficiency in growth signals*”, which will be a first step towards loss of growth regulation in a normal cell. The tumour cell becomes independent of exogenous growth stimuli, as e.g. the tumour cell produces their own growth factors in an autocrine mechanism. As an example, PDGF (platelet-derived growth factor) and TNF $\alpha$  (tumour necrosis factor  $\alpha$ ) is produced by glioblastomas and sarcomas [17].
- “*Insensitivity to antigrowth-signals*”: Mutations in tumour suppressor genes may induce the proliferative potential of a tumour cell, when the tumour suppressor gene normally protects cells of uncontrolled proliferation by regulation of the transition of G1- to S-phase in the cell cycle and normally force cells into the quiescent (G0) state. These signals are mainly transduced by soluble growth inhibitors or inhibitors embedded in the extracellular matrix (ECM) or located on the surface of neighbouring cells. Tumour cells often interfere with the Rb (retinoblastoma) tumour suppressor, which controls most of the antiproliferative signals in the cell, by mutation or hypophosphorylation [18;19]. Alternatively, cells may be induced to permanently relinquish their proliferative potential by being induced to enter into postmitotic states, usually associated with acquisition of specific differentiation-associated traits. Another way to avoid the antiproliferating state is the downregulation of integrins which mediate various intracellular signals. By this, integrins not only define cellular shape and mobility but also regulate the cell cycle. Integrins essentially contribute to cell division, cell survival, cellular differentiation and apoptosis.

- "*Evasion of apoptosis*" which means that cancer cells acquires resistance towards apoptosis and do not undergo apoptosis, if the cells have been damaged. Therefore, tumour cells disrupt sensors for apoptosis by e.g. mutations in the tumour suppressor gene p53, which affords unlimited replication. On the other hand downregulation of Fas receptors and killing of activated T-lymphocytes through the constitutive expression of Fas-ligand by tumour cells has been suggested as a mechanism for pathologic suppression of immune surveillance [19], and has been demonstrated in melanomas and colon cancers as an important antiapoptotic mechanism [20;21].
- "*Limitness of replicative lifespan*" can be obtained in a tumour cell by upregulation of e.g. the enzyme telomerase, which maintains the length of telomeres [22] and therefore contributes to the capability of unlimited replication.
- "*Sustained angiogenesis*" is achieved by changing the balance of angiogenic inducers and inhibitors to induce and sustain angiogenesis [23] e.g. by increased expression of proangiogenic factors such as vascular endothelial growth factor (VEGF) and/or fibroblast growth factor (FGF).
- "*Tissue invasion and metastasis*": To transform a primary tumour into an invasive and metastasising tumour, which is able to invade local tissues and blood as well as lymphatic vessels, changes in the expression pattern of adhesion molecules like cell-cell adhesion molecules (CAM's) and integrines are necessary to make the tumour less adhesive [24]. Furthermore, upregulation of extracellular matrix-degrading proteases supports the evasion of tumour cells through the basal cell membrane across blood vessel walls and into connective tissues. Such a cell-to-cell interaction molecule is e.g. E-cadherine, which is also involved in  $\beta$ -catenin signalling [25]. Recently, it was shown that expression of E-cadherin correlates with the presence of nodal metastases at the time of diagnosis in SCC of the head and neck [26;27].

This very general overview on cancer demonstrates that the cause of cancer is not linked to a single molecular event but in contrast, tumourigenesis encompasses complex molecular interactions and deregulation of signaling cascades in which single proteins are involved. Some of these altered proteins may play an essential role, others may only be regarded as passenger alterations (mutations).

"Oncogene addiction" describes the acquired dependence of tumour cells on an activated oncogene for their survival and/or proliferation. This phenomenon has

important implications for the success of targeted cancer therapies [28;29]. It was first discussed for mutations in the EGFR gene of human NSCLCs [30;31].

## ***Epithelial and Squamous Cell Carcinoma (SCC)***

An epithelium is defined as a layer of cells that is located at the boundary of body cavities and the connective tissues. Epithelial cells are arranged along the basement membrane, which mainly consists of collagens. As shown in Figure 1, different types of epithelial structures are classified by shape, stratification and specialisation. Squamous epithelium can be distinguished by two types of “simple squamous epithelia”, which is single-layered, and the type of stratified squamous epithelia, which is multilayered (Figure 1). Squamous epithelial exhibits a typically flat and scale-like shape. Several molecular biomarkers for squamous epithelium were identified, which are human desmocollin 3 (DSC3) [32], keratin 5 (KRT5) [33], desmoglein 3 (DSG3) [34], plakophilin 1 (PKP1) [35], plakophilin 3 (PKP3) [36], PERP [37], and syndecan [38].

Squamous cell carcinoma (SCC) specifically derives from squamous epithelial cells and may occur in many different organs, including skin, lung, cervix, prostate, esophagus, urinary bladder, and the head and neck region.

Accounting for approximately 20 % of cutaneous malignancies, SCC is the second leading cause of skin cancer in Caucasians [39] (after basal cell carcinoma, but more common than melanoma) with over 250,000 new cases per year estimated in the United States, whereby incidence appears to be in the rise [40]. Most cases of head and neck cancer are due to SCC. About 30 % of all lung cancers are SCCs. Two thirds of all SCCs are located in the central lung, the remaining one third is peripheral.

In the carcinoma *in situ* (the earliest form), the squamous epithelium is replaced by malignant squamous cells and with ongoing growth, tumour cells invade the sub-epithelial basement membrane. Carcinomas *in situ* do not necessarily progress to invasive carcinomas, but they can spontaneously regress to normal mucosa. The histological pattern of SCC appears as intracellular bridging, horn pearl formation and individual cell keratinisation; these features become more and more characteristic, the higher such a tumour is differentiated. About 5 % of SCCs are invasive and metastasise to different sites in the body [41]. For most of the SCCs there exists a high medical need for novel targeted therapies. Especially in recurrent and/or

metastatic SCC of the head and neck, there have been no improvements in survival in last decade [42]. Therefore, the identification of SCC-specific proteins is a key element to gain additional prognostic markers and a prerequisite to develop novel chemical and immunological therapeutic strategies for treatment of SCCs.

### Types of Epithelium

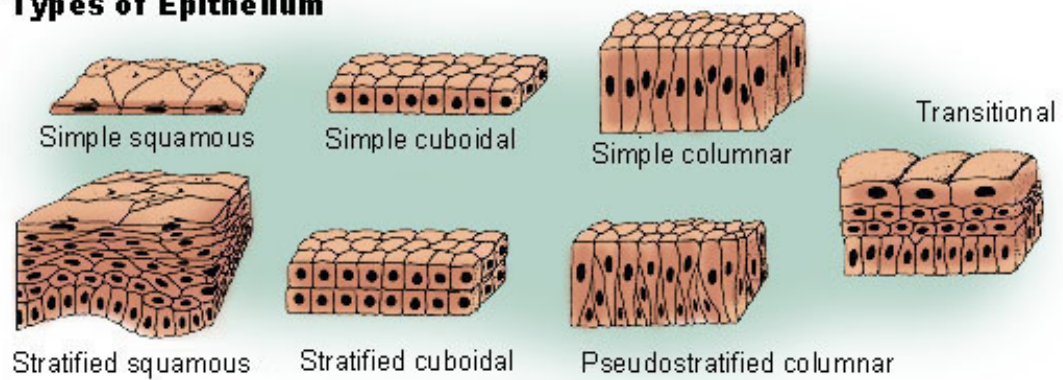


**Figure 1. Different types of epithelia**

(Taken from [http://training.seer.cancer.gov/module\\_anatomy/unit2\\_2\\_body\\_tissues1\\_epithelial.html](http://training.seer.cancer.gov/module_anatomy/unit2_2_body_tissues1_epithelial.html))

### Identification of the Novel Tumour-Specific Gene CLCA2

Combination of subtractive hybridisation using a pool of lung squamous cell carcinoma (lung-SCC) as tester and a pool of 11 critical normal tissues as driver on cDNA microarrays lead to the identification of the human calcium-activated chloride channel 2 (CLCA2) as one gene being highly expressed in lung-SCC [1]. In addition, selected HLA-A2-restricted peptides from CLCA2 have been selected and by using *in vitro* priming, T cell lines against the CLCA2-derived KLLGNCLPTV, LLGNCLPTV, and SLQALKVTV peptides have been generated. These primed T cells also recognised allogeneic tumour cells in an antigen-specific and HLA-restricted fashion. Moreover, peptide LLGNCLPTV was also independently recognised by CD8(+) T cells expanded from pancreatic carcinoma/T cell cocultures whereas CLCA2-specific CD8(+) T cells were absent from the peripheral blood of healthy donors. These data indicate that an immune response can be induced against CLCA2, which thus may become an important antigen for anti-tumour vaccination approaches [2]. However, the contribution of CLCA2 in tumour growth and/or survival and its biological role in tumourigenesis is still unknown.

## ***The CLCA (CaCC) Family of Putative Calcium-Activated Chloride Channels***

The CLCA gene family is a growing family of trans-membrane proteins with a putative role in chloride conductivity across the outer cell membrane, that is regulated by the intracellular concentration of calcium [3]. CLCA proteins are of high interest for respiratory disorders with chronic mucus overproduction, including asthma, chronic obstructive pulmonary disease (COPD), and cystic fibrosis.

To date, 17 homologous genes have been identified so far in mammals. The family consists of the two bovine founder molecules: bCLCA1 (alias CaCC) [43;44] and bCLCA2 (alias Lu-ECAM-1) [45;46]; six murine homologues: mCLCA1 [47;48], mCLCA2 [49], mCLCA3 (alias gob-5) [50], mCLCA4 [51], mCLCA5 [52] and mCLCA6 [52]; four human homologues: hCLCA1 [53;54], hCLCA2 [55;56], hCLCA3 [4], hCLCA4 (CaCC2) [54]; one porcine homologue: pCLCA1 [57]; a rat homologue: rCLCA1 [58] and two rat-brain homologues: rbCLCA1 [59] and rbCLCA2 [60]; one equine homologue: eCLCA1 [61]; and one canine homologue: cCLCA1 [62].

All members of this gene family map to the same site on chromosome 1p31-p22 [63] and share high degrees of homology in size, sequence, and predicted structure; but they differ significantly in their tissue distribution and in cellular expression pattern.

With the exception of the truncated secreted member human CLCA3 [64], all are synthesised as an 902-943 amino acid precursor trans-membrane glycoprotein of approximately 125 kDa weight, which is rapidly cleaved into 90 and 35 kDa subunits [4]. Another common feature is a symmetrical multiple Cysteine motif in the amino-terminal tail. For human CLCA1 a novel conserved metallo-hydrolase structural domain was shown [65].

Despite the well characterised biophysical property as chloride channels, demonstrated by cell transfection and patch clamp studies, other functions and their physiological significance are poorly understood. Independently of their alleged role in ion conductance, the field of functionalities seems to be quite broad. Certain CLCA family members may serve as cell-adhesion molecules and may play a role in tumour metastasis. Aberrant morphology of cells overexpressing murine CLCA2 has been interpreted as evidence for modulation of the cell cycle by CLCA proteins [66]. A mechanism of tumour suppressive effects of CLCA proteins has been reported, but is not understood in detail yet.

## ***Human CLCA2: Present Status and Rationale***

The human CLCA2 protein is highly homologous to murine CLCA5 [52]. It is expressed as a 943 amino acid precursor whose N-terminal signal sequence is removed, followed by internal cleavage near amino acid position 670. Biochemical analysis of human CLCA2 suggested five trans-membrane domains [64], three of which were predicted to be located in the larger amino-terminal part and two in the smaller ~ 38 kD carboxy-terminal cleavage product. More recent investigations of trans-membrane geometry predict that a C-terminal 22-amino-acid hydrophobic segment comprises the only trans-membrane pass [67]. However, the native structure remains unclear.

A tumour suppressive effect of human CLCA2 has been suggested through pro-apoptotic action: Stable transfection of CLCA2 into a human breast carcinoma cell line reduced its invasive growth *in vitro* and slowed their tumourigenicity *in vivo* [66;68]. The von Willebrand factor type A (vWA) domain has been discovered in CLCA2 [69], and was shown to play a role in adhesion by being involved in the binding of Integrin  $\beta 4$  to human CLCA2.

In contrast to other family members, human CLCA2 displays a very restricted tissue expression profile. It is selectively expressed in human lung, trachea and mammary gland [55]. Expression in uterus, prostate, testis was also reported [54], as well as in corneal epithelium [56]. Since this protein is expressed predominantly in trachea and lung, it is suggested that CLCA2 might play a role in the complex pathogenesis of cystic fibrosis. It may also serve as adhesion molecule for lung metastatic cancer cells, mediating vascular arrest, and colonisation.

In a tumour attachment model the expression of human CLCA2 on lung endothelial cells was demonstrated to mediate the attachment of breast cancer cells, by binding to Integrin  $\beta 4$  [70]. The additional function of this family of proteins as adhesion molecules is supported by the prediction of a von Willebrand factor type A adhesion domain [71]. This domain was first described as the adhesion element in blood-clotting proteins. Binding between murine CLCA1 and Integrin  $\beta 4$  was demonstrated to induce the activation of the focal adhesion kinase in cancer cells [72]. The adhesion function of this class of proteins was further demonstrated by the fact that the lung epithelial bovine CLCA2 was shown to mediate lung metastasis of melanoma cells in mice [73].

Multiple tissue Northern blot analysis revealed a very restricted expression profile in normal tissues as it was only detected in larynx and esophagus. In addition, a weak expression was detected in skin and testis (PhD-Thesis of Ulrich König 2001, Boehringer Ingelheim Austria). These findings are supported by the work from Pauli and Gruber [54;55]. *In situ* hybridisations and a large set of comparative hybridisations on cDNA arrays followed by real time PCR studies supported this result; 100 % of lung SCC patient samples exhibit high upregulation of human CLCA2, whereas residual normal lung was negative for human CLCA2.

Suggesting CLCA2 as a novel marker for SCC, these data served as the basis for the present PhD-Thesis, with the aim of the functional characterisation of CLCA2 in human tumour cells. Recent data of gene expression profiling of primary and metastatic melanoma reported differential gene expression of human CLCA2 between metastatic melanoma and non-metastatic cutaneous tumours [74], and confirmed data which have been obtained during this PhD-Thesis.

Based on previous studies of our group and others (see above), there is profound evidence that CLCA2 is a tumour-associated protein which might play an important role in squamous cell carcinogenesis. However, very little is known about the function of CLCA2 and its essential contribution to tumour cell growth and/or survival.

Therefore, the aims of this PhD-Thesis can be summarised as follows:

- performing a detailed *in silico* expression profile analysis utilising mainly the in-house expression database BioExpress (GeneLogic Inc.),
- functional characterisation of CLCA2 by gain- and loss-of-function studies in selected SCC cell lines,
- identification of functionally essential amino acids of CLCA2 by mutational analyses (putative metallo-hydrolase domain),
- analysing the effect of wild type and mutant CLCA2 in 3D culture,
- expression profiling on Affymetrix GeneChips of cell lines upon induction with wild type and mutated CLCA2, selecting differentially induced genes and analysing those genes by RT-qPCR and Western blot analysis, and finally
- utilising data mining algorithms to bring CLCA2 and the differentially induced genes into a biological context.



## RESULTS

This PhD-Thesis is based on data of previous projects in the Sommergruber lab at Boehringer Ingelheim Austria, which aimed at the identification of novel putative targets for anti-cancer therapy. In these studies, Stefan Amatschek compared during his diploma thesis tumourous and non-tumourous patient samples by analysing 20 breast carcinomas, 11 lung squamous cell carcinomas (SCC), 11 lung adenocarcinomas (AC), 8 renal cell arcinomas (RCC), and 16 corresponding normal tissues utilising PCR-based cDNA subtraction analyses combined with subsequent cDNA microarray analyses. The obtained data allowed the discrimination between mRNA transcripts, which are exclusively expressed in lung SCC and/or lung ACs [1]. One of these transcripts was identified as the human calcium-activated chloride channel, family member 2 (CLCA2).

During his PhD-Thesis, Ulrich König could confirm the lung SCC-specific mRNA expression of CLCA2 by different methods such as Northern blot, RT-qPCR, *in situ* hybridisation and others. Additionally, he could identify an overexpression of CLCA2 mRNA transcript in esophageal SCCs in comparison to normal esophageal tissue. In addition, he could show that selected HLA-A2-restricted peptides from CLCA2 can be used for *in vitro* priming T cell lines [2].

### ***In Silico Analysis of Expression Data***

The expression levels of CLCA2 mRNA were investigated in available normal tissue samples, tumourous tissue samples and tumour cell lines utilising Boehringer Ingelheims proprietary BioExpress database (GeneLogic Inc.), which includes expression data from ~ 14.000 human tissue samples, analysed on Affymetrix GeneChips.

## Expression Profiling of CLCA2 in Normal Tissue Samples

By comparison of 31 different normal tissues using BioExpress database (GeneLogic Inc.), CLCA2 expression could only be found in normal skin, larynx and esophagus (Figure 2).

The expression of CLCA2 mRNA seems to be tightly regulated, as its mRNA is only found in a small number of normal tissues and is not ubiquitously expressed.

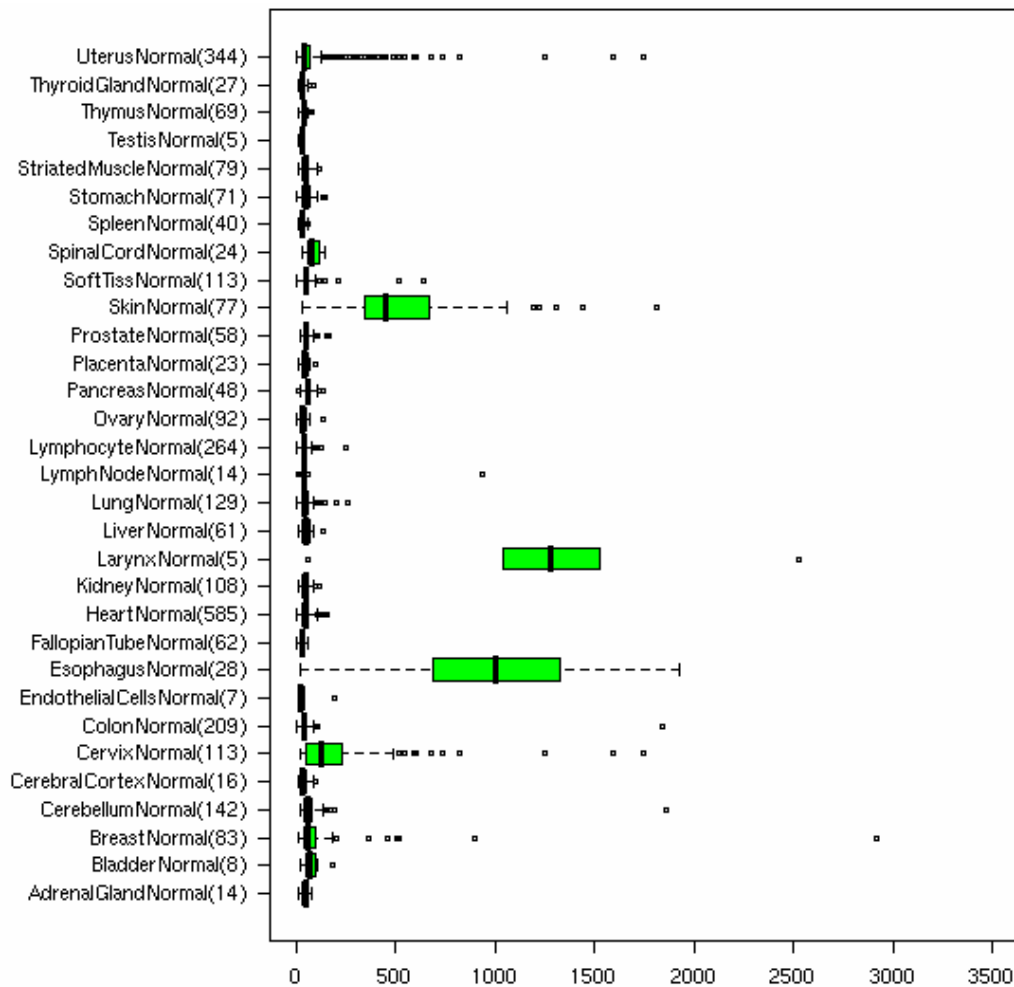


**Figure 2. CLCA2 mRNA expression in normal tissue samples**

CLCA2 mRNA expression was analysed using Affymetrix GeneChip technology. The Affymetrix identification code for CLCA2 is 206165\_s\_at. The expression levels of CLCA2 mRNA are shown in box-plots. The vertical centre line in the box indicates the median. The box itself represents the interquartile range (IQR) between the first and third quartiles. Whiskers extend to 1.5 times the IQR; the position of extreme values, if above the upper whisker limits, are marked by open circles. The human sample collection has been described by the originator of the BioExpress database (GeneLogic Inc.). Numbers in brackets indicate the sample numbers. All samples have been MAS5-normalised [75].

### **Expression Profiling of CLCA2 in Tumourous Tissue Samples**

The expression levels of CLCA2 were examined in those available tumourous and corresponding normal tissue samples, where the disease annotation was confirmed by the revision of the clinical history by an experienced pathologist. The verified diagnostic sample annotation was taken as the primary quality criteria for sample selection.

Varying portions of tumour cells on the individual tissue sections could distort some of the relative expression values. In-depth statistical analyses of those samples, of which the percentage of tumour cells per section was available and accordingly correlated (data not shown), resulted in negligible corrections of the relative expression values.

Data for cervix carcinomas could only be linked to squamous cell carcinomas (SCC). For those two indications no further tumour type sub-classification could be found in BioExpress database (GeneLogic Inc.). Tumours from the lung were subdivided into small cell lung cancers (SCLC), adenocarcinomas (AC), adenosquamous carcinomas (AdSqCa), large cell carcinomas (LCC), and squamous cell carcinomas (SCC). For a fraction of SCCs from the head and neck region it was possible to classify those samples into two sub-categories (esophageal and laryngeal tumours), since data of the corresponding normal tissue were also available. For tumours of the urinary bladder mainly data on transitional cell carcinomas (TCC), the most common type of bladder carcinomas, were available. Lymph node metastases were subcategorised, corresponding to the tumour subtype of the primary tumour they descend from, namely melanoma (Mel), adenocarcinomas (AC), and squamous cell carcinomas (SCC).

As previously mentioned, CLCA2 expression was already detected in esophageal and lung SCCs by Northern blotting and RT-qPCR. As shown in Figure 4, analyses of the expression pattern in the BioExpress database (GeneLogic Inc.) confirmed these data and indicated a preferential overexpression of CLCA2 for lymph node metastases of SCCs (LNSCCMet) as well as for SCCs of the larynx, the cervix, the head and neck region, and of a subpopulation of the infiltrating ductal breast carcinoma and mycosis fungoides.

There is a clear preference of elevated levels of CLCA2 mRNA transcript in SCCs such as larynx SCC, head and neck SCC or cervix SCC (Figure 4).

After in-depth analyses of the available clinical history of the normal skin samples a discrimination between skin samples derived from healthy individuals and skin samples from cancer patients was possible. As the expression levels for CLCA2 are significantly higher in most of the skin samples, which were taken from cancer patients distant from the primary tumour site (Figure 3), it is very likely that the expression levels of CLCA2 in tumour-associated normal samples of larynx and esophagus are similarly altered by distant primary tumours. However, for these tissues samples no reliable clinical history was available.

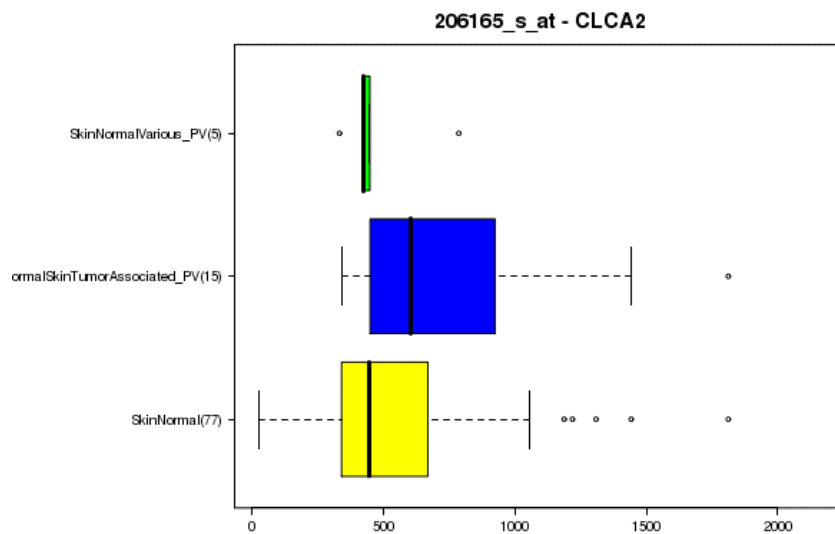


**Figure 3. CLCA2 mRNA expression in skin samples of different origins**

PV: Verified by pathologist; green: Skin-derived from non-tumour (normal) samples; blue: Normal skin tumour-associated samples; yellow: Normal skin samples w/o assignment. CLCA2 mRNA expression was analysed using Affymetrix GeneChip technology. The Affymetrix identification code for CLCA2 is 206165\_s\_at. The expression levels of CLCA2 mRNA are shown in box-plots. The vertical centre line in the box indicates the median. The box itself represents the interquartile range (IQR) between the first and third quartiles. Whiskers extend to 1.5 times the IQR; the position of extreme values, if above the upper whisker limits, are marked by open circles. The human sample collection has been described by the originator of the BioExpress database (GeneLogic Inc.). Numbers in brackets indicate the sample numbers. All samples have been MAS5-normalised.

In contrast to SCCs, overexpression of CLCA2 is neither detected in ACs and their corresponding lymph node metastasis, nor in tumours of the hematopoietic or lymphatic system indicating again its highly SCC-specific expression (Figure 4).

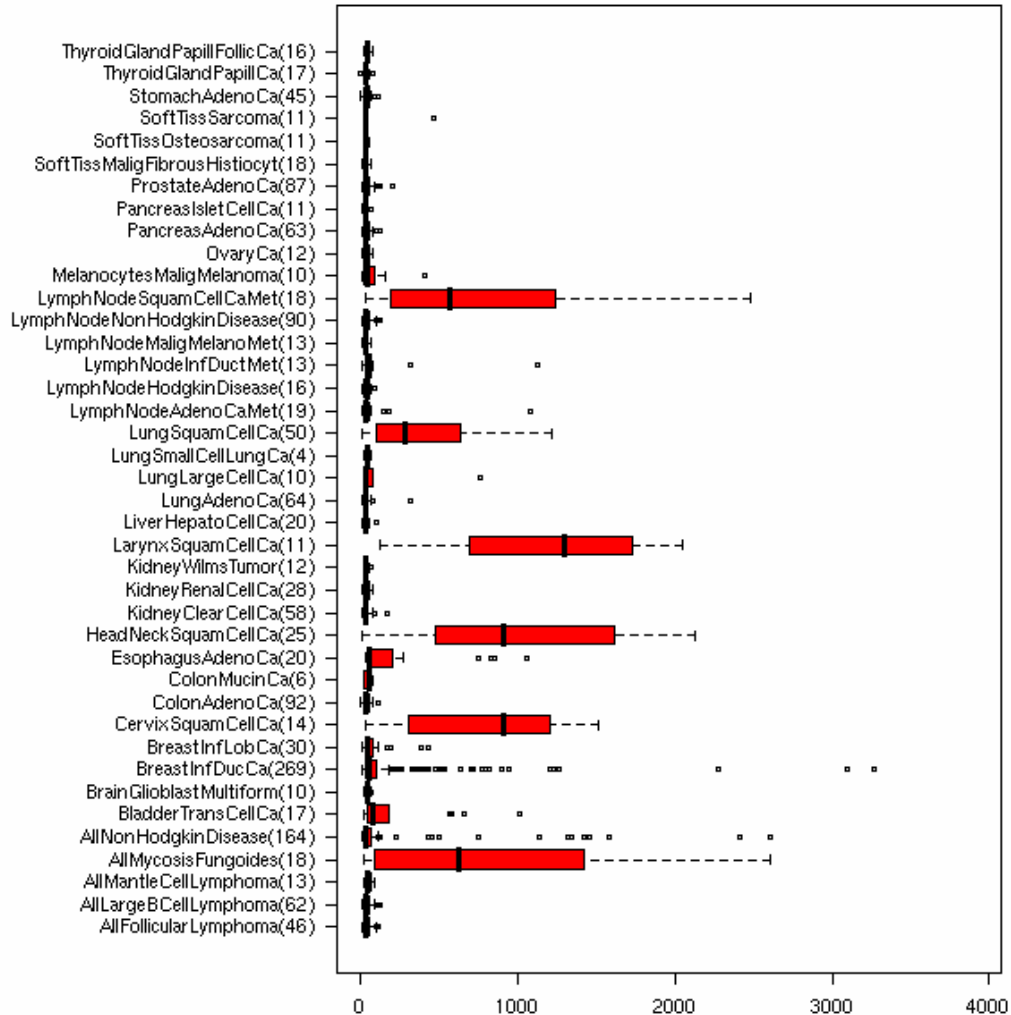


**Figure 4. CLCA2 mRNA expression in various tumours**

All: Acute lymphocytic leukaemia, Ca: Carcinoma, Met: Metastases, Tiss: Tissue, Squam: Squamous, InfDuc: Infiltrating ductal, InfLob: Infiltrating lobular, PapillFollic: Papillary and follicular, Malig: Malignant, TransCellCa: Trans cell carcinoma, ColonMucinCa: Mucinous colon carcinoma, GlioblastMultiform: Glioblastoma multiforme. CLCA2 mRNA expression was analysed using Affymetrix GeneChip technology. The Affymetrix identification code for CLCA2 is 206165\_s\_at. The expression levels of CLCA2 mRNA are shown in box-plots. The vertical centre line in the box indicates the median. The box itself represents the interquartile range (IQR) between the first and third quartiles. Whiskers extend to 1.5 times the IQR; the position of extreme values, if above the upper whisker limits, are marked by open circles. The human sample collection has been described by the originator of the BioExpress database (GeneLogic Inc.). Numbers in brackets indicate the sample numbers. All samples have been MAS5-normalised.

Figure 5 comprises a comparison of the major therapeutically relevant tumour types versus their corresponding normal tissues. Elevated levels of CLCA2 mRNA transcript were detected only in lung SCC and could not be found in lung AC or the corresponding normal tissues. In prostate and colon carcinomas no CLCA2 expression was found (Figure 5).

In breast cancer, a subpopulation of the infiltrating ductal carcinomas shows overexpression of CLCA2, which is represented by the high amount of outliers in Figure 5. However, it remains unclear whether distinct chromosomal aberrations or different differentiation stages lead to the induction of and/or dependence on CLCA2 in this subset of breast cancer samples. In this context it has to be mentioned that Her2 amplification is also found only in a subset (outlier) of breast cancer samples.

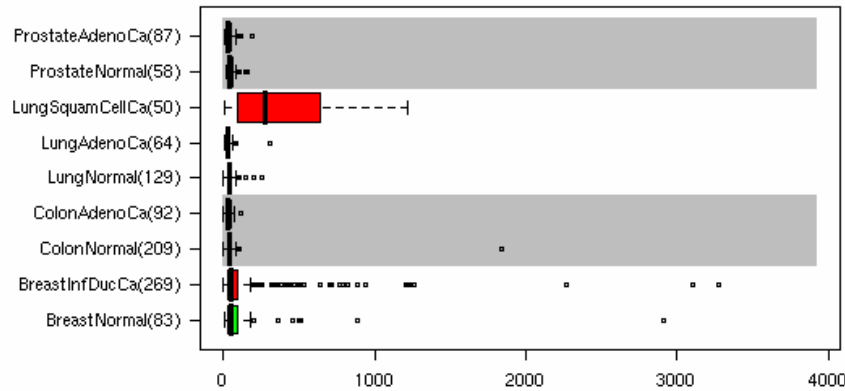


**Figure 5. CLCA2 mRNA expression in tumourous tissues: Major therapeutically important tumour types**  
CLCA2 mRNA expression was analysed using Affymetrix GeneChip technology. The Affymetrix identification code for CLCA2 is 206165\_s\_at. The expression levels of CLCA2 mRNA are shown in box-plots. The vertical centre line in the box indicates the median. The box itself represents the interquartile range (IQR) between the first and third quartiles. Whiskers extend to 1.5 times the IQR; the position of extreme values, if above the upper whisker limits, are marked by open circles. The human sample collection has been described by the originator of the BioExpress database (GeneLogic Inc.). Numbers in brackets indicate the sample numbers. All samples have been MAS5-normalised. Abbreviations see Figure 4.

In Figure 6 lymph node metastases are compared with a set of “minor indications” and their corresponding normal tissues. Again, CLCA2 overexpression could only be detected in lymph node metastases derived from SCC but not AC-driven metastases.

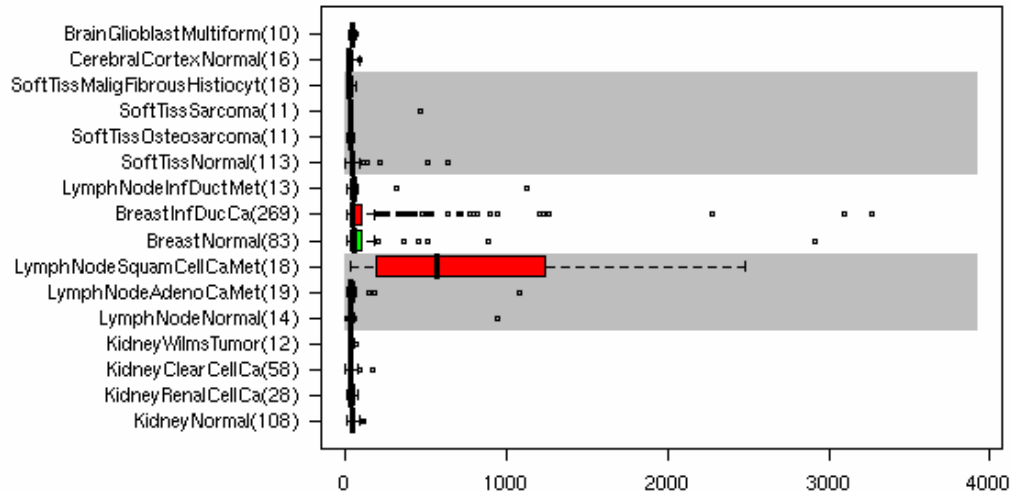


**Figure 6. CLCA2 mRNA expression in lymphnode metastases**

SoftTissMalignFibrousHistiocyt: Soft tissue malignant fibrous histiocytoma; other abbreviations see Figure 4. CLCA2 mRNA expression was analysed using Affymetrix GeneChip technology. The Affymetrix identification code for CLCA2 is 206165\_s\_at. The expression levels of CLCA2 mRNA are shown in box-plots. The vertical centre line in the box indicates the median. The box itself represents the interquartile range (IQR) between the first and third quartiles. Whiskers extend to 1.5 times the IQR; the position of extreme values, if above the upper whisker limits, are marked by open circles. The human sample collection has been described by the originator of the BioExpress database (GeneLogic Inc.). Numbers in brackets indicate the sample numbers. All samples have been MAS5-normalised.

In the view of elevated CLCA2 transcript levels in tumour-associated skin biopsies (see Figure 3) it is of interest that a dramatic increase of CLCA2 mRNA was identified in mycosis fungoides (Figure 7). Mycosis fungoides is the most common type of cutaneous T cell lymphoma (CTCL). It is a Non-Hodgkin lymphoma, which is predominantly related to skin. It generally affects the skin, but may progress internally over time. As shown in Figure 3, mRNA expression of CLCA2 seems to be induced in tumour-associated skin rather than in normal skin. Similarly, mycosis fungoides might make use of CLCA2 for its colonisation of the skin during its course of progression. In contrast, no CLCA2 expression is found in Hodgkin lymphomas. In summary, it seems that formation of SCC-derived metastases are somehow linked with CLCA2 expression (Figure 6) supporting the idea that CLCA2 might play a crucial role in the formation of SCC-derived metastases and for the progression of mycosis fungoides (Figure 7).

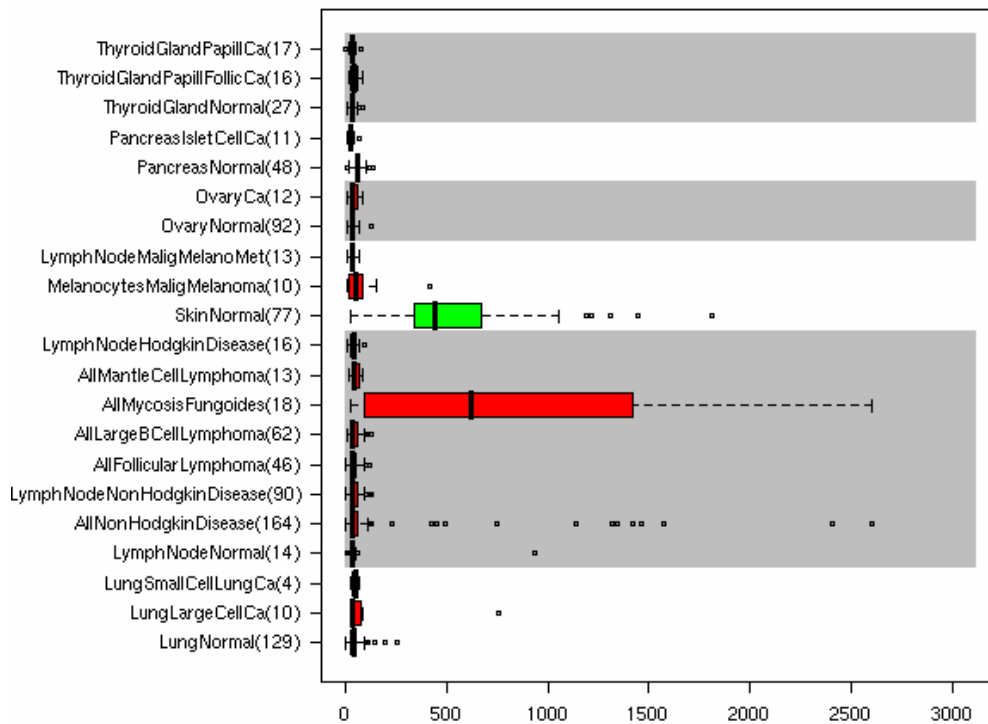


**Figure 7. CLCA2 mRNA expression in lymphomas and mycosis fungoides**

CLCA2 mRNA expression was analysed using Affymetrix GeneChip technology. The Affymetrix identification code for CLCA2 is 206165\_s\_at. The expression levels of CLCA2 mRNA are shown in box-plots. The vertical centre line in the box indicates the median. The box itself represents the interquartile range (IQR) between the first and third quartiles. Whiskers extend to 1.5 times the IQR; the position of extreme values, if above the upper whisker limits, are marked by open circles. The human sample collection has been described by the originator of the BioExpress database (GeneLogic Inc.). Numbers in brackets indicate the sample numbers. All samples have been MAS5-normalised. Abbreviations see Figure 4.



In contrast to mycosis fungoides no (elevated) expression of CLCA2 was detectable in B cell and T cell lymphomas and their corresponding normal tissues (Figure 8, Figure 9 and Figure 10).

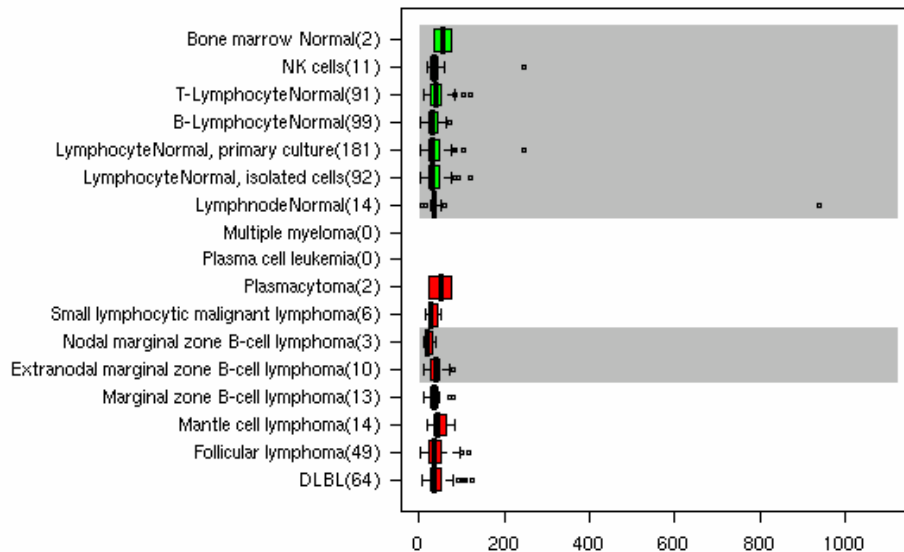


**Figure 8. CLCA2 mRNA expression in a panel of lymphomas and B cell leukaemias and their corresponding normal tissues**

CLCA2 mRNA expression was analysed using Affymetrix GeneChip technology. The Affymetrix identification code for CLCA2 is 206165\_s\_at. The expression levels of CLCA2 mRNA are shown in box-plots. The vertical centre line in the box indicates the median. The box itself represents the interquartile range (IQR) between the first and third quartiles. Whiskers extend to 1.5 times the IQR; the position of extreme values, if above the upper whisker limits, are marked by open circles. The human sample collection has been described by the originator of the BioExpress database (GeneLogic Inc.). Numbers in brackets indicate the sample numbers. All samples have been MAS5-normalised. DLBL: Diffuse large B cell lymphoma; other abbreviations see Figure 4.

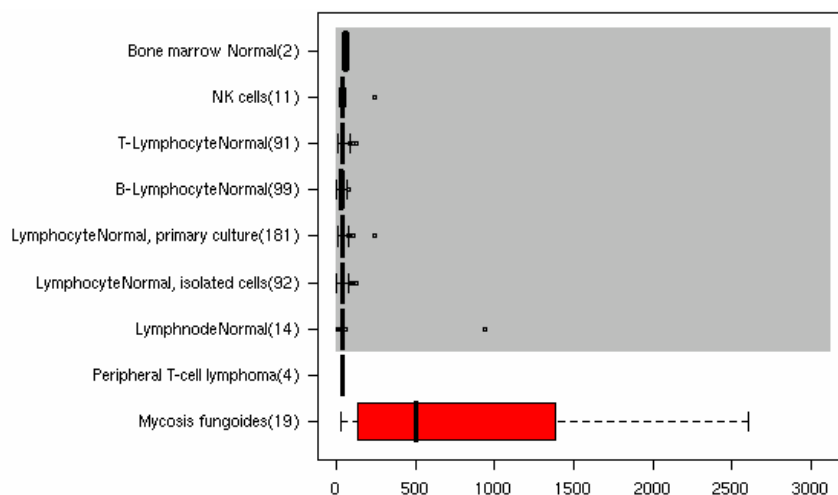


**Figure 9. CLCA2 mRNA expression in T cell and B cell lymphomas and their corresponding normal tissues**

CLCA2 mRNA expression was analysed using Affymetrix GeneChip technology. The Affymetrix identification code for CLCA2 is 206165\_s\_at. The expression levels of CLCA2 mRNA are shown in box-plots. The vertical centre line in the box indicates the median. The box itself represents the interquartile range (IQR) between the first and third quartiles. Whiskers extend to 1.5 times the IQR; the position of extreme values, if above the upper whisker limits, are marked by open circles. The human sample collection has been described by the originator of the BioExpress database (GeneLogic Inc.). Numbers in brackets indicate the sample numbers. All samples have been MAS5-normalised. Abbreviations see Figure 4.

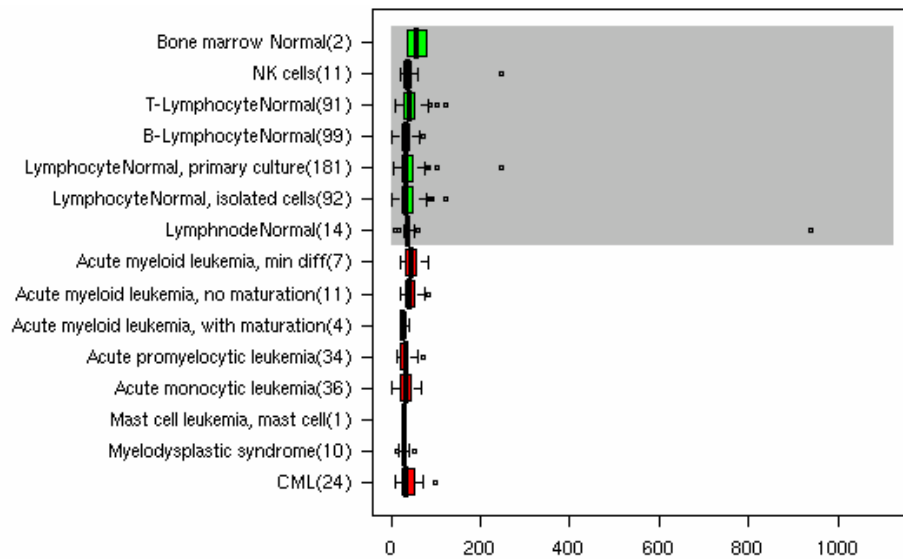


**Figure 10. CLCA2 mRNA expression in acute leukaemias such as acute myeloid, acute promyelocytic, and acute monocytic leukaemia**

CLCA2 mRNA expression was analysed using Affymetrix GeneChip technology. The Affymetrix identification code for CLCA2 is 206165\_s\_at. The expression levels of CLCA2 mRNA are shown in box-plots. The vertical centre line in the box indicates the median. The box itself represents the interquartile range (IQR) between the first and third quartiles. Whiskers extend to 1.5 times the IQR; the position of extreme values, if above the upper whisker limits, are marked by open circles. The human sample collection has been described by the originator of the BioExpress database (GeneLogic Inc.). Numbers in brackets indicate the sample numbers. All samples have been MAS5-normalised. CML: Chronic myelogenous leukemia; other abbreviations see Figure 4.

As different generations of Affymetrix GeneChips have been used, an *in silico* comparison was performed to test for the robustness and reproducibility of the expression profile of CLCA2. As clearly seen in Figure 11, the expression profile of CLCA2 is independent from the type of GeneChip used. In all cases only SCCs exhibit the dramatic overexpression of CLCA2. For testing the Exon GeneChip generation only a subset of the human lung samples have been used. Although different types of arrays have been used for the expression profiling no statistically relevant variation can be observed in the mRNA levels of the same sample set among different GeneChips. It has to be indicated that for a given tissue sample the relative expression values between the different GeneChips cannot be directly compared with each other (e.g. median for CLCA2 in SCC on U133AB Array is ~ 600, on U133 Plus 2.0 is ~ 800 and on Exon Array ~ 300, respectively).

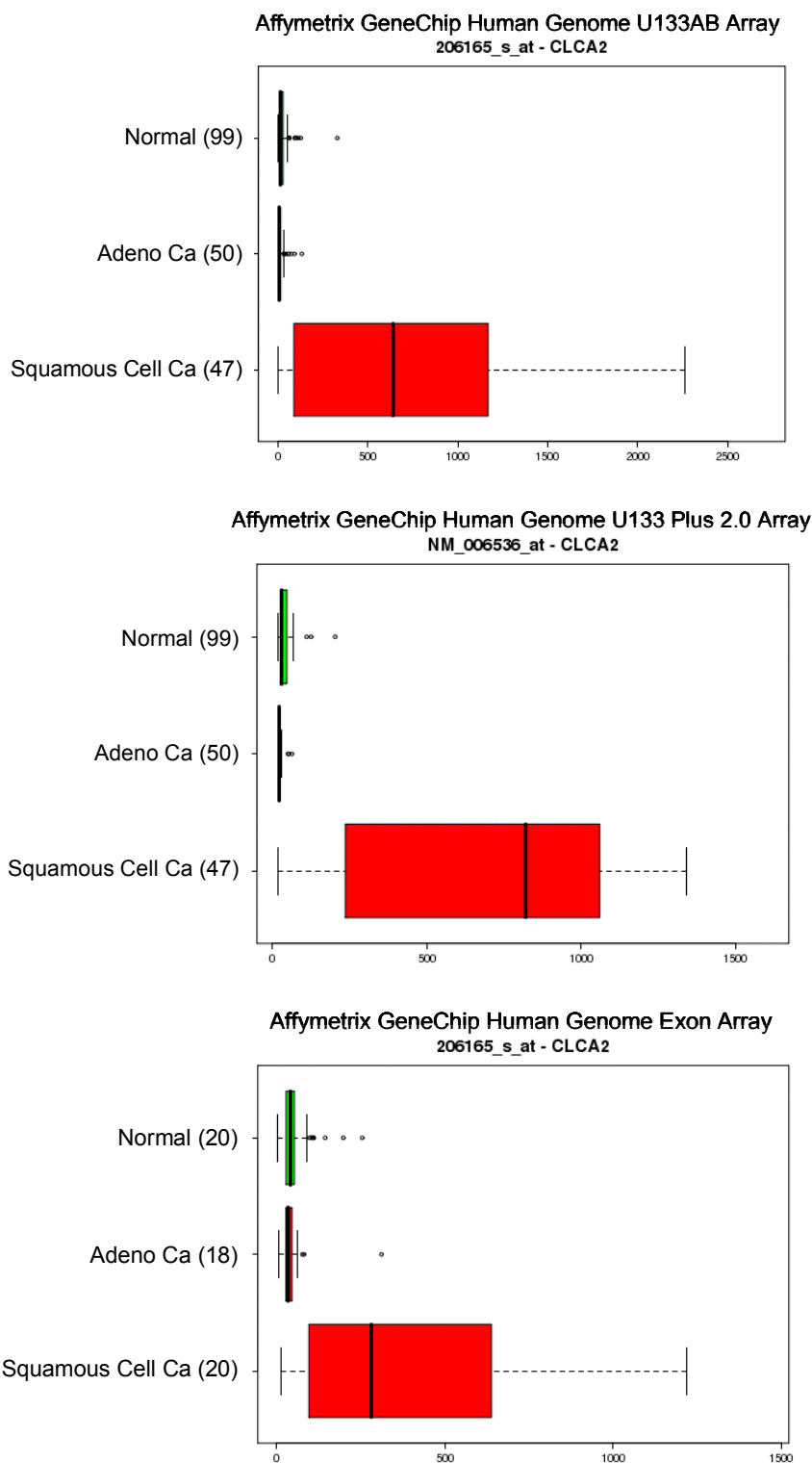


**Figure 11. Comparison of CLCA2 expression profiles of a set of human normal and lung tumour (AC and SCC) samples utilising different types of Affymetrix GeneChips**

Note that the identification code for CLCA2 is different, depending on the array type used. The expression levels of CLCA2 mRNA are shown in box-plots. The vertical centre line in the box indicates the median. The box itself represents the interquartile range (IQR) between the first and third quartiles. Whiskers extend to 1.5 times the IQR; the position of extreme values, if above the upper whisker limits, are marked by open circles. The human sample collection has been described by the originator of the BioExpress database (GeneLogic Inc.). Numbers in brackets indicate the sample numbers. All samples have been MAS5-normalised. Abbreviations see Figure 4.

The infiltration of a number of non-tumourous cell types (e.g. macrophages, lymphocytes) into the tumour tissue and the presence of surrounding non-tumourous tissue (tumour stroma) in whole tissue preparations often leads to falsification in the interpretation of *ex vivo* tissue expression data. To exclude relevant contribution of cells of the tumour stroma, the CLCA2 expression pattern in several laser-capture-microdissected (LCM) tissue samples of lung carcinomas in comparison to non-neoplastic lung tissue samples was analysed (Figure 12). Based on this *in silico* analysis, expression of CLCA2 in tumour stroma could be excluded and the tumour-specific expression pattern of CLCA2 could be confirmed. For a better comparability the total RNA from all cell types and LCM-dissected epithelial cells from different sections of the identical frozen tumour samples was analysed. The expression of CLCA2 transcript is exclusively found in the epithelial tumour cell fraction and if indeed expressed in any stromal compartment, would have led to a decrease in normalised expression levels in epithelial tumour cells, when compared with the corresponding normal tissue. As the relative expression level in the tumour cell population even increased after LCM sample preparation, it can be argued that the detected expression of CLCA2 transcript in all other tissue samples of different origin, which were analysed without LCM dissection, originates exclusively from epithelial tumour cells (see also Figure 2 and Figure 3).

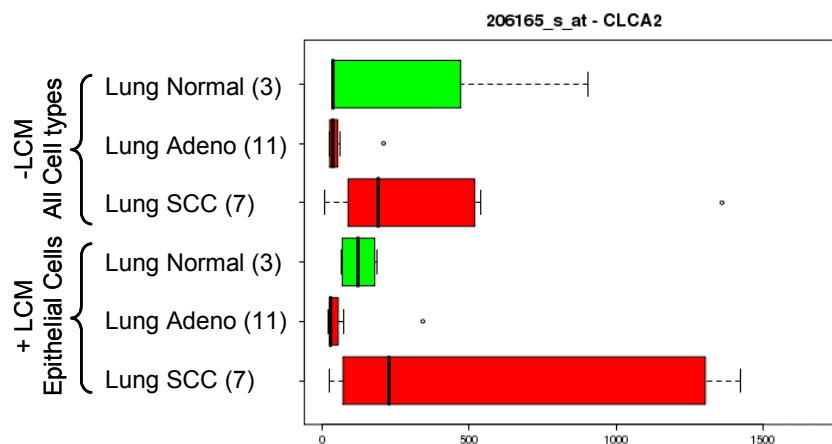


**Figure 12. CLCA2 mRNA expression in LCM-dissected lung tumour samples**

Samples were analysed with and without LCM-dissection (with: +LCM / without: -LCM) of epithelial tumour cells. CLCA2 mRNA expression was analysed using Affymetrix GeneChip technology. The Affymetrix identification code for CLCA2 is 206165\_s\_at. The expression levels of CLCA2 mRNA are shown in box-plots. The vertical centre line in the box indicates the median. The box itself represents the interquartile range (IQR) between the first and third quartiles. Whiskers extend to 1.5 times the IQR; the position of extreme values, if above the upper whisker limits, are marked by open circles. Numbers in brackets indicate the sample numbers. All samples have been MAS5-normalised.

As expression of CLCA2 is detected in esophagus tissue, an interesting aspect was whether CLCA2 is also expressed in other parts of the digestive tract. Therefore the expression levels of CLCA2 were compared in various tissues of the entire digestive tract. As clearly seen in Figure 13, no additional expression is found in other parts of the digestive tract, again underlining the restricted expression pattern of CLCA2.

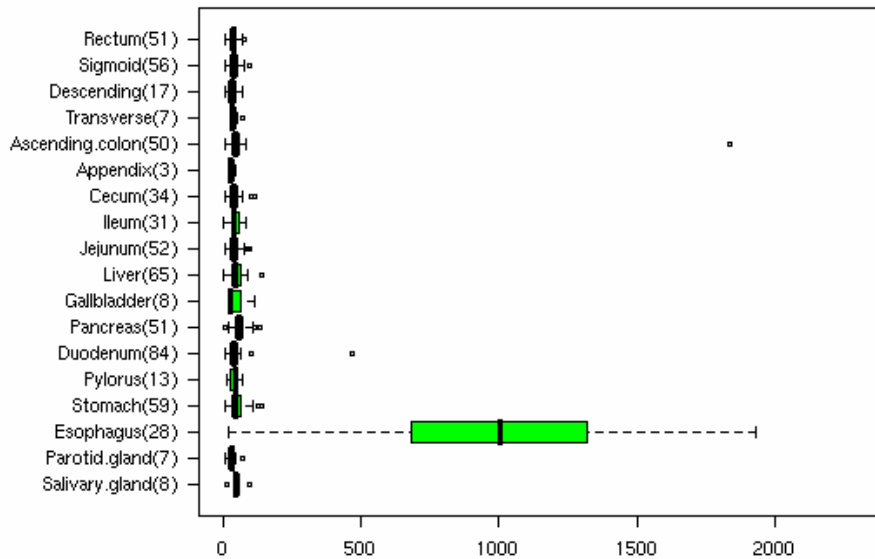


**Figure 13. CLCA2 mRNA expression in normal tissues of the digestive tract**

CLCA2 mRNA expression was analysed using Affymetrix GeneChip technology. The Affymetrix identification code for CLCA2 is 206165\_s\_at. The expression levels of CLCA2 mRNA are shown in box-plots. The vertical centre line in the box indicates the median. The box itself represents the interquartile range (IQR) between the first and third quartiles. Whiskers extend to 1.5 times the IQR; the position of extreme values, if above the upper whisker limits, are marked by open circles. The human sample collection has been described by the originator of the BioExpress database (GeneLogic Inc.). Numbers in brackets indicate the sample numbers. All samples have been MAS5-normalised.

That CLCA2 expression might have an influence on development of metastasis as shown in Figure 14. To analyse if there is a correlation of CLCA2 overexpression with development of metastases, it was made use of expression data derived from cell lines and their corresponding developing tumours in xenograft models. It is of great interest that xenografts originating from SSC cell lines such as A431 (cervix carcinoma), H520 (lung carcinoma) and HNOE (head and neck/ esophagus carcinoma) all exhibit a dramatic upregulation of CLCA2 (Figure 14). Except for the pancreatic cell line BxPC3 and MDA-MB-453 (mamma carcinoma) no AC-derived cell line leads to such a pronounced upregulation of CLCA2 in xenografts. In the case of MDA-MB-453 a high expression level of CLCA2 is already observed in 2D culture (Figure 14).

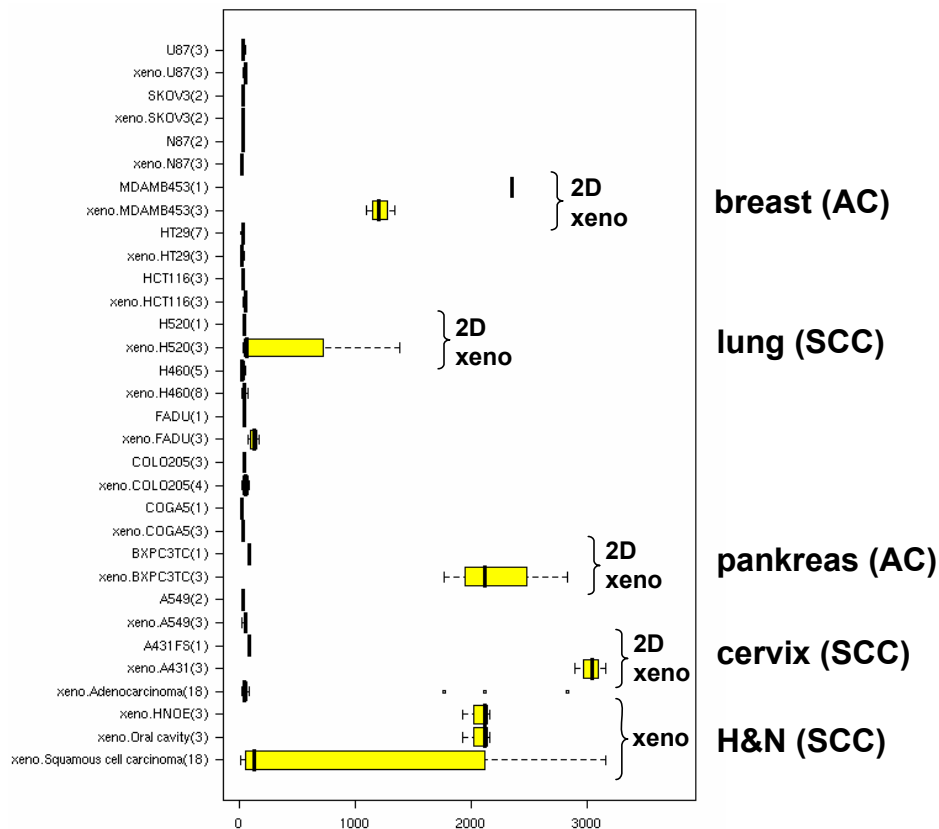


**Figure 14. Induction of CLCA2 in xenografts versus 2D cell culture**

CLCA2 mRNA expression was analysed using Affymetrix GeneChip technology. The Affymetrix identification code for CLCA2 is 206165\_s\_at. The expression levels of CLCA2 mRNA are shown in box-plots. The vertical centre line in the box indicates the median. The box itself represents the interquartile range (IQR) between the first and third quartiles. Whiskers extend to 1.5 times the IQR; the position of extreme values, if above the upper whisker limits, are marked by open circles. The human sample collection has been described by the originator of the BioExpress database (GeneLogic Inc.). Numbers in brackets indicate the sample numbers. All samples have been MAS5-normalised. 2D refers to cell lines cultivated in tissue culture and xeno the corresponding xenografts. Other abbreviations see Figure 4.

### **Expression Profiling of CLCA2 in Tumour Cell Lines**

Additional support for a restricted expression profile of CLCA2 comes from the expression profiling analysis of different human carcinoma cell lines (Figure 15). Expression was only detected in the human glioblastoma cell line SNB75, in two SCC cell lines HN5 (head and neck) and A431 (cervix carcinoma) and in the breast carcinoma cell line MDA-MB-453.

Two cell lines were selected for knock-down experiments, HN5 a squamous head and neck carcinoma cell line and MDA-MB-453 (mamma carcinoma) as a representative of an AC cell line with high levels of CLCA2 expression.

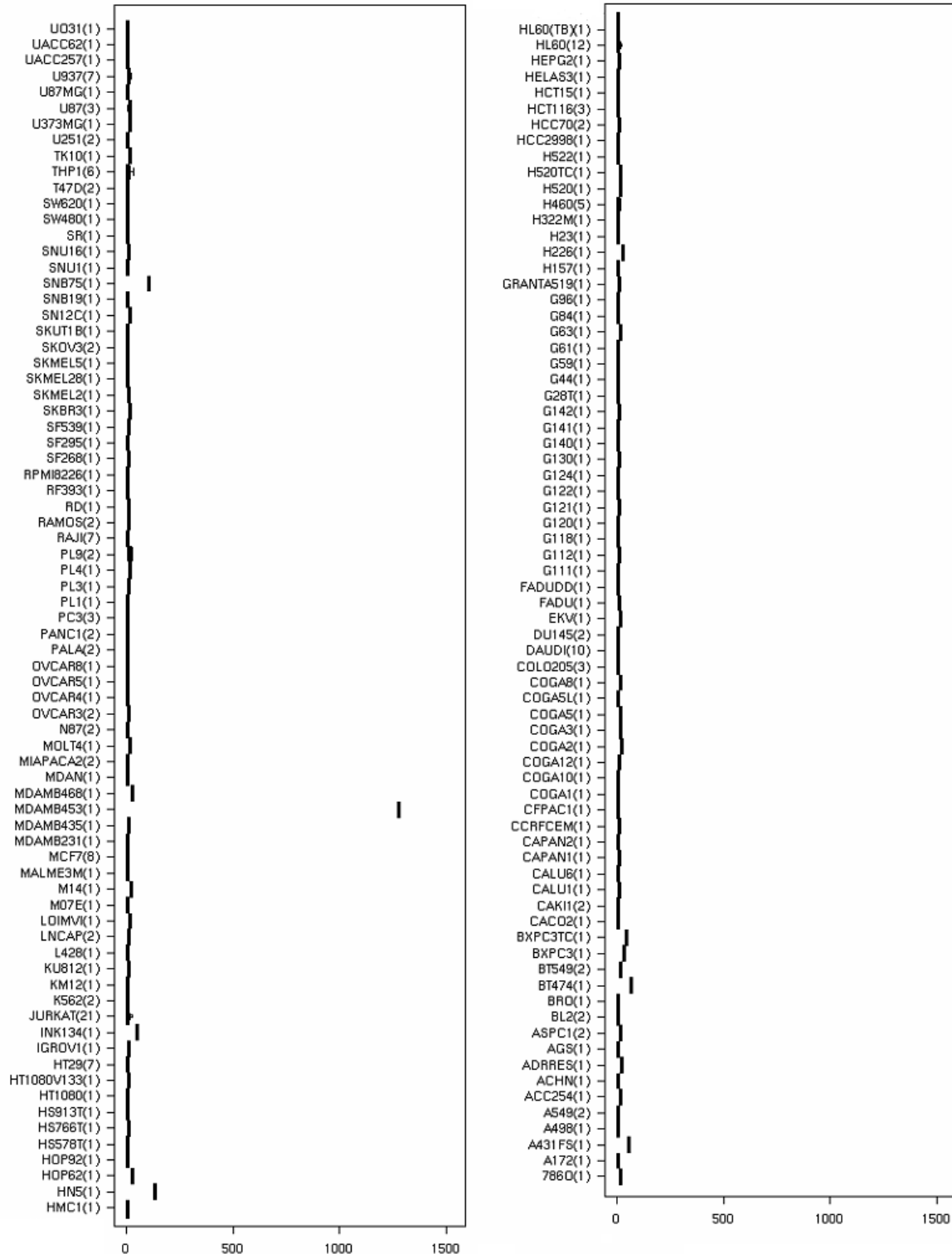


**Figure 15. CLCA2 mRNA expression in various human tumour cell lines**

CLCA2 mRNA expression was analysed using Affymetrix GeneChip technology. The Affymetrix identification code for CLCA2 is 206165\_s\_at. The expression levels of CLCA2 mRNA are shown in box-plots. The vertical centre line in the box indicates the median. The box itself represents the interquartile range (IQR) between the first and third quartiles. Whiskers extend to 1.5 times the IQR; the position of extreme values, if above the upper whisker limits, are marked by open circles. Cell line description is according to the nomenclature of the provider (in most cases ATCC (American Type Culture Collection): <http://www.atcc.org/home.cfm>, DSMZ (Deutsche Sammlung für Mikroorg. und Zellkulturen): <http://www.dsmz.de/index.html>, and ECACC (European Collection of Animal Cell Cultures): <http://fuseiv.star.co.uk/camr/>). Numbers in brackets indicate the sample numbers. All samples have been MAS5-normalised. Corresponding tumour types to cell lines are shown in Appendix.



A correlation of CLCA2 expression in metastases of breast cancer with detection of metastases in different sites is shown in Figure 16. To exclude any interference of cells from the tumour stroma, only laser-capture-microdissected (LCM) tissue samples were used for this analysis (for details see Figure 3).

Sample sets which showed no evidence of disease including metastases (NED) were compared to metastases-positive samples (POS). Only samples from patients with a five year observation time have been included in this analysis. Except for metastases to bone, CLCA2 overexpression is obviously needed for formation of metastases in brain, lung, liver, and lymph node respectively. The data shown in Figure 16 strongly supports the results in our xenograft models (Figure 14): CLCA2 expression plays a crucial role in tumour progression and metastasis.

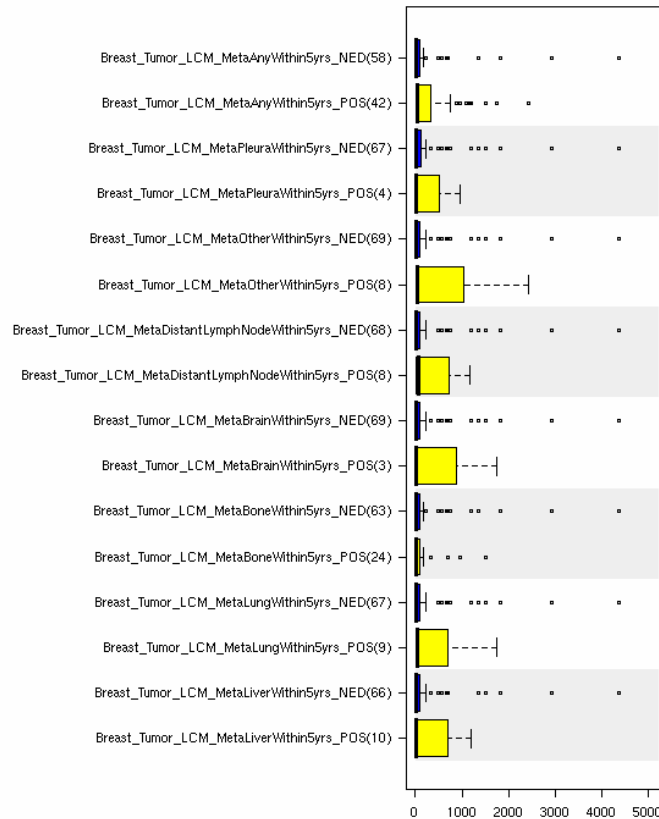


**Figure 16. Correlation of metastasis status with CLCA2 expression in LCM breast cancer samples**  
CLCA2 mRNA expression was analysed using Affymetrix GeneChip technology. The Affymetrix identification code for CLCA2 is 206165\_s\_at. The expression levels of CLCA2 mRNA are shown in box-plots. The vertical centre line in the box indicates the median. The box itself represents the interquartile range (IQR) between the first and third quartiles. Whiskers extend to 1.5 times the IQR; the position of extreme values, if above the upper whisker limits, are marked by open squares. Numbers in brackets indicate the sample numbers. All samples have been MAS5-normalised. LCM: Laser-capture-microdissected, Meta: Metastases, NED: No evidence of disease (blue), POS: Metastases-positive (yellow). Data generated in the course of the GEN-AU Project (Joint Project: “Genomic Approaches to Tumour Invasion and Metastasis”).

A correlation was also found between CLCA2 expression and receptor- and lymphnode status in breast cancer (Figure 17). In the case of Her2 amplification (aggressive status; poor prognosis; [76]) CLCA2 expression is upregulated as compared to tumour samples where Her2 is not amplified. In contrast, if the tumour is still estrogen-sensitive (estrogen receptor status POS; good prognosis; [77]), CLCA2 expression is very low, but becomes upregulated in samples of negative estrogen receptor status (insensitive to estrogen; poor prognosis).

These results support the present view on the essential contribution of CLCA2 to tumour formation, progression, and induction of metastases (Figure 14, Figure 16, Figure 17).

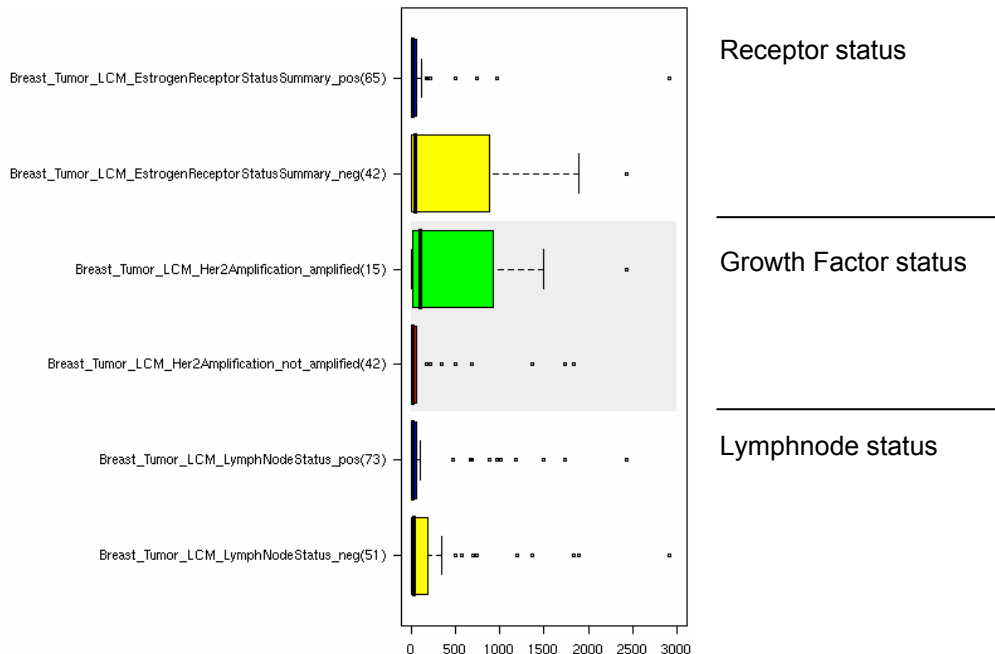


**Figure 17. Correlation of receptor and lymphnode status with CLCA2 expression**

CLCA2 mRNA expression was analysed using Affymetrix GeneChip technology. The number of samples (n) for each tissue is given. The expression levels of CLCA2 (206165\_s\_at) mRNA in ER positive and ER negative, in Her2 amplified and Her2 non-amplified and in lymph node positive and negative breast cancer patient samples are shown in box-plots. The vertical centre line in the box indicates the median; the box itself represents the interquartile range (IQR) between the first and third quartiles. Whiskers extend to 1.5 times the IQR. Positions of extreme values are marked by open circles, if they were above the upper whisker limits. Only data from samples which have been laser-capture-microdissected were included in the *in silico* analysis. Data generated in the course of the GEN-AU Project (Joint Project: "Genomic Approaches to Tumour Invasion and Metastasis").

### Chromosomal Amplifications of CLCA2 Locus in Tumour Cell Lines

Interestingly, most squamous cell carcinoma cell lines with an increased expression level of CLCA2 also exhibit amplification of the chromosomal locus of CLCA2: 1p22-31 [63], possibly reflecting the link between genomic and transcriptional status in various SCCs. Using Affymetrix SNP-Chip analysis (SNP: Single nucleotide polymorphism), chromosomal amplification or deletion patterns in different human tumours and tumour cell lines were analysed and are shown in Figure 18 and Figure 19. For instance, in FaDu, a head and neck SCC cell line, the copy number (CN) of the CLCA2 locus is amplified (CN ~ 3).

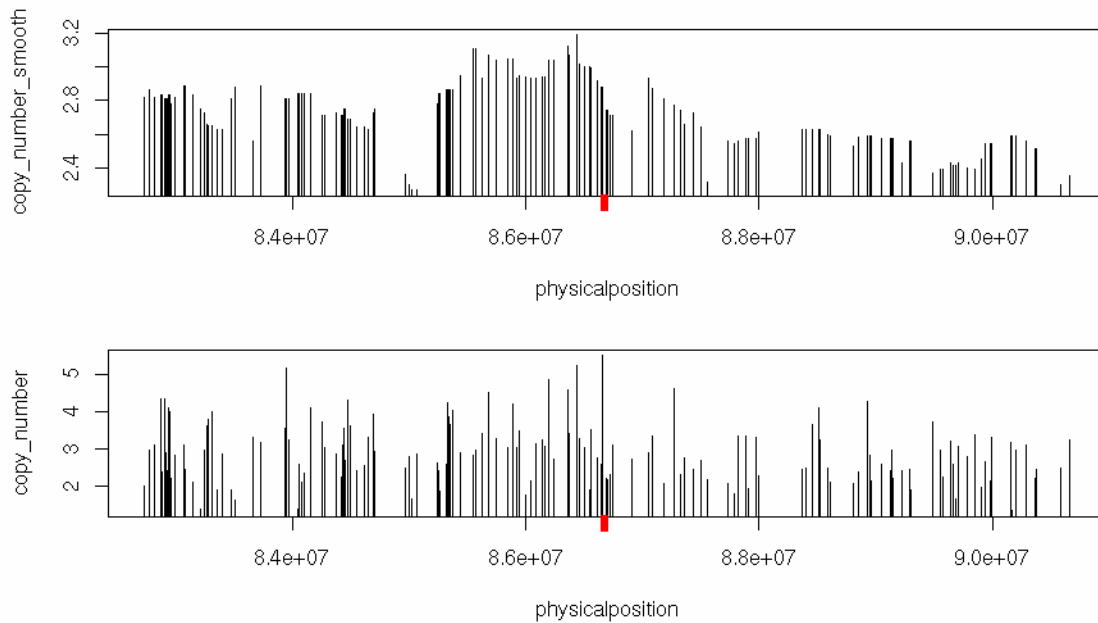


**Figure 18. Chromosomal amplification of CLCA2 locus in the SCC cell line FaDu**

Using Affymetrix SNP-Chip technology, the chromosomal amplification pattern was analysed in FaDu, a head and neck squamous cell carcinoma cell line. Position of CLCA2 is marked in red. For analysis two algorithms have been used (copy number and copy number smooth).

A set of various colon and breast carcinoma cell lines is shown in Figure 19. Whereas no colon carcinoma cell line contains amplified CLCA2 loci, breast carcinoma cell lines MDA-MB-231, BT-549, and HS-578T exhibit amplification of the CLCA2 loci (marked in yellow).

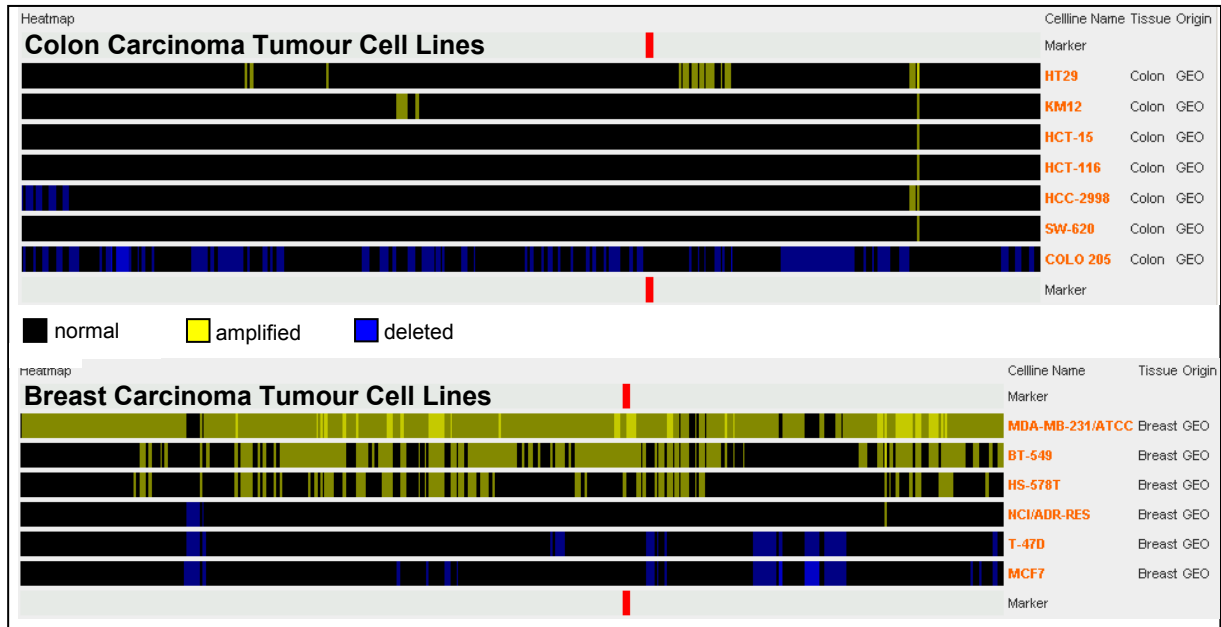


**Figure 19. Heatmap of amplification of the chromosomal CLCA2 locus in various human tumour cell lines**  
Using Affymetrix SNP-Chip technology, the chromosomal amplification pattern was analysed in different human tumour cell lines. Yellow indicated amplified loci, black normal, and blue deleted loci. Corresponding tumour types to cell lines are shown in Appendix.

Based on SNP-Chip data and utilising a new algorithm “GLAD” [78] the copy number of genes located at chromosome 1 (chr1) has been studied in more detail (higher resolution) in breast cancer patient samples and three SCC cell lines. As shown in Figure 20, not only a small part of the chromosomal region around CLCA2 (1p32-p22) is found to be amplified, but huge parts or even the entire chromosome arm are amplified. In contrast to Her2, no focal amplification pattern was identified.

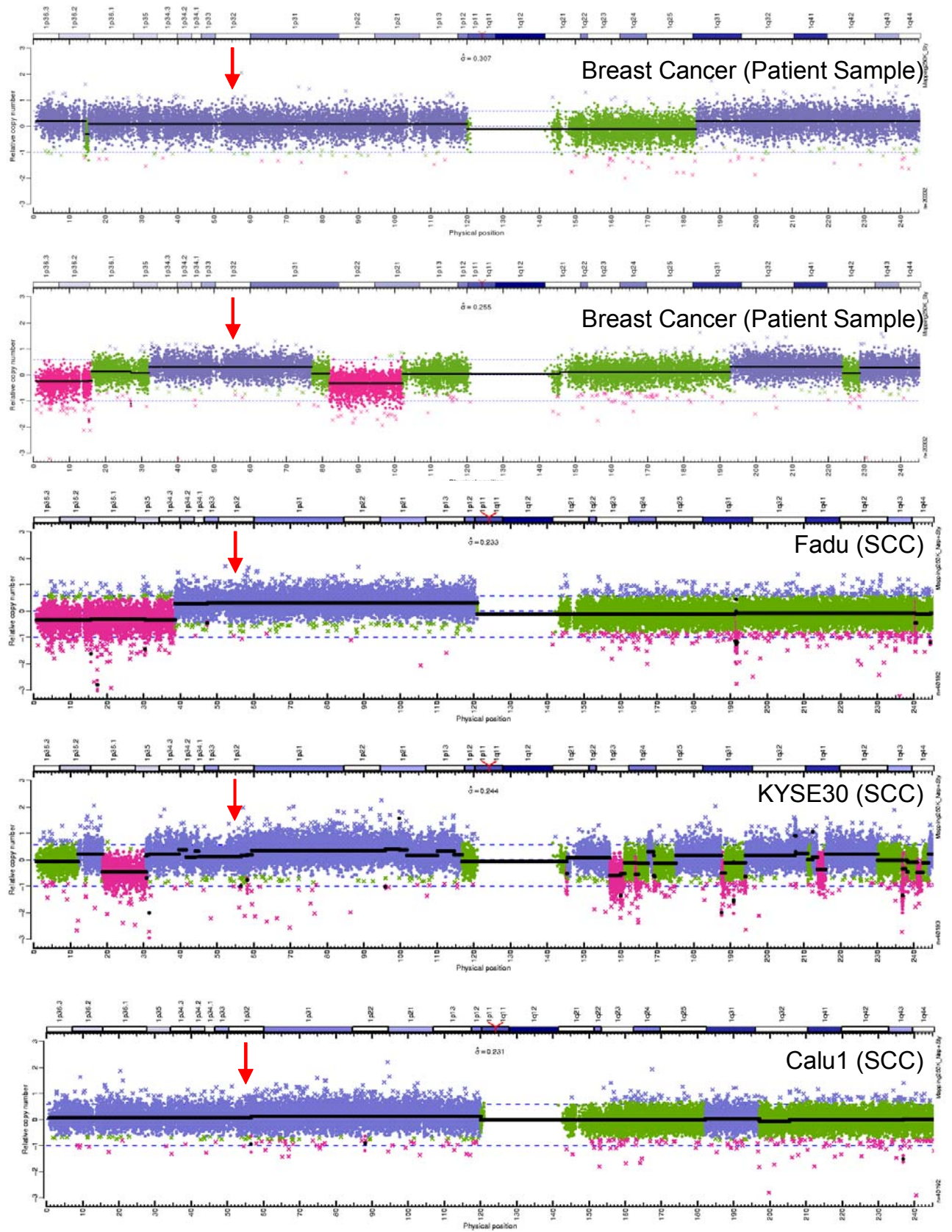


**Figure 20. Chromosomal status of chr1 in human breast cancer samples and SCC cell lines**  
Using Affymetrix SNP-Chip technology, the chromosomal amplification pattern was analysed. Blue indicates amplification, red deletion and green refers to a normal chromosomal status. The red arrow indicates the position of CLCA2 at 1p32-p22. Tissue DNA copy numbers were analysed using the GLAD algorithm [78].

### **Identification of Differential Gene Expression Profiles**

To identify transcripts which show a similar expression pattern to that of CLCA2, statistical analyses which correlated normalised expression values of the BioExpress database (GeneLogic Inc.) were performed.

The expression values of CLCA2 were correlated to the expression values of all available probe sets. Thereby the relative differences between the mean expression values of normal and tumourous tissues were used for correlation. In a first analysis the relative expression differences of CLCA2 between normal tissues and SCCs of the lung, cervix, larynx, esophagus, lymphnode metastasis, and skin, respectively, were compared. During the second round of analyses, the focus was laid on the differences in normal tissues and SCCs of the lung, cervix, and lymph nodes.

As expected, all four annotated probe sets for CLCA2 ranked first in both correlation analyses. Among the highest correlated probe sets within both analyses, different markers for stratified epithelia were found. These were, to name but a few, desmocollin (DSC3), desmoglein 3 (DSG3), TP53 apoptosis effector (PERP), plakophilin 1 (PKP1), and keratin 5 (KRT5). The expression of those epithelial differentiation markers seems to be maintained during the transition from a stratified epithelial cell into a hyper-proliferating SCC cell, and could therefore be essential for the establishment of SCCs.

Genes already described to be involved in tumourigenesis, such as ladinin 1 (LAD1/CD18), tripartite motif-containing 29 (TRIM29), stratifin (14-3-3 sigma/SDN), or RAB38, a member of the RAS oncogene family were also identified.

Correlated probe sets which seem to represent yet unidentified markers for stratified epithelia and/or the tumourigenesis of SCCs were found as well.

One of the identified probe sets (219936\_s\_at), which showed in both analyses nearly an identical expression profile as CLCA2, corresponds to GPR87 and has not been associated with stratified epithelia or the establishment of SCCs before.

The investigation of GPR87 was basis for the PhD-Thesis of Sebastian Glatt with the title "Contribution of hGPR87 and hARHV to squamous cell carcinogenesis", which was done in the Sommergruber lab at Boehringer Ingelheim. The work was recently published in the Int. J. of Cancer [79].

## ***Knock-Down of CLCA2 in CLCA2-Positive Tumour Cells***

To minimise off-target effects of the siRNA treatment, commercially available non-targeting control siRNA (siCONTROL#1, Dharmacon; further named “siCTRL”) and mock transfections were additionally performed in parallel for all siRNA experiments.

### **siRNA Experiments in Human Head and Neck SCC Tumour Cell Line HN5**

Based on the relatively high expression level of CLCA2 (see section “Expression Profiling”), the cell line HN5 was chosen to study CLCA2 loss-of-function by siRNA-mediated knock-down and its implication on cell survival and proliferation.

#### **Evaluation of CLCA2 siRNAs**

First, siGENOME SMART pool (Dharmacon) containing a mixture of four designed siRNAs targeting CLCA2 mRNA, was tested in HN5 cell line for efficient downregulation of the specific mRNA by performing RT-qPCR analysis.

Downregulation of protein levels could not be tested in HN5, because untagged CLCA2 protein could not be detected on Western blots due to lack of an appropriate antibody.

After SMART pool treatment, a reduction of CLCA2 mRNA transcript below 10 % could be determined in HN5 cells (Figure 21).

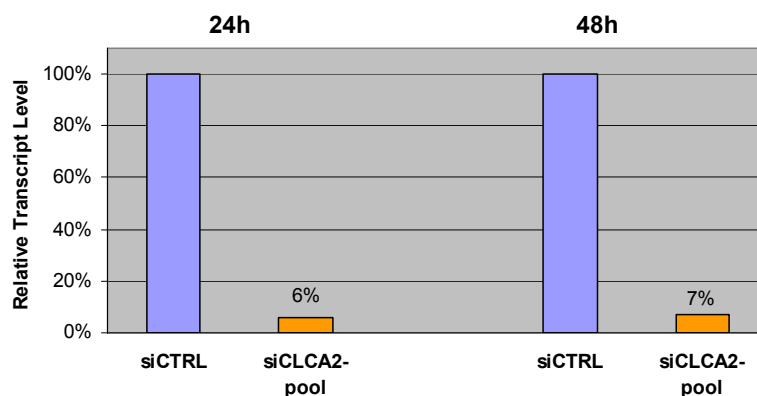


**Figure 21. siRNA-mediated knock-down of CLCA2 in human head and neck SCC tumour cell line HN5: Testing siGENOME SMART pool (RT-qPCR)**

150,000 cells per well of a 6-well-plate were transfected with CLCA2-siGENOME SMART pool of Dharmacon (siCLCA2-pool), at a concentration of 20 nM siRNA, using Dharmafect 4 transfection reagent. RNA was harvested 24 h and 48 h post transfection. Transcribed cDNA was tested in RT-qPCR using a pool of CLCA2-specific oligonucleotides for the individual siRNAs siCLCA2-2, siCLCA2-4, siCLCA2-5 and siCLCA2-5 – all of Dharmacon; for sequence see section “Material and Methods”. CLCA2 mRNA levels were normalised against the endogenous control gene  $\beta$ -2-microglobulin. As control, CLCA2 expression was compared to HN5 cells transfected under same conditions with non-targeting control siRNA CONTROL#1 of Dharmacon (siCTRL).



In a next step, the four individual siRNAs were tested separately under identical conditions and both were shown to exhibit comparable and efficient downregulation of the specific mRNA in RT-qPCR (Figure 22). It was decided, to use only the two most efficient siRNA oligonucleotides, siCLCA2-2 and siCLCA2-4 for further experiments as they lead to a reduction of about 6 % or 10 % at 24 h, and 3 % or 1 % at 48 h, respectively (Figure 22).

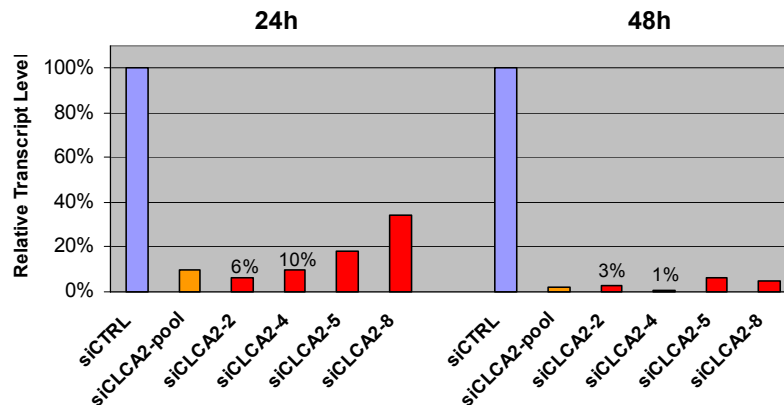


**Figure 22. siRNA-mediated knock-down of CLCA2 in human head and neck SCC tumour cell line HN5: Testing individual siRNAs of siGENOME SMART pool (RT-qPCR)**

150,000 HN5 cells per well of a 6-well-plate were transfected with CLCA2-siGENOME SMART pool (Dharmacon) (siCLCA2-pool) and in parallel with the individual siRNAs of CLCA2-siGENOME SMART pool (siCLCA2-2, siCLCA2-4, siCLCA2-5, siCLCA2-8) at a concentration of 20 nM siRNA using Dharmafect 4 transfection reagent. RNA was harvested 24 h and 48 h post transfection. cDNA was tested in RT-qPCR using a CLCA2-specific primer pair. CLCA2 mRNA levels were normalised against the endogenous control gene  $\beta$ -2-microglobulin. As control, CLCA2 expression was compared to HN5 cells transfected under identical conditions with non-targeting control siRNA CONTROL#1 of Dharmacon (siCTRL).

For optimisation of siRNA concentration, different concentrations of the two most efficient siRNA oligonucleotides were transfected into HN5 cells. In this experiment lysates were analysed after 48 h, because it was shown before, that in general the knock-down effect was more efficient 48 h post transfection (Figure 22).



Furthermore, the two most efficient siRNA oligonucleotides were pooled and analysed for a possible additive effect. As shown in Figure 23, the knock-down efficiency seems to be relatively independent of the siRNA concentration and ranges for all concentrations between 0 and 23 %.

Pooling of the two most efficient siRNA oligonucleotides siCLCA2-2 and siCLCA2-4 seems to slightly improve the knock-down effect (reduction of CLCA2 mRNA transcript to 4-10 %).

In general, efficient knock-down could be achieved under all conditions and higher concentrations did not lead to better results. Therefore, it was decided to perform further experiments at the originally applied concentration of 20 nM siRNA.

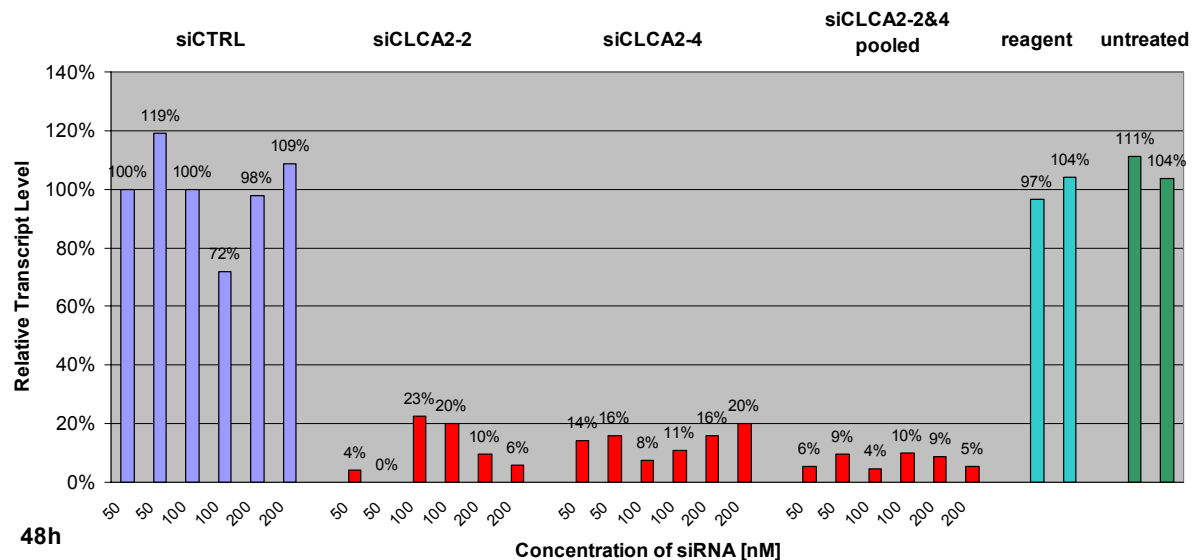


**Figure 23. siRNA-mediated knock-down of CLCA2 in human head and neck SCC tumour cell line HN5: Testing different concentrations of siRNA (RT-qPCR)**

5,000 HN5 cells per well of a 96-well-plate were transfected with different concentrations of the individual siRNAs siCLCA2-2 and siCLCA2-4 and cells were also transfected with a pool of both (siCLCA2-2&4 pooled) using Dharmafect 4 transfection reagent. RNA was harvested 48 h post transfection. cDNA was tested in RT-qPCR using a CLCA2-specific primer pair. CLCA2 mRNA levels were normalised against the endogenous control gene  $\beta$ -2-microglobulin. As control, CLCA2 expression was compared to HN5 cells transfected under identical conditions with non-targeting control siRNA CONTROL#1 of Dharmacon (siCTRL) to untreated HN5 cells (untreated), and to HN5 cells which were treated with transfection reagent alone (reagent).

To analyse if the cell number has an effect on the knock-down efficiency, different cell numbers of HN5 were transfected (6-well-plate) with the two most efficient siRNA oligonucleotides. No significant dependence of the knock-down efficiency on the cell number could be demonstrated (Figure 24). Transfecting either 50,000 or 100,000 cells with siCLCA2-2, lead in both cases to a knock-down of CLCA2 mRNA transcript to 15 %. Using siRNA siCLCA2-4, a knock-down of the CLCA2 transcript to 31 % (50,000 cells) and to 18 % (100,000 cells), respectively, was achieved (Figure 24). Based on these data and previous results the cell number seems not to be the determining factor for knock-down efficacy.

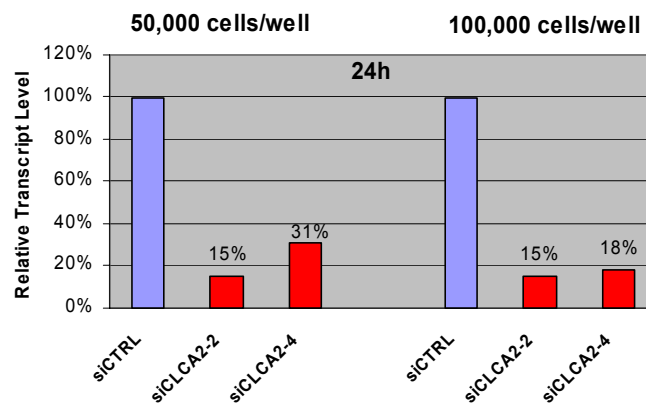


**Figure 24. siRNA-mediated knock-down of CLCA2 in human head and neck SCC tumour cell line HN5: Testing different cell numbers (RT-qPCR)**

50,000 and 100,000 HN5 cells per well of a 6-well-plate were transfected with the individual siRNAs siCLCA2-2 and siCLCA2-4 at a concentration of 20 nM siRNA using Dharmafect 4 transfection reagent. RNA was harvested 24 h post transfection. cDNA was tested in RT-qPCR using a CLCA2-specific primer pair. CLCA2 mRNA levels were normalised against the endogenous control gene  $\beta$ -2-microglobulin. As control, CLCA2 expression was compared to HN5 cells transfected under identical conditions with non-targeting control siRNA CONTROL#1 of Dharmacon (siCTRL).

### Proliferation Assay

To analyse whether knock-down of CLCA2 has any effect on proliferation of HN5 cells, the proliferation of CLCA2 siRNA-treated HN5 cells was analysed in an Alamar Blue Assay. Thereby GPR87 siRNA was used as a positive control. It has been shown previously that downregulation of GPR87 in HN5 cells lead to inhibition of proliferation, to reduction in viability and subsequently to induction of apoptosis [79]. As shown in Figure 25 the  $IC_{50}$  values of siCLCA2-2 and of siCLCA2-4 are in the same range of the  $IC_{50}$  value for siGPR87, indicating that both, CLCA2 and GPR87 play an essential role for proliferation in HN5 cells.

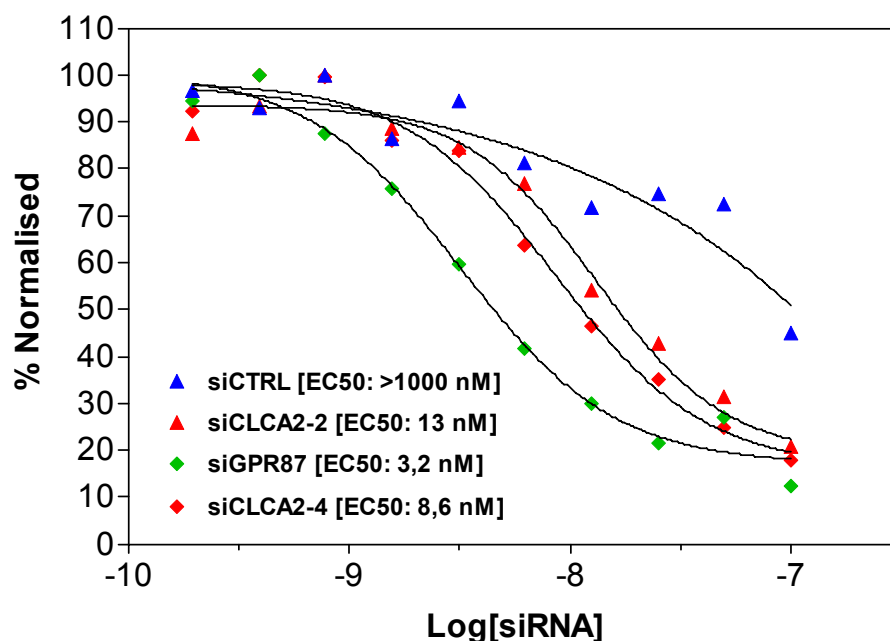


**Figure 25. siRNA-mediated knock-down of CLCA2 in human head and neck SCC tumour cell line HN5: Effect on proliferation (Alamar Blue Assay)**

5,000 HN5 cells per well of a 96-well-plate were transfected with the individual siRNAs siCLCA2-2 and siCLCA2-4 and as negative control with non-targeting siRNA CONTROL#1 of Dharmacon (siCTRL) and as positive control with GPR87-targeting siRNA siGPR87 at concentrations of 390 pM up to 100 nM siRNA using Dharmafect 4 transfection reagent. For normalisation untreated cells (non-altered proliferation level) and a boiled cell extract (background) was used. Alamar Blue Assay was performed 72 h post transfection.

## Apoptosis

Cleavage of PARP (Poly ADP-ribose polymerase), a protein involved in a number of cellular processes which are mainly linked to DNA repair and programmed cell death, is an appropriate indicator of apoptosis as PARP-cleavage is observed upon induction of apoptosis. Protein lysates of siRNA-treated HN5 cells were analysed for PARP-cleavage with an anti-PARP-antibody detecting both, full-length and cleaved PARP on Western blot.

48 h after transfection with siCLCA2-4 a pronounced induction of apoptosis (Figure 26) could be detected in HN5 cells, whereas PARP-cleavage in siCLCA2-2-transfected cells was only comparable to the siCTRL-transfected cells. These data again support the previous findings (Figure 25) that siCLCA2-4 is more efficient in knocking-down than siCLCA2-2.

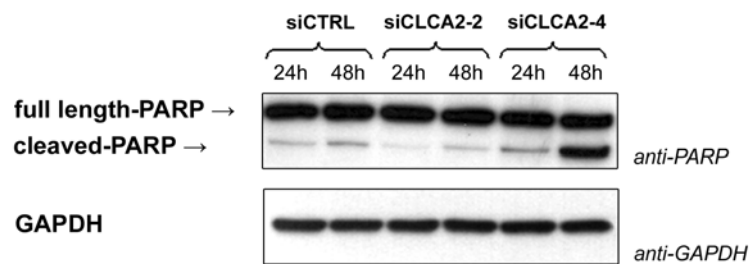


**Figure 26. siRNA-mediated knock-down of CLCA2 in human head and neck SCC tumour cell line HN5: Effect on induction of apoptosis (PARP-cleavage)**

150,000 HN5 cells per well of a 6-well-plate were transfected with the individual siRNAs siCLCA2-2 and siCLCA2-4 and as control with non-targeting control siRNA CONTROL#1 of Dharmacon (siCTRL) at a concentration of 20 nM siRNA using Dharmafect 4 transfection reagent. Protein lysates were harvested 24 h and 48 h post transfection. For Western blot 50 µg protein was loaded per lane; an anti-PARP antibody was used for detection of cleaved and uncleaved PARP. GAPDH served as loading control.

To not only rely on PARP-cleavage as a read out for induction of apoptosis, a detailed analysis of further effects on changes in apoptotic parameters of siRNA-transfected HN5 cells was performed by investigating the change of nuclear area, nuclear fragmentation, membrane-permeability, mitochondrial status, and nuclear fragmentation. All these processes are linked with induction of apoptosis. For details on the high content screening technology see section “Material and Methods”.

In siCLC2-4-transfected HN5 cells dramatical changes in membrane permeability (Figure 27, yellow bar), in the mitochondrial status (Figure 27, black bar) and the nuclear fragmentation (Figure 27, green bar) could be observed, supporting data obtained from PARP-cleavage experiments shown before. As already demonstrated for siCLC2-2-transfected HN5 cells (Figure 25, Figure 26), no significant changes could be detected (Figure 27).

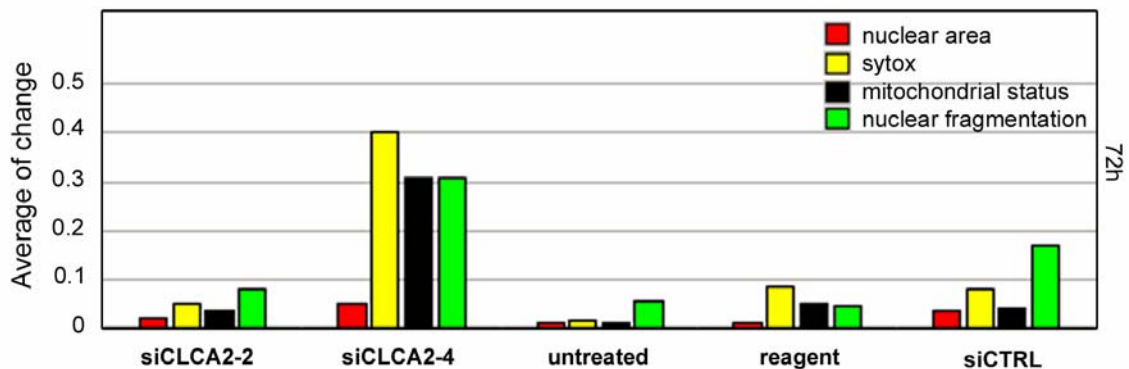


**Figure 27. siRNA-mediated knock-down of CLCA2 in human head and neck SCC tumour cell line HN5: Effects on apoptotic parameters (HCS Reader, Cellomics)**

5,000 HN5 cells per well of a 96-well-plate were transfected with the individual siRNAs siCLCA2-2 and siCLCA2-4 and as control with non-targeting control siRNA CONTROL#1 of Dharmacon (siCTRL) at a concentration of 20 nM siRNA using Dharmafect 4 transfection reagent. Further controls were untreated cells (untreated) and cells, which were treated with transfection reagent only (reagent). 72 h post transfection, cells were analysed for changes in the apoptotic parameters by using appropriate antibodies for respective stainings which could be evaluated by the ArryScan HCS Reader (Cellomics).

## Cell Cycle

The CLCA2 knock-down in siCLCA2-2- and siCLCA2-4-treated HN5 cells, leads also to a significant shift in cell cycle 72 h after transfection in comparison to controls (Figure 28). The cell count in G1-phase (2n) was clearly reduced, and cells were arrested in G2, whereby polyploidy was increased. Most likely apoptosis is being initiated in these polyploidic cells (Figure 27). Again, for siCLC2-2-transfected HN5 cells only minor changes of the cell cycle profile could be observed which is in line with previous observations (Figure 25, Figure 26, and Figure 27).

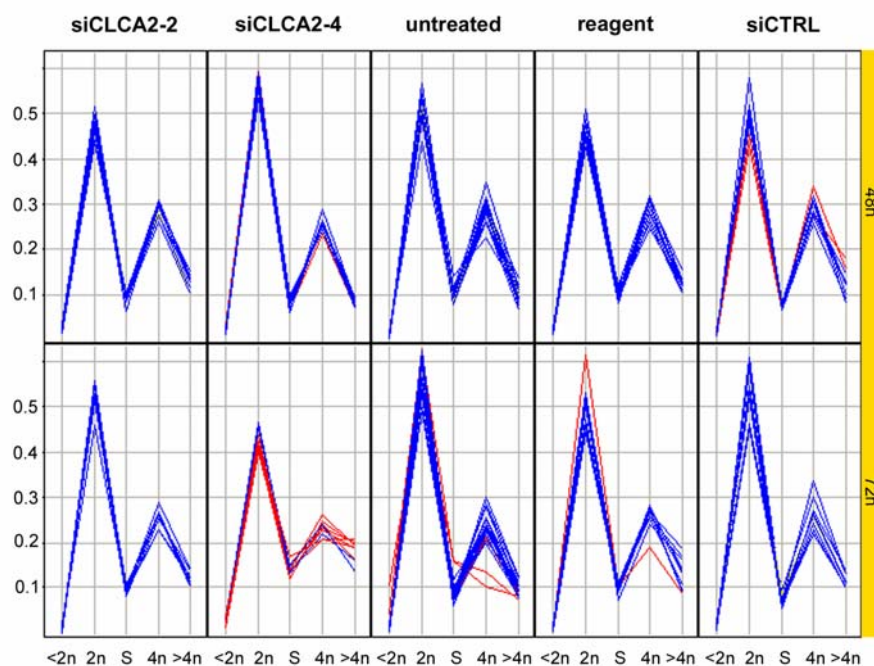


**Figure 28. siRNA-mediated knock-down of CLCA2 in human head and neck SCC tumour cell line HN5: Effects on cell cycle (HCS Reader, Cellomics)**

5,000 HN5 cells per well of a 96-well-plate were transfected with the individual siRNAs siCLCA2-2 and siCLCA2-4 and as control with non-targeting control siRNA CONTROL#1 of Dharmacon (siCTRL) at a concentration of 20 nM siRNA using Dharmafect 4 transfection reagent. Further controls were untreated cells (untreated) and cells, which were treated with transfection reagent only (reagent). 48 h and 72 h post transfection, cells were stained with DAPI and analysed on the ArryScan HCS Reader (Cellomics).

Red lines indicate statistically relevant changes.

X-axis: The abbreviations <2n, 2n, s, 4n, and >4n represent percentage of cells in sub G1- or G0-phase (<2n), in G1-phase (2n), in S-phase (S), in G2-phase (4n), and polyploidic cells (>4n), respectively.

### siRNA Experiments in Human Breast Carcinoma Cell Line MDA-MB-453

According to the BioExpress database (GeneLogic Inc.), the human breast carcinoma cell line MDA-MB-453 exhibits very high CLCA2 expression levels (Figure 15) and was therefore selected for siRNA experiments as well.

As shown in Figure 29, siRNA transfection utilising siCLCA2-2 and siCLCA2-4 revealed that the high levels of naturally expressed CLCA2 in MDA-MB-453 cells could also be knocked-down with these siRNAs to 15 % (siCLCA2-2) and 31 % (siCLCA2-4), respectively, in comparison to non-targeting control siRNA (siCTRL). In contrast to HN5 cells, the efficiency of knock-down is more pronounced with siCLCA2-2 than with siCLCA2-4 (Figure 29, Figure 30). One explanation for this phenomena might be the different transfection reagent (for HN5: Dharmafect 4; for MDA-MB-453: Dharmafect 2) used in this approach (Table 7).

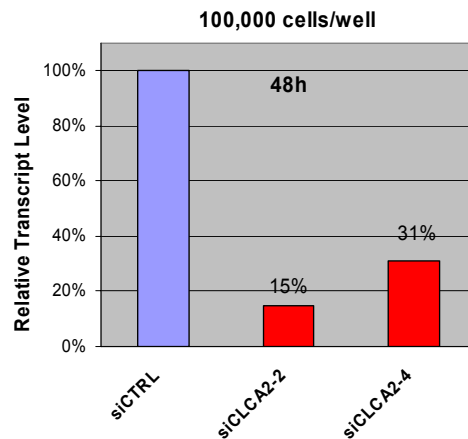


**Figure 29. siRNA-mediated knock-down of CLCA2 in breast carcinoma cell line MDA-MB-453: Testing siCLCA2-2 and siCLCA2-4 of siGENOME SMART pool, Dharmacon (RT-qPCR)**

100,000 MDA-MB-453 cells per well of a 6-well-plate were transfected with the individual siRNAs siCLCA2-2 and siCLCA2-4, respectively, at a concentration of 20 nM siRNA using Dharmafect 2 transfection reagent. RNA was harvested 48 h post transfection. cDNA was tested in RT-qPCR using a CLCA2-specific primer pair. CLCA2 mRNA levels were normalised against the endogenous control gene  $\beta$ -2-microglobulin. As control, CLCA2 expression is compared to HN5 cells transfected under identical conditions with non-targeting control siRNA CONTROL#1 of Dharmacon (siCTRL).

Next, the siRNA concentration for an efficient downregulation in MDA-MB-453 cells was optimised (Figure 30). Transfection with 50 up to 200 nM siCLCA2-2 results in knock-down of CLCA2 mRNA transcript ranging between 3-12 % compared to cells transfected with non-targeting siRNA (siCTRL). For siCLCA2-4 the results are similar, ranging between 6-12 % but nevertheless siCLCA2-4 seems to be inferior to siCLCA2-2. Co-transfections with both siRNAs are resulting in knock-down of 6-8 %. As the efficiency of downregulation was also demonstrated at lower concentrations of siRNA oligonucleotide and the off-target effects of control siRNA are also less at lower concentrations, it was decided to use a concentration of 20 nM siRNA throughout all further experiments.

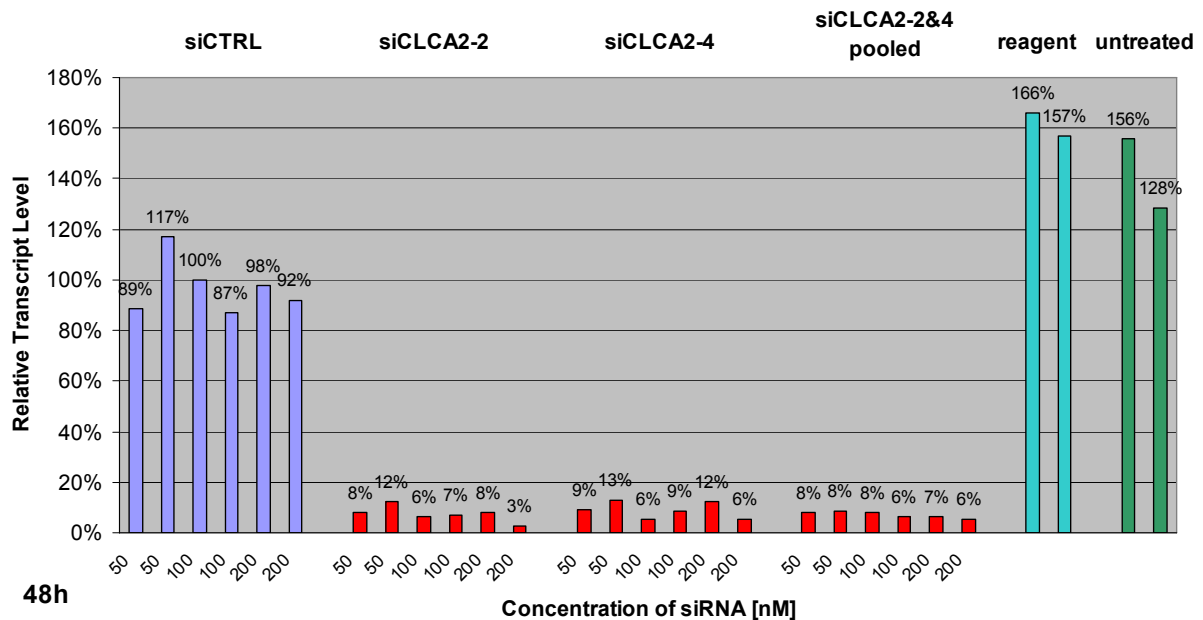


**Figure 30. siRNA-mediated knock-down of CLCA2 in human breast carcinoma cell line MDA-MB-453: Testing different concentrations of siRNA (RT-qPCR)**

5,000 MDA-MB-453 cells per well of a 96-well-plate were transfected with different concentrations of the individual siRNAs siCLCA2-2 and siCLCA2-4 and cells were transfected with a pool of both as well (siCLCA2-2 and siCLCA2-4 pooled) using Dharmafect 2 transfection reagent. RNA was harvested 48 h post transfection. Transcribed cDNA was tested in RT-qPCR using a CLCA2-specific primer pair. CLCA2 mRNA levels were normalised against the endogenous control gene  $\beta$ -2-microglobulin. As control, CLCA2 expression is compared to MDA-MB-453 cells transfected under same conditions with non-targeting control siRNA CONTROL#1 of Dharmacon (siCTRL), to untreated MDA-MB-453 cells (untreated), and to MDA-MB-453 cells which were treated with transfection reagent only (reagent).



Next, the question whether the cell number per well has an impact on the knock-down efficiency of the CLCA2 mRNA transcript was addressed. As shown in Figure 31, the optimal cell number per well of a 6-well-plate for an efficient knock-down to 10 % is about 50,000. However, increasing the number of cells per well (75,000 to 200,000) leads only to a knock-down efficiency ranging between 26 and 31 %.

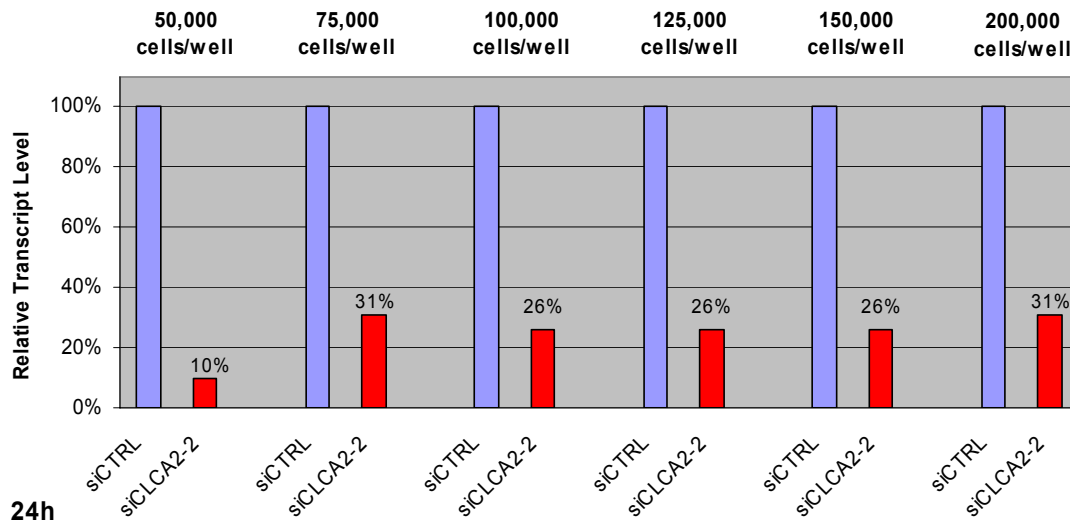


**Figure 31. siRNA-mediated knock-down of CLCA2 in human breast carcinoma cell line MDA-MB-453: Testing different cell numbers (RT-qPCR)**

As indicated, 50,000 up to 200,000 MDA-MB-453 cells per well of a 6-well-plate were transfected with the individual siRNA (siCLCA2-2) and the control siRNA (siCTRL) each at a concentration of 20 nM using Dharmafect 2 transfection reagent. RNA was harvested 24 h post transfection. cDNA was tested in RT-qPCR using a CLCA2-specific primer pair. CLCA2 mRNA levels were normalised against the endogenous control gene  $\beta$ -2-microglobulin. As control, CLCA2 expression is compared to MDA-MB-453 cells transfected under same conditions with non-targeting control siRNA CONTROL#1 of Dharmacon (siCTRL).

In contrast to HN5 cells, MDA-MB-453 cells were insensitive towards knock-down of CLCA2 when tested in a proliferation assay (Alamar Blue Assay). However, it has to be mentioned that MDA-MB-453 cells only very weakly react with the Alamar Blue reagent and therefore normalisation to untreated MDA-MB-453 cells generated only a small “read out window” (Figure 32).

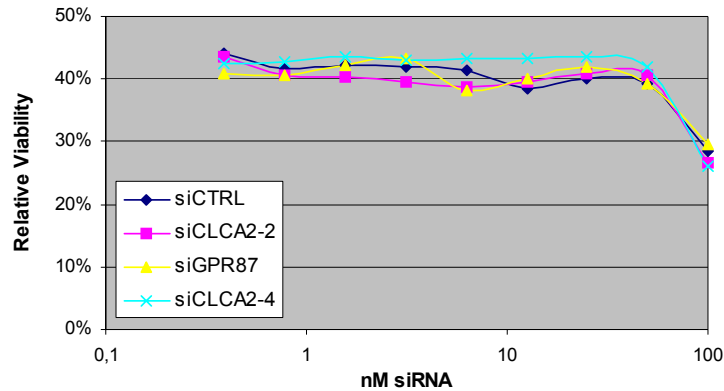


**Figure 32. siRNA-mediated knock-down of CLCA2 in human breast cancer cell line MDA-MB-453: Effect on proliferation/viability (Alamar Blue Assay)**

5,000 MDA-MB-453 cells per well of a 96-well-plate were transfected with the individual siRNAs siCLCA2-2 and siCLCA2-4 and as negative control with non-targeting siRNA CONTROL#1 of Dharmacon (siCTRL) and as positive control with GPR87-targeting siRNA siGPR87 at concentrations of 390 pM up to 100 nM siRNA using Dharmafect 2 transfection reagent. For normalisation untreated cells (non-altered proliferation level) and a boiled cell extract (background) was used. Alamar Blue Assay was performed 72 h post transfection.

### siRNA Experiments in a Stable CLCA2-Constitutively-Expressing T47D Clone

Due to the lack of a specific antiserum against CLCA2 it was not possible to show siRNA-mediated knock-down on protein level for HN5 or MDA-MB-453 cells.

To proof the efficiency of used CLCA2 siRNAs for knock-down of CLCA2 on the protein level, stable CLCA2-expressing T47D clones were established, with CLCA2 being C-terminally HA-tagged. One of these recombinant cell lines constitutively expressing HA-tagged CLCA2 was used for siRNA transfections: “CLCA2-constitutively-expressing T47D clone #47”. For generation of this clone see section “Establishment of Stable wt-CLCA2 Clones”.

For Western blot (Figure 33) an anti-HA-antibody detecting both, the full-length CLCA2 and the cleaved C-terminal fragment was used, resulting in two bands on Western blot. In cells transfected with siCLCA2-2 or siCLCA2-4 no or only traces of CLCA2 protein could be detected, whereas in the control cells (untreated cells and cells transfected with non-targeting siRNA) the HA-tagged CLCA2 protein could be visualised as strong bands (Figure 33).

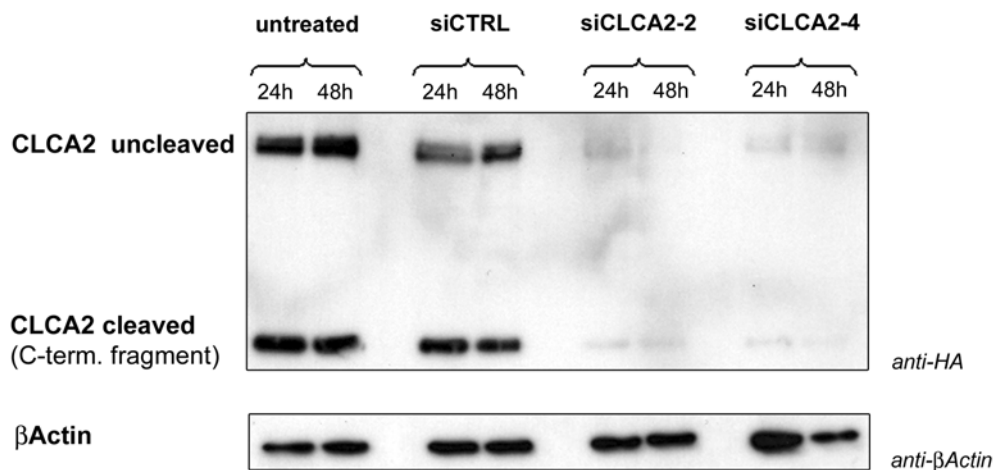


**Figure 33. siRNA-mediated knock-down of CLCA2 in CLCA2-constitutively-expressing T47D clone on protein level (Western blot)**

150,000 cells of the CLCA2-constitutively-expressing T47D clone #47 per well of a 6-well-plate were transfected with the individual siRNAs siCLCA2-2 and siCLCA2-4 at a concentration of 20 nM siRNA using Dharmafect 4 transfection reagent. As control served untreated cells, and cells transfected with non-targeting siRNA CONTROL#1 of Dharmacon (siCTRL) under same conditions. Protein lysates were harvested 24 h and 48 h post transfection. For Western blot 50 µg protein was loaded per lane; an anti-HA-tag antibody was used for detection of HA-tagged CLCA2. β-Actin served as loading control.

The same protein lysates were further tested for siRNA-mediated PARP-cleavage. In contrast to HN5 cells, no PARP-cleavage could be detected in a CLCA2-constitutively-expressing T47D clone that was treated with CLCA2 siRNA (Figure 34).

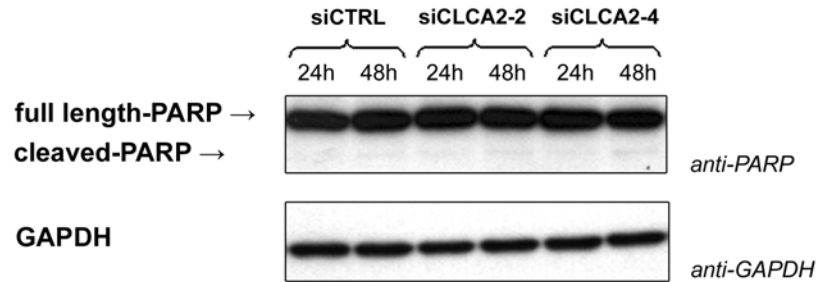


**Figure 34. siRNA-mediated knock-down of CLCA2 in CLCA2-constitutively-expressing T47D clone: Effect on apoptosis (PARP-cleavage)**

150,000 cells of the CLCA2-constitutively-expressing T47D clone #47 per well of a 6-well-plate were transfected with the individual siRNAs siCLCA2-2 and siCLCA2-4 at a concentration of 20 nM siRNA using Dharmafect 4 transfection reagent. As control non-targeting siRNA CONTROL#1 of Dharmacon (siCTRL) was transfected under same conditions. Protein lysates were harvested 24 h and 48 h post transfection. For Western blot 50  $\mu$ g protein was loaded per lane; an anti-PARP antibody was used for detection of cleaved and uncleaved PARP. GAPDH served as loading control.

## ***Antibody Generation***

Due to the lack of a commercially available CLCA2-specific antibody, it was repeatedly tried to generate specific antisera against human CLCA2. Rabbits were immunised with peptides derived from identified CLCA2-specific epitopes which discriminate between other members of the CLCA family (for details see chapter “Material and Methods”).

However, fractions of affinity-purified sera tested on Western blot (data not shown), did not lead to generation of a specific signal. Also peptides linked to proteins such as KHL could not improve the specific immune response. Therefore, it was necessary to generate an HA-tagged CLCA2 expression vector, which – after transfection into the cell line of interest – allowed the detection of CLCA2 on Western blots. However, a polyclonal antiserum was generated which could be used successfully in immunohistochemistry (IHC) studies.

### **Selection of Peptides for Generation of Antisera**

First, specific epitopes which can be used for synthesising small 10 to 20 AA long peptides and for immunisation of rabbits, had to be identified. Appropriate peptides have to exhibit a series of chemical, physical and immunological properties in order to serve as effective immunogens. Algorithms are available which allow the prediction of these characteristics for linear epitopes.

In order to correlate the respective amino acid sequence to secondary structure motifs in CLCA2 (alpha, beta regions as well as turns and coils), mainly the prediction algorithms from Chou and Fasman or from Garnier and colleagues (Figure 35) [80-82] were used. In addition both, hydrophobicity and hydrophilicity play an important role for solubility of the respective epitope peptide, features which essentially contribute to the successful generation of peptide antisera [83-85].

Another important tool for selection of peptide antigens is the determination of the accessibility of selected protein regions. Those flexible regions are more likely exposed to the surface of a protein than highly structured regions [86]. The antigenic index prediction of linear/sequential peptide motifs is based on the knowledge of known and experimentally verified peptide epitopes [87]. This approach not only describes the antigenic behaviour of a peptide (protein region) alone, but also takes into account the structural characteristics such as the “protrusion index” [88-92].

BLAST search was performed in order to learn more about the species specificity (“epitope overlap”) of CLCA2; for example, percentage of identity within the CLCA2 peptide epitope among other proteins of the same species (human) is a measure for the background signal to be expected on Western blots. If the epitope is conserved among other species, especially in those animals where the antisera have to be generated (e.g. rabbits), immune tolerance can lead to a weak or almost no immune reaction towards the epitope peptide in the animal. Furthermore, the generation of intra/intra-peptidale secondary structures (e.g. formation of disulfide bridges) was avoided by selecting peptide epitopes without Cys residues. Those secondary structures can efficiently reduce the spatial flexibility of a peptide allowing only a limited number of different configurations in solution and thereby reducing the number of different antibody species in a polyclonal antiserum. Finally, the PROSITE database was used to search for functional epitopes such as Ca-binding motifs, potential glycosylation sites, active sites, etc. within the selected peptide epitopes of CLCA2. For instance, targeting potential glycosylation sites, would lead to less efficient antibodies, as the bulky sugar residues “protect” the immune epitope and by this interfere with the recognition of the linear peptide motif within the CLCA2 [93]. In the absence of any 3D-structure for CLCA2 it could not be speculated, whether the selected peptide epitopes are in principle spatially accessible, as the minimal spatial requirement for an antibody to recognise its epitope is ~ 35 Å. Therefore, it is often observed that high titers towards the peptide can be generated, but the polyclonal antiserum recognises only the protein on IHC slides, but not on Western blots. Based on these algorithms putative peptide epitopes were selected for immunisation, utilising the program “LaserGene 6.1 Protean” comprising almost all algorithms discussed above (Figure 35 and Table 1).

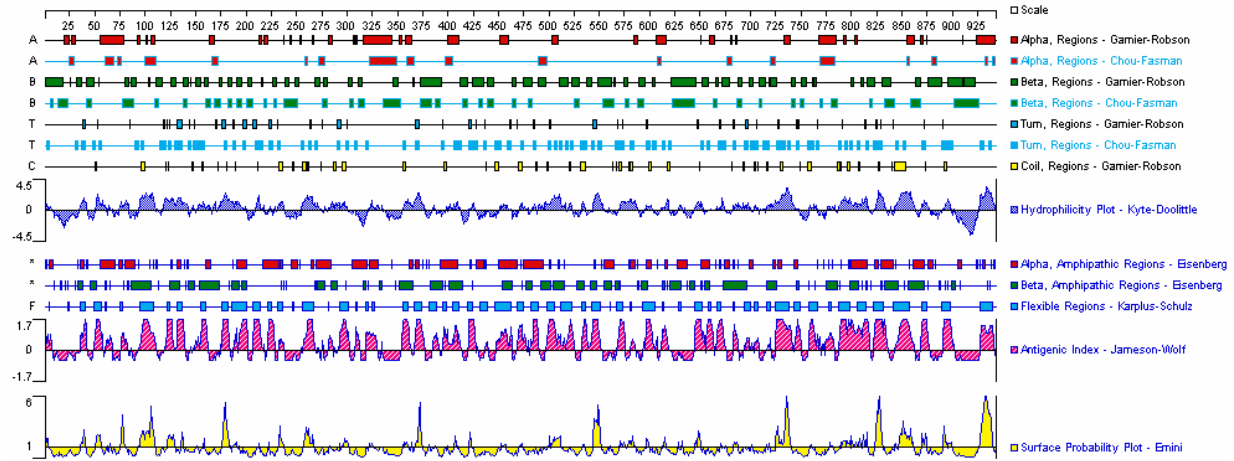


**Figure 35. Prediction of structural features of human CLCA2 protein**

The indicated programs were used to predict the most promising immunogenic peptide epitopes of CLCA2 for immunising rabbits. The selected peptide epitopes are listed in Table 1.

Amino Acid Pos. in CLCA2 Protein Sequence	Peptide Sequence
K94 – N110	KANNNSKIKQESYEKAN
N179 – D199	NDKPFYINGQNQIKVTRCSSD
E498 – T513	ESTGENVKPHHQLKNT
H690 – H708	HVNHSPSISTPAHSIPGSH
T643 – L656	TVEPETGDPVTLRL

**Table 1. Putative immune epitopes selected for synthesis of peptides used to generate antisera**

## Anti-CLCA2 Polyclonal Peptide Antisera and Their Use for Western Blots

Three rabbits were immunised, two of them with two peptides in parallel – rabbit #1 (K94-N110 + N179-D199), rabbit #2 (E498-T513 + H690-H708) and rabbit #3 (T643-L656). Fractions of affinity-purified sera were tested on Western blot (data not shown), but none of these antibodies generated a specific signal. Also peptides linked to proteins such as KHL could not improve the specific immune response. Therefore, it was necessary to generate an HA-tagged CLCA2 expression vector, which – after transfection into the cell line of interest – allowed a detection of CLCA2 on Western blots.

## ***Immunohistochemistry***

In contrast to CLCA2-specific antisera used for Western blotting, one of these affinity-purified antisera exhibits a high titer towards peptide K94-N110 (KANNNSKIKQESYEKAN) and showed a specific staining of tumour cells in human SCC lung tumour samples, utilising a pre-immune serum as a negative control (Figure 36). The different techniques used for antigen retrieval (citrate buffer or proteinase K treatment) lead to slightly different staining pattern; acidic retrieval generate a more spot-like pattern whereas Proteinase K treatment a more diffuse pattern. However, both retrieval methods lead to a specific and pronounced tumour cell staining.

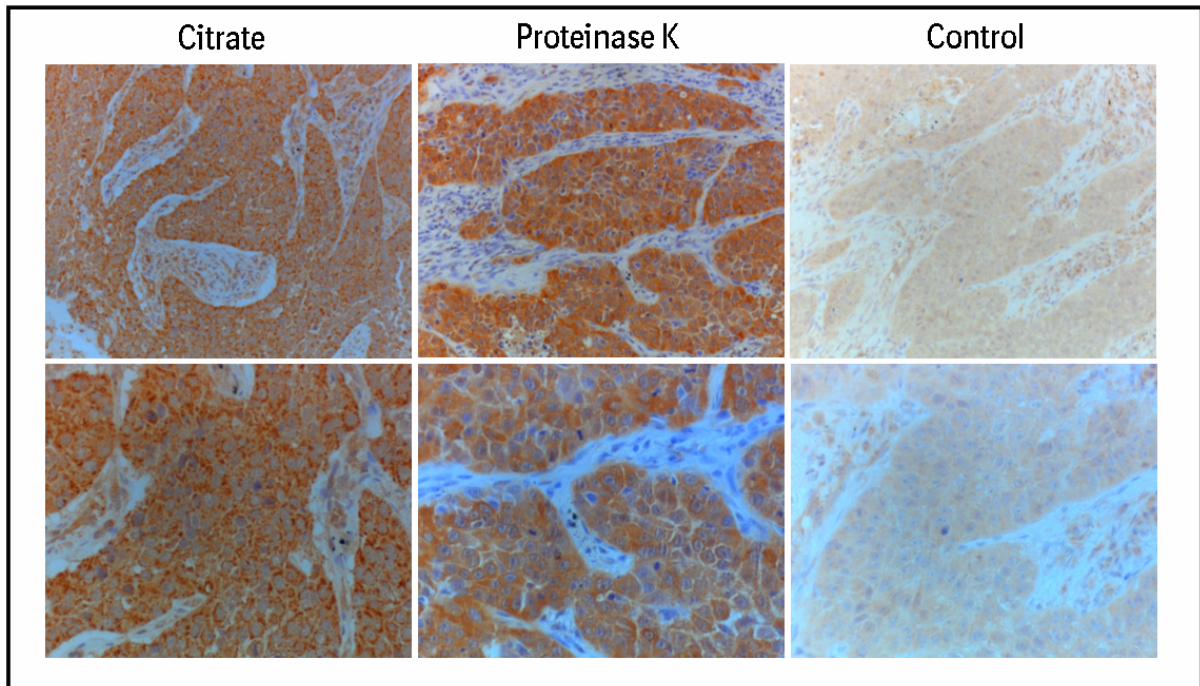


**Figure 36. Immunohistochemistry analysis of two human SCC lung cancer samples (NSCLC)**

For antigen retrieval samples were either treated with citrate buffer (Citrate: 10 mM, pH: 6.0) or by incubation with Proteinase K (for details see "Material and Methods"). As control a pre-immune serum was used for staining generating a weak and unspecific background signal (Control).





The “pGEM T-Easy-CLCA2” vector was digested with BamHI (for cutting out CLCA2) and with ScaI for discriminating with another resulting fragment of nearly the same size. The resulting 1838bp fragment was discarded; the 4037bp fragment was isolated and cut with NotI. The resulting 2841bp fragment was inserted into each of the pCMV-tag vectors (as described above), which had been digested with NotI and BamHI before. As a result, a panel of pCMV expression vectors carrying various tagged CLCA2 genes, were obtained. Figure 38 exemplarily shows the pCMV-CLCA2 vector wherein CLCA2 is tagged with 8F5.

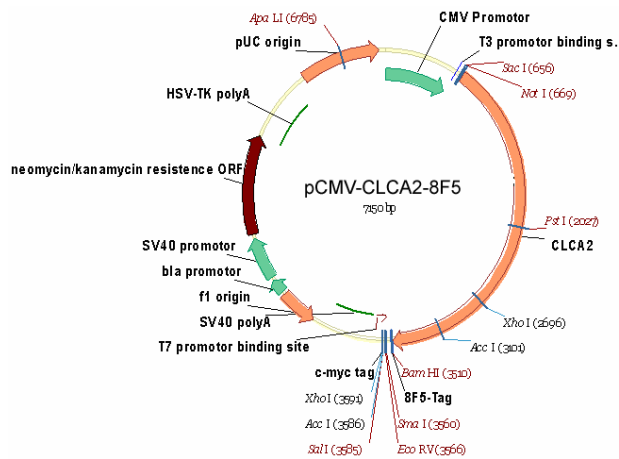


**Figure 38. Map of expression vector pCMV-8F5 with inserted CLCA2 cDNA**  
CLCA2 was inserted between the NotI- and BamHI-site.

### Cloning CLCA2-Tag to Expression Vector pTRE2pur

To benefit from an inducible expression system, the differently tagged CLCA2 genes were finally cloned from the pCMV vectors to the pTRE2pur vector of the “Tet-on Gene Expression System” (Clontech) by restriction digestion with NotI and EcoRV, which both are single cutters in the used vectors. Exemplarily, a schematic map of pTRE2pur-CLCA2-HA is shown in Figure 39.

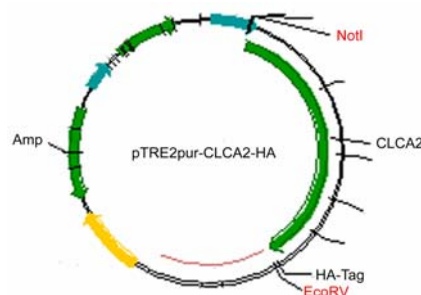


**Figure 39. Schematic map of expression vector pTRE2pur with the inserted CLCA2-HA cDNA**  
The CLCA2-HA-fragment is inserted between the NotI- and EcoRV-site.

### Evaluation of Tags on Western Blot

All resulting pTRE2pur-CLCA2-tag expression vectors were individually transfected to T47D Tet-on cells, and lysates of induced and non-induced cells were analysed on Western blot with antibodies detecting the respective tags. As shown in Figure 40, best results were obtained with HA-tag and V5-tag. The cleaved and uncleaved CLCA2-fragment could be detected in the induced sample; the signal in the non-induced sample is extremely low, which demonstrates the strict control of the Tet-on system in T47D Tet-on cells. The strongest signal was found for HA-tagged CLCA2 protein. The antibodies for detection of 8F5 (monoclonal antibody recognising an epitope of VP2 in HRV2 [94]) and myc-tag did not give rise to a valid signal on Western blots and the antibody detecting the His-tag lead to detection of additional bands. Based on these data the construct with the HA-tag was chosen for further investigation.

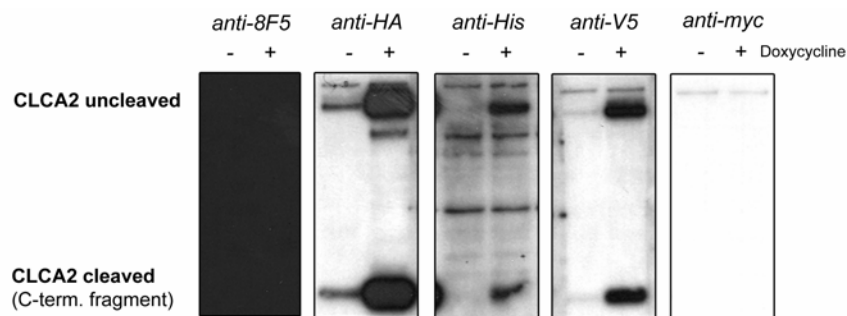


**Figure 40. CLCA2 expression with various tags on Western blot**

150,000 T47D Tet-on cells were seeded into 6-well-plates and each of pTRE2pur expression vectors containing CLCA2 fused to an 8F5-, HA-, His-, V5-, or myc-tag respectively, was transiently transfected. Expression of tagged CLCA2 was non-induced (-) and induced (+) with Doxycycline 24 h after transfection. Protein lysates were harvested 48 h post induction. For Western blot 50 µg protein was loaded per lane; an antibody detecting the respective tag was used.

## ***Establishment of Stable wt-CLCA2 Clones***

As the pTRE2pur-CLCA2-HA construct was chosen for further investigation, this construct was used for establishment of stable wt-CLCA2-expressing clones in the cell line T47D Tet-on, with CLCA2 being C-terminally HA-tagged. The cell line T47D Tet-on was chosen, to benefit from the inducible expression system.

Therefore, 100 clones were picked after selection with Puromycin for 3 weeks and than analysed. All clones were induced and both, induced and non-induced protein lysates were analysed on Western blots with an anti-HA-antibody for detection of HA-tagged CLCA2. The inducible clones were kept in culture and after testing all 100 clones, the most efficiently expressing candidates were compared against each other. In Figure 41 one individual Western blot with five selected inducible clones (#3, 4, 26, 44, 46) is shown, whereby only in induced lysates CLCA2 expression could be detected and non-induced cells did not express detectable amounts of CLCA2.

During the selection process, one clone was identified as a constitutively CLCA2-expressing clone, which wasn't needed to be induced first: "CLCA2-constitutively-expressing T47D clone #47". This clone deemed to be useful to be kept for further experiments and was e.g. used for siRNA experiments (see section "siRNA Experiments in a Stable CLCA2-Constitutively-Expressing T47D Clone").

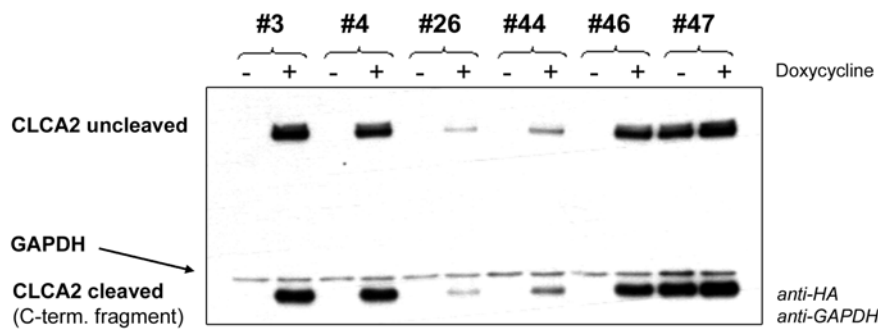


**Figure 41. Stable CLCA2-expressing T47D Tet-on clones: Inducible/constitutive expression of HA-tagged CLCA2**

Clones #3, #4, #26, #44, #46 expresses CLCA2 inducibly; clone #47 expresses CLCA2 constitutively. Clones were selected for 3 weeks with Puromycin. 300,000 cells were seeded into 6-well-plates and induced with Doxycycline. Protein lysates were harvested 48 h post induction. For Western blot 50 µg protein was loaded per lane; an anti-HA-tag antibody was used for detection of HA-tagged CLCA2. GAPDH served as loading control.

For experiments with an inducible clone, clone #3 ("CLCA2-expressing T47D Tet-on Clone #3") was chosen for further investigations.

To evaluate the concentration of Doxycycline which is necessary for induction of expression of CLCA2, clone #3 was induced with various concentrations and CLCA2 expression was analysed on Western blot. As shown in Figure 42 the expression of CLCA2 could not be dramatically enhanced, using more than 2 µg/ml Doxycycline in media. So this concentration was chosen for all further experiments.

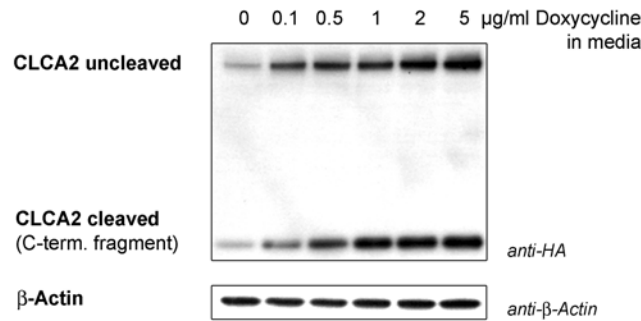


**Figure 42. Doxycycline-induced induction of CLCA2 expression in stable T47D Tet-on clone: Concentration-dependency**

300,000 cells were seeded into 6-well-plates and CLCA2 expression induced with 0, 0.1, 0.5, 1, 2, 5 µg/ml Doxycycline in media. Protein lysates were harvested 48 h post induction. For Western blot 50 µg protein was loaded per lane; an anti-HA-tag antibody was used for detection of HA-tagged CLCA2. β-Actin served as loading control.

In Figure 43 a time-kinetic of expression of CLCA2 in clone #3 is shown. In parallel, cells were induced and non-induced and protein lysates harvested after variable time-periods. CLCA2 expression was analysed on Western blots.

CLCA2 expression could be detected already 24 h post induction, after 48 h expression was not further increased.

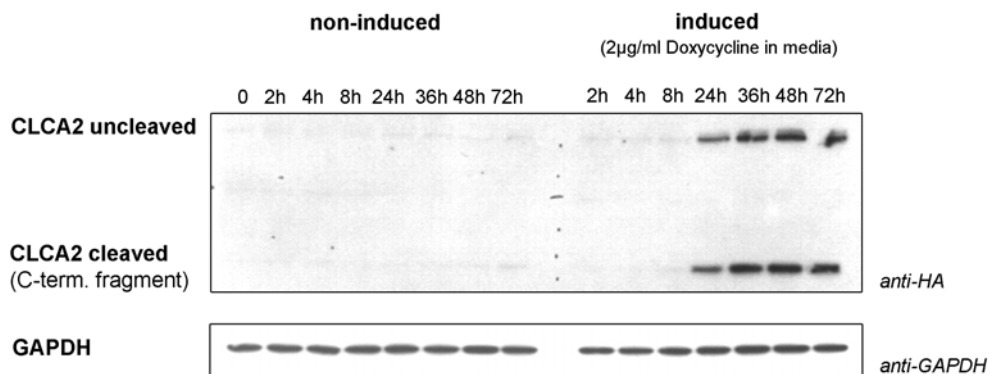


**Figure 43. Doxycycline-induced induction of CLCA2 expression in stable T47D Tet-on clone: Time-dependency**

300,000 cells were seeded into 6-well-plates and non-induced/induced with 2 µg/ml Doxycycline in media. Protein lysates were harvested 2 h, 4 h, 8 h, 24 h, 36 h, 48 h and 72 h post induction. For Western blot 50 µg protein was loaded per lane; an anti-HA-tag antibody was used for detection of HA-tagged CLCA2. GAPDH served as loading control.

These results clearly demonstrate the time-dependent induction of CLCA2 expression, which was only in induced lysates of clone #3 detectable, but no in protein lysates of non-induced cells.

## Proteolytic Processing

In May 2006 Pawlowski published that CLCA1 has a hydrolase domain responsible for processing mature full-length CLCA1 [65]. As from peptide-design for immunisation (see above) it was already known, that the homology within the CLCA family is quite high, it was assumed that CLCA2 might also contain such a hydrolase domain. Therefore, experiments with matrixmetalloprotease-inhibitors such as Phenantrolin, Diprotin B, Bestatin, Amastatin and others were performed as the internal hydrolase activity of CLCA1 was supposed to be a member of the metalloproteinase family (data not shown). Besides Phenantrolin, no effect on cleavage of CLCA2 by treatment with these inhibitors (at concentrations recommended by conventional literature) could be demonstrated. As Phenantrolin was quite toxic for the CLCA2-expressing T47D Tet-on cell line, no final conclusion could be drawn from this experiment. To learn more about the putative internal hydrolase activity of CLCA2, first an alignment of CLCA1 and CLCA2 protein sequence was made (Figure 45) with the idea that the hydrolase domain which was found by Pawlowski in CLCA1 might be conserved in the whole protein family. Indeed, a high homology within the hydrolase domain of CLCA1 and respective segment in CLCA2 (equivalent sequence in CLCA2 is located at AA 29-208) could be identified (Figure 44).

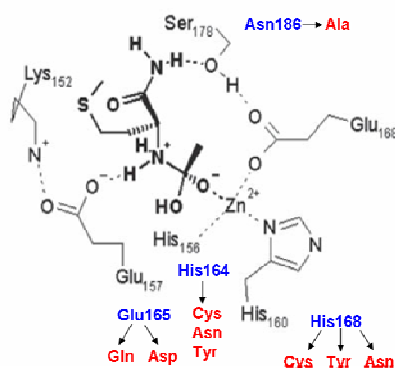


**Figure 44. Catalytic unit of hydrolase domain of CLCA1 and corresponding sites in CLCA2**

The Picture is modified from Pawlowski et al. 2006 [65]. Schematic representation showing polar interactions (dashed lines) between sTI (bold) and putative catalytic site residues.

Black letters indicate the respective AA positions of CLCA1, blue ones refer to corresponding positions in CLCA2 and red letters describe planned mutations within the catalytic center of the putative hydrolase domain of CLCA2.



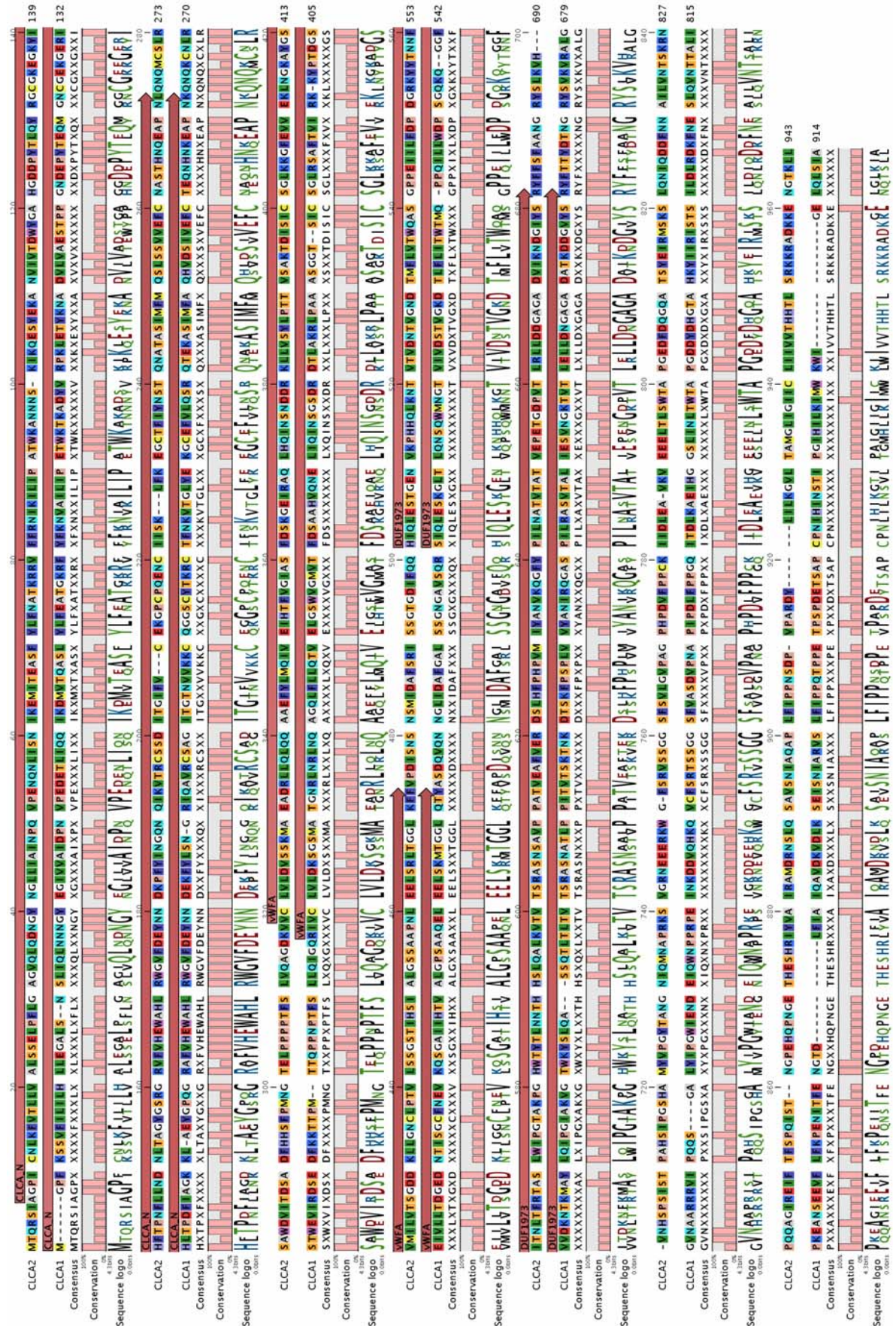


**Figure 45. Amino acid sequence alignment of CLCA1 and CLCA2**  
Protein Sequences of CLCA1 and CLCA2 were aligned utilising CLC Bio.

As Cysteines not only play an essential role in the formation of protein structure, but also can be part of the catalytic site, those Cys residues within the proposed hydrolase domain were identified, which are conserved between CLCA1 and CLCA2. These Cysteines are in CLCA2 protein sequence located at the following amino acid (AA) positions: C132, C196, C206, C211, and C216 (Figure 46). These Cys residues were also selected for mutational analysis.

### Mutating Conserved Cysteines

The conserved Cysteines within CLCA1 and CLCA2 protein structure (in CLCA2: C132, C196, C206, C211, and C216) were mutated to Alanine and in the case of C132 to Alanine and Serine. These point mutations were directly introduced into the expression vector pTRE2pur-CLCA2-HA carrying the HA-tagged wt-CLCA2, by utilisation of the “QuikChange II XL Site-Directed Mutagenesis Kit” (Stratagene). Mutation constructs were sequenced and transiently transfected into T47D Tet-on cells, where the expression of mutated CLCA2 was induced. Protein lysates were tested on Western blot using an anti-HA-antibody.

As shown in Figure 46, cleavage of CLCA2-bearing mutations C211A or C216A is heavily impaired, whereas mutations at C132, C196, and C206 completely abolish the proteolytic processing.

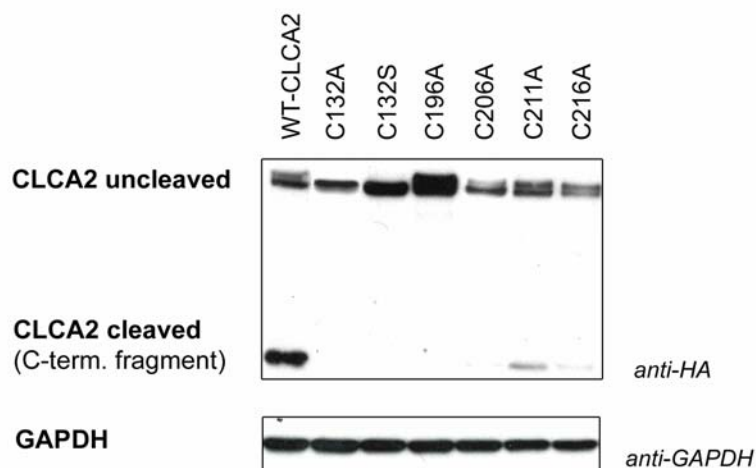


**Figure 46. Mutations of conserved Cysteines of CLCA2 and their effects on its proteolytic processing**  
150,000 T47D Tet-on cells were seeded into 6-well-plates and transiently transfected with various constructs of pTRE2pur expression vector, expressing either HA-tagged wt-CLCA2 or bearing one of the following mutations: C132A, C132S, C196A, C206A, C211A, and C216A. Expression was induced with Doxycycline 24 h post transfection. Protein lysates were harvested 48 h post induction. For Western blot 50 µg protein was loaded per lane; an anti-HA-tag antibody was used for detection of HA-tagged wt/mutant CLCA2. GAPDH served as loading control.



## Mutational Analysis of the Putative Hydrolase Domain

As the homology search with CLCA1 and CLCA2 protein sequences predicted a putative hydrolase domain for CLCA2 for AA 29-208, it was decided to point mutate respective sites in CLCA2 which might be involved in the formation of the catalytic site. Figure 47 summarises the influence of the mutations within the putative hydrolase domain on the proteolytic cleavage of CLCA2. N186A is the only mutation being tolerated, all other mutations completely abolish cleavage of CLCA2.

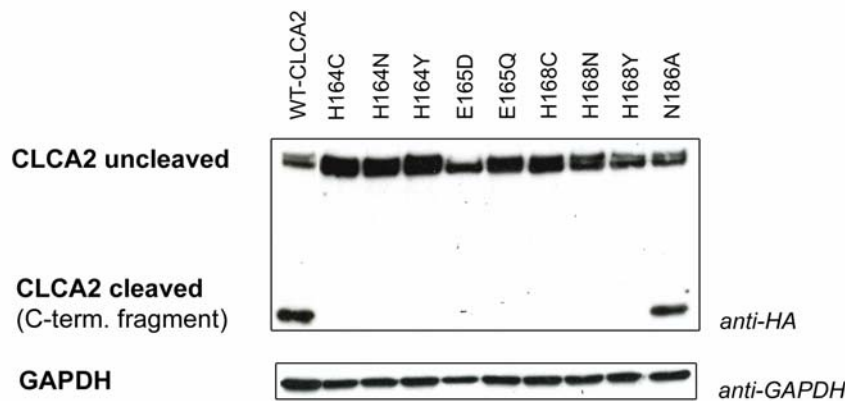


**Figure 47. Mutations in the putative hydrolase domain of CLCA2 and their effects on its proteolytic processing**

150,000 T47D Tet-on cells were seeded into 6-well-plates and transiently transfected with various constructs of pTRE2pur expression vector, expressing either HA-tagged wt-CLCA2 or bearing one of the following mutations: H164C, H164N, H164Y, E165D, E165Q, H168C, H168N, H168Y, and N186A. Expression was induced with Doxycycline 24 h post transfection. Protein lysates were harvested 48 h post induction. For Western blot 50 µg protein was loaded per lane; an anti-HA-tag antibody was used for detection of HA-tagged wt/mutant CLCA2. GAPDH served as loading control.

In Figure 48 a schematic overview of the impact on the proteolytic processing of all analysed mutations within the putative hydrolase domain of CLCA2 is presented.

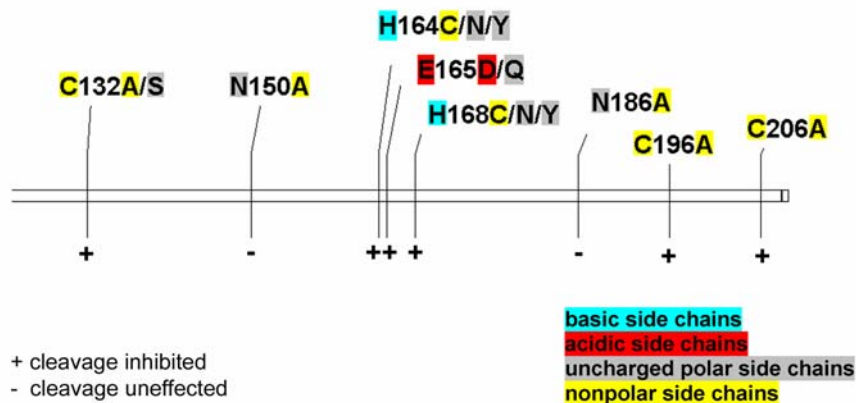


**Figure 48. Summary of effects of mutations within the putative hydrolase domain of CLCA2**

+ indicates complete inhibition of CLCA2 cleavage as analysed on Western blots (no cleaved fragment detectable)

- indicates no influence of the mutation on CLCA2 cleavage (Western blot pattern similar to that of wt-CLCA2)

Red coloured amino acids have an acidic side chain, blue ones a basic side chain, yellow ones have a non-polar side chain and grey ones a polar side chain.

### Mutational Analysis of the Putative Cleavage Site

As known from bioinformatic analysis and literature [95], there is a mono basic cleavage site predicted at position R674.

Mutational analyses were first done by Alanine-walking starting from predicted positions P5 to P4' (R670 to R678) by subsequent and stepwise substitution of the respective amino acid to an Alanine. These studies were further improved by introducing (especially at position R674 of the predicted mono basic cleavage site) at least one of each class of amino acids (i.e. amino acids with either a basic, acidic, non-polar or uncharged polar side chain). Western blot data on cleavage efficiency of mutated CLCA2 proteins are shown in Figure 49 and the effects are summarised in Figure 50. These data indicate that position R674 might serve as the P1 cleavage site, as this position strictly not allows any exchange of Arginine, besides Lysine which is also tolerated, due to the fact, that both are amino acids with basic side chains.

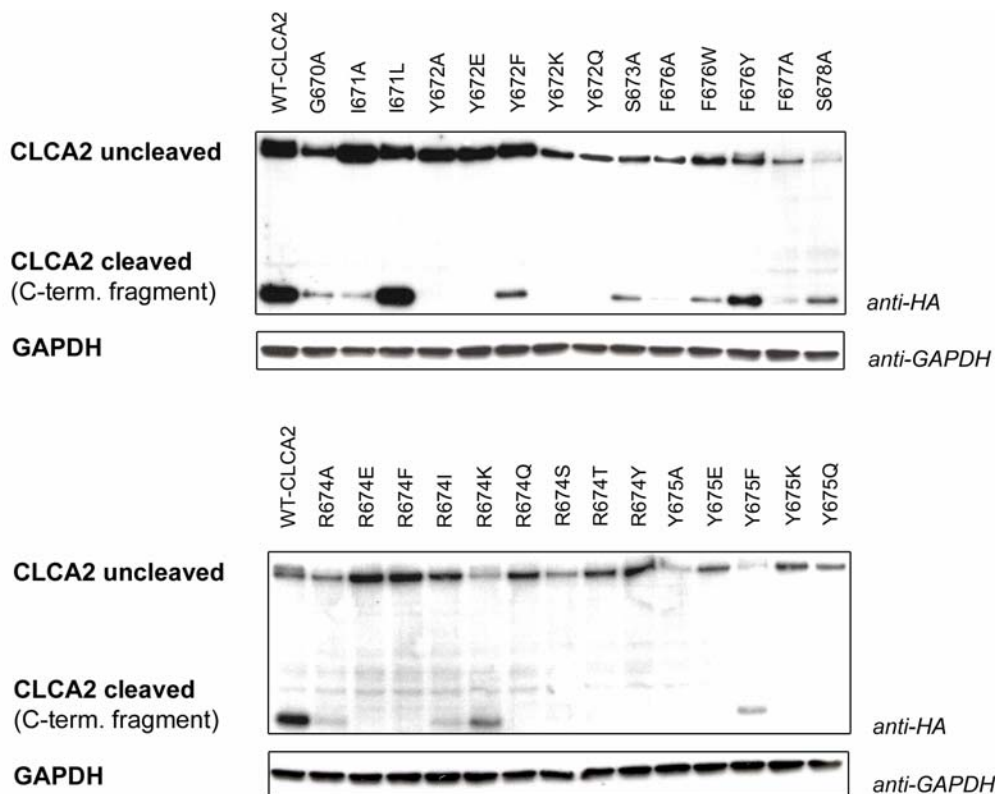


**Figure 49. Mutations in the putative cleavage site of CLCA2 and their effects on its proteolytic processing**

150,000 T47D Tet-on cells were seeded into 6-well-plates and transiently transfected with various constructs of pTRE2pur expression vector, expressing either HA-tagged wt-CLCA2 or bearing one of the following mutations: 670A, I671A/L, Y672A/E/F/K/Q, S673A, F676A/W/Y, F677A, F678A, R674A/E/F/I/K/Q/S/T/Y and Y675A/E/F/K/Q. Expression was induced with Doxycycline 24 h post transfection. Protein lysates were harvested 48 h post induction. For Western blot 50 µg protein was loaded per lane; an anti-HA-tag antibody was used for detection of HA-tagged wt/mutant CLCA2. GAPDH served as loading control.

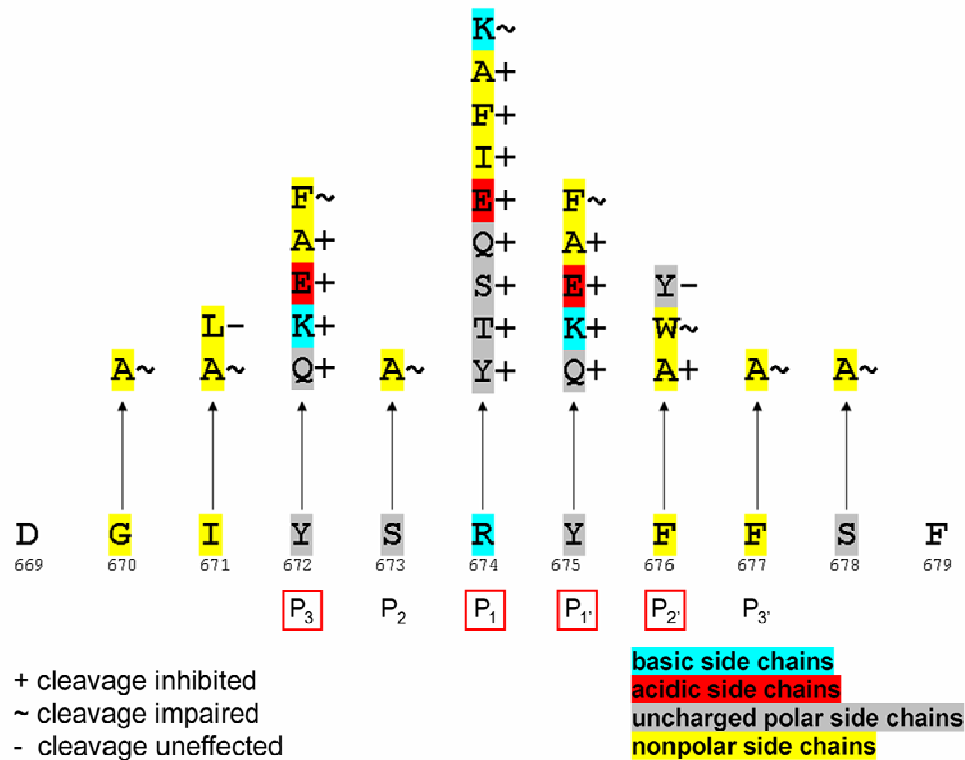


**Figure 50. Summary of effects of mutations in the putative cleavage site of CLCA2 on its proteolytic processing**

+ indicates complete inhibition of CLCA2 cleavage by analysis on Western blot (no cleaved fragment detectable)  
 ~ indicates impaired CLCA2 cleavage (detectable cleavage fragment on Western blot is reduced in comparison to wt-CLCA2)  
 - indicates no influence on CLCA2 cleavage (pattern on Western blot is similar with that of wt-CLCA2)  
 Red coloured amino acids have an acidic side chain, blue ones a basic side chain, yellow ones have a non-polar side chain and grey ones a polar side chain. Red-boxed positions indicate most sensitive residues within predicted cleavage site.

## Establishment of Stable Mutant-CLCA2 Clones

As for wt-CLCA2, it was decided to establish stable cell lines, expressing mutated CLCA2, which are devoid of cleavage ability. Therefore, constructs with either point mutations in the catalytic unit (E165Q or H186N), or with a point mutation in the monobasic cleavage site were transfected into T47D Tet-on cells.

All mutations were originally directly introduced into the expression vector pTRE2pur-CLCA2-HA carrying the HA-tagged wt-CLCA2, by utilisation of the “QuikChange II XL Site-Directed Mutagenesis Kit” (Stratagene). The cell line T47D Tet-on was chosen, to benefit from the inducible expression system and to allow comparison to wt-CLCA2 clones.

For establishment of stable clones, 100 clones were picked after selection with Puromycin for 3 weeks and analysed. All clones were induced and protein lysates

(induced and non-induced) were analysed on Western blots utilising an anti-HA-antibody for detection of (wild type/mutated) CLCA2. Inducible clones were kept in culture and after testing 100 clones, the most promising clones were compared against each other. In Figure 51 Western blot analysis of the most efficiently inducible clones for various CLCA2 mutants is shown.

Double bands seen for HA-tagged CLCA2 on Western blots for e.g. clones #3 and #32 might be due to incomplete glycosylation as a result of tremendous overexpression.

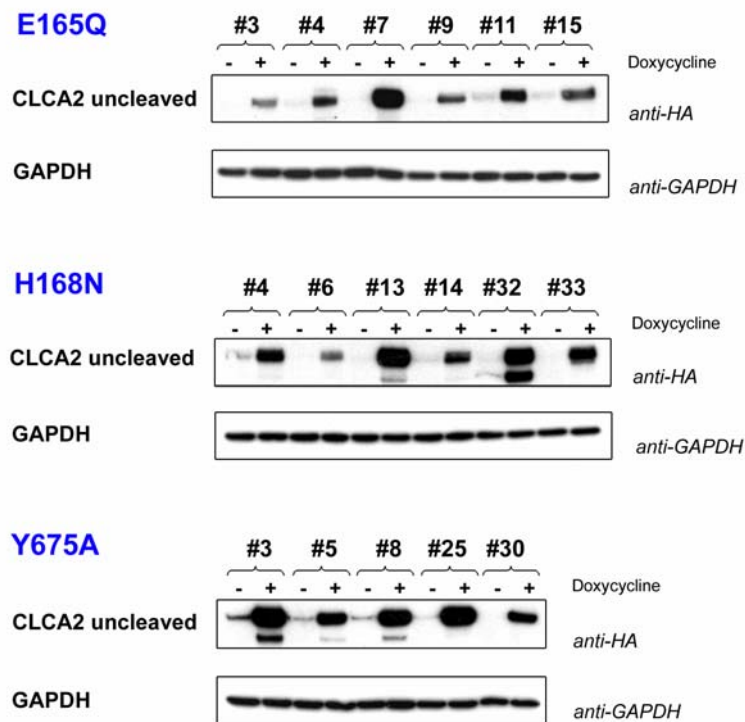


**Figure 51. Stable mutant-CLCA2-expressing T47D Tet-on clones:**  
**Inducible/constitutive expression of HA-tagged CLCA2 mutants E165Q, H168N, Y675A**

Clones were selected for 3 weeks with Puromycin. 300,000 cells were seeded into 6-well-plates and induced with Doxycycline. Protein lysates were harvested 48 h post induction. For Western blot 50 µg protein was loaded per lane; an anti-HA-tag antibody was used for detection of HA-tagged wt/mutant CLCA2. GAPDH served as loading control.

The following clones were chosen for further investigations:

- mutant-CLCA2(E165Q)-expressing T47D Tet-on clone #7
- mutant-CLCA2(H168N)-expressing T47D Tet-on clone #13
- mutant-CLCA2(Y675A)-expressing T47D Tet-on clone #25

### Inhibition of Post-Translational Modifications

Most of cell surface proteins are post-translationally modified by the attachment of different sugar- and/or lipid-residues (glycosylation, isoprenylation) for transport and/or stabilisation of the correct conformation of proteins within the cell membrane. The stability and processing of CLCA2 was analysed in the presence of the glycosylation inhibitor Tunicamycin and the isoprenylation inhibitor Perillic acid, utilising stable CLCA2-expressing T47D Tet-on cell lines (inducible expression system). Cells were treated with increased concentrations of the corresponding inhibitors and protein lysates analysed on Western blot, by detection of CLCA2 protein via the HA-tag, using an anti-HA-antibody. As seen in Figure 52 the stability of CLCA2 seems to be dependent on its post-translational glycosylation. Furthermore, glycosylation influences proteolytic processing: At a concentration of 0.5  $\mu\text{g}/\mu\text{l}$  of Tunicamycin no proteolytic processing is observed anymore.

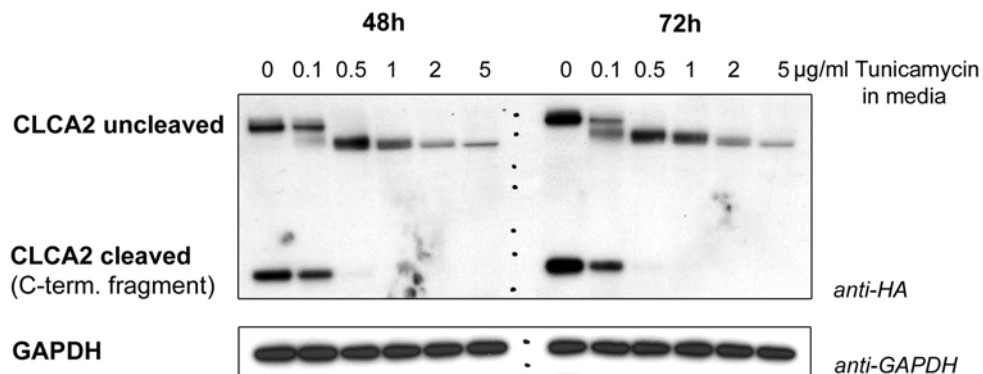


**Figure 52. CLCA2 stability and post-translational proteolytic processing of CLCA2 in the presence of the glycosylation inhibitor Tunicamycin**

300,000 cells of CLCA2-expressing T47D Tet-on clones #3 were seeded into 6-well-plates and treated with 0, 0.1, 0.5, 1, 2, 5  $\mu\text{g}/\text{ml}$  Tunicamycin in media. CLCA2 expression was induced with Doxycycline. Protein lysates were harvested 48 h post induction. For Western blot 50  $\mu\text{g}$  protein was loaded per lane; an anti-HA-tag antibody was used for detection of HA-tagged CLCA2. GAPDH served as loading control.

Analyses with several glycosylation site prediction software tools resulted in prediction of the putative glycosylation sites N150 and N822. However, mutation of these amino acids by exchanging Asparagine with Alanine did not influence the proteolytic processing of CLCA2 (Figure 53). Therefore, N150 and N822 seem not to be the major glycosylation sites in CLCA2.

However, N822 is located within the C-terminal fragment of CLCA2 and interestingly, a point mutation at this position influences the proteolytic processing resulting in a shorter C-terminal fragment on Western blots (Figure 53).

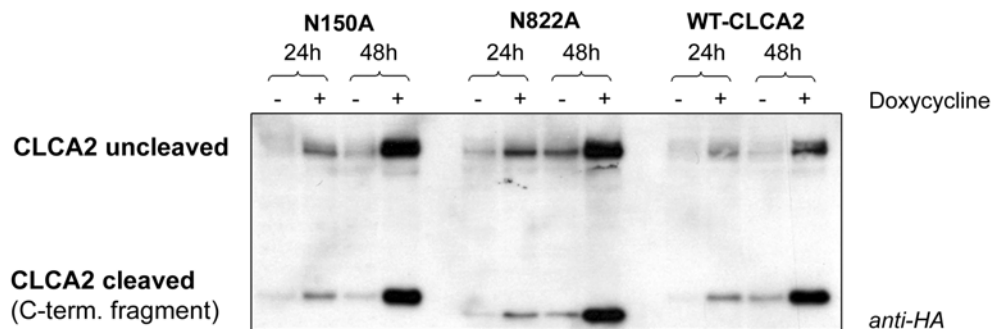


**Figure 53. Mutations of putative glycosylation sites N150A and N822A of CLCA2 and their effects on its stability and proteolytic processing**

150,000 T47D Tet-on cells were seeded into 6-well-plates and transiently transfected with constructs of pTRE2pur expression vector, expressing either HA-tagged wt-CLCA2 or bearing one of the following mutations: N150A, N822A. Expression was non-induced (-) and induced (+) with Doxycycline 24 h post transfection. Protein lysates were harvested 24 h and 48 h post induction. For Western blot 50 µg protein was loaded per lane; an anti-HA-tag antibody was used for detection of HA-tagged wt/mutant CLCA2.

In contrast to inhibition of glycosylation (Figure 52), isoprenylation does not play an important role for stability or efficient proteolytic cleavage of CLCA2 (Figure 54).

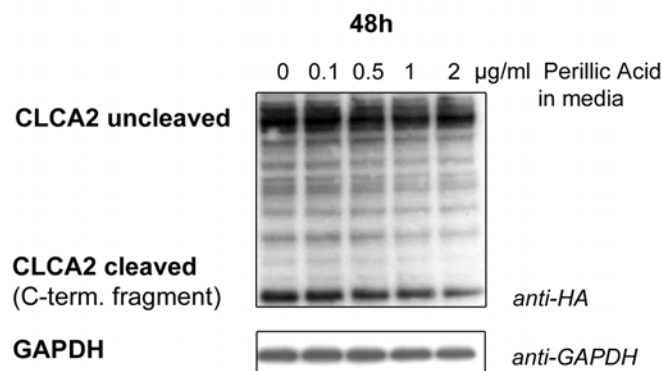


**Figure 54. CLCA2 stability and post-translational proteolytic processing of CLCA2 in the presence of the isoprenylation inhibitor Perillic acid**

300,000 cells of CLCA2-expressing T47D Tet-on clones #3 were seeded into 6-well-plates and treated with 0, 0.1, 0.5, 1, 2, 5 µg/ml Perillic acid in media. CLCA2 expression was induced with Doxycycline. Protein lysates were harvested 48 h post induction. For Western blot 50 µg protein was loaded per lane; an anti-HA-tag antibody was used for detection of HA-tagged CLCA2. GAPDH served as loading control.

## Integrin $\beta 4$

Abdel-Ghany found Integrin  $\beta 4$  to be coprecipitated with CLCA2. He also described a strong correlation between the level of Integrin  $\beta 4$  and adhesion of HEK293 cells expressing CLCA2 and a correlation *in vivo* between Integrin  $\beta 4$  expression in tumourigenic cell lines and the number of lung metastases detected in nude mice [70]. Upregulated Integrin  $\beta 4$  levels were also found in microarray studies of lung cancer metastases [74].

It could be shown that induction of CLCA2 expression in CLCA2-expressing T47D Tet-on clones #3 leads to enhanced Integrin  $\beta 4$  expression (Figure 55).

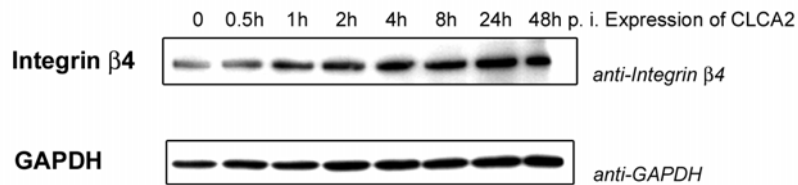


**Figure 55. Expression of Integrin  $\beta 4$  upon induction of CLCA2 expression**

Expression of CLCA2 was induced in CLCA2-expressing T47D Tet-on clone #3 by addition of Doxycycline. Protein lysates were harvested at indicated time points post induction. CLCA2 expression of lysates was confirmed before use. For Western blot 50  $\mu$ g protein was loaded per lane; an anti-Integrin  $\beta 4$  antibody was used for detection of Integrin  $\beta 4$ . GAPDH served as loading control.

Due to the lack of phospho-specific antibodies towards Integrin  $\beta 4$ , no conclusion could be drawn whether Integrin  $\beta 4$  becomes not only upregulated, but also activated upon induction of CLCA2.

### **Integrin-Mediated Cell Adhesion Assay**

Based on the data from Abdel-Ghany et al. [70] and to gain a more detailed understanding about the specific induction of integrins upon induced CLCA2 expression, the “Integrin-Mediated Cell Adhesion Arrays” (Chemicon) were used. (For details see section “Material and Methods”).

Especially the protein family of integrins (cell surface receptors) is involved in cell attachment to proteins of the extracellular matrix. Integrins therefore play an important role during metastasis, regulating not only dissemination but also homing of metastasising tumour cells. The “Integrin-Mediated Cell Adhesion Arrays” from Chemicon are efficient tools to screen cell surface protein profiles. These kits are composed of stripwells with each well pre-coated with an antibody detecting an individual integrin or extracellular matrix protein and one negative control well coated with bovine serum albumin (BSA). Utilising the established inducible expression system for CLCA2, it was possible to screen for induction of  $\alpha$ - and  $\beta$ -integrins in dependence on induction of wt or mutant CLCA2 expression in T47D Tet-on cells. As a control T47D cells with “empty” expression were used. As seen in Figure 56 out of the  $\alpha$ -integrin family no specific induction could be detected, whereas for  $\beta$ -integrin family member B2 a specific induction depending on wt-CLCA2 induced expression could be demonstrated for Clone #4 (Figure 57).



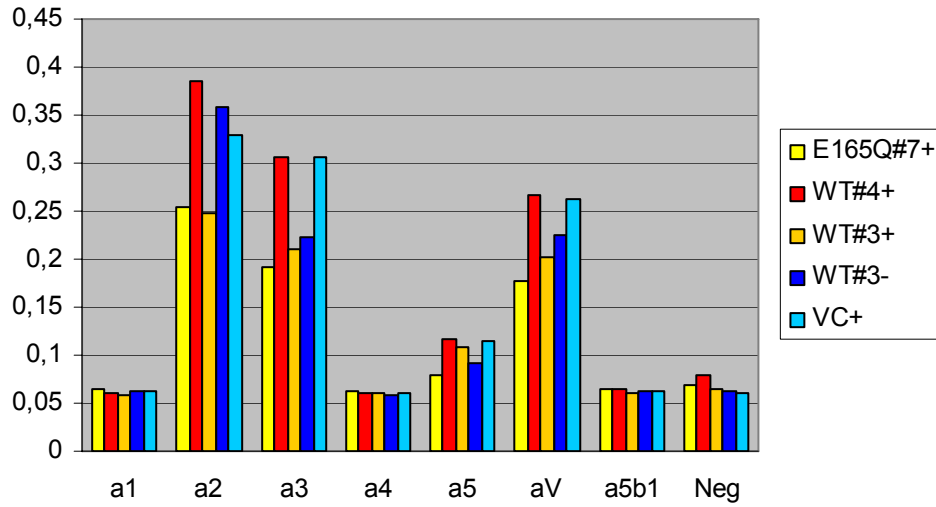


**Figure 56.  $\alpha$ -integrin-mediated cell adhesion of CLCA2-expressing and non-expressing cells**  
 Expression of wt-CLCA2 was induced in T47D Tet-on clone #4 (red), T47D Tet-on clone #3 (orange); expression of mutant-CLCA2 (E165Q) was induced in T47D Tet-on clone #7 (yellow). As control served non-induced T47D Tet-on clone #3 (dark-blue) and T47D cells with the empty vector (light-blue). Lysates were tested in the “Alpha-Integrin-Mediated Cell Adhesion Array” from Chemicon.

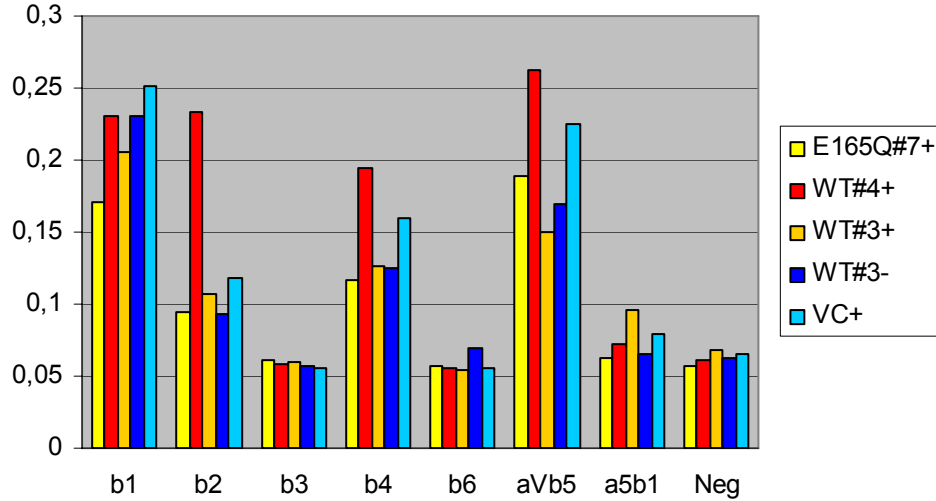


**Figure 57.  $\beta$ -integrin-mediated cell adhesion of CLCA2-expressing and non-expressing cells**  
 Expression of wt-CLCA2 was induced in T47D Tet-on clone #4 (red), T47D Tet-on clone #3 (orange); expression of mutant-CLCA2 (E165Q) was induced in T47D Tet-on clone #7 (yellow). As control served non-induced T47D Tet-on clone #3 (dark-blue) and T47D cells with the empty vector (light-blue). Lysates were tested in the “Beta-Integrin-Mediated Cell Adhesion Array” from Chemicon.

### **3D-In Vitro Carcinoma Assay: Spheroids**

For a better simulation of the situation in a tumour, CLCA2-expressing clones were not only grown in 2D cell culture, but also in multicellular tumour spheroids, which are *in vitro* 3D models that simulate malignant cell contacts within a tumour. Multicellular tumour spheroids can for instance also be used to evaluate tumour response to therapeutic agents. In this approach the *in vitro* 3D model was used for analysis of the influence of CLCA2 expression on cell growth and viability in a 3D model.

For this purpose 250 cells, each of the various T47D-CLCA2 clones were cultivated with methylcellulose and transferred into 96-well-plates for suspension culture. The methylcellulose causes cells to grow in three-dimensional cultures as opposed to mono-layer, forming a spheroid.

After forming stable spheroids, they were transferred to a collagen gel or Matrigel (Becton Dickinson) and grown until the spheroids became necrotic due to increased volume and the lack of supply with nutrients and oxygen in the centre of the 3D spheroid, as angiogenesis-induced vessels in a tumour would do.

After 3, 5, 7, and 10 days in the gel, spheroids were monitored under the microscope. Growth was estimated by measurement of the area of spheroids with AxioVision Software (Zeiss). To analyse the apoptotic status of cells within a spheroid, cells were stained with the intercalating and fluorescent agent Propidium iodide that pervades cell membranes of dead cells only.

Before forming spheroids, stable CLCA2 expression of T47D Tet-on clones was confirmed on Western blot (data not shown).

The following cell clones were used in this study:

- wt-CLCA2-expressing T47D Tet-on clone #3 (in induced/non-induced status)
- wt-CLCA2-constitutively-expressing T47D clone #47
- mutant-CLCA2(E165Q)-expressing T47D Tet-on clone #7 (in induced status)
- control cells, which stably carry the “empty” expression vector pTRE2pur (no CLCA2 expression) and which were pseudo-induced with Doxycycline to search for any specific Doxycycline-dependent effect.

Spheroids of non-induced wt-CLCA2-expressing T47D Tet-on clone #3 are shown in Figure 58 and can be directly compared with spheroids of the same clone, but in an induced status, as shown in Figure 59. Exemplarily, two representative pictures are shown for the time points 3, 5, 7, and 10 days growth of spheroids in Matrigel. No

distinct difference could be observed between induced and non-induced clone #3, but in contrast a pronounced difference in area, representative for cell growth and apoptotic status of cells within the spheroid was found, as compared to the constitutive expressing clone #47 (Figure 60). It seems that constitutive expression triggers cell growth in a way that these spheroids become considerably bigger from day 3 on in Matrigel. It is also of interest that in spheroids of clone #47 considerably more apoptotic cells were found than in clone #3, where CLCA2 expression was induced only when spheroids were transferred to the Matrigel. Therefore, constitutive CLCA2 expression during spheroid-formation lead to generation of larger spheroids and subsequently to more apoptosis activity due to enhanced cell growth, supporting previous findings that CLCA2 essentially contributes to proliferation and/or viability of tumour cells.

Control cells, which stably carry the “empty” expression vector pTRE2pur and which were “pseudo-induced” with Doxycycline, are shown in Figure 61 and look very similar to non-induced clone #3 (Figure 58). Cells expressing mutant CLCA2 protein (E165Q), which are exhibiting a deficient proteolytic processing, were undistinguishable from other spheroids (Figure 62). Apparently proteolytic processing did not have any influence on spheroid formation or other properties of spheroids concerning cell growth or apoptotic status of cells within a spheroid. The same holds true for other CLCA2 expressed mutants (data not shown).

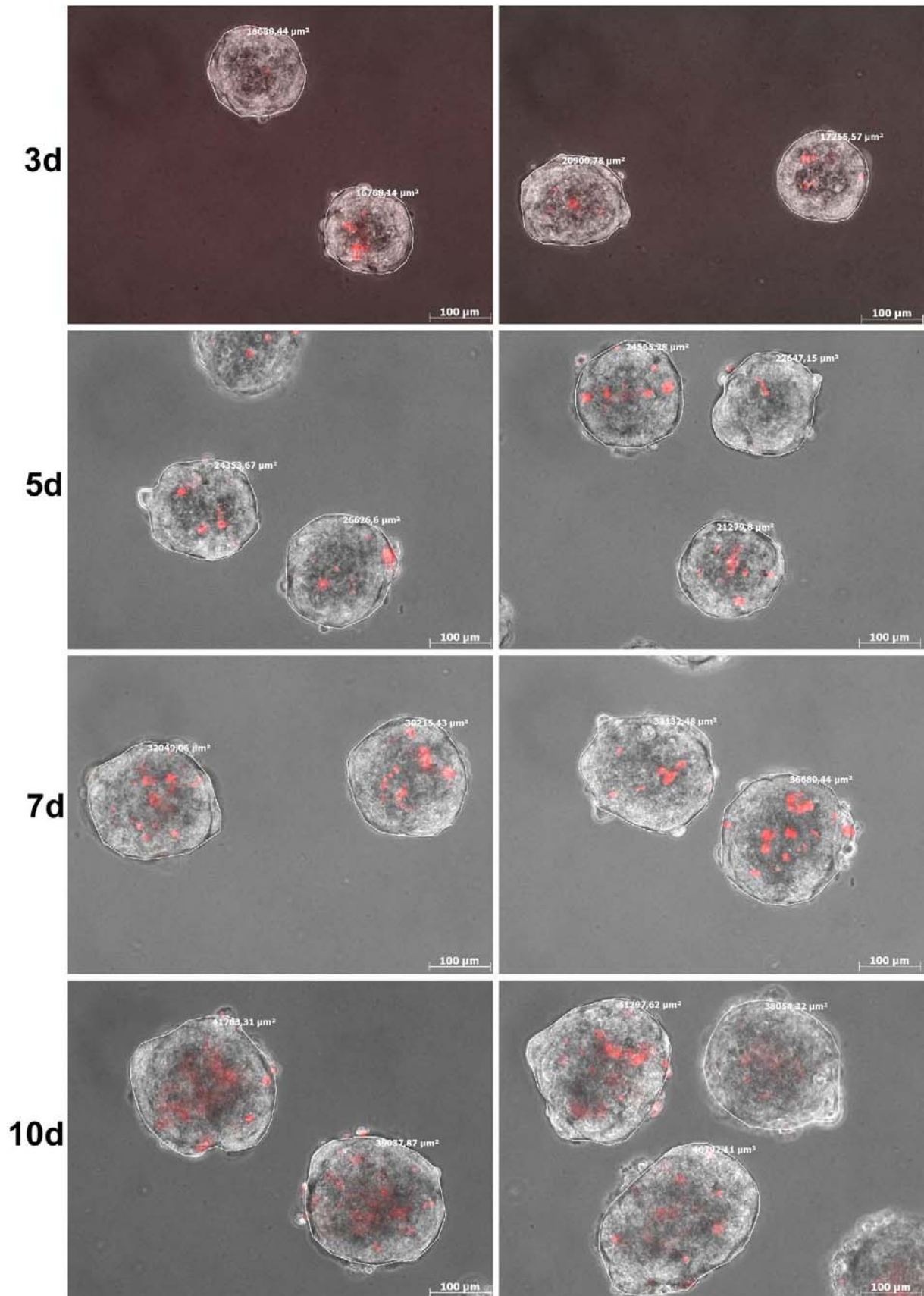


**Figure 58. Spheroids of wt-CLCA2-expressing T47D Tet-on clone #3 – non-induced**  
Exemplarily two pictures are shown after growth for 3 d, 5 d, 7 d, and 10 d in Matrigel.  
Red: Propidium iodide-stained apoptotic cells.

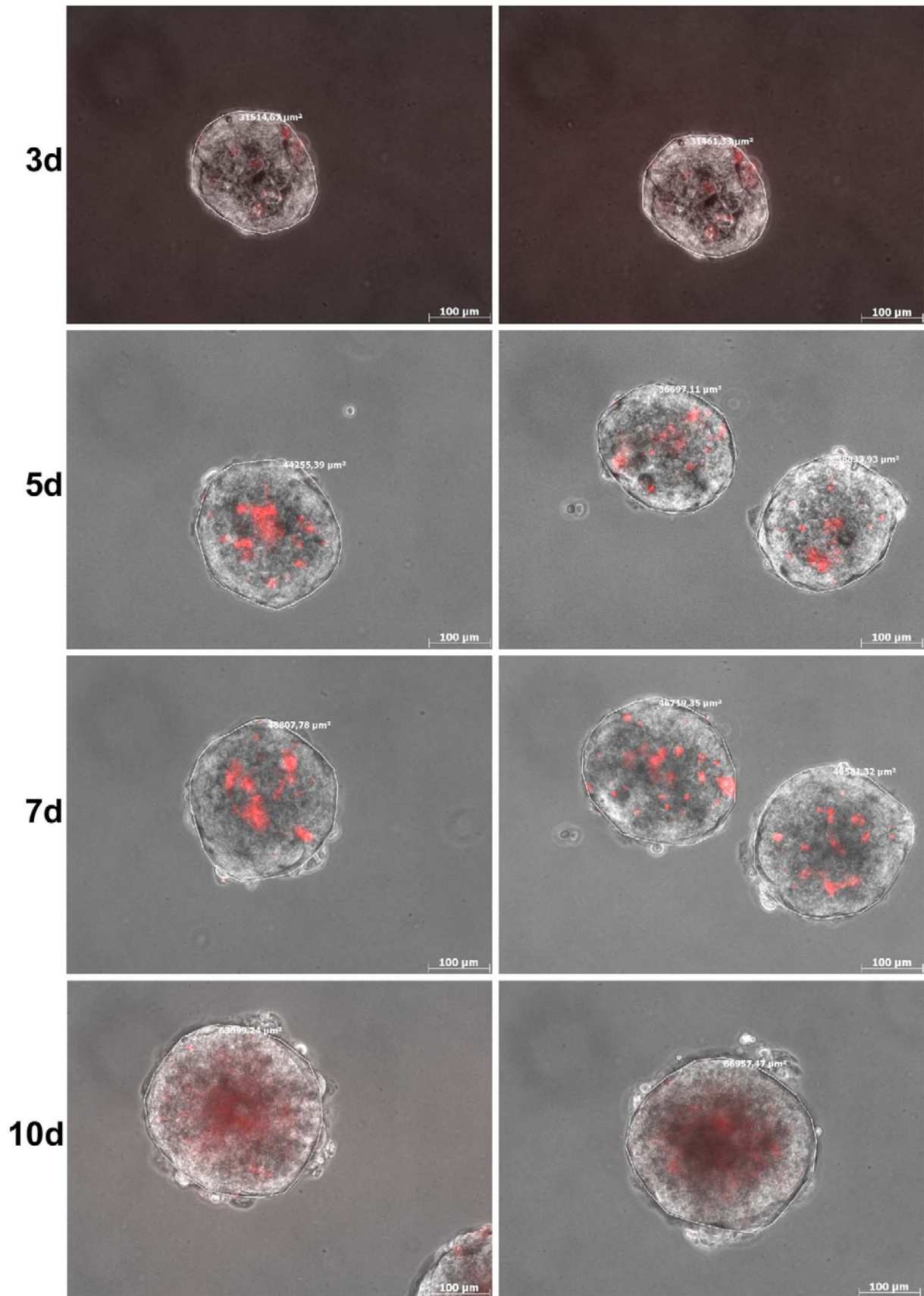


**Figure 59. Spheroids of wt-CLCA2-expressing T47D Tet-on clone #3 – induced**  
Exemplarily two pictures are shown after growth for 3 d, 5 d, 7 d, and 10 d in Matrigel.  
Red: Propidium iodide-stained apoptotic cells.



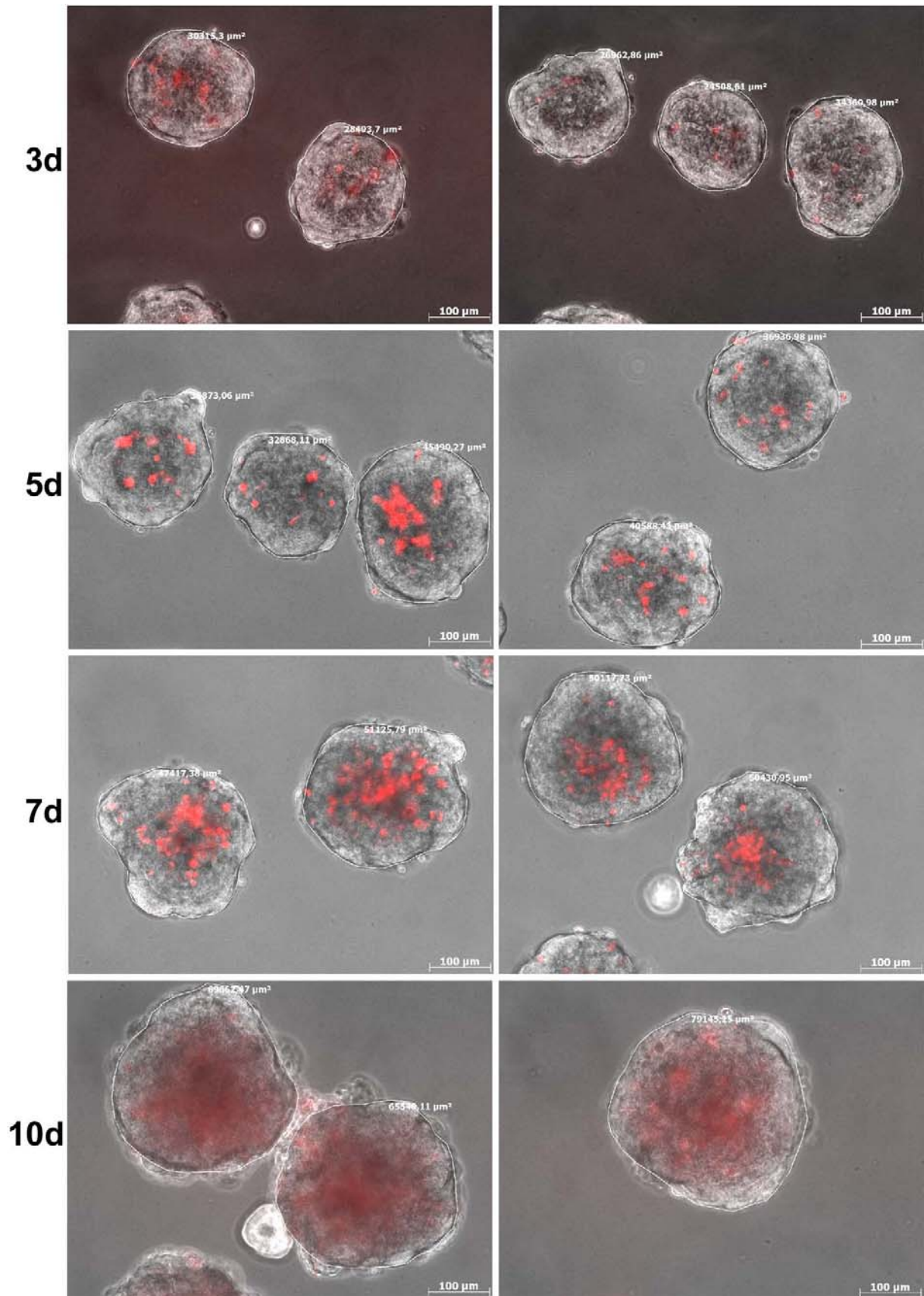


**Figure 60. Spheroids of wt-CLCA2-constitutively-expressing T47D clone #47**  
Exemplarily two pictures are shown after growth for 3 d, 5 d, 7 d, and 10 d in Matrigel.  
Red: Propidium iodide-stained apoptotic cells.

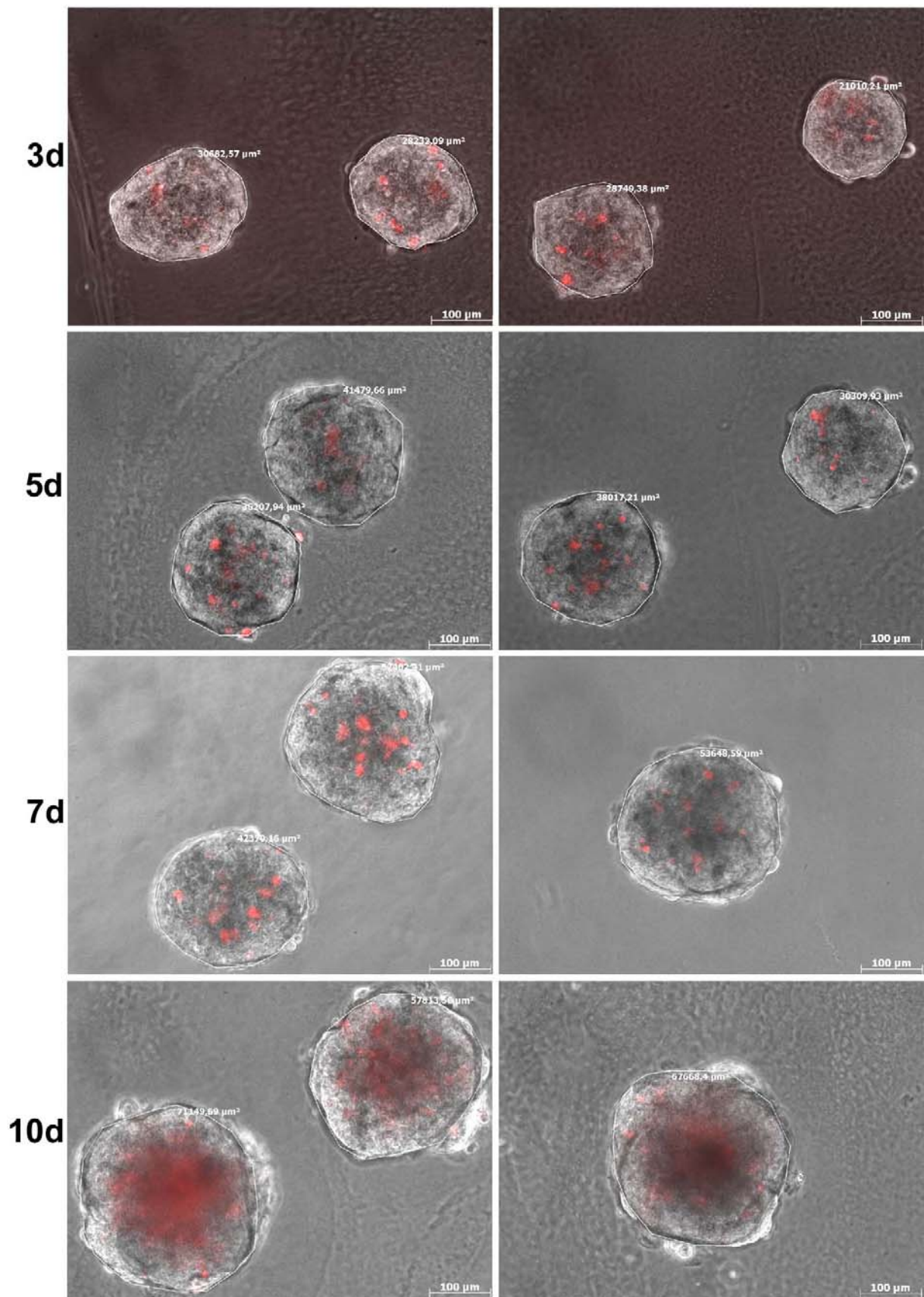


**Figure 61. Spheroids of control cells (T47D Tet-on cells with empty vector, Doxycycline-treated)**  
Control cells stably carrying the “empty” expression vector pTRE2pur were pseudo-induced with Doxycycline for analysis of any Doxycycline effect. Exemplarily two pictures are shown after growth for 3 d, 5 d, 7 d, and 10 d in Matrigel. Red: Propidium iodide-stained apoptotic cells.



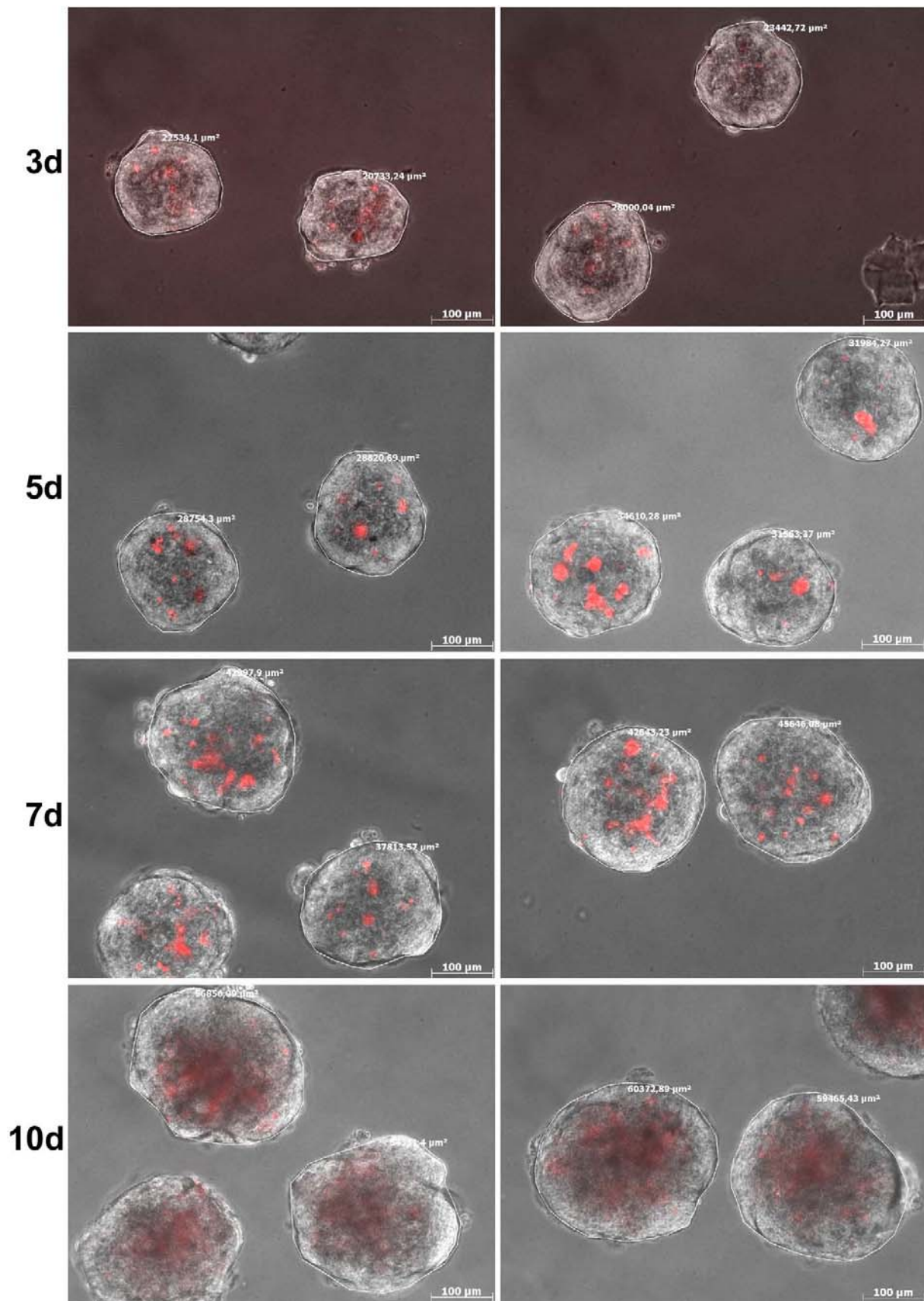


**Figure 62. Spheroids of mutant-CLCA2(E165Q)-expressing T47D Tet-on clone #7 – induced**  
Exemplarily two pictures are shown after growth for 3 d, 5 d, 7 d, and 10 d in Matrigel.  
Red: Propidium iodide-stained apoptotic cells.



**Growth Curve of CLCA2-Expressing Clones (T47D Tet-on): 2D versus 3D**

As it could be shown, that cell growth in the spheroid 3D-model is enhanced in CLCA2-constitutively-expressing T47D clone #47 compared to induced or non-induced CLCA2-expressing T47D Tet-on clones #3. Cell growth of these clones was also compared in 2D-tissue culture. Therefore, 2D-growth curves were generated, based on cell numbers of cells which had been trypsinised and counted after 3-10 days in 2D-cell culture. Interestingly, in 2D no distinct difference between non-induced or induced clone #3 could be observed.

Next, a 3D-growth curve was generated by measurement of the area of various spheroids, which was calculated with AxioVision Software after 3-10 days in Matrigel. In a statistically meaningful setting the relative cell growth of 2D- (counting viable cells) with that of 3D-cultures (determination of area [ $\mu\text{m}^2$ ]; Figure 63) were compared over a period of 3 to 10 days. Although, the relative cell growth of induced versus non-induced clone #3 did not show a difference in 2D-cultures, it indeed exhibited a pronounced difference ( $> 2.5$ -fold) between 2D- and 3D-culturing. In contrast to inducible clone #3, the constitutive clone #47 showed already an enhanced relative cell growth in 2D-culture, which was similar to that found in 3D-cultures. Spheroids of inducible cell clones expressing other CLCA2-mutants were also analysed in this assay, but none of them showed a statistically relevant different behaviour in growth, when compared to inducible CLCA2 clones (data not shown).

In general, the 3D-model is more sensitive than 2D-cultures to show differences in cell proliferation, and it allows to demonstrate the impact of CLCA2 on the three-dimensional growth of tumour cells.

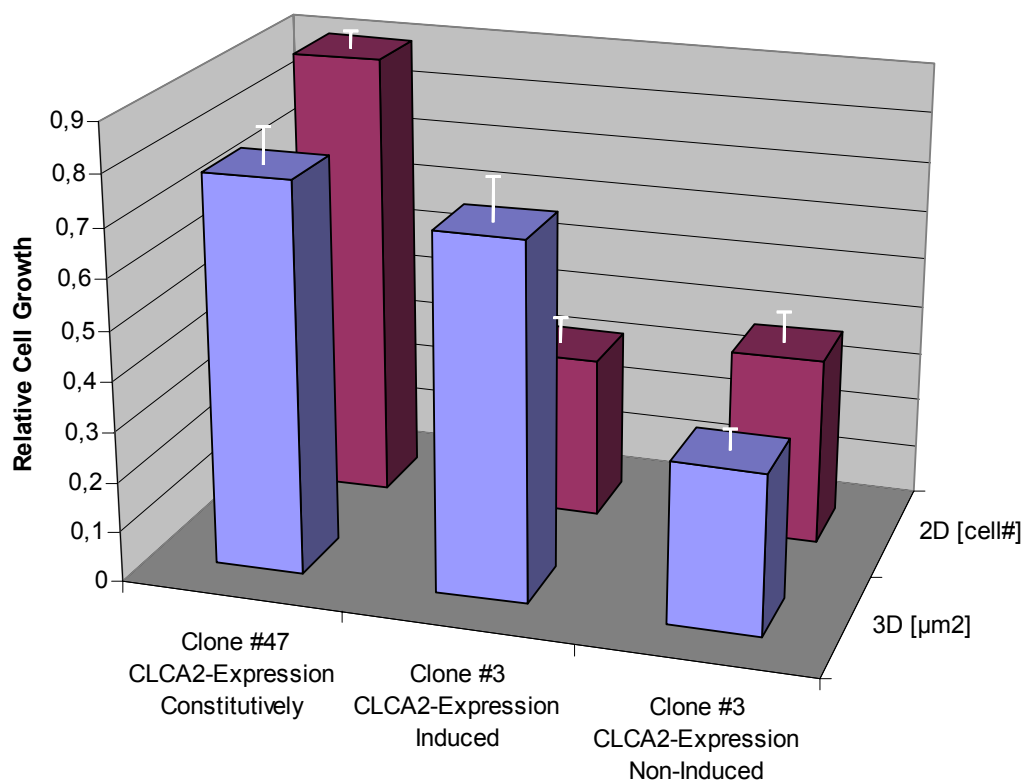


**Figure 63. Relative cell growth in 2D and 3D of T47D clones with constitutive, induced, and non-induced CLCA2 expression**

Left: CLCA2-constitutively-expressing T47D clone

Middle: CLCA2-expressing T47D Tet-on clones #3 – induced

Right: CLCA2-expressing T47D Tet-on clones #3 – non-induced

For 2D-growth curve, cells were trypsinised and counted after 3-10 days in 2D-cell culture.

For 3D-growth curve, area of spheroids was estimated with AxioVision Software after 3-10 d in Matrigel.

The value of area is the average of all measured spheroids (5 up to 11 spheroids per time point).

## Affymetrix Microarray Studies

To study the effects of overexpression of CLCA2 on gene expression, expression profiling using the Affymetrix GeneChip Human Genome U133 Array was performed by testing stable cell clones with inducible expression of CLCA2.

First, different wt-CLCA2-expressing T47D Tet-on clones (Figure 41) were tested for CLCA2 expression both, on the protein level performing Western blots and on the transcript level performing real-time quantitative PCR (RT-qPCR). Freshly thawed clones #3, #4 and #46 still proved as the best inducible cell lines as shown previously (Figure 41). These clones exhibit the most efficient induction profile (Figure 64).

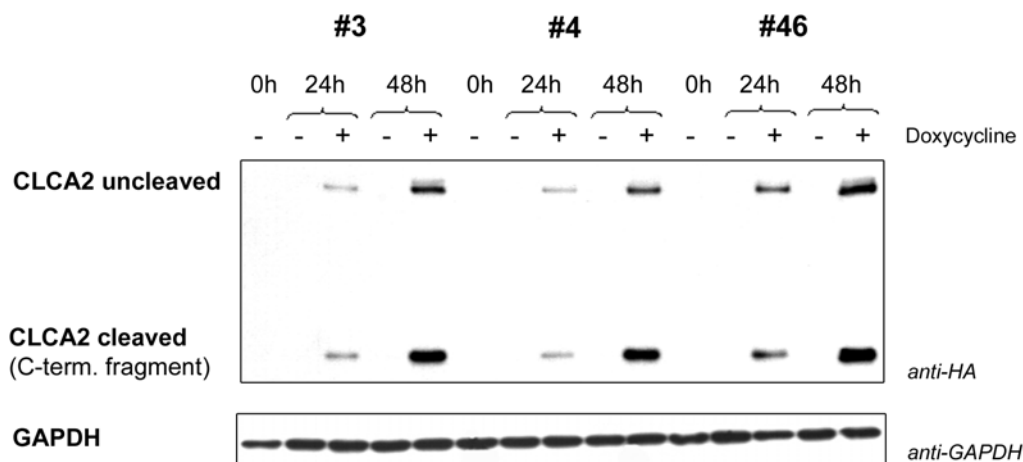


**Figure 64. CLCA2 protein expression of inducible CLCA2-expressing T47D Tet-on clones used for Affymetrix microarray studies**

300,000 cells of CLCA2-expressing T47D Tet-on clone #3, #4, and #46 were seeded each into 6-well-plates and induced with Doxycycline. Protein lysates were harvested 24 h and 48 h post induction. For Western blot 50 µg protein was loaded per lane; an anti-HA-tag antibody was used for detection of HA-tagged CLCA2. GAPDH served as loading control.

Expression of CLCA2 transcript in clone #3 was monitored by performing RT-qPCR with cDNA samples taken at different time points. As shown in Figure 65 the CLCA2 transcript could only be detected in induced lysates. CLCA2 transcript level increased between 8 h and 24 h post induction. In non-induced lysates the CLCA2 transcript stayed within the background level of control cells (Figure 65).

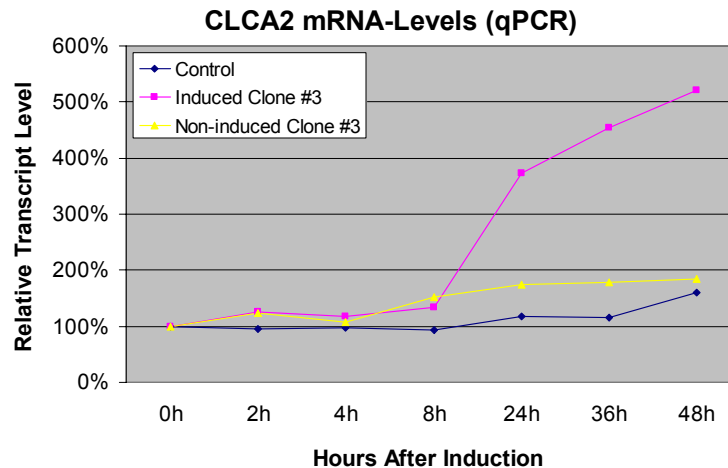


**Figure 65. CLCA2 mRNA levels of induced and non-induced CLCA2-expressing T47D Tet-on clone #3 versus control cells (T47D Tet-on cells with empty vector, Doxycycline-treated)**

300,000 cells were seeded into 6-well-plates and induced with Doxycycline. RNA lysates were harvested 24 h post induction and transcribed into cDNA. For detection of the CLCA2 transcript by RT-qPCR a CLCA2-specific primer pair (see “Material and Methods”) was used in a duplex assay together with the internal control  $\beta$ -2 microglobulin for normalisation.

After testing primer pairs for various housekeeping genes in these lysates (data not shown),  $\beta$ -2-microglobulin was chosen for use as the most robust internal reference for normalisation of CLCA2 transcript levels.

Protein lysates were prepared at various time points and stored at  $-80^{\circ}\text{C}$ . cDNA preparations of clones #4 and #46 were analysed on Affymetrix GeneChip Human Genome U133 Array (for details see “Material and Methods”). Expression profiles are shown in Figure 66.

Blue bars indicate CLCA2-transcript levels in non-induced cells and red bars CLCA2 transcript levels in induced cells, respectively. In all three clones induction of CLCA2 expression can be detected at 24 h and 48 h after treatment with Doxycycline. In contrast to other clones, clone #46 exhibits already elevated CLCA2 levels without induction. However, the relative induction range is similar compared to clone #3 and #4. Clone #46 obviously contains a “leaky” expression control for CLCA2.

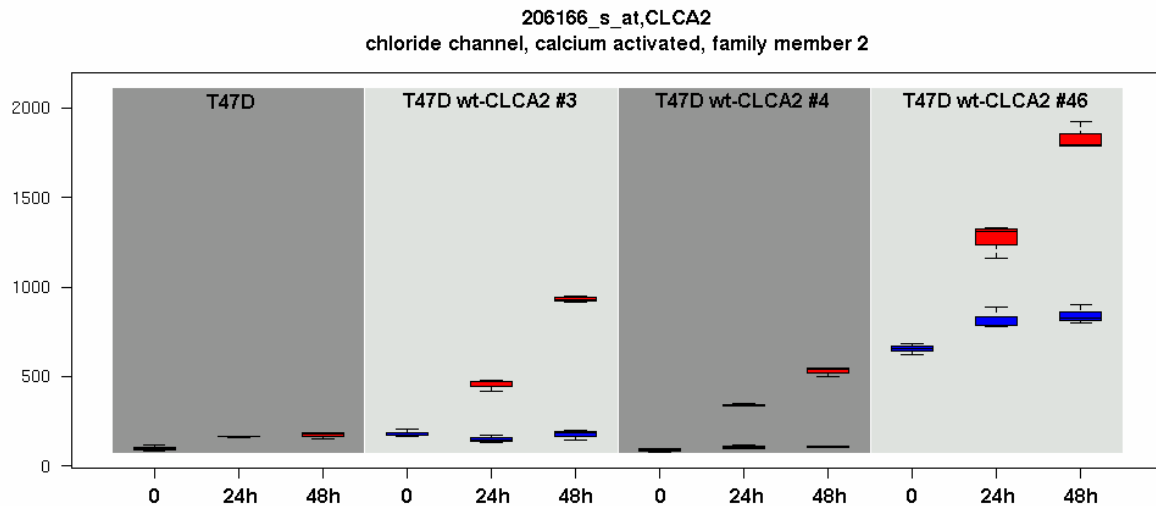


**Figure 66. CLCA2 mRNA levels of inducible CLCA2-expressing T47D Tet-on clones #3, #4 and #46 compared with T47D (control) on Affymetrix GeneChip Human Genome U133 Array**

The MAS5-normalised expression levels of CLCA2 (206166\_s\_at) mRNA is shown in box-plots. Red box-plots indicate CLCA2 transcript levels of cells with induced CLCA2 expression, blue box-plots represent CLCA2 transcript levels of non-induced cells. The vertical centre line in the box indicates the median; the box itself represents the interquartile range (IQR) between the first and third quartiles.

In a next step, genes whose induction is dependent on the presence/induction of CLCA2 should be identified; i.e. these are transcripts which are induced in CLCA2-inducibly-expressing cell lines, but not expressed in non-induced or control cells (“empty” vector bearing cells). Selected top hits are shown in Table 2. To reduce complexity of data this “correlation analysis” was only performed for clone #3.

Probeset	Gene Symbol	Gene Title	Chromosomal Location	Correlation Factor (r)
206166_s_at	CLCA2	chloride channel, calcium activated, family member 2	1p31-p22	1
212134_at	PHLDB1	pleckstrin homology-like domain, family B, member 1	11q23.3	0.98308
223212_at	ZDHHC16	zinc finger, DHHC-type containing 16	10q24.1	0.98276
229399_at	C10orf118	chromosome 10 open reading frame 118	10q25.3	0.98070
202733_at	P4HA2	procollagen-proline, 2-oxoglutarate 4-dioxygenase (proline 4-hydroxylase), alpha polypeptide II	5q31	0.97973
200974_at	ACTA2	actin, alpha 2, smooth muscle, aorta	10q23.3	0.97693
215120_s_at	SAMD4	sterile alpha motif domain containing 4	14q22.2	0.97123
209922_at	BRAP	BRCA1 associated protein	12q24	0.96837
1557104_at	NA	Zinc finger protein	NA	0.96594
203408_s_at	SATB1	special AT-rich sequence binding protein 1 (binds to nuclear matrix/scaffold-associating DNA's)	3p23	0.95899
1552621_at	POLR2J2	DNA directed RNA polymerase II polypeptide J-related gene	7q11.22	0.95825
203050_at	TP53BP1	tumor protein p53 binding protein, 1	15q15-q21	0.95779
233750_s_at	C1orf25	chromosome 1 open reading frame 25	1q25.2	0.95680
232754_at	NA	NA	NA	0.95256
223629_at	PCDHB5	protocadherin beta 5	5q31	0.95240
1556339_a_at	NA	NA	NA	0.95147
224321_at	TMEFF2	transmembrane protein with EGF-like and two follistatin-like domains 2 /// transmembrane protein with EGF-like and two follistatin-like domains 2	2q32.3	0.95135
201295_s_at	WSB1	WD repeat and SOCS box-containing 1	17q11.1	0.95100
208589_at	TRPC7	transient receptor potential cation channel, subfamily C, member 7	5q31.1	0.94950
1554895_a_at	RHBDL2	rhomboid, veinlet-like 2 (Drosophila)	1p34.3	0.94919
211762_s_at	KPNA2	karyopherin alpha 2 (RAG cohort 1, importin alpha 1) /// karyopherin alpha 2 (RAG cohort 1, importin alpha 1)	17q23.1-q23.3	0.94716
235756_at	NA	CDNA FLJ26187 fis, clone ADG04782	NA	0.94685
224280_s_at	FAM54B	family with sequence similarity 54, member B	1p36.11	0.94434
207904_s_at	LNPEP	leucyl/cystinyl aminopeptidase	5q15	0.94389
1553740_a_at	IRAK2	interleukin-1 receptor-associated kinase 2	3p25.3	0.94332

**Table 2. “Correlation Analysis” on expression pattern of microarray studies**

The Table lists an extract of genes with a high correlation factor showing an induction upon induced expression of CLCA2 in clone #3 after 0, 24 h and 48 h. A correlation factor of 1,000 represents the induction of CLCA2 (probeset 206166\_s\_at). The right column refers to the respective correlation factor r.

As clone #4 and #46 had also been analysed on Affymetrix GeneChips in parallel, the selected top-correlating probesets (genes) listed in Table 2 could be manually compared with the corresponding expression pattern of clone #4 and #46. Those genes showing a similar expression profile in clone #4 and #46 were selected and subjected to RT-qPCR to confirm the expression pattern by an independent method. Individual results are shown in Figure 67 to Figure 83, always comparing the respective expression profile from the Affymetrix GeneChip analysis with the corresponding one from RT-qPCR analysis.

## SFI1

SFI1 homolog, spindle assembly associated (yeast) is involved in initiation of centrosome duplication. SFI1 has been identified as a binding partner for the calcium-binding protein centrin suggesting a role in the dynamic behavior of centrosomes. SFI1 binds to multiple centrin molecules and the complex forms calcium sensitive contractile fibers that function to reorient centrioles and alter centrosome structure [96]. So far no correlation to tumour cell growth has been reported. However, according to our *in silico* analysis SFI1 is found upregulated in many tumors, with highest expression levels found in various B-cell lymphomas and B-cell leukemias (data not shown).

Results from Affymetrix microarray analysis indicating an upregulation of SFI1 upon induction of CLCA2 expression could be confirmed in RT-qPCR as shown in Figure 67.

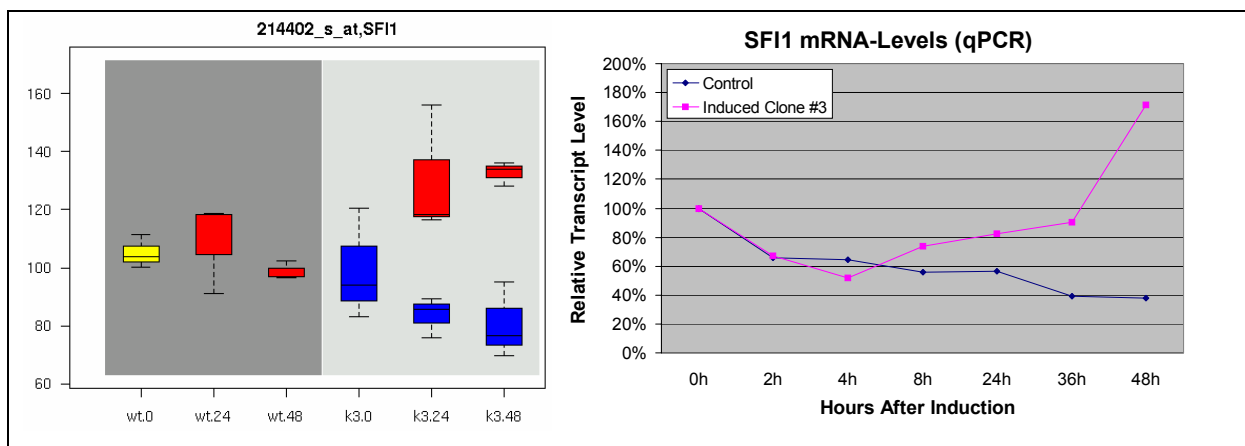


**Figure 67. SFI1 mRNA levels in induced CLCA2-expressing T47D Tet-on clone #3 versus control**

**Left: Affymetrix microarray studies using Affymetrix GeneChip Human Genome U133 Array**

The MAS5-normalised expression levels of SFI1 mRNA are shown in box-plots. The vertical centre line in the box indicates the median; the box itself represents the interquartile range (IQR) between the first and third quartiles. Whiskers extend to 1.5 times the IQR. In the left dark grey field, expression levels in control cells (T47D Tet-on) are shown. In the right light grey field, expression levels in T47D Tet-on clone #3 (k3) are represented.

Red box-plots indicate SFI1 transcript levels of cells with induced CLCA2 expression; blue box-plots represent SFI1 transcript levels of non-induced cells. The yellow box plot represents the transcript level in control cells at the time point of induction. 0, 24 and 48 indicate the time points (h) of lysate preparation post induction

**Right: RT-qPCR in duplex assay with β-2-microglobulin as internal reference for normalisation**

Normalised SFI1 mRNA levels of induced clone #3 are shown in relation to mRNA levels in control cells (T47D Tet-on with empty expression vector).

## TP53BP1

Alteration of the tumour protein TP53BP1 (p53 binding protein 1), during skin carcinogenesis is associated with genomic instability [97]. The expression pattern of TP53BP1 from microarray analysis is shown in Figure 68, left side suggesting an overexpression of TP53BP1 if CLCA2 expression is induced. However, higher levels of TP53BP1 could also be detected in control cells after 48 h of treatment with Doxycycline. In addition, overexpression of TP53BP1 could also not be confirmed with RT-qPCR (Figure 68, right side). Therefore, expression of TP53BP1 has to be regarded as a non-specific induction. This example supports the application of an independent method for validation of expression profiles.

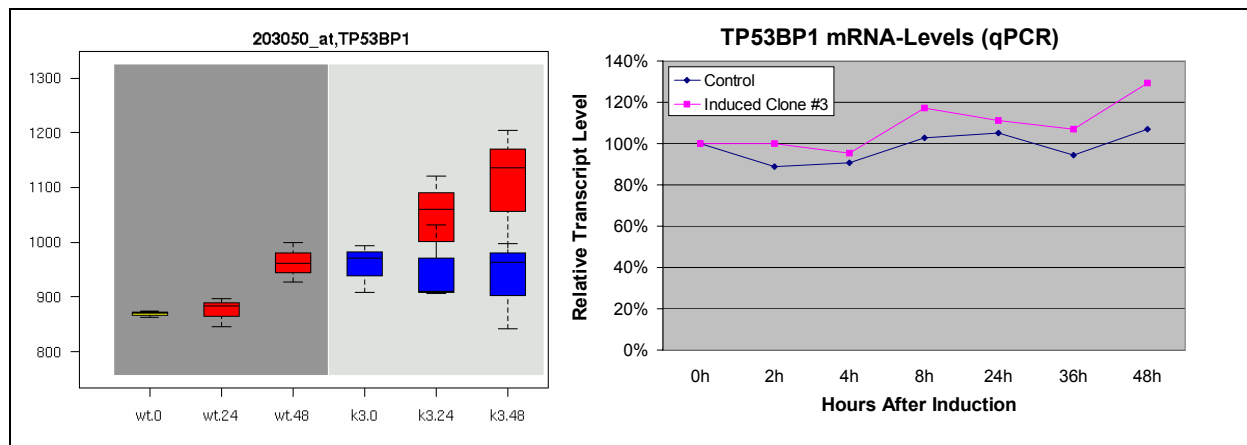


**Figure 68. TP53BP1 mRNA levels in induced CLCA2-expressing T47D Tet-on clone #3 versus control**

**Left: Affymetrix microarray studies using Affymetrix GeneChip Human Genome U133 Array**

The MAS5-normalised expression levels of TP53BP1 mRNA are shown in box-plots. The vertical centre line in the box indicates the median; the box itself represents the interquartile range (IQR) between the first and third quartiles. Whiskers extend to 1.5 times the IQR. In the left dark grey field, expression levels in control cells (T47D Tet-on) are shown. In the right light grey field, expression levels in T47D Tet-on clone #3 (k3) are represented. Red box-plots indicate TP53BP1 transcript levels of cells with induced CLCA2 expression; blue box-plots represent TP53BP1 transcript levels of non-induced cells. The yellow box plot represents the transcript level in control cells at the time point of induction. 0, 24 and 48 indicate the time points (h) of lysate preparation post induction.

**Right: RT-qPCR in duplex assay with  $\beta$ -2-microglobulin as internal reference for normalisation**

Normalised TP53BP1 mRNA levels of induced clone #3 is shown in relation to mRNA levels in control cells (T47D Tet-on with empty expression vector).



## CDIPT

CDP-diacylglycerol-inositol 3-phosphatidyltransferase (phosphatidylinositol synthase) is a gene whose inhibition causes small cell lung carcinoma cells to arrest in G1 [98]. It further has been suggested to be involved in oral carcinogenesis [99]. Inostamycin, an inhibitor of CDIPT, led to a decrease in cyclin D1 mRNA and protein expression accompanied by suppression of phosphorylated retinoblastoma susceptibility gene product (pRB-P) levels. Inostamycin might be a useful agent for tumour dormant cytostatic therapy for oral SCC.

Overexpression of CDIPT was found in microarray studies and was confirmed in RT-qPCR, as shown in Figure 69.

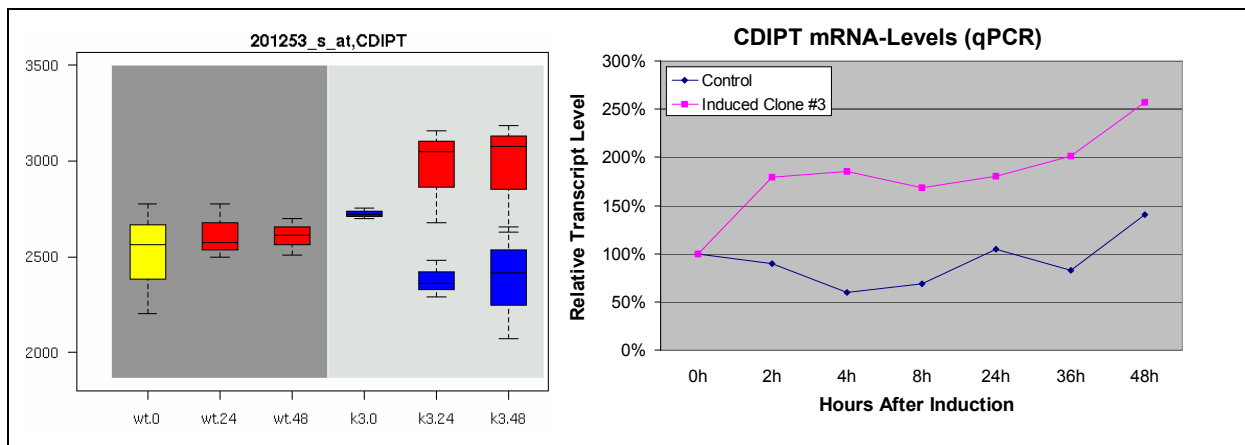


**Figure 69. CDIPT mRNA levels in induced CLCA2-expressing T47D Tet-on clone #3 versus control**

**Left: Affymetrix microarray studies using Affymetrix GeneChip Human Genome U133 Array**

The MAS5-normalised expression levels of CDIPT mRNA are shown in box-plots. The vertical centre line in the box indicates the median; the box itself represents the interquartile range (IQR) between the first and third quartiles. Whiskers extend to 1.5 times the IQR. In the left dark grey field, expression levels in control cells (T47D Tet-on) are shown. In the right light grey field, expression levels in T47D Tet-on clone #3 (k3) are represented. Red box-plots indicate CDIPT transcript levels of cells with induced CLCA2 expression; blue box-plots represent CDIPT transcript levels of non-induced cells. The yellow box plot represents the transcript level in control cells at the time point of induction. 0, 24 and 48 indicate the time points (h) of lysate preparation post induction.

**Right: RT-qPCR in duplex assay with β-2-microglobulin as internal reference for normalisation**

Normalised CDIPT mRNA levels of induced clone #3 are shown in relation to mRNA levels in control cells (T47D Tet-on with empty expression vector).

## MLL2

Myeloid/lymphoid or mixed-lineage leukemia 2 gene plays a role in apoptosis and in alterations of cell adhesion. MLL2 is a member of the human MLL family, which belongs to a larger SET1 family of histone methyltransferases. MML2 is a transcriptional activator that induces the transcription of target genes by covalent histone modification. It appears to be involved in the regulation of adhesion-related cytoskeletal events, which might affect cell growth and survival [100]. Members of the MLL protein family have been found to cause acute leukemia. Deletion studies revealed that alterations of the CxxC domain (Zn-binding domain) disrupts its oncogenic potential [101]. Loss-of-function mutations within the coding sequence of NF-kappaB inhibitory molecules such as IkappaBalpha or p100 leads to constitutive NF-kappaB activation in haematological malignancies. Hut-78, a truncated form of p100, constitutively generates p52 and contributes to the development of T-cell lymphomas and was recently shown to induce MMP9 gene expression. Conversely, MMP9 gene expression is impaired in p52-depleted HUT-78 cells. Interestingly, MLL1 and MLL2 H3K4 methyltransferase complexes are tethered by p52 on the MMP9 but not on the IkappaBalpha promoter, and the H3K4 trimethyltransferase activity recruited on the MMP9 promoter is impaired in p52-depleted HUT-78 cells. Moreover, MLL1 and MLL2 are associated with Hut-78 in a native chromatin-enriched extract. This molecular mechanism recruits a H3K4 histone methyltransferase complex on the promoter of a NF-kappaB-dependent gene induces its expression and potentially the invasive potential of lymphoma cells harbouring constitutive activity of the alternative NF-kappaB-activating pathway [102].

Overexpression following CLCA2 induction could be observed in microarray studies and was confirmed by RT-qPCT (Figure 70).

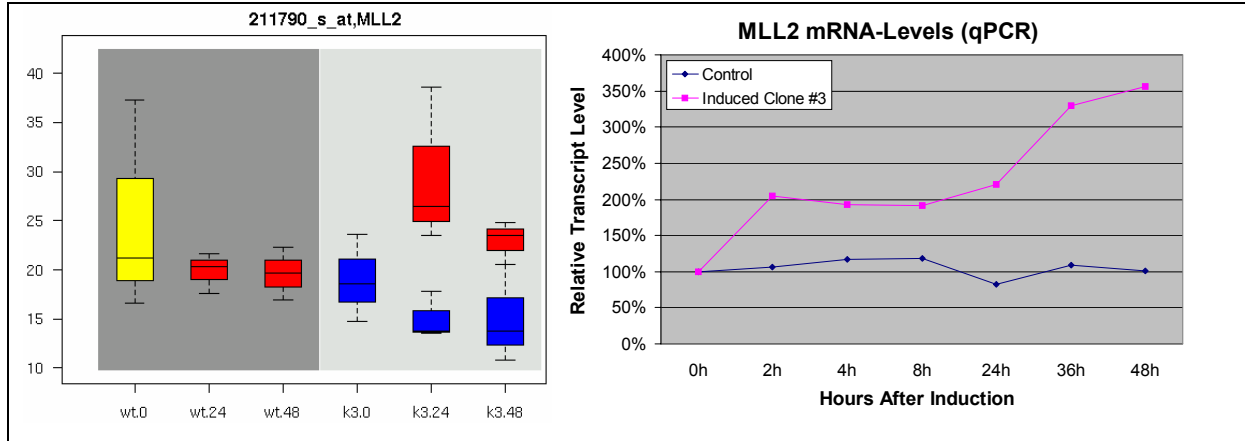


**Figure 70. MLL2 mRNA levels in induced CLCA2-expressing T47D Tet-on clone #3 versus control**  
**Left: Affymetrix microarray studies using Affymetrix GeneChip Human Genome U133 Array**  
The MAS5-normalised expression levels of MLL2 mRNA are shown in box-plots. The vertical centre line in the box indicates the median; the box itself represents the interquartile range (IQR) between the first and third quartiles. Whiskers extend to 1.5 times the IQR. In the left dark grey field, expression levels in control cells (T47D Tet-on) are shown. In the right light grey field, expression levels in T47D Tet-on clone #3 (k3) are represented. Red box-plots indicate MLL2 transcript levels of cells with induced CLCA2 expression; blue box-plots represent MLL2 transcript levels of non-induced cells. The yellow box plot represents the transcript level in control cells at the time point of induction. 0, 24 and 48 indicate the time points (h) of lysate preparation post induction.  
**Right: RT-qPCR in duplex assay with β-2-microglobulin as internal reference for normalisation**  
Normalised MLL2 mRNA levels of induced clone #3 are shown in relation to mRNA levels in control cells (T47D Tet-on with empty expression vector).

## AFF4 (MCEF)

AF4/MR2 family member 4 (also known as MCEF), the newest member of the AF4 family of transcription factors involved in leukemia, is a positive transcription elongation factor-b-associated protein [103].

Its overexpression after CLCA2 induction shown on microarray arrays was confirmed by RT-qPCR (Figure 71).

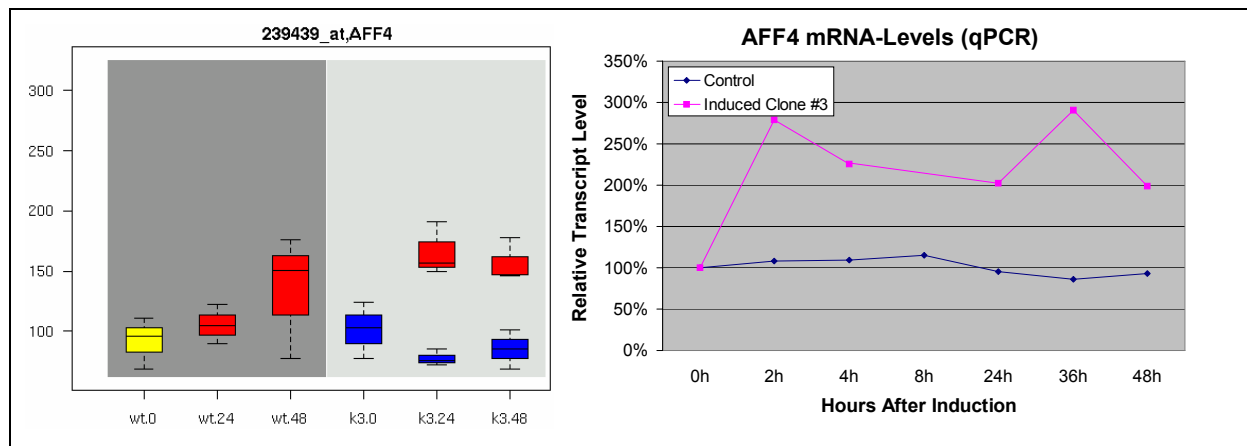


**Figure 71. AFF4 mRNA levels in induced CLCA2-expressing T47D Tet-on clone #3 versus control**

**Left: Affymetrix microarray studies using Affymetrix GeneChip Human Genome U133 Array**

The MAS5-normalised expression levels of AFF4 mRNA are shown in box-plots. The vertical centre line in the box indicates the median; the box itself represents the interquartile range (IQR) between the first and third quartiles. Whiskers extend to 1.5 times the IQR. In the left dark grey field, expression levels in control cells (T47D Tet-on) are shown. In the right light grey field, expression levels in T47D Tet-on clone #3 (k3) are represented. Red box-plots indicate AFF4 transcript levels of cells with induced CLCA2 expression; blue box-plots represent AFF4 transcript levels of non-induced cells. The yellow box plot represents the transcript level in control cells at the time point of induction. 0, 24 and 48 indicate the time points (h) of lysate preparation post induction.

**Right: RT-qPCR in duplex assay with β-2-microglobulin as internal reference for normalisation**

Normalised AFF4 mRNA levels of induced clone #3 are shown in relation to mRNA levels in control cells (T47D Tet-on with empty expression vector).

## UNC84A

UNC84A belongs to the conserved family of SUN proteins. Human UNC84A (Sun1) is a homolog of *C. elegans* UNC-84, a protein involved in nuclear anchorage and migration. Targeting of UNC84A to the nuclear envelope revealed that the N-terminal 300 amino acids are crucial for efficient nuclear envelope localisation of UNC84A whereas the conserved C-terminal SUN domain is not required. Localisation and anchoring of UNC84A is not dependent on the lamin proteins, in contrast to what had been observed for *C. elegans* UNC-84. If UNC84A can also interact with cytoplasmic tracts of transmembrane proteins such as CLCA2 to contribute to ECM interaction/migration is not yet known [104].

The transcript is found upregulated both, by Affymetrix GeneChip analysis and RT-qPCR (Figure 72).

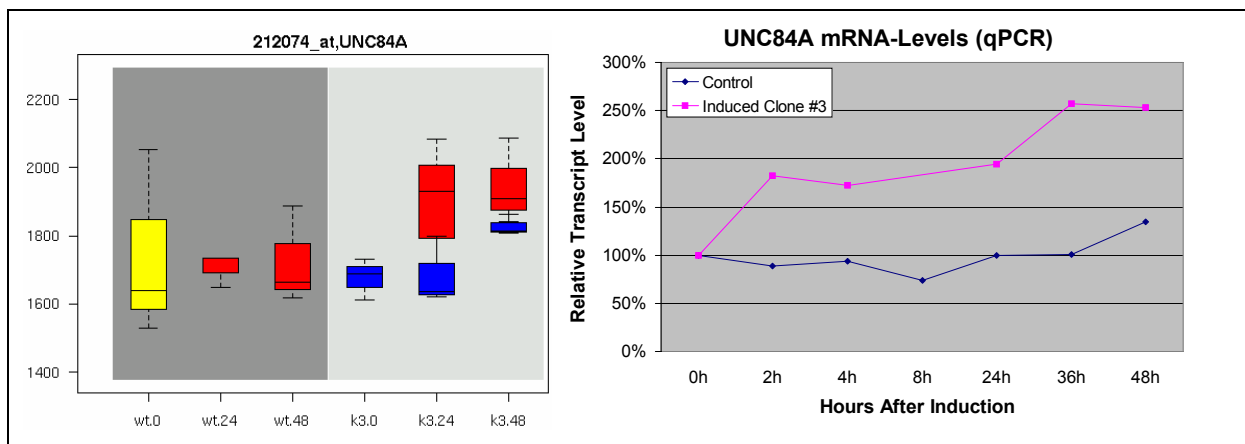


**Figure 72. UNC84A mRNA levels in induced CLCA2-expressing T47D Tet-on clone #3 versus control**  
**Left: Affymetrix microarray studies using Affymetrix GeneChip Human Genome U133 Array**

The MAS5-normalised expression levels of UNC84A mRNA are shown in box-plots. The vertical centre line in the box indicates the median; the box itself represents the interquartile range (IQR) between the first and third quartiles. Whiskers extend to 1.5 times the IQR. In the left dark grey field, expression levels in control cells (T47D Tet-on) are shown. In the right light grey field, expression levels in T47D Tet-on clone #3 are represented. Red box-plots indicate UNC84A transcript levels of cells with induced CLCA2 expression; blue box-plots represent UNC84A transcript levels of non-induced cells. The yellow box plot represents the transcript level in control cells at the time point of induction. 0, 24 and 48 indicate the time points (h) of lysate preparation post induction.

**Right: RT-qPCR in duplex assay with β-2-microglobulin as internal reference for normalisation**

Normalised UNC84A mRNA levels of induced clone #3 are shown in relation to mRNA levels in control cells (T47D Tet-on with empty expression vector).

## DTX2 (Deltex2)

The *deltex* null mutant indicates tissue-specific *deltex*-dependent Notch signaling in *Drosophila*. It was further shown, that in *Drosophila* *deltex* mediates suppressor of hairless-independent and late-endosomal activation of Notch signaling. In addition, the *Drosophila* Nedd4-like protein suppressor of Deltex, Su(dx), has been characterised as a negative regulator of Notch receptor signaling, an intercellular signaling pathway of fundamental importance for multiple cell fate decisions [105;106].

Upregulation of DTX2 could be confirmed on the Affymetrix GeneChip and by RT-qPCR (Figure 73).

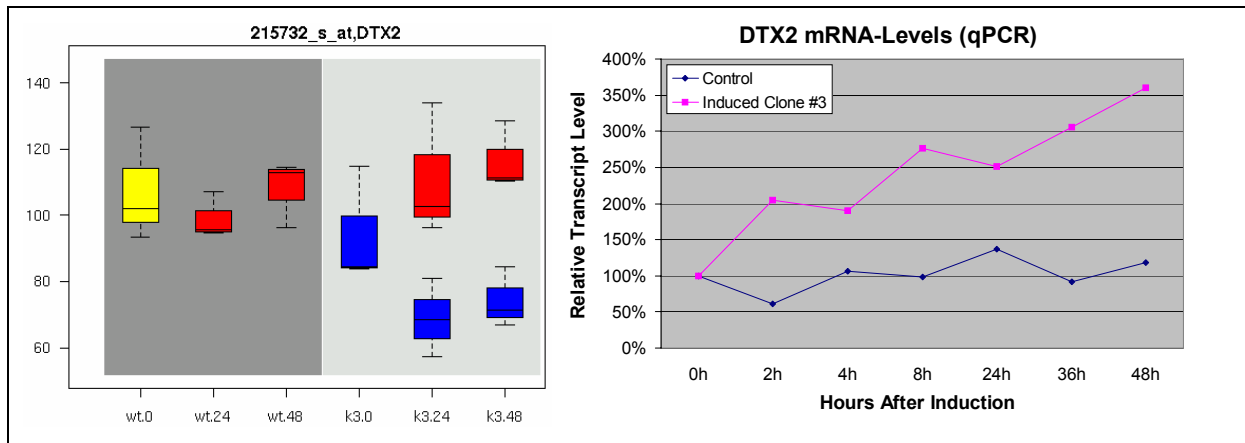


**Figure 73. DTX2 mRNA levels in induced CLCA2-expressing T47D Tet-on clone #3 versus control**

**Left: Affymetrix microarray studies using Affymetrix GeneChip Human Genome U133 Array**

The MAS5-normalised expression levels of DTX2 mRNA are shown in box-plots. The vertical centre line in the box indicates the median; the box itself represents the interquartile range (IQR) between the first and third quartiles. Whiskers extend to 1.5 times the IQR. In the left dark grey field, expression levels in control cells (T47D Tet-on) are shown. In the right light grey field, expression levels in T47D Tet-on clone #3 (k3) are represented. Red box-plots indicate DTX2 transcript levels of cells with induced CLCA2 expression; blue box-plots represent DTX2 transcript levels of non-induced cells. The yellow box plot represents the transcript level in control cells at the time point of induction. 0, 24 and 48 indicate the time points (h) of lysate preparation post induction.

**Right: RT-qPCR in duplex assay with β-2-microglobulin as internal reference for normalisation**

Normalised DTX2 mRNA levels of induced clone #3 are shown in relation to mRNA levels in control cells (T47D Tet-on with empty expression vector).

## C10orf118

Chromosome 10 open reading frame 118 of unknown function was found upregulated after CLCA2-induction on the Affymetrix GeneChip and was confirmed by RT-qPCR (Figure 74).

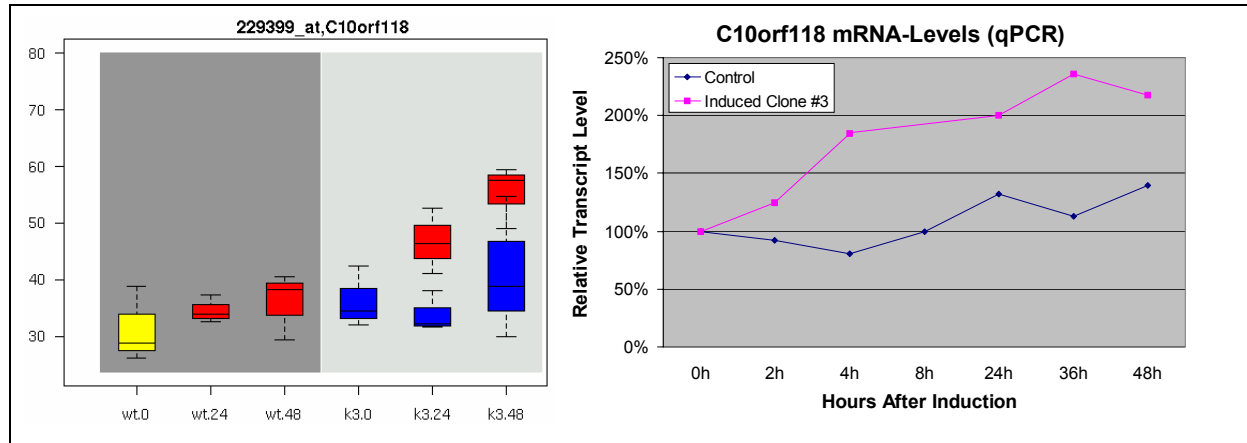


**Figure 74. C10orf118 mRNA levels in induced CLCA2-expressing T47D Tet-on clone #3 versus control**  
**Left: Affymetrix microarray studies using Affymetrix GeneChip Human Genome U133 Array**

The MAS5-normalised expression levels of C10orf118 mRNA are shown in box-plots. The vertical centre line in the box indicates the median; the box itself represents the interquartile range (IQR) between the first and third quartiles. Whiskers extend to 1.5 times the IQR. In the left dark grey field, expression levels in control cells (T47D Tet-on) are shown. In the right light grey field, expression levels in T47D Tet-on clone #3 (k3) are represented. Red box-plots indicate C10orf118 transcript levels of cells with induced CLCA2 expression; blue box-plots represent C10orf118 transcript levels of non-induced cells. The yellow box plot represents the transcript level in control cells at the time point of induction. 0, 24 and 48 indicate the time points (h) of lysate preparation post induction.

**Right: RT-qPCR in duplex assay with β-2-microglobulin as internal reference for normalisation**

Normalised C10orf118 mRNA levels of induced clone #3 are shown in relation to mRNA levels in control cells (T47D Tet-on with empty expression vector).

## SATB1

SATB1 is a genome organizer that tethers multiple genomic loci and recruits chromatin-remodelling enzymes to regulate chromatin structure and gene expression. It was shown that SATB1 is expressed by aggressive breast cancer cells and its expression level has high prognostic significance, independent of lymph-node status [107]. Knock-down of SATB1 in highly aggressive cancer cells altered the expression of lots of genes, reversing tumourigenesis by restoring breast-like acinar polarity and inhibiting tumour growth and metastasis *in vivo*. Conversely, ectopic SATB1 expression in non-aggressive cells led to gene expression patterns consistent with aggressive-tumour phenotypes, acquiring metastatic activity *in vivo*. SATB1 delineates specific epigenetic modifications at target gene loci, directly upregulating metastasis-associated genes while downregulating tumour-suppressor genes. SATB1 reprogrammes chromatin organisation and the expression profiles of breast tumours to promote growth and metastasis [107].

The upregulation found on Affymetrix GeneChip could not be confirmed by RT-qPCR (Figure 75).

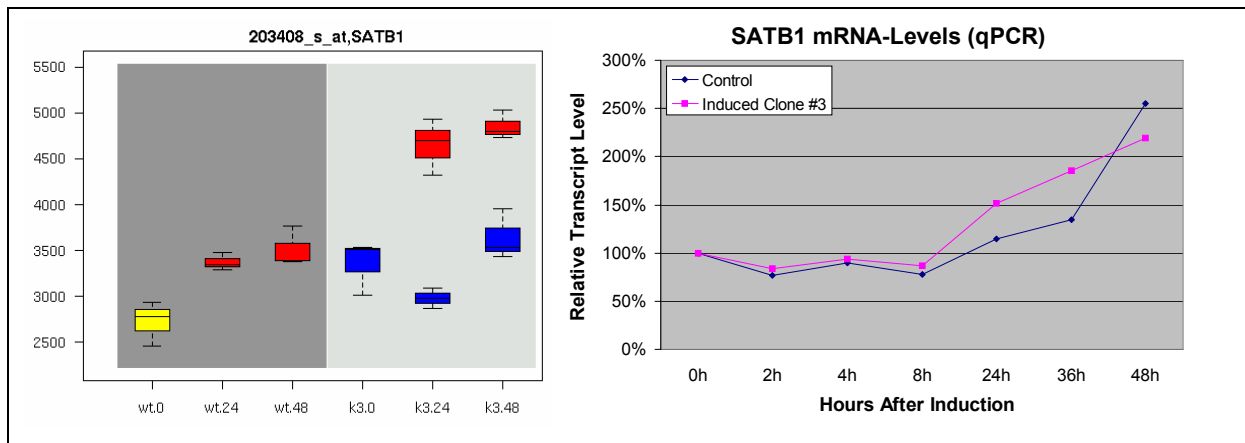


**Figure 75. SATB1 mRNA levels in induced CLCA2-expressing T47D Tet-on clone #3 versus control**

**Left: Affymetrix microarray studies using Affymetrix GeneChip Human Genome U133 Array**

The MAS5-normalised expression levels of SATB1 mRNA are shown in box-plots. The vertical centre line in the box indicates the median; the box itself represents the interquartile range (IQR) between the first and third quartiles. Whiskers extend to 1.5 times the IQR. In the left dark grey field, expression levels in control cells (T47D Tet-on) are shown. In the right light grey field, expression levels in T47D Tet-on clone #3 (k3) are represented. Red box-plots indicate SATB1 transcript levels of cells with induced CLCA2 expression; blue box-plots represent SATB1 transcript levels of non-induced cells. The yellow box plot represents the transcript level in control cells at time point of induction. 0, 24 and 48 indicate the time points (h) of lysate preparation post induction.

**Right: RT-qPCR in duplex assay with β-2-microglobulin as internal reference for normalisation**

Normalised SATB1 mRNA levels of induced clone #3 are shown in relation to mRNA levels in control cells (T47D Tet-on with empty expression vector).



## EP300

The transcriptional coactivator E1A binding protein p300 is a ubiquitous nuclear phosphoprotein and transcriptional cofactor with intrinsic acetyltransferase activity. p300 controls the expression of numerous genes in cell-type and signal-specific manner, and plays a pivotal role in cellular proliferation, apoptosis, and embryogenesis [108].

Although the expression profile of EP300 was contradictory, it was analysed by RT-qPCR and found to be downregulated (Figure 76). One reason for this discrepancy might be the presence of various isoforms or splice variants of EP300, generating a contradictory profile on Affymetrix GeneChips.

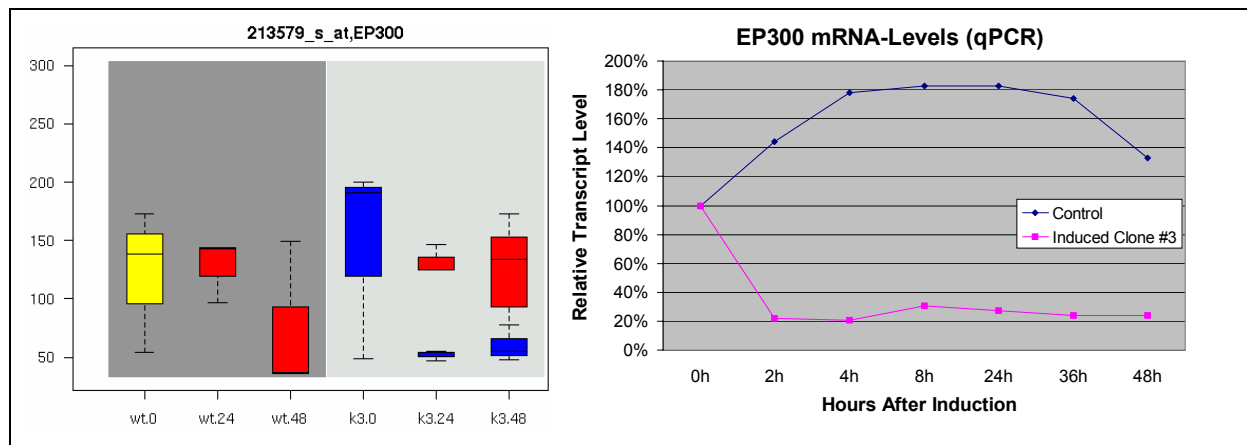


**Figure 76. EP300 mRNA levels in induced CLCA2-expressing T47D Tet-on clone #3 versus control**

**Left: Affymetrix microarray studies using Affymetrix GeneChip Human Genome U133 Array**

The MAS5-normalised expression levels of EP300 mRNA are shown in box-plots. The vertical centre line in the box indicates the median; the box itself represents the interquartile range (IQR) between the first and third quartiles. Whiskers extend to 1.5 times the IQR. In the left dark grey field, expression levels in control cells (T47D Tet-on) are shown. In the right light grey field, expression levels in T47D Tet-on clone #3 (k3) are represented. Red box-plots indicate EP300 transcript levels of cells with induced CLCA2 expression; blue box-plots represent EP300 transcript levels of non-induced cells. The yellow box plot represents the transcript level in control cells at the time point of induction. 0, 24 and 48 indicate the time points (h) of lysate preparation post induction.

**Right: RT-qPCR in duplex assay with  $\beta$ -2-microglobulin as internal reference for normalisation**

Normalised EP300 mRNA levels of induced clone #3 are shown in relation to mRNA levels in control cells (T47D Tet-on with empty expression vector).

## LTBP1

Overexpression of Latent transforming growth factor beta binding protein 1 (LTBP1) in association with TGF-beta 1 was found in ovarian carcinoma [109].

LTBP1 is impressively upregulated when analysed on GeneChips. Although RT-qPCR confirmed upregulation, the level of upregulation is significantly lower (Figure 77).

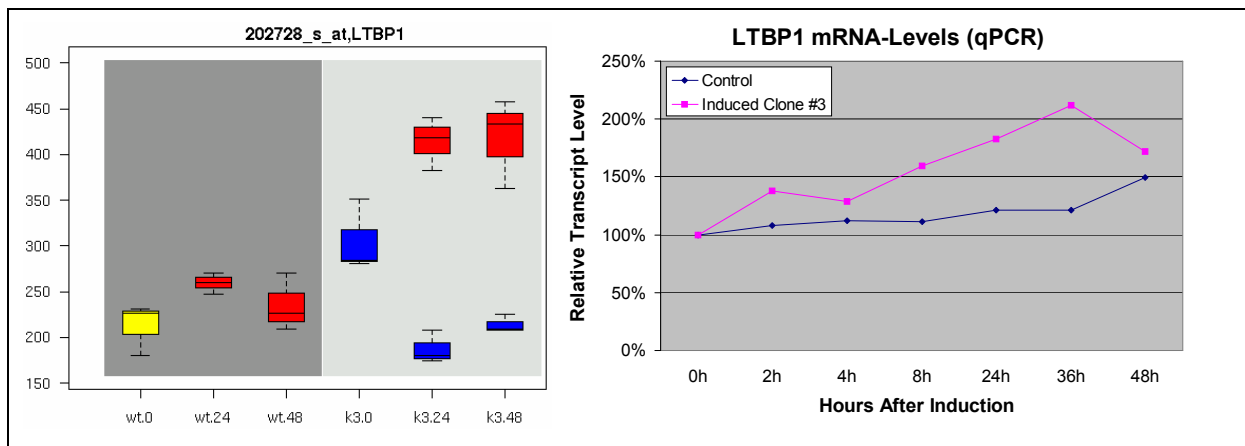


**Figure 77. LTBP1 mRNA levels in induced CLCA2-expressing T47D Tet-on clone #3 versus control**

**Left: Affymetrix microarray studies using Affymetrix GeneChip Human Genome U133 Array**  
The MAS5-normalised expression levels of LTBP1 mRNA are shown in box-plots. The vertical centre line in the box indicates the median; the box itself represents the interquartile range (IQR) between the first and third quartiles. Whiskers extend to 1.5 times the IQR. In the left dark grey field, expression levels in control cells (T47D Tet-on) are shown. In the right light grey field, expression levels in T47D Tet-on clone #3 (k3) are represented. Red box-plots indicate LTBP1 transcript levels of cells with induced CLCA2 expression; blue box-plots represent LTBP1 transcript levels of non-induced cells. The yellow box plot represents the transcript level in control cells at the time point of induction. 0, 24 and 48 indicate the time points (h) of lysate preparation post induction.

**Right: RT-qPCR in duplex assay with β-2-microglobulin as internal reference for normalisation**  
Normalised LTBP1 mRNA levels of induced clone #3 are shown in relation to mRNA levels in control cells (T47D Tet-on with empty expression vector).

## TSC1

Tuberous sclerosis complex 1 is a tumour suppressor gene which is involved in the mTOR pathway. Interestingly, a recently published study suggests the involvement of TSC genes and other members of the mTOR signaling pathway in the pathogenesis of oral squamous cell carcinoma [110].

TSC1 was also shown to be involved in induction of autophagy. The role of autophagy in oncogenesis is manifold: At the early stages of tumor formation, autophagy acts as a tumor suppressor. During tumor progression, autophagy contributes to tumor growth. For instance, inhibition of autophagy by siRNAs targeting essential autophagy genes such as TSC1, sensitises cancer cells to the induction of apoptosis by radiotherapy and a wide range of chemotherapeutic agents. Inhibition of autophagy sensitises breast cancer cells to killing by the estrogen receptor antagonist tamoxifen, prostate cancer cells to androgen deprivation, colon cancer cells to amino-acid or glucose deprivation, and Bax<sup>-/-</sup> HCT116 cells to TRAIL-induced apoptosis. Similar effects have been observed sensitising tumor cells to anoikis (apoptosis due to detachment from the extracellular matrix) [111].

Upregulation of TSC1 in cells with induced CLCA2 expression could be confirmed by both methods (Figure 78).

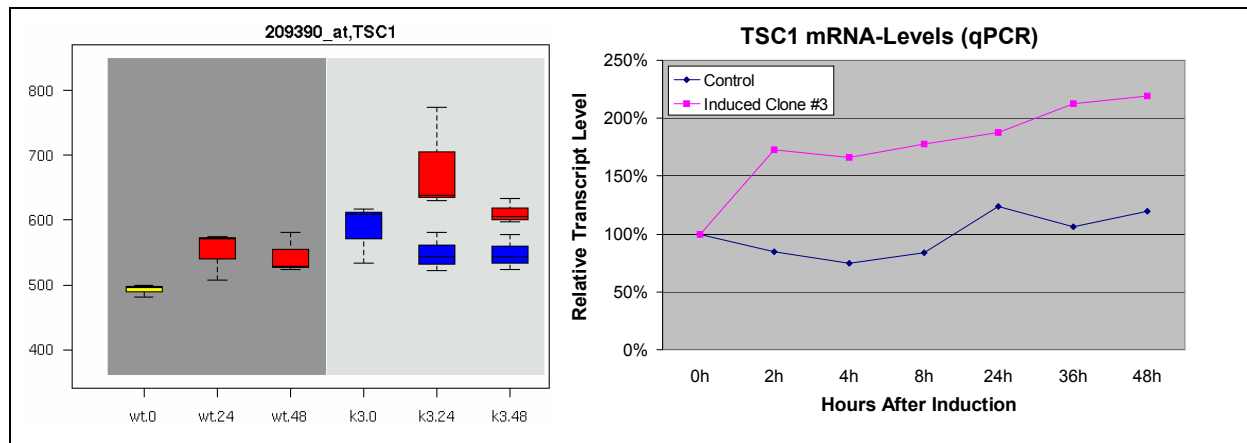


**Figure 78. TSC1 mRNA levels in induced CLCA2-expressing T47D Tet-on clone #3 versus control**

**Left: Affymetrix microarray studies using Affymetrix GeneChip Human Genome U133 Array**

The MAS5-normalised expression levels of TSC1 mRNA are shown in box-plots. The vertical centre line in the box indicates the median; the box itself represents the interquartile range (IQR) between the first and third quartiles. Whiskers extend to 1.5 times the IQR. In the left dark grey field, expression levels in control cells (T47D Tet-on) are shown. Red box-plots indicate TSC1 transcript levels of cells with induced CLCA2 expression; blue box-plots represent TSC1 transcript levels of non-induced cells. The yellow box plot represents the transcript level in control cells at the time point of induction. 0, 24 and 48 indicate the time points (h) of lysate preparation post induction.

**Right: RT-qPCR in duplex assay with β-2-microglobulin as internal reference for normalisation**

Normalised TSC1 mRNA levels of induced clone #3 are shown in relation to mRNA levels in control cells (T47D Tet-on with empty expression vector).

## MACF1

Microtubule-actin crosslinking factor 1 is involved in the Wnt signaling pathway [112]. An upregulation after CLCA2-induction could be observed on the Affymetrix GeneChip and at later time points applying RT-qPCR (Figure 79).

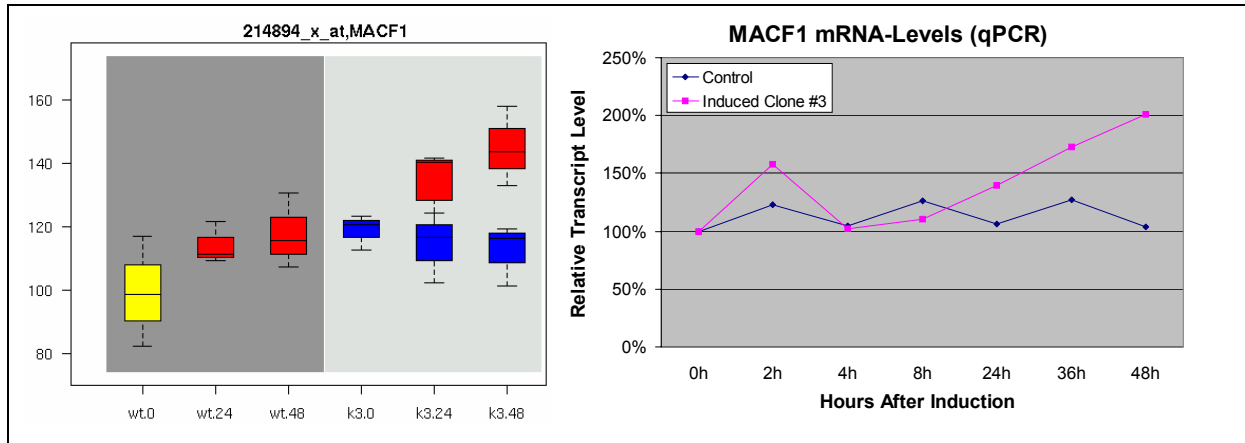


**Figure 79. MACF1 mRNA levels in induced CLCA2-expressing T47D Tet-on clone #3 versus control**  
**Left: Affymetrix microarray studies using Affymetrix GeneChip Human Genome U133 Array**

The MAS5-normalised expression levels of MACF1 mRNA are shown in box-plots. The vertical centre line in the box indicates the median; the box itself represents the interquartile range (IQR) between the first and third quartiles. Whiskers extend to 1.5 times the IQR. In the left dark grey field, expression levels in control cells (T47D Tet-on) are shown. In the right light grey field, expression levels in T47D Tet-on clone #3 (k3) are represented. Red box-plots indicate MACF1 transcript levels of cells with induced CLCA2 expression; blue box-plots represent MACF1 transcript levels of non-induced cells. The yellow box plot represents the transcript level in control cells at the time point of induction. 0, 24 and 48 indicate the time points (h) of lysate preparation post induction.

**Right: RT-qPCR in duplex assay with β-2-microglobulin as internal reference for normalisation**

Normalised MACF1 mRNA levels of induced clone #3 are shown in relation to mRNA levels in control cells (T47D Tet-on with empty expression vector).

## CHD6

Chromodomain helicase DNA binding protein 6 is a DNA-dependent ATPase that localises at nuclear sites of mRNA synthesis [113]. CHD proteins have drawn increased attention, because some of them were found to form large multi-subunit complexes, involved in transcription-related events like gene activation, suppression, or histone modification [113].

CHD6 was found upregulated after CLCA2-induction both, on the Affymetrix GeneChips and by RT-qPCR (Figure 80).

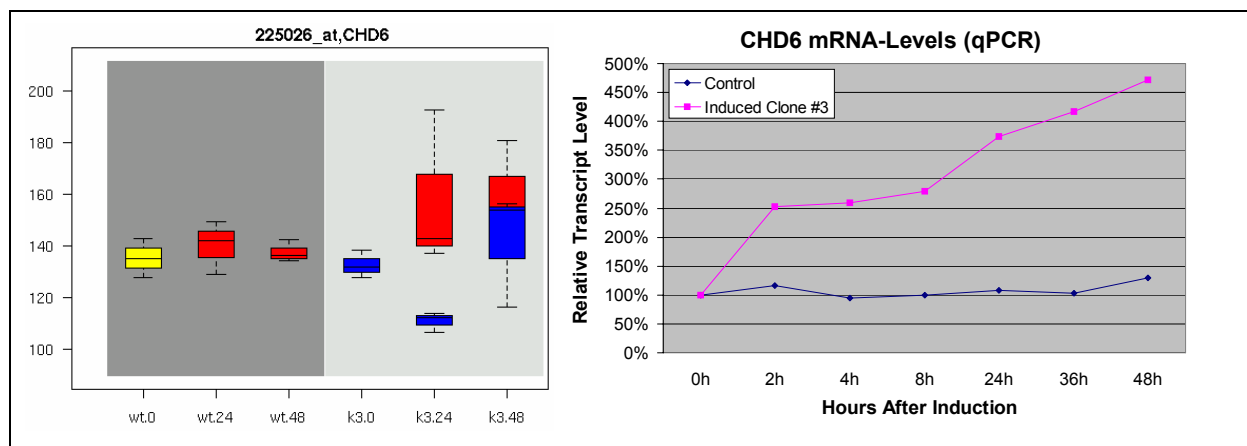


**Figure 80. CHD6 mRNA levels in induced CLCA2-expressing T47D Tet-on clone #3 versus control**

**Left: Affymetrix microarray studies using Affymetrix GeneChip Human Genome U133 Array**

The MAS5-normalised expression levels of CHD6 mRNA are shown in box-plots. The vertical centre line in the box indicates the median; the box itself represents the interquartile range (IQR) between the first and third quartiles. Whiskers extend to 1.5 times the IQR. In the left dark grey field, expression levels in control cells (T47D Tet-on) are shown. In the right light grey field, expression levels in T47D Tet-on clone #3 (k3) are represented. Red box-plots indicate CHD6 transcript levels of cells with induced CLCA2 expression; blue box-plots represent CHD6 transcript levels of non-induced cells. The yellow box plot represents the transcript level in control cells at the time point of induction. 0, 24 and 48 indicate the time points (h) of lysate preparation post induction.

**Right: RT-qPCR in duplex assay with β-2-microglobulin as internal reference for normalisation**

Normalised CHD6 mRNA levels of induced clone #3 are shown in relation to mRNA levels in control cells (T47D Tet-on with empty expression vector).

## RUTBC3

RUN and TBC1 domain containing 3 gene belongs to the RUN domain protein family [114]. RUN domains are present in several proteins that are linked particularly to the functions of GTPases in the Rap and Rab families. They could hence play an important role in multiple Ras-like GTPase signaling pathways [115].

RUTBC3 was found to be upregulated after induction of CLCA2 expression in both assays (Figure 81).

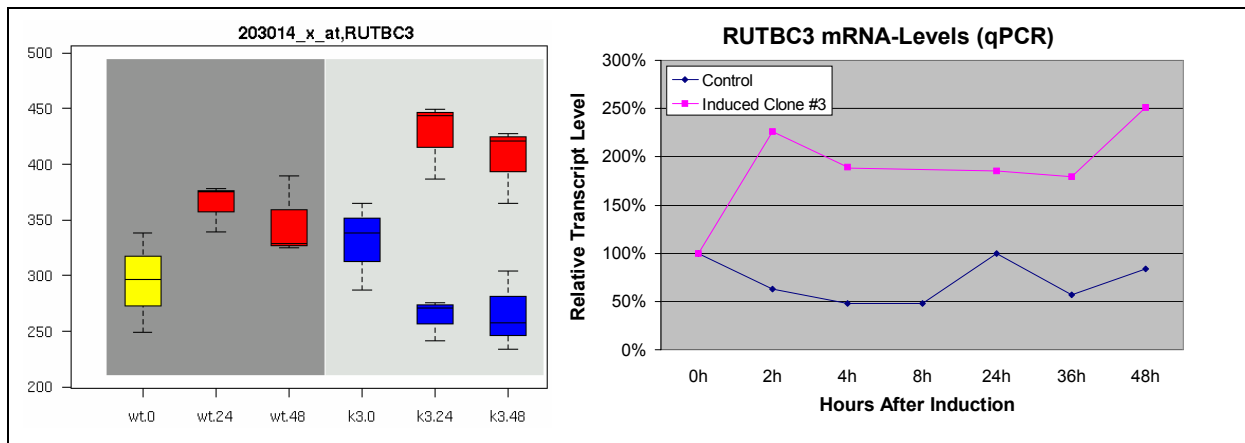


**Figure 81. RUTBC3 mRNA levels in induced CLCA2-expressing T47D Tet-on clone #3 versus control**  
**Left: Affymetrix microarray studies using Affymetrix GeneChip Human Genome U133 Array**

The MAS5-normalised expression levels of RUTBC3 mRNA are shown in box-plots. The vertical centre line in the box indicates the median; the box itself represents the interquartile range (IQR) between the first and third quartiles. Whiskers extend to 1.5 times the IQR. In the left dark grey field, expression levels in control cells (T47D Tet-on) are shown. In the right light grey field, expression levels in T47D Tet-on clone #3 (k3) are represented. Red box-plots indicate RUTBC3 transcript levels of cells with induced CLCA2 expression; blue box-plots represent RUTBC3 transcript levels of non-induced cells. The yellow box plot represents the transcript level in control cells at the time point of induction. 0, 24 and 48 indicate the time points (h) of lysate preparation post induction.

**Right: RT-qPCR in duplex assay with β-2-microglobulin as internal reference for normalisation**

Normalised RUTBC3 mRNA levels of induced clone #3 are shown in relation to mRNA levels in control cells (T47D Tet-on with empty expression vector).

## P4HA2

Prolyl-4 hydroxylase-2 belonging to the procollagen hydroxylase protein family was shown earlier to be differentially regulated upon ERBB2 (HER2/neu) overexpression in human mammary luminal epithelial cells [116]. Furthermore, P4HA2 is suggested to be a potent molecular classifier able to discriminate between papillary thyroid carcinoma and non-malignant thyroid [117]. In this study P4HA2 was found to be upregulated after CLCA2-induction when analysed on Affymetrix GeneChips. However, no specific CLCA2-driven induction of this gene was detected in the RT-qPCR (Figure 82).

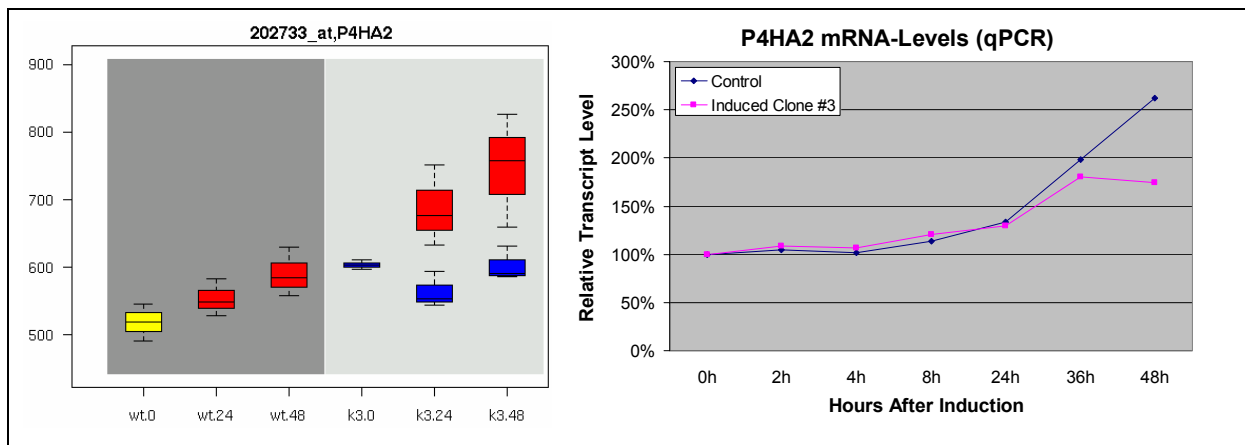


**Figure 82. P4HA2 mRNA levels in induced CLCA2-expressing T47D Tet-on clone #3 versus control**

**Left: Affymetrix microarray studies using Affymetrix GeneChip Human Genome U133 Array**

The MAS5-normalised expression levels of P4HA2 mRNA are shown in box-plots. The vertical centre line in the box indicates the median; the box itself represents the interquartile range (IQR) between the first and third quartiles. Whiskers extend to 1.5 times the IQR. In the left dark grey field, expression levels in control cells (T47D Tet-on) are shown. In the right light grey field, expression levels in T47D Tet-on clone #3 (k3) are represented. Red box-plots indicate P4HA2 transcript levels of cells with induced CLCA2 expression; blue box-plots represent P4HA2 transcript levels of non-induced cells. The yellow box plot represents the transcript level in control cells at the time point of induction. 0, 24 and 48 indicate the time points (h) of lysate preparation post induction.

**Right: RT-qPCR in duplex assay with β-2-microglobulin as internal reference for normalisation**

Normalised P4HA2 mRNA levels of induced clone #3 are shown in relation to mRNA levels in control cells (T47D Tet-on with empty expression vector).

## ASPM

Asp (abnormal spindle)-like, microcephaly associated (drosophila) gene was recently found as a novel marker for vascular invasion, early recurrence, and poor prognosis of hepatocellular carcinoma [118]. Overexpression after CLCA2-induction was found on the Affymetrix GeneChip. Although a similar expression profile in CLCA2-induced and control cells was shown by RT-qPCR, the levels of CLCA2 transcript were higher in CLCA2-expressing cells (Figure 83).

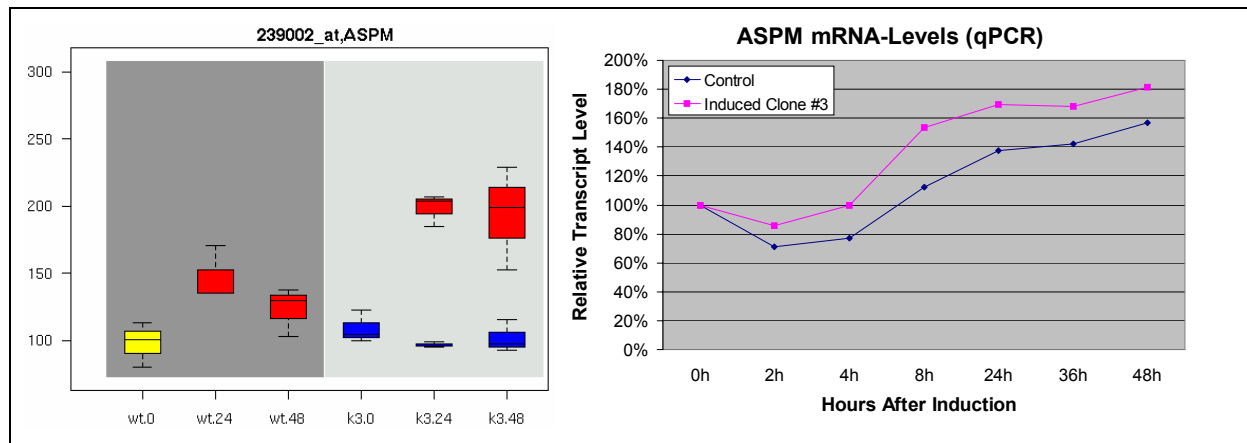


**Figure 83. ASPM mRNA levels in induced CLCA2-expressing T47D Tet-on clone #3 versus control**

**Left: Affymetrix microarray studies using Affymetrix GeneChip Human Genome U133 Array**

The MAS5-normalised expression levels of ASPM mRNA are shown in box-plots. The vertical centre line in the box indicates the median; the box itself represents the interquartile range (IQR) between the first and third quartiles. Whiskers extend to 1.5 times the IQR. In the left dark grey field, expression levels in control cells (T47D Tet-on) are shown. In the right light grey field, expression levels in T47D Tet-on clone #3 (k3) are represented. Red box-plots indicate ASPM transcript levels of cells with induced CLCA2 expression; blue box-plots represent ASPM transcript levels of non-induced cells. The yellow box plot represents the transcript level in control cells at the time point of induction. 0, 24 and 48 indicate the time points (h) of lysate preparation post induction.

**Right: RT-qPCR in duplex assay with β-2-microglobulin as internal reference for normalisation**

Normalised ASPM mRNA levels of induced clone #3 are shown in relation to mRNA levels in control cells (T47D Tet-on with empty expression vector).



To identify CLCA2 coregulated genes upon induced CLCA2 expression, expression profiles at different time points were analysed and mainly confirmed by RT-qPCR. These analyses were performed with two limitations: i) only a small number of genes out of a about 250 statistically relevant and differentially induced genes were selected for detailed analysis and ii) both assays (hybridisation on GeneChips and RT-qPCR) were performed only once, but samples from different time points were analysed. Nevertheless, as seen in Table 3 a good correlation between both approaches was achieved, only 2 out of 18 analysed expression profiles are questionable (Table 3).

GENE ID	Chip	qPCR
AFF4	u	u
ASPM	u	u?
C10orf118	u	u
CDIPT	u	u
CHD6	u	u
CLCA2	u	u
DTX2	u	u
EP300	d/i	d
LTBP1	u	u
MACF1	u	u
MLL2	u	u
P4HA2	i	i
RUTBC3	u	u
SATB1	i	i
SFI1	u	u
TP53BP1	i	i
TSC1	u	u
UNC84A	u	u

u upregulated  
d downregulated  
i indifferet

**Table 3. Comparison of expression data derived from Affymetrix microarray analysis and RT-qPCR**  
Status of gene regulation from microarray and RT-qPCR studies are opposed.

## Linking Profiles of Cells with Induced CLCA2 Expression to Canonical Pathways

As described above, a comprehensive study was performed on Affymetrix GeneChips in clones with inducible CLCA2 expression. Approximately 150 genes were shown to be specifically up- or downregulated in a statistically relevant mode (fold change > 1.8; p-value < 0.0001). In order to link these expression profiles of regulated genes to canonical pathways and bring them into a biological context, these data were analysed with the Ingenuity Pathways Analysis (IPA; Software of Ingenuity Systems Inc.). This program is a text- and data-mining program, which not only links gene and protein functions/interactions based on the knowledge of published data in the most relevant journals, but also allows to bring these interactions into a context of biological functions, regulatory cascades and functional groups (e.g. oncology/metastasis/prostate). It has to be mentioned that the presented studies can only be regarded as preliminary as the outcome of these *in silico* analyses have to be proven in experimental settings. On the other hand these data allow a much more focussed procedure for future experiments as this program not only describes protein-protein interactions, but also other types of reciprocal action such as protein-nucleic acid interactions. Based on these *in silico* analyses several interaction-networks were identified. Some exemplary statistically relevant networks are shown in Figure 85, Figure 86, Figure 87, and Figure 88.

For understanding the display of the following networks, an overview of the used symbols is given in Figure 84.

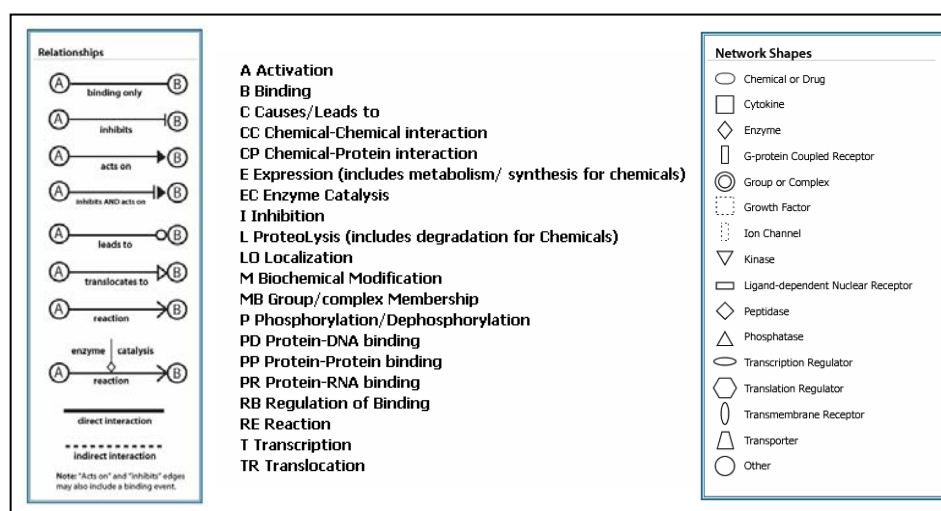


**Figure 84. Abbreviations and explanation of relationships and network shapes used for Ingenuity Pathway Analyst (IPA) Software of Ingenuity Systems, Inc.**





Network III (Figure 87) brings some of the differentially upregulated genes into the context of the ERK–MAPK signaling cascade with ERK as the knot of this network.

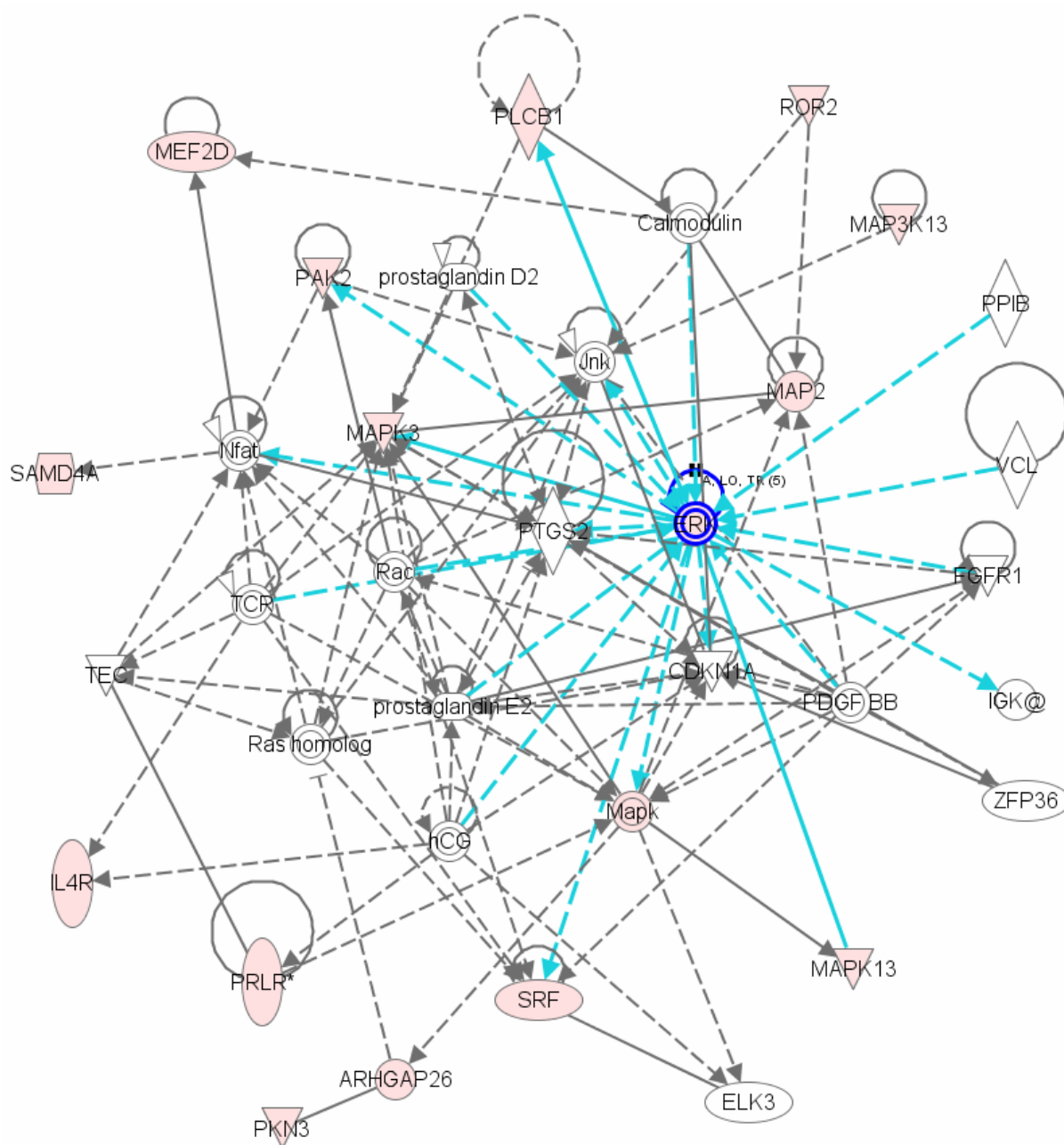


**Figure 87. Network III: Link to the ERK–MAPK pathway**

Display of interactions based on the Ingenuity Pathway Analyst (IPA) Software of Ingenuity Systems, Inc. Red-coloured genes have been identified on Affymetrix GeneChips as differentially expressed upon CLCA2 overexpression. A detailed description of symbols and abbreviations used is given in Figure 84. Lines/arrows in blue indicate interactions of ERK.

In Figure 88 merging of the most significant networks is shown, focussing exclusively on protein-protein interactions. As already mentioned, utilising this program, also other interactions such as protein-DNA interactions can be visualised. For the sake of simplicity only the protein-protein interaction is presented, highlighting biologically interesting clusters such as the cluster of v-src (involved in regulation of many different signaling cascades) or the polypyrimidine tract binding protein 1 (PTBP1) which is essentially involved in translational control (Figure 88).

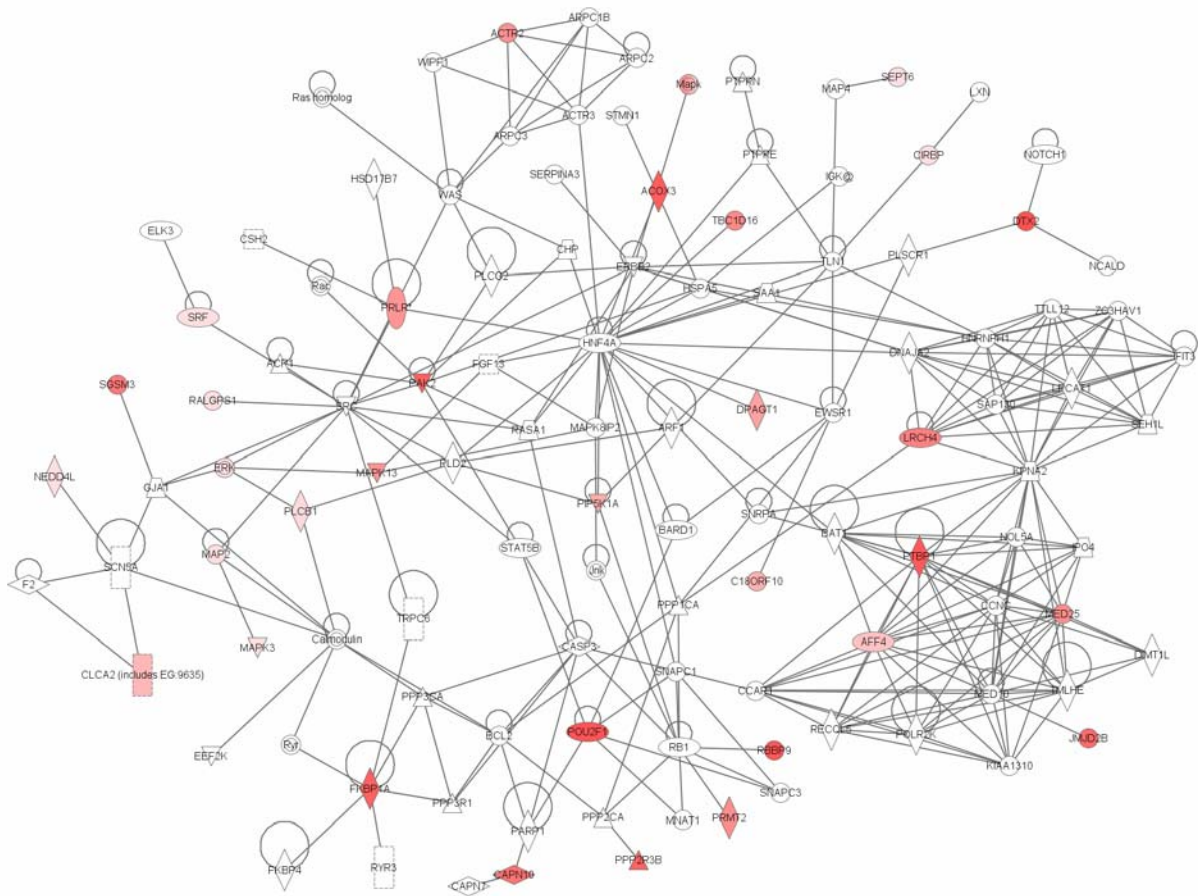


**Figure 88. Merging most significant networks**

Display of interactions based on the Ingenuity Pathway Analyst (IPA) Software of Ingenuity Systems, Inc. Red-coloured genes have been identified on Affymetrix GeneChips as differentially expressed upon CLCA2 overexpression. The intensity of the red colour indicates the level of differential regulation on GeneChips. A detailed description of symbols and abbreviations used is given in Figure 84.

### **Phospho-Proteomic Studies: Canonical Signaling Transduction Pathways**

Utilising the IPA software (see above), only data derived from expression profiling were applied so far. In order to learn more about the contribution of some important executor proteins of canonical pathways, which might be found activated/deactivated (=phosphorylated/dephosphorylated) in the experimental setting of CLCA2 induction, cell lysates which were taken at various time points of induced and non-induced T47D Tet-on clone #3 cells, were analysed on Western blots and on phospho-proteomic antibody arrays.

## Western Blots

Antibodies listed in Table 4 were used for Western blots.

Target Protein Name	Phospho Site	Company	Cat. No.
Akt	S473	Cell Signaling	#9271
Akt	S308	Cell Signaling	#9275
Akt	Y326	Cell Signaling	#2968
Akt	pan	Cell Signaling	#9272
GSK-3beta	S9	Cell Signaling	#9336
PTEN	S380	Cell Signaling	#9551
PDK1	S241	Cell Signaling	#3061
PDK1	pan	Cell Signaling	#3062
PI3K	p85 Y458 / p55 Y199	Cell Signaling	#4228
FAK	Y861	Biosource	44-626G
iKkalpha/beta	S176/180	Cell Signaling	#2697S
NF-KB p65	S536	Cell Signaling	#3031
NF-KB p65	pan	Cell Signaling	#3034
MEK 1/2	S217/221	Cell Signaling	#9121
p44/42 MAP Kinase	T202/Y204	Cell Signaling	#9101
p38 MAPK	T180/Y182	Cell Signaling	#9211
p90RSK	S380	Cell Signaling	#9341
RSK1	S221/S227	Biosource	44-924G
RSK1	S363/S369	Biosource	44-926G
Elk1	S383	Cell Signaling	#9181
Raf	S259	Cell Signaling	#9421
c-Raf	S338	Biosource	#9427
ERK 1 & 2	T185/Y187	Biosource	44-680G
Erk 1&2	pan	Biosource	44-654G
p70 S6 Kinase	T389	Cell Signaling	#9234S
p70 S6 Kinase	pan	Cell Signaling	#9202
mTOR	S2448	Cell Signaling	#2971
mTOR	S2481	Cell Signaling	#2974
4E-BP1	T37/46	Cell Signaling	#2855
4E-BP1	T70	Cell Signaling	#9455
4E-BP1	S65	Cell Signaling	#9451
FoxO1	S319	Cell Signaling	#2487
FoxO3a	S318/321	Cell Signaling	#9465
FoxO3a	S253	Cell Signaling	#9466
Stat1	Y701	Cell Signaling	#9171
Stat2	Y690	Cell Signaling	#4471
Stat3	Y705	Cell Signaling	#9131
Stat3	S727	Cell Signaling	#9134
Stat3	Y705	Cell Signaling	#9131
Stat5	Y694	Cell Signaling	#9351
Stat6	Y641	Cell Signaling	#9361
NPM/B23 (Nucleophosmin 1)	T234/T237	BioLegend	#619101
PKCe	pan	Biosource	AHO0743
p27	pan	novocastra	NCL-p27
Histon H3	S10	Upstate	#06-570
TSC2	T1462	Cell Signaling	#3611
TSC2	S1254	Cell Signaling	#3616
KI67	pan	Dako Cytomation	M7240

phosphorylated  
phosphorylated ?  
dephosphorylated  
dephosphorylated ?

**Table 4. Phospho-antibodies tested on protein lysates of induced/non-induced CLCA2-expressing T47D Tet-on clone #3**

Genes marked in green were found to be phosphorylated upon induction of CLCA2 expression.

Genes marked in yellow were found to be dephosphorylated upon induction of CLCA2 expression.



In Figure 89 Western blots of proteins which were found to be phosphorylated upon CLCA2-induction are shown. An increase in phosphorylation of AKT (S473; Figure 89a), ERK 1&2 (T185/Y187; Figure 89c), MAPK (T202/Y204; Figure 89d), RAF (S259; Figure 89e), CRAF (S338; Figure 89f), and PDK1 (S241; Figure 89g) was observed. No change in the phosphorylation pattern was seen for AKT at position S308. These data confirm previous predictions made through the usage of the IPA software, indicating a link to the ERK–MAPK canonical pathway.

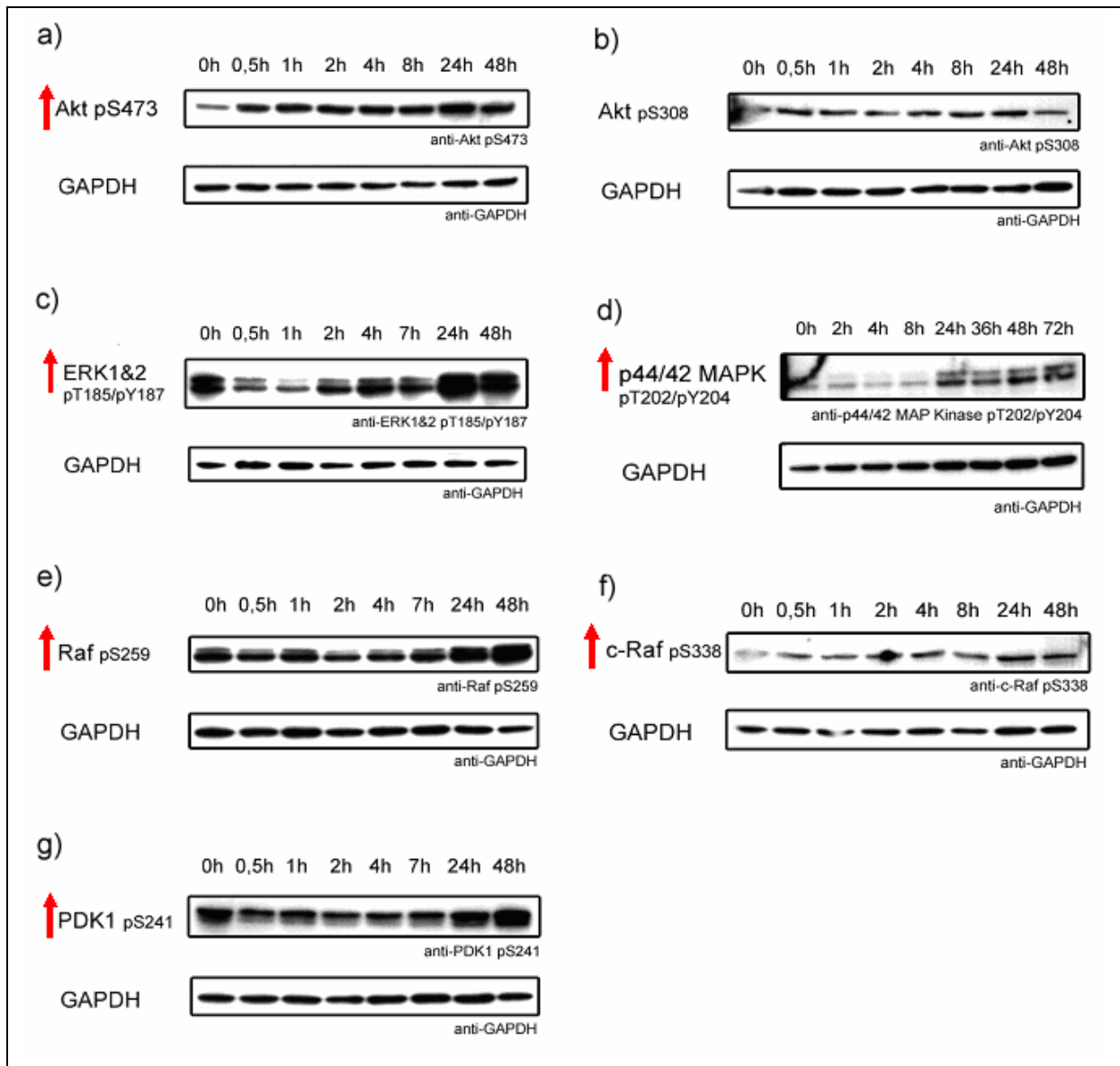


**Figure 89. Proteins involved in the AKT–ERK–MEK canonical pathway exhibiting an increase in phosphorylation upon induction of CLCA2 expression**

Expression of CLCA2 was induced in CLCA2-expressing T47D Tet-on clone #3 by addition of Doxycycline. Protein lysates were harvested at indicated time points post induction. CLCA2 expression of lysates was confirmed before use. For Western blot 50 µg protein was loaded per lane; the phosphorylation status of indicated proteins was tested with a respective phospho-antibody (for detailed information on antibodies see Table 4). GAPDH served as loading control.

In Figure 90 Western blots of identical protein lysates are shown. In contrast to Figure 83, proteins analysed were found dephosphorylated upon CLCA2-induction including mTOR (p2448; Figure 90a), 4E-BP1 (T37/T47; Figure 90b), STAT1 (Y701; Figure 90c), and NPM (T234/T237; Figure 90d), respectively. Nucleophosmin (NPM), for instance, is involved in cytoskeletal regulation [120], whereas deregulation of STAT1 indicates a link of CLCA2 expression to translational control.

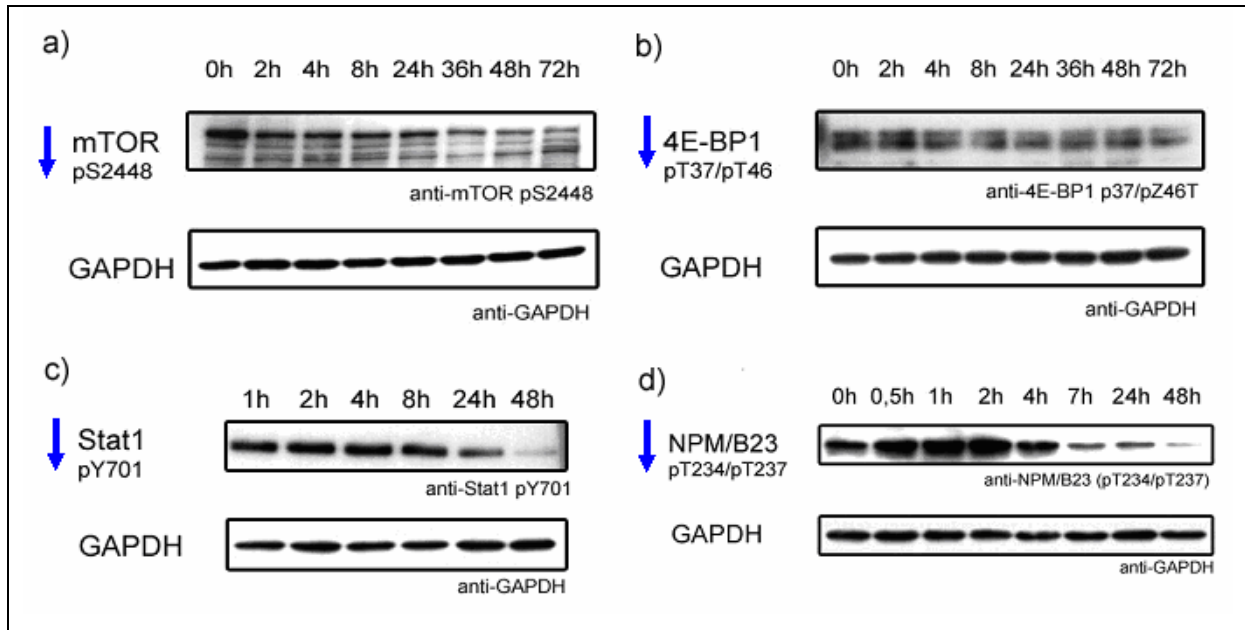


**Figure 90. Proteins exhibiting a decrease in phosphorylation upon induction of CLCA2 expression**

Expression of CLCA2 was induced in CLCA2-expressing T47D Tet-on clone #3 by addition of Doxycycline. Protein lysates were harvested at indicated time points post induction. CLCA2 expression of lysates was confirmed before use. For Western blot 50 µg protein was loaded per lane; the phosphorylation status of indicated proteins was tested with a respective phospho-antibody (for detailed information on antibodies see Table 4). GAPDH served as loading control.

Western blots of those antibodies listed in Table 4 which did not show any effect on the phosphorylation status of the respective protein upon CLCA2-induction, are not shown.

**Antibody Arrays: Proteome Profiler**

“Human Phospho-MAPK Array Kit” (Cat.# ARY002) and “Human Phospho-RTK Array Kit” (Cat.# ARY001) of R&D Systems were tested on lysates of CLCA2-expressing T47D Tet-on clones and on CLCA2-constitutively-expressing T47D clone.

The principle of the assays is that capture and control antibodies have been spotted in duplicates on nitrocellulose membranes. Cell lysates are diluted and incubated with the “Human Phospho-Array Kit”. After binding both, phosphorylated and non-phosphorylated proteins, unbound material is washed off. A cocktail of phospho-site-specific biotinylated antibodies is then used to detect phosphorylated kinases via Streptavidin-HRP and chemiluminescence.

The phosphorylation status of all three major families of mitogen-activated protein kinases (MAPKs), the extracellular signal-regulated kinases (ERK1/2), c-Jun N-terminal kinases (JNK1-3), different p38 isoforms ( $\alpha/\beta/\delta/\gamma$ ), other intracellular kinases such as Akt, GSK-3, and p70 S6 kinases was analysed, using the “Human Phospho-MAPK Array Kit” from R&D Systems and for analysis of the relative levels of phosphorylation of 42 different receptor tyrosine kinases, the “Human Phospho-RTK Array Kit” from R&D Systems (Cat.# ARY001) was used.

As shown in Figure 91, the duplicates of B3 and B4, representing ERK1 and the duplicates C3 and C4, representing ERK3 (red squares) show a higher phosphorylation level in CLCA2-constitutively-expressing T47D clone #47, than in control cells with the empty vector (blue squares).

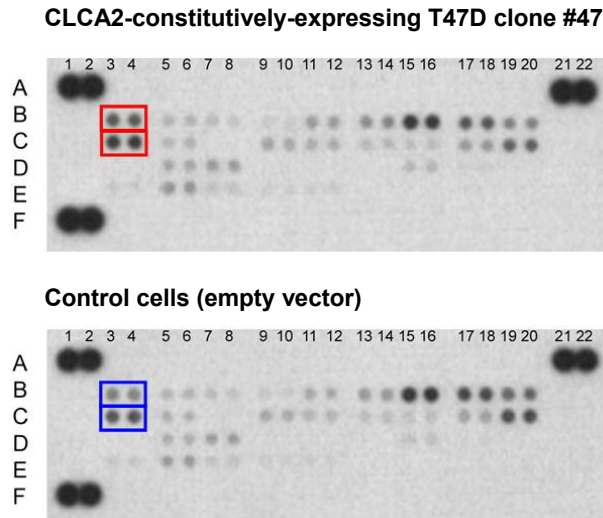


**Figure 91. Phosphorylation status of MAPKs, ERK1/2, JNK1-3, different p38 isoforms and other intracellular kinases upon expression of CLCA2 on antibody arrays**  
Protein lysates of CLCA2-constitutively-expressing T47D Clone #47 and “pseudo-induced” control cells with empty vector were harvested; CLCA2 expression of lysates was confirmed before use. The lysates were tested for the phosphorylation status of various proteins of the MAPK pathway using the “Human Phospho-MAPK Array Kit” from R&D Systems (Cat.# ARY002).

As shown in Figure 92 the duplicates of B3 and B4, representing EGF-R and the duplicates B17 and B18, representing Insulin-R and the duplicated B19 and B20, representing IGF-I R (red squares) show a higher phosphorylation level in CLCA2-inducibly-expressing T47D clone #3, than in control cells with the empty vector (blue squares). These data point to a possible activation of these three RTKs by CLCA2.

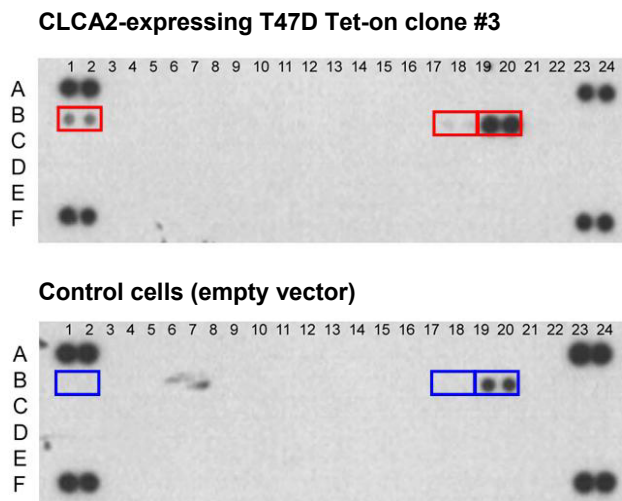


**Figure 92. Phosphorylation status of different receptor tyrosine kinases upon induction of CLCA2 expression on antibody arrays**  
Protein lysates of induced CLCA2-expressing T47D Tet-on Clone #3 and “pseudo-induced” control cells with the empty vector were harvested 48 h post induction; CLCA2 expression of lysates was confirmed before use. The lysates were tested for the phosphorylation status of 42 different receptor tyrosine kinases using the “Human Phospho-RTK Array Kit” from R&D Systems (Cat.# ARY001).

## DISCUSSION

### ***Introductory Remarks: General Reflections on Targeted Therapy in Oncology***

Cancer incidence is increasing worldwide with a tendency to be concentrated in developing countries (WHO estimation: 66 % of all new cases will be diagnosed within such regions). As the majority of patients are diagnosed in advanced stage, “classical” chemotherapy very often is still the first choice in treatment modality. As this therapy acts mainly in a non-specific manner, significant toxicity is observed. Indisputably, there is a high medical need to identify novel target molecules for more focused therapies in oncology. However, identification of such novel molecular targets requires a better understanding of the biology of cancer cells and their metabolic functioning. The knowledge about molecules and processes that are unique to cancerous cells or at least to a given cancer type is a prerequisite in the development of novel therapeutic approaches in cancer patients, leading to “targeted therapy”.

Over the last few years, a set of potential targets for cancer-directed therapy has been explored. Targeted therapy is defined as a drug or molecule causing tumour cell kill by interacting with predefined target(s) present on malignant cells [121]. Besides others, such an approach has the obvious advantage that it would selectively attack molecules and/or signaling transduction cascades that are unique to the tumour cells. Such kind of therapy has the potential to exclude normal cells to be hit, resulting in the reduction of side effects and general toxicity of the therapy, to have greater efficacy and to improve quality of life. Depending on the mode of action and the defined targets, various agents can be classified in subcategories such as monoclonal antibodies like Trastuzumab [122], tyrosine kinase inhibitors [123-127], antiangiogenic agents [128;129], cyclin-dependent kinases (CDK) and mitotic kinase inhibitors [130-132], proteasome inhibitors [133], and Cox-2 inhibitors [134] to name but a few.

Targeted therapies generate additional benefits and a higher efficacy in tumour patients. However, both, benefits and efficacy need to be evaluated carefully [121].

Cancer is a multistep process and genetic events (deletions, amplifications, rearrangements, mutations, epigenetic regulation etc.) result in the activation of

(proto-)oncogenes or the inactivation of tumour suppressor genes. As a result, the proliferation and growth of a tumour cell increases. It is of interest that the experimental inactivation of even a single oncogene can be sufficient to induce sustained tumour regression or vice versa, although tumourigenesis is thought to be a multistep process. Tumours become irrevocably addicted to these oncogenes. “Oncogene addiction” describes therefore, the phenomenon by which some cancers that contain multiple genetic and epigenetic abnormalities remain dependent on (addicted to) one or a few genes for both maintenance of the malignant phenotype and cell survival/proliferation. One explanation for this phenomenon is that activated oncogenes (e.g. mutated EGFR) result in a constitutive activation of a signaling cascade leading to sustained proliferation and survival [28]. On the other hand, a single oncogene is not sufficient to fulfill all requirements of a “full-blown” tumour cell and to overcome all physiologic barriers and safety mechanisms [16;135]. Therefore, it was suggested that oncogene activation initiates tumourigenesis mainly because it directly overrides physiologic programs inducing a state of “cellular amnesia”, not only inducing constitutive proliferation, but also bypassing checkpoint mechanisms that are essential for cellular mortality, self-renewal, and genomic integrity [136;137]. Correspondingly, in a tumour exhibiting the status of “oncogene addiction”, the inactivation of a single oncogene can restore some of these pathways resulting in proliferative arrest, differentiation, cellular senescence, and/or apoptosis. According to Felsher and colleagues “oncogenes induce cancer because they induce a cellular state of enforced oncogenic amnesia in which, only upon oncogene inactivation, the tumour becomes aware of its transgression” [138]. Novel techniques of systems biology will provide methods for analysing the entire circuitry of cancer cells and thus facilitate identification of these pathways of “oncogene addiction” or “oncogene amnesia” in specific types of human cancer. Regardless whether we call it “oncogene addiction” or “oncogene amnesia”, a prerequisite for the development of a targeted therapy is the identification of tumour-specific target genes which might not only be used as targets for mono-therapies but also be applied in combination with other anticancer agents [139].

Oncogenes and tumour suppressors are derived from all protein families, not only bearing an enzymatic function such as kinases, GPCRs, phosphatases, oxidoreductases, proteases etc., but also exhibiting transport [140;141], transcriptional [142;143] or structural/topologic functions [144;145]. For many of

these proteins the contribution to carcinogenesis has been univocally demonstrated (e.g. receptor tyrosine kinases), for others it remains to be determined (e.g. transporters, ion channels).

Often tumour-associated overexpression is the first hint that a gene might be involved in tumourigenesis. However, overexpression per se explains neither its essential contribution to tumour growth, survival or maintenance nor whether a gene (gene function) is able to drive tumour formation (“oncogene addiction”). A expression profile also does not allow to draw any conclusions about the mode of action of how a certain gene becomes overexpressed (e.g. chromosomal amplification, epigenetic regulation).

In the context of targeted therapy, ion channels are representing promising players. Specific stages of cancer progression are marked and regulated by expression and activity of different channels. Their contribution to the neoplastic phenotype ranges from control of cell proliferation and apoptosis, to regulation of invasiveness and metastatic spread. Often the contribution of these channels are independent of ion flow (e.g. shown for potassium ( $K^+$ ) channels) but the underlying molecular mechanisms are poorly understood [146]. Ion channels frequently exert pleiotropic effects on the tumour cell such as regulating membrane potential and thereby controlling calcium ion ( $Ca^{2+}$ ) fluxes and subsequently interfering with the cell cycle machinery [146;147]. The effect on mitosis might depend on the regulation of cell volume as shown in HeLa cells [146;148]. However, ion channels seem also to play an important role at late stage tumourigenesis by supporting angiogenesis, mediating the cell-matrix interaction, and regulating cell motility e.g. AQP1-null mice show defective tumour angiogenesis resulting from impaired endothelial cell migration whereas AQP3-null mice are resistant to skin tumourigenesis [140]. This is of interest as during this study it was found that CLCA2 might play an important role during colonisation of mycosis fungoides (cutaneous T cell lymphoma) into the skin (see section “*In Silico* Analysis of Expression Data”).

Another important contribution of ion channels to tumourigenesis is executed via formation of protein complexes with other membrane proteins such as integrins or growth factor receptors. These interactions may trigger a variety of different signaling cascades. First evidence that calcium channel blockers suppress the growth of human cancer cells, both *in vitro* and *in vivo* has been published recently [149]. A major drawback of all these approaches is that often ion channel blockers produce

serious side effects, such as cardiac arrhythmias and are not yet sufficiently specific enough [146]. This also holds true for members of the CLCA protein family for which no specific blocking compounds are available yet.

### ***In Silico Analysis of Expression Data***

Prior to the biological characterisation of CLCA2 a detailed *in silico* expression profile analysis was performed to learn more about its contribution to tumourigenesis. Based on the PhD-Thesis of Ulrich König and the Diploma Thesis of Stefan Amatschek [1], a lung SCC-specific expression profile of the human calcium-activated chloride channel, family member 2 (CLCA2) was suggested. Therefore, it was started to analyse the expression levels of CLCA2 mRNA in normal and tumourous tissue samples, as well as in tumour cell lines and xenografts thereof by utilising Boehringer Ingelheims proprietary BioExpress database (GeneLogic Inc.), which includes expression data from ~ 14.000 human tissue samples, analysed on Affymetrix GeneChips. Although different types of GeneChips have been used for the expression profiling, no statistically relevant variation was observed in the mRNA levels of the corresponding sample set among different GeneChips.

Analyses of the expression pattern in the BioExpress database (GeneLogic Inc.) indicated a preferential overexpression of CLCA2 not only in SCCs of the lung, but also in SCCs of the cervix, the larynx, the head and neck region, in lymph node metastasis of SCCs, in mycosis fungoides a cutaneous T cell lymphoma and in a subset of infiltrating ductal breast cancers.

Interestingly, adenocarcinomas of the esophagus show only minimal levels of CLCA2 transcript in comparison to their corresponding normal esophageal tissue, whereas laryngeal SCC maintain the high expression level of CLCA2 transcript throughout transformation. It cannot be excluded, that the relatively high CLCA2 transcript levels in normal esophageal and laryngeal tissue stems from the presence of an adjacent SCC and/or an inflammatory disease due to the fact that often the “normal” tissue is excised from the adjacent tissue of a tumour. Also a paracrine induction of CLCA2 in the surrounding tissue cannot be excluded. The uncategorised head and neck SCCs show an elevation of CLCA2 transcript levels in comparison to the corresponding normal tissue samples.



Comparison of the expression pattern of CLCA2 in esophagus with that in other tissues of the digestive tract, exhibits no additional expression in other parts of the digestive tract, underlining the restricted expression pattern of CLCA2.

In breast cancer a subpopulation of the infiltrating ductal carcinomas shows overexpression of CLCA2. It remains unclear whether distinct chromosomal aberrations or various differentiation stages lead to the induction of and/or dependence on CLCA2 in this subset of breast cancer samples. In this context it has to be mentioned that Her2 amplification is also found only in a subset of breast cancer samples [150-152].

In the view of elevated CLCA2 transcript levels in tumour-associated skin biopsies, it is of interest that a dramatic increase of CLCA2 mRNA was identified in mycosis fungoides, which is the most common type of cutaneous T cell lymphoma. It is a Non-Hodgkin lymphoma, which is predominantly related to skin. It generally affects the skin, but may progress internally over time. Disease may also progress involving nodes, blood and internal organs, or transform into a higher-grade lymphoma. As shown in this study, expression of CLCA2 seems to be induced in tumour-associated skin rather than in normal skin. Similarly, mycosis fungoides might make use of CLCA2 for its colonisation of the skin during its course of progression. In contrast, no CLCA2 expression is found in Hodgkin lymphomas.

To exclude relevant contribution of cells of the tumour stroma, the CLCA2 expression pattern was also investigated in several laser-capture-microdissected (LCM) tissue samples of lung carcinomas in comparison to non-neoplastic lung tissue samples. Based on data from the *in silico* analysis, an expression of CLCA2 in tumour stroma could be excluded and the tumour-specific expression pattern of CLCA2 was confirmed.

It seems that formation of SCC-derived metastases are somehow linked with CLCA2 expression, supporting the idea that CLCA2 might play a crucial role in the formation of SCC-derived metastases and being essentially involved in the progression of mucosis fungoides. In contrast to mycosis fungoides no (elevated) expression of CLCA2 was detectable in B cell and T cell lymphomas and their corresponding normal tissues/cells.

The analysis of CLCA2 transcript levels in lymph node metastases from different primary tumour subtypes showed, that SCC cells, which metastasise into the lymph node, maintain their high CLCA2 transcript levels during the infiltration of the lymph

node. Again a highly specific expression pattern was found as lymph node metastases descending from primary melanomas and adenocarcinomas do not express CLCA2.

All SCC tissues with elevated levels of CLCA2 transcript (as compared to their corresponding normal tissues) do not show overexpression in their corresponding adenocarcinomas; CLCA2 overexpression is clearly restricted to SCCs.

By comparison of the CLCA2 expression level in breast cancer specimens with that in their corresponding metastases, it was found that CLCA2 overexpression in breast cancer seems to be needed for formation of brain-, lung-, liver-, and lymphnode-metastases (see Figure 16). A correlation between CLCA2 overexpression and the development of metastases, was also indicated by analysis of expression data derived from cell lines and their corresponding developing tumours in xenograft models. All xenografts originating from SCC cell lines such as A431 (cervix carcinoma), H520 (lung carcinoma) and HNOE (head and neck/esophagus carcinoma) exhibit a dramatic upregulation of CLCA2 when xenografted into nude mice (Figure 14). Except for the pancreatic tumour cell line BxPC3 and MDA-MB-453 (breast cancer cell line) none of the adenocarcinoma-derived cell lines lead to such a pronounced upregulation of CLCA2 in xenografts. In the case of MDA-MB-453 a high expression level of CLCA2 is already detectable in 2D culture (Figure 14). Altogether, these data support the idea that CLCA2 plays a crucial role in tumour progression.

In addition, correlation of CLCA2 expression with receptor- and lymph node status in human breast cancer samples reveals that CLCA2 expression is mainly found in estrogen receptor-negative or in Her2-positive specimens.

Analysis of a panel of different human carcinoma cell lines again underlines the restricted expression of CLCA2 as it is limited to SCC or human breast cancer cell lines (Figure 15).

Analysis of chromosomal amplifications of the CLCA2 locus on Affymetrix SNP-Chips in human tumour cell lines showed that most SCC cell lines with an increased expression level of CLCA2 also exhibit amplification of 1p22-31 [63]. A copy number of 3 of the CLCA2 loci was found e.g. for FaDu, a head and neck SCC cell line, possibly reflecting the link between genomic and expressional status in various SCCs.

In statistical analyses – correlating normalised expression values of the BioExpress database (GeneLogic Inc.) – the next step was to search for transcripts exhibiting a

similar expression pattern. Among those genes various markers of stratified epithelia, such as desmocollin (DSC3), desmoglein 3 (DSG3), TP53 apoptosis effector (PERP), plakophilin 1 (PKP1), and keratin 5 (KRT5) were extracted. The expression of those epithelial differentiation markers seems to be maintained during the transition from a stratified epithelial cell into a hyper-proliferating SCC cell, and could therefore be essential for the establishment of SCCs. Further identified genes, which were already described to be involved in tumorigenesis, are: Ladinin 1 (LAD1/CD18), tripartite motif-containing 29 (TRIM29), stratifin (14-3-3 sigma/SDN), or RAB38, a member of the RAS oncogene family. Another set of genes with a similar expression profile may represent yet unidentified markers for stratified epithelia and/or genes involved in the tumorigenesis of SCCs. One of these genes, which showed a more or less identical expression profile is the G-protein-coupled receptor GPR87. Its association with stratified epithelia and essential contribution to SCC carcinogenesis was shown recently by S. Glatt, a PhD student of our group [79]. Whether GPR87 and CLCA2 are directly interacting with each other is not known yet. However, interaction of GPCRs and ion channels for regulation of signal transduction has already been demonstrated [153;154].

### ***Knock-Down of CLCA2 in CLCA2-Positive Tumour Cells***

With loss-of-function studies by siRNA-mediated knock-down of CLCA2, the implication on cell survival and proliferation of CLCA2 was investigated. In proliferation assays could be shown that downregulation of CLCA2 in HN5 cells (SCC cell line) leads to inhibition of proliferation, to reduction in viability and subsequently to induction of apoptosis. The same holds true for GPR87 [79], which exhibits a nearly identical expression profile as CLCA2 and was used as a control target gene for siRNA experiments. Downregulation was monitored by RT-qPCR. Testing different siRNA oligonucleotides, the two most efficient ones (siCLCA2-2 and siCLCA2-4) were selected for further studies. In general, siRNA oligonucleotide siCLCA2-4 lead to the most pronounced biological effects in all experimental settings.

Investigation of various apoptosis parameters by a high content screening approach (Cellomics) utilising siRNA-transfected HN5 cells revealed dramatic changes in the membrane permeability and in the mitochondrial status. In addition, a pronounced

nuclear fragmentation could be observed, which supports data obtained from PARP-cleavage experiments on Western blots reflecting induction of apoptotic events.

CLCA2 knock-down in siRNA-treated HN5 cells also lead to a significant shift in the cell cycle. The cell count in G1-phase (2n) was clearly reduced, and cells were arrested in G2, whereby polyploidy increased. Most likely apoptosis was already initiated in these polyploidic cells. Altogether, these data indicate that both, CLCA2 and GPR87 play an essential role for proliferation of HN5 cells.

As MDA-MB-453 cells (breast cancer cell line) exhibit much higher CLCA2 expression levels than HN5 cells, they were also used in siRNA experiments. Interestingly, in contrast to HN5 cells, MDA-MB-453 cells were insensitive towards knock-down of CLCA2 when tested in a proliferation assay.

Furthermore, no PARP-cleavage could be detected in siRNA-treated, CLCA2-constitutively-expressing T47D clone #47. T47D is also a breast cancer cell line which – in contrast to MDA-MB-453 – has only a hundred-fold lower expression level for CLCA2.

In contrast to the SCC cell lines HN5, the breast cancer cell line MDA-MB-453 (although exhibiting high levels of CLCA2 transcript) seems not to be dependent on CLCA2 for proliferation and survival in 2D-culture. Also gain-of-function in the breast cancer cell line T47D did not change the growth behaviour or generates a sensitivity towards siRNA-mediated downregulation of CLCA2. As both breast cancer cell lines are derived from adenocarcinomas, we conclude that downregulation of CLCA2 leads only to severe effects in cell lines of SCC origin (as e.g. HN5).

### ***Antibody Generation and Immunohistochemistry***

Due to the lack of commercially available CLCA2-specific antisera it was repeatedly tried to generate specific antisera against human CLCA2. Rabbits were immunised with peptides derived from identified CLCA2-specific epitopes which discriminate between other members of the CLCA family (for details see “Results”).

Fractions of affinity-purified sera of immunised rabbits were tested on Western Blot, but none of these antibodies generated a specific signal. Therefore, it was decided to recombinantly introduce an HA-tag to the wild type CLCA2 coding sequence in order to allow detection of CLCA2 expression at least in stably or transiently transfected cells utilising an anti-HA-antibody. The time-dependent induction of inducible HA-

tagged CLCA2 expression could be confirmed with HA-specific antibodies in stably transfected T47D.

Interestingly, one of the affinity-purified antisera, which was not suitable for detection of CLCA2 on Western blots but exhibiting a high titer towards peptide K94-N110 of CLCA2, showed a specific staining of tumour cells in human SCC lung tumour samples confirming its tumour-specific expression (tumour stroma and normal tissue is negative). A pre-immune serum was used as a negative control. The signal could also be competed with a peptide which was applied for generating the antiserum. Staining of adenocarcinomas, however, are not conclusive yet, as immunohistochemical analyses of these tumour types lead to aggregation of the antiserum. Therefore, these data have to be regarded as preliminary, also because (due to availability) only a small number of human SCCs have been analysed yet.

## ***Proteolytic Processing***

### **Putative Hydrolase Domain**

Pawlowski and colleagues published in 2006 that CLCA1 contains a hydrolase domain which is responsible for the processing of mature full-length CLCA1 [65]. Detailed sequence comparison revealed that the homology within the CLCA family is quite high. Making use of the established inducible expression of HA-tagged CLCA2 in T47-D cells, it was first tried to detect a C-terminal fragment on Western blots. Indeed, the cleavage product could only be detected upon Tet-induced CLCA2 expression in a time- and concentration-dependent manner. Non-induced cells under the same conditions did not show any specific band on Western blots (Figure 41, Figure 43). An alignment of CLCA1 and CLCA2 protein sequence exhibited a high homology within the segment where the proposed hydrolase is located (in CLCA2 at AA 29-208). As the essential residues which might be involved in the formation of the predicted hydrolase domain are conserved, it was started to analyse the proteolytic activity of CLCA2 in more detail. Experiments with matrixmetalloprotease-inhibitors such as Phenantrolin, Diprotin B, Bestatin, Amastatin and others did not allow to draw any valid conclusions as most of these compounds are quite toxic and can only be used at very low and thus ineffective concentrations in tissue culture. Next, all conserved Cysteine residues in the coding region of CLCA2 which are located within the region where the putative hydrolase domain is embedded were exchanged. Mutation of conserved Cysteines at position C211 and C216 still allowed a residual

proteolytic activity to take place although at a very low level. Mutations at C132, C196, and C206 completely abolish the proteolytic processing (Figure 46, Figure 48). Whether the inhibitory effects of the respective mutations are due to the influence on the correct formation of the active site or are due to a more general influence on the overall structure and/or stability is not clear yet. C132 corresponds to the Cysteine residue which is suggested to keep H140 (equivalent AA in CLCA1: H133) the proposed structural metal site ( $\text{Zn}^{2+}$  coordination) in correct orientation. Next, the corresponding sites in CLCA2 which might be directly involved in the formation of the catalytic site were mutated. The exchange of basic Histidines H164 and H168 with Cysteine (polar), Tyrosine (polar) or Asparagine (polar) completely inhibits cleavage of CLCA2. Exchange of Glutamic acid E165 with Aspartic acid or Glutamine also completely inhibits cleavage. Based on the modelling data from Pawlowski et al. [65] these residues are supposed to take part in the formation of the putative catalytic site. These results strongly supports the presence of a zincin-like hydrolase domain in the N-terminal region of CLCA2 as well. Furthermore, by generating hydrolase dead mutants it could be shown that the proteolytic activity is an autocleavage rather than a trans cleavage event managed by an additional cellular protease. Whether this autocatalytic activity is performed in cis or trans is still open. However, to clearly demonstrate a 1/1 molar ratio of the CLCA2 protein and  $\text{Zn}^{2+}$  further experiments are needed [155].

### **Putative Cleavage Site**

As known from bioinformatic analyses and literature [95], a mono basic cleavage site is predicted at position AA674. Mutational analysis by “Alanine-walking”, starting from predicted positions P5 to P4’ (AA670 to AA678) by subsequent and stepwise substitution of the respective amino acid to an Alanine, were performed. Additionally, at those positions where the cleavage activity could be abolished after introduction of an Alanine, additional exchanges were performed at the respective position. In particular at positions P3, P1, P1’, and P2’ all classes of amino acids i.e. amino acids with basic, acidic, non-polar or uncharged polar side chain) were introduced. These positions have been chosen as they are in most cases the cleavage specificity-determining amino acids [156]. Data from this study support this idea as predicted position P1 (AA674) strictly not allows any exchange of Arginine with others than Lysine (both AA contain a basic side chains). According to the mutational analysis

the cleavage recognition site might be as follows: P3(Tyr/Phe) – P2(X) – P1(Arg/Lys) – P1'(Tyr/Phe) – P2'(Phe/Ala).

### **Inhibition of Post-Translational Modifications**

For investigation of post-translational modifications of CLCA2 (glycosylation, isoprenylation) and their contribution to stabilisation and/or proteolytical processing, expression of CLCA2 was studied in the presence of the glycosylation inhibitor Tunicamycin and the isoprenylation inhibitor Perillic acid. By utilising the T47D Tet-on inducible expression system for wt-CLCA2 it could be shown that both, the stability and the proteolytic processing are impaired when glycosylation is inhibited. How glycosylation influences the post-translational processing is unclear. Two scenarios are conceivable: Either impaired glycosylation leads to incorrect folding and protection of the cleavage site or leads to a misguided cellular localisation where proteolytic processing cannot take place. Another explanation would be that the cleavage product of non-glycosylated CLCA2 becomes degraded and therefore cannot be detected on Western blots.

Based on these data it was decided to mutate the putative glycosylation sites in CLCA2. The use of several glycosylation site prediction software tools resulted in prediction of the putative glycosylation sites N150 (located within the predicted hydrolase domain) and N822. Point mutations resulting in exchange of Asparagine to Alanine of these two sites had no influence on the cleaving efficacy. However, mutating N822 resulted in a shorter C-terminal fragment after cleavage, indicating that an incorrect positioning of the cleavage site (e.g. triggered by loss of glycosylation) leads to processing at another site with a related amino acid motif.

### ***Integrin $\beta$ 4***

Abdel-Ghany found Integrin  $\beta$ 4 to be coprecipitated with CLCA2 [70]. He also identified a strong correlation between the level of Integrin  $\beta$ 4 and adhesion of HEK293 cells expressing CLCA2, and a correlation between Integrin  $\beta$ 4 expression in tumourigenic cell lines *in vivo* and the number of lung metastases detected in nude mice [70]. Upregulated Integrin  $\beta$ 4 levels were also found in microarray studies of lung cancer metastases [74].

Based on data of expression profiling on Affymetrix GeneChips, it could also be identified an enhanced Integrin  $\beta$ 4 expression upon induction of CLCA2 expression.

Whether the upregulation leads also to an enhanced activation status of Integrin  $\beta 4$  or not, could not be answered due to the lack of any functional phospho-specific antibodies for Integrin  $\beta 4$ . As members of the integrin protein family are known to be involved in cell attachment to proteins of the extracellular matrix, integrins therefore play an important role in metastasis, regulating not only dissemination, but also homing of metastasising tumour cells [157]. To gain a more detailed understanding about the specific induction of integrins upon induced CLCA2 expression, integrin-mediated cell adhesion assays were performed. The “Integrin-Mediated Cell Adhesion Arrays” (Chemicon) are efficient tools to screen cell surface protein profiles. The method is based on stripwells with each well pre-coated with an antibody detecting an individual integrin or extracellular matrix protein. Utilising the established inducible expression system for CLCA2, it was possible to screen for induction of  $\alpha$ - and  $\beta$ -integrins in dependence on induction of wt- or mutant-CLCA2 expression in T47D Tet-on cells (control: T47D cells which stably carry the “empty” expression vector). Out of the  $\alpha$ -integrin family no specific induction could be detected, whereas for  $\beta$ -integrin family member B2 a specific induction upon CLCA2-induced expression could be demonstrated (Figure 56, Figure 57).

### **3D-In Vitro Carcinoma Assay: Spheroids**

For a better simulation of the situation in a tumour, CLCA2-expressing clones were also grown in multicellular tumour spheroids, which are *in vitro* 3D models that recapitulate malignant cell contacts within a tumour. Multicellular tumour spheroids can for instance also be used to evaluate the tumour’s response to therapeutic agents or the interaction with cells of the tumour stroma, e.g. the von Willebrand factor domain in CLCA2 was previously shown to have a role in adhesion by binding at Integrin  $\beta 4$  [158] and preliminary experiments confirmed at least the interaction with members of the  $\beta$ -integrin family (see above).

In the course of this study the *in vitro* 3D model [159] was used for analysis of the influence of expression of active and inactive CLCA2 on three-dimensional cell growth and viability. Since not all cell lines or cell types are capable of forming spheroids, first a cell line capable of spheroid formation had to be selected. Fortunately, cell line T47D which was used to establish constitutive and inducible CLCA2-expressing clones could be cultivated as spheroids. Stable spheroids were transferred to a collagen gel or Matrigel and grown until they became necrotic and/or



apoptotic due to the lack of supply with nutrients and oxygen in the centre of the 3D spheroid, which are normally provided by *de novo* formed vessels, docking the growing tumour to the existing blood vessel system of the organism (neoangiogenesis).

In a statistically meaningful setting the relative cell growth of 2D- (counting viable cells) with that of 3D-cultures (determination of area [ $\mu\text{m}^2$ ]; Figure 63) was compared over a period of 3 to 10 days. Although, the relative cell growth of CLCA2-expressing T47D Tet-on clone #3 in induced versus non-induced status did not show a difference in 2D-cultures, it indeed exhibited a pronounced difference ( $> 2.5$ -fold) between 2D- and 3D-culturing. In contrast to CLCA2-inducible clone #3, the constitutive clone #47 showed already an enhanced relative cell growth in 2D-culture which was similar to that found in 3D-cultures. In general, constitutive CLCA2 expression during spheroid-formation lead to generation of larger spheroids and subsequently to enhanced apoptosis due to a higher proliferation rate. Without using the 3D-spheroid model, detection of the essential contribution of CLCA2 for a three-dimensional growth wouldn't have been possible. It is also of interest that CLCA2 mutants defective in their proteolytic processing apparently had no influence on spheroid formation or growth properties of spheroids. Therefore, maturation processing of CLCA2 seems not to have an impact on the three-dimensional growth of this cell line.

### ***Affymetrix Microarray Studies***

To study the effects of overexpression of CLCA2 on gene expression, expression profiling using the Affymetrix GeneChip Human Genome U133 Array was performed by comparing cell clones with induced expression of CLCA2 with their uninduced counterparts. In a separate experimental setting, the expression pattern for selected transcripts was confirmed by RT-qPCR. Among those (and besides CLCA2, which served as an internal control), genes such as CDIPT, MLL2 and SFI1 were identified. CDIPT (CDP-diacylglycerol-inositol 3-phosphatidyltransferase; phosphatidy inositol synthase) is a gene whose inhibition causes small cell lung carcinoma cells to arrest in G1 [98]. It further has been suggested to be involved in oral carcinogenesis [99]. MLL2 (myeloid/lymphoid or mixed-lineage leukemia 2) plays a role in apoptosis and in alterations of cell adhesion. MLL2 is a member of the human MLL family, which belongs to a larger SET1 family of histone methyltransferases. MLL2 is a

transcriptional activator that induces the transcription of target genes by covalent histone modification. MLL2 appears to be involved in the regulation of adhesion-related cytoskeletal events, which might affect cell growth and survival [100]. Members of the MLL protein family have been found to cause acute leukemia. Recently, deletion studies revealed that alterations of the CxxC domain (Zn-binding domain) disrupts its oncogenic potential [101]. SFI1 (SFI1 homolog, spindle assembly associated; yeast) is involved in initiation of centrosome duplication. SFI1 has been identified as a binding partner for the  $\text{Ca}^{2+}$ -binding protein centrin, suggesting a role in the dynamic behavior of centrosomes. SFI1 binds to multiple centrin molecules and the complex forms  $\text{Ca}^{2+}$ -sensitive contractile fibers that function to reorient centrioles and alter centrosome structure [96]. So far no correlation to tumour cell growth has been reported. However, according to the *in silico* analysis of this study, SFI1 is found upregulated in many tumours, with highest expression levels found in various B cell lymphomas and B cell leukemias (data not shown).

In total, approximately 150 genes were shown to be differentially up- or downregulated in a statistically relevant mode (fold change > 1.8; p-value < 0,0001). In order to link these expression profiles of regulated genes to canonical pathways and bring them into a biological context, these data were analysed with the Ingenuity Pathways Analysis Software (IPA; of Ingenuity Systems Inc.). This program is a text- and data-mining program which not only links gene and protein functions/interactions based on the knowledge of published data in the most relevant journals, but also allows to bring these interactions into a context of biological functions, regulatory cascades and functional groups (e.g. oncology/metastasis/prostate). It has to be mentioned that the presented studies can only be regarded as preliminary as the outcome of these *in silico* analyses has to be proven in experimental settings. On the other hand these data allow a much more focused proceeding for future experiments as this text- and data-mining program not only describes protein-protein interactions, but also other types of reciprocal action such as protein-nucleic acid interactions.

Based on these *in silico* analyses several interaction-networks were identified.

Network I (Figure 85) indicates that a group of specifically induced genes upon induction of CLCA2 is strongly linked to the interaction-axis of SMAD3–TP53–MYC–HNF4A–ERBB2. It has been shown recently that HNF4 $\alpha$ 1 (HNFA4) and the

proliferation factor c-Myc may compete for control of genes involved in cell proliferation and differentiation [160].

Network II (Figure 86) comprises a link to the TNF–IL2–IL10 interaction network. Interestingly, treatment of SCCs of the skin with a Toll-like receptor agonist such as imiquimod contained a decreased percentage of regulatory T (T reg) cells producing less IL10 and TGF-beta, thereby inhibiting their suppressive activity. This means that SCCs evade the immune response at least in part by recruiting T reg cells via modulation of the IL10 pathway [119].

Network III (Figure 87) brings some of the differentially upregulated genes into the context of the ERK–MAPK signaling cascade with ERK as the center of this network. The most significant networks were then merged (Figure 88), for the sake of simplicity focusing exclusively on protein-protein interactions, highlighting biologically interesting clusters such as the cluster of v-src (involved in regulation of many different signaling cascades), HNFA4, ERBB2, and KPNA2. Karyopherin 2 (KPNA2), for instance, is a member of the karyopherin (importin) family, which is part of the nuclear transport protein complex. KPNA2 is responsible for transfer of the repair complex RAD50–MRE11–NBS1 into the nucleus. The cytoplasmic portion of NBS1 promotes tumorigenesis through the binding and activation of the PI3-kinase/AKT pathway which is dependent on KPNA2 [161]. Previously KPNA2 overexpression was identified as a prognostic marker in breast cancer correlating with poor survival [162]. KPNA2 was also shown to be highly upregulated in esophageal cancer [163].

In a next step, the involvement of canonical signaling transduction pathways were investigated by phospho-proteomic studies. To learn more about the contribution of some important executor proteins of canonical pathways, which might be found activated/deactivated (=phosphorylated/dephosphorylated) in experimental settings of CLCA2 induction, cell lysates of induced and non-induced T47D Tet-on clone #3 cells (taken at various time points) were analysed on Western blots utilising phospho-specific antisera.

An increase in phosphorylation of AKT (S473), ERK 1&2 (T185/Y187), MAPK (T202/Y204), RAF (S259), CRAF (S338), and PDK1 (S241) was observed. No change in the phosphorylation pattern was seen for AKT at position S308. These data confirm the predictions made through the usage of the IPA software, indicating a link to the ERK–MAPK canonical pathway. From literature it is known that in oropharyngeal squamous cell cancer patients phosphorylation of AKT at S473 is

linked with a poor clinical outcome [164]. The malignant potential of SCC cell lines was shown to be significantly higher in CRAF-expressing cells and CRAF expression maintained also the radiation-resistant phenotype indicating that CRAF plays an important role in the squamous cell carcinogenesis [165]. Phosphoinositide-dependent kinase 1 (PDK1), a downstream target of PI3-K, has been recently suggested to take part in the signaling cascade of gastrin releasing peptide [(GRP)-Src-PI3K-PDK1-TACE-amphiregulin-EGFR] with multiple points of interaction leading to induction of proliferation of human head and neck squamous cells [166].

Analysed proteins which were found to be dephosphorylated upon CLCA2-induction are: mTOR (p2448), 4E-BP1 (T37/T47), STAT1 (Y701), and NPM (T234/T237). Deregulation of mTOR, 4E-BP1, STAT1 indicates a strong impact of CLCA2 to translational modulation whereas nucleophosmin (NPM) is involved in cytoskeletal regulation [120].

The phosphorylation and dephosphorylation upon CLCA2-induction of selected proteins was also analysed with the “Human Phospho-MAPK Array Kit” and “Human Phospho-RTK Array Kit” of R&D Systems. Performing these assays, a higher phosphorylation and therefore activation level for ERK1 and ERK3 could be confirmed in CLCA2-constitutively-expressing T47D clone #47 compared to control cells (empty vector). In addition, a higher phosphorylation level of EGF-R, Insulin-R, and IGF-I R was found in T47D clone #3 cells upon induction of CLCA2. The biological meaning of these findings is supported by recent publications e.g. showing that a worse tumour differentiation and a positive nodal stage in head and neck SCC are significantly associated with EGFR overexpression. In contrast to NSCLC, protein overexpression rather than mutation might be responsible for activation of the EGFR pathway in head and neck SCC [167].

## ***Summary***

In the context of targeted therapy, ion channels are representing promising players. However, very little is known about their specific contribution to tumourigenesis. In the course of this Thesis a preferential overexpression of CLCA2 in human squamous cell carcinomas (SCC) of different origins including their lymph node metastases could be demonstrated. In addition, overexpression was also detected in mycosis fungoides, a cutaneous T cell lymphoma and in a subset of infiltrating ductal breast cancers. Preliminary IHC analyses confirmed expression in human SCC

samples. *In silico* expression analyses identified a dramatic increase in CLCA2 expression when SCC cell lines are xenografted into nude mice supporting that CLCA2 plays an important role in late stage tumourigenesis.

Loss-of-function studies in SCC cell lines by siRNA-mediated knock-down of CLCA2 leads to inhibition of proliferation, to reduction in viability, subsequently to induction of apoptotic processes, and to an arrest in G2. In contrast, breast cancer cell lines stayed unaffected at least in 2D-tissue culture. Inducible expression of CLCA2 in tumour cells in combination with a detailed mutational analysis demonstrated a proteolytic (most likely autocatalytic) processing (hydrolase) activity of CLCA2 and proposed a structural metal site for Zn<sup>2+</sup> coordination. Altogether, these data strongly supports the presence of a zincin-like hydrolase domain in the N-terminal region of CLCA2. As predicted by bioinformatic analyses and in analogy to CLCA1 a mono basic cleavage site was predicted and could be confirmed by “Alanine-walking” mutagenesis with a predicted cleavage recognition site of P3(Tyr/Phe) – P2(X) – P1(Arg/Lys) – P1'(Tyr/Phe) – P2'(Phe/Ala). Inhibition of glycosylation revealed that both, the stability and the proteolytic processing are impaired when glycosylation is inhibited.

For a better simulation of the situation in a tumour, CLCA2-expressing clones were also grown in multicellular tumour spheroids. In statistically meaningful experimental settings, the relative cell growth rate of 2D- and 3D-cultures was compared and indeed a > 2.5-fold increase in proliferation in the three-dimensional system could be demonstrated upon induction of CLCA2 expression.

For a better understanding of the involvement of CLCA2 in signal transduction a comprehensive expression profiling study on Affymetrix GeneChips was performed, followed by RT-qPCR and phospho-proteom studies with selected genes. In total ~ 150 genes were shown to be differentially regulated upon induction of CLCA2 expression. Among those genes are CDIPT, MLL2, and SFI1, which play an important role in cell cycle regulation. Utilising Ingenuity Pathways Analysis – a text- and data-mining program – several interaction-networks were identified. All of them could be linked with important canonical signal transduction cascades or interaction networks such as the TNF–IL2–IL10 interaction network or the ERK–MAPK signaling cascade. Phospho-proteom studies confirmed these findings and additionally identified a strong impact of CLCA2 on translational modulation.

Although these expression profiling data can only be regarded as preliminary, they however, offer the basis for further focused studies for the characterisation of CLCA2 as a promising target in SCC tumourigenesis.

## MATERIAL AND METHODS

### *Molecular Biology*

#### **Total RNA Isolation**

The medium was removed and cells were directly lysed on the plates using 1 ml Trizol reagent (Invitrogen, Cat.# 15596-018) per 10 cm<sup>2</sup> of tissue plate. To ensure total lysis of the cells the suspension was pipetted up and down several times. The lysate was stored at -20°C, or used directly for RNA isolation.

For RNA isolation, the lysate was incubated for at least 5 min at RT (room temperature) to ensure complete dissociation of nucleoprotein complexes. 0.2 ml Chloroform (CHCl<sub>3</sub>) per ml Trizol was added, vortexed for about 15 sec and incubated for 2-3 min at RT. Afterwards the lysate was centrifuged at 10,000 rpm for 5 min at 4°C and the upper aqueous phase was transferred into a fresh RNase free tube.

The RNA was precipitated using 0.5 ml isopropanol per ml Trizol by incubating at least 10-15 min at 4°C. Subsequently the RNA was spun down by centrifugation at 15,000 rpm for 5 min at 4°C. The RNA pellet was washed with 75 % RNase-free Ethanol and centrifuged at 15,000 rpm for 5 min at 4°C. The supernatant was then removed and the pellet was air dried.

Finally, the RNA was resuspended in 10 µl DEPC-H<sub>2</sub>O and frozen at -20°C or used immediately for single strand cDNA (ss cDNA) synthesis.

Frozen tumour samples were sectioned and subsequently lysed in 200 µl RLT buffer of RNeasy Kit (Qiagen, Cat.# 74104) and total RNA was isolated following instructions of the provider.

#### **Single Strand cDNA Synthesis (First Strand Synthesis)**

For ss cDNA synthesis the extracted total RNA was reverse transcribed using the “Sprint™ PowerScript™ PrePrimed SingleShots with Random Hexamer Primers” from Clontech (Cat.# 639562).

To eliminate putative contaminations with genomic DNA, 1 µg total RNA was digested with 1 U DNaseI for 30 min at 37°C. The reaction was stopped by the addition of 2.5 mM EDTA and incubation at 65°C for 10 min. For ss cDNA synthesis 10 µl DEPC-H<sub>2</sub>O (di-ethyl-propyl carbonate-treated H<sub>2</sub>O) was added to the

lyophilised kit components and the DNA-free RNA was also added. The reaction was incubated for 60 min on 42°C. The ss cDNA was stored at -20°C, or used for further investigations.

### Real-Time Quantitative PCR (RT-qPCR)

For RT-qPCR cDNA samples were prepared following the instructions as described above. Analyses were performed with commercially available gene-specific “TaqMan Gene Expression Assays” of Applied Biosystems for the genes listed in Table 5.

<b><i>Gene of Interest</i></b>	<b><i>Cat.# and Label</i></b>
CLCA2	Hs00197957, FAM
SATB1	Hs00161515, FAM
SFI1	Hs00826823, FAM
MLL2	Hs00231606, FAM
EP300	Hs00914223, FAM
CDIPT	Hs00197004, FAM
TP53BP1	Hs00996818, FAM
LTBP1	Hs00386448, FAM
TSC1	Hs00184423, FAM
MACF1	Hs00201468, FAM
DTX2	Hs00539707, FAM
CHD6	Hs00260089, FAM
AFF4	Hs00232683, FAM
UNC84A	Hs00391956, FAM
RUTBC3	Hs00210437, FAM
P4HA2	Hs00188349, FAM
C10orf118	Hs00215984, FAM
ASPM	Hs00411505, FAM

**Table 5. Genes which were tested in “TaqMan Gene Expression Assays” (Applied Biosystems)**

In all gene expression assays, a FAM-dye labelled minor-groove-binder probe linked to a non-fluorescent quencher is used in combination with two non-labelled flanking primers. Probe and primers are sequence-specific for the respective gene of interest. The fluorescent signal is generated due to the release of the quencher from the FAM-labelled probe after the induction of DNA-synthesis from the two flanking primers.

As endogenous control the “Taq Man Gene Expression Assays” of the “housekeeping gene”  $\beta$ -2-microglobulin (Applied Biosystems, Cat.# 4326319E) was used, which is VIC-labelled and can be measured parallel to the FAM-channel.

For all assays the “Taq Man Gene Expression Master Mix” (Applied Biosystems, Cat.# 4369016) was used. Quantification and analyses were performed by the Mx4000 device from Stratagene, using the provided software package.



For RT-qPCR the following reagents were combined:

<i>reagent</i>	<i>μl per reaction tube</i>
cDNA-sample	2
2x TaqMan Gene Expression Master Mix	12.5
20x target primers and probe	1.25
20x control primers and probe (of B2M)	1.25
nuclease-free water	8
<i>total volume</i>	<i>25</i>

Cycling Parameters for RT-qPCR using MX4000, Stratagene:

1 cycle:	10 min	95°C
40 cycles:	15 sec	95°C
	1 min	60°C
hold at:		4°C

## PCR (Polymerase Chain Reaction)

### PCR-Amplification

This method was used to amplify specific DNA-fragments by using rapid changes in temperature and a DNA-Polymerase in connection with dNTPs and specific primers for the DNA sequences of interest.

For amplification of CLCA2, the commercially available vector „Human Full-Length cDNA Clone in pCMV6-XL4” from Origene (Cat.# TC116023, Acc. NM\_006536: Human calcium-activated chloride channel, family member 2 (CLCA2)) was used as template.

For the amplification reaction the following reagents were combined:

<i>reagent</i>	<i>μl per reaction tube</i>
aqua dest.	30
10x Pfx amplification buffer	5
10 mM dNTP mixture	1.5
PCR primer forward (5 pmol/μl)	5
PCR primer reverse (5 pmol/μl)	5
50 mM MgSO <sub>4</sub>	1
DNA template (plasmid: 10 ng/μl)	2
Platinum Pfx DNA polymerase (2.5 U/μl)	0.5
<i>total volume</i>	<i>50</i>

The following amplification parameters were designed to be used in a “PE GeneAmp PCR System 2400” or “PE GeneAmp PCR System 9700”:

1 cycle:	2 min	94°C
30 cycles:	15 sec	94°C
	30 sec	55°C
	3 min	68°C
1 cycle:	10 min	68°C
hold at:		4°C

Aliquots of 5 µl per reaction were analysed by electrophoresis on ethidiumbromide-(EtBr) stained 4 % agarose gels and amplified DNA-fragments were visualised on an UV-transilluminator.

### Colony Screening

Colony PCR screening was used for rapid determination of positive transformants. Bacterial colonies were picked from the agar plate, boiled for 10 min in 100 µl TE, either in water bath or in a thermocycler. The suspension was cooled down on ice and 2 µl suspension was pipetted into a PCR tube for amplification.

The following reagents were combined:

<i>reagent</i>	<i>µl per reaction tube</i>
aqua dest.	12.2
10x PCR buffer	2
dNTP mix (2.5 mM each)	1.6
PCR primer down (5 pmol/µl)	1
PCR primer up (5 pmol/µl)	1
boiled <i>E. coli</i> solution	2
Taq polymerase (5 U/µl)	0.2
<i>total volume</i>	<i>20</i>

The following amplification parameters were chosen in a “PE GeneAmp PCR System 2400” or “PE GeneAmp PCR System 9700” with a minimum of 1 min of elongation time and per additional 1000 bp one extra min for elongation.

1 cycle:	3 min	94°C
28 cycles:	1 min	94°C
	1 min	55°C
	1 min	72°C
1 cycle:	7 min	72°C
hold at:		4°C

Aliquots of 5 µl per reaction were analysed by electrophoresis on EtBr-stained 4 % agarose gels and amplified DNA-fragments were visualised on an UV-transilluminator. Colonies corresponding to samples, which showed an amplification product of the correct size, were picked and grown in 2 ml respective medium o/n and used for plasmid purification.

### Cloning PCR Products (TA-Cloning)

The method is based on the non-template-dependent activity of Taq polymerase which adds a single desoxadenosine to the 3'-end of a PCR product. The fragment can then be ligated to a vector (pGEM-T Easy Vector of the "pGEM-T Easy Vector System" (Promega, Cat.# A1380)) containing a desoxythymidine residue overhang. Usually, 3 µl of fresh PCR product (10-20 ng/µl) was directly ligated to the pGEM-T Easy Vector (50 ng/µl).

If the PCR product was amplified via a polymerase with proof-reading activity (e.g. Platinum Pfx from Invitrogen), a desoxadenosine had to be added to the 3'-end of the purified PCR product (see "A-Tailing of PCR-Products").

The ligation reaction was performed o/n at 14°C into 50 ng vector in a total volume of 10 µl containing 1 µl 10x ligation buffer, 1 µl pGEM-T Easy Vector (50 ng) and 1 µl T4 DNA ligase (3 U/µl). For highest efficacy the molar ratio (vector : PCR product) should be between 1:1 and 1:3. The ligation product was immediately used for transformation or stored at -20°C.

### A-Tailing of PCR Products

To add a desoxadenosine to the 3'-end of the purified PCR product, which is relevant if such PCR product should be directly cloned to the pGEM-T Easy Vector, the following reagents were combined:

<i>reagent</i>	<i>µl per reaction tube</i>
purified DNA-sample	7
dATP 2 mM	1
10x buffer	1
rTaq-polymerase (e.g. TakaRa) 5 U/µl	1
<i>total volume</i>	<i>10</i>

The reaction mixture was incubated for 30 min at 70°C and then directly ligated to the pGEM-T Easy Vector. For this, the following reagents were combined:

<i>reagent</i>	<i>µl per reaction tube</i>
A-getailte DNA-Lsg.	7
pGEM-T Easy Vector	1
10x Ligation buffer (Fermentas)	1
T4-Ligase (Fermentas)	1
<i>total volume</i>	<i>10</i>

The ligation was performed at 14°C o/n.

## Restriction Digestion

DNA was digested with restriction endonucleases for about 2 h at 37°C in the appropriate buffer with 3-fold excess (3 U/μg DNA) of restriction enzyme; standard enzymes from e.g. Fermentas, New England Biolabs, Invitrogen were used.

After digestion the enzymes were heat-inactivated at 70°C for 10 min.

The reaction mixture was directly used for further reactions, purified with “QIAquick PCR Purification Kit”, or the DNA was precipitated or separated on agarose gels.

## Filling 5'-Overhangs with dNTPs

The 5'-3' polymerase activity of “DNA Polymerase I Large (Klenow) Fragment” can be used to fill in 5'-protruding ends, which result from restriction digestion with dNTPs. The optimal reaction conditions are:

1-4 μg	digested DNA
50 mM	Tris-HCl (pH 7.2)
10 mM	MgSO <sub>4</sub>
0.1 mM	DTT
40 μM	of each dNTP
20 μg/μl	acetylated BSA
1 U/μg DNA	Klenow fragment

Klenow fragment is active in many restriction enzyme buffers, so in most cases the heat-inactivated reaction mix from restriction digestion was directly taken for filling, 1.5 μl dNTP mix (2.5 mM each) and 1 μl Klenow fragment (5 U/μl) were added.

In some cases DNA was first purified by phenol/chloroform extraction and ethanol precipitation or by using the QIAquick PCR purification Kit. After resuspending DNA the Klenow 10 x Buffer, 1.5 μl dNTP mix (2.5 mM each) and 1 μl Klenow fragment (5 U/μl) were added.

The reaction mix was incubated at RT for 10 min.

The reaction was stopped by heating the mixture for 10 min at 75°C.

## Converting a 3'-Overhang to a Blunt End

T4 DNA Polymerase exhibits 5'-3' polymerase activity, and 3'-5' exonuclease activity as well, and can be used for the generation of blunt ends from DNA molecules with 3'-overhangs, or for fill 5'-protruding ends with dNTPs.

For converting a 3'-overhang to a blunt end, DNA was digested in a volume of 50 μl with a restriction enzyme that generates a 3'-overhang.

The optimal reaction conditions are:

0.5-2 µg	digested DNA
33 mM	Tris-Ac (pH 7.9)
66 mM	KAc
10 mM	MgAc <sub>2</sub>
0.5 mM	DTT
0.1 mg/ml	BSA
5 U/µg DNA	T4 DNA polymerase

T4 DNA Polymerase can also be used directly in restriction enzyme buffer.

In most cases 2 µl T4 DNA Polymerase (3 U/µl) was added directly to the heat-inactivated reaction mix of the restriction enzyme digestion.

This reaction mix was then incubated at 37°C for 5 min.

The reaction was stopped by heating the mixture for 10 min at 75°C.

### ***In Vitro Site-Directed Mutagenesis***

Site-specific mutations in double stranded (expression-) plasmids were inserted by using the „QuikChange II XL Site-Directed Mutagenesis Kit” from Stratagene (Cat.# 200522).

The method is based on the utilisation of *PfuUltra* high-fidelity (HF) DNA polymerase for mutagenic primer-directed replication of both plasmid strands. The basic procedure utilises a supercoiled double-stranded DNA vector with an insert of interest and two synthetic oligonucleotide primers, both containing the desired mutation. The primers, each complementary to opposite strands of the vector, are extended during temperature cycling by DNA polymerase, without primer displacement. Extension of the oligonucleotide primers generates a mutated plasmid containing staggered nicks. Following temperature cycling, the product is treated with *DpnI*, an endonuclease specific for methylated and hemimethylated DNA, which is used to digest the parental DNA template and to select for mutation-containing synthesised DNA. The nicked vector DNA containing the desired mutations is then transformed into competent cells.

The primer length should be between 25 and 45 bases, with a melting temperature (T<sub>m</sub>) of ≥ 78°C. The desired mutation should be in the middle of the primer with ~ 10-15 bases of correct sequence on both sides. The primers should have a minimum GC content of 40 % and should terminate in one or more C or G bases.

For mutant strand synthesis reaction the following reagents were combined:

<i>reagent</i>	<i>μl per reaction tube</i>
10x reaction buffer	5
template (50 ng/μl)	1
forward Primer (5 pmol/μl)	2.5
reverse Primer (5 pmol/μl)	2.5
dNTPmix	1
QuikSolution reagent	3
H <sub>2</sub> O	34
<i>PfuUltra</i> polymerase (2.5 U/μl)	1
<i>total volume</i>	<i>50</i>

The following amplification parameters were chosen in a “PE GeneAmp PCR System 2400” or “PE GeneAmp PCR System 9700”:

1 cycle:	1 min	95°C
18 cycles:	50 sec	95°C
	50 sec	60°C
	9 min	68°C
1 cycle:	7 min	68°C
hold at:		4°C

1 μl of the *DpnI* restriction enzyme (10 U/μl) was added directly to each amplification reaction and incubated for 60 min at 37°C. 2 μl of the *DpnI*-treated amplified DNA was transformed to *E. coli* (for details see “Transformation of Bacteria”). The DNA of at least 3 colonies was isolated by “Miniprep” and sequenced.

### Purification of DNA

For purification of DNA, the “QIAquick PCR Purification Kit” of Qiagen (Cat.# 28104) was used. This method is adapted to purify single- or double-stranded DNA-fragments from PCR and other enzymatic reactions. Fragments ranging from 100 bp to 10 kb are purified from primers, nucleotides, polymerases, and salts.

5 volumes of buffer PB was added to 1 volume of the sample and mixed. The sample was then applied to a QIAquick column and centrifuged for 30-60 sec at 13,000 rpm. The flow-through was discarded and the column placed back to the same tube. To wash bound DNA, 0.75 ml buffer PE was added to the QIAquick column and centrifuged for 30-60 sec. The flow-through was discarded, the column placed back to the same tube. Then the column was centrifuged for additional 1 min, the flow-through was again discarded and the column placed in a clean 1.5 ml tube. To elute DNA, first 15 μl buffer EB was added to the centre of the QIAquick membrane and after 1 min centrifuged for 1 min. To increase DNA concentration another 10 μl buffer

EB was added and after 1 min centrifuged for 1 min. The average eluate volume is 22 µl from 25 µl elution buffer volume.

### **Phenol/Chloroform Extraction of DNA**

This method removes proteins from nucleic acid solutions.

Equal volumes of phenol/chloroform/isoamylalcohol 25:24:1 (v/v/v) and DNA solution were mixed by vortexing for 20 sec and centrifuged 5 min at RT with 15,000 rpm. The upper aqueous phase was transferred to a fresh tube and extracted with 24:1 (v/v) chloroform/isoamylalcohol. The sample was again mixed by vortexing for 20 sec, centrifuged for 5 min at RT and the aqueous upper phase transferred to another fresh tube. DNA was precipitated with ethanol.

### **Precipitation of DNA/RNA**

DNA was precipitated by adding 0.1 volumes of 3 M NaAc, pH 5.2 and 2.5 volumes of ice-cold 96 % ethanol for at least 3 h at -80°C. The most quantitative precipitation will be achieved when incubating at -20°C o/n and centrifugation for 30 min at 15,000 rpm at 4°C. The supernatant was removed and the pellet was washed with 500 µl 70 % ethanol (-20°C) and air dried or briefly dried under vacuum in a vacuum concentrator (Speedvac). The DNA pellet was dissolved in an appropriate amount of elution buffer EB (10 mM Tris-HCl, pH 8.5). For precipitation of RNA the same protocol is valid, but DEPC-treated solutions have to be used.

Alternatively, DNA or RNA can be precipitated with 1 volume of isopropanol without sodium acetate. This is of advantage for large volumes.

### **Agarose Gel Electrophoresis**

Depending on the expected DNA-fragment length agarose-gels ranging from 0.7-4 % agarose were prepared. The agarose was suspended in 1x TBE and shortly boiled in the microwave until the agarose was completely dissolved. The agarose solution was cooled to approximately 50°C and supplemented with EtBr from a stock solution (10 mg/ml) to a final concentration of 1 µg/ml. The mixture was pored into a gel tray and an appropriate comb was stacked into the tray. When the gel was completely solidified the comb was removed and the gel tray was put into the gel chamber containing 1x TBE as running buffer. The samples were mixed in a ratio of 6:1 with 6x loading buffer. Gels were run at 50-200 V depending on the gel size (3-5 V/cm in horizontal configuration).

### **Recovery of DNA from Agarose Gels**

With the “QIAEX II Agarose Gel Extraction Kit” of Qiagen (Cat.# 20021), DNA of 40 bp to 50 kb can be extracted and purified from standard or low-melting agarose gels in TAE or TBE buffers. Up to 400 mg Agarose can be processed per spin column.

The DNA fragments were separated on an agarose gel and fragments of interest were excised with a clean, sharp scalpel. The agarose pieces were transferred into 2 ml Eppendorf tubes and weighted before filling and afterwards. 3 volumes of buffer QG was added to 1 volume of agarose gel and incubated for 10 min in an Eppendorf thermoblock at 50°C to achieve total dissolution of the gel matrix. Then 1 gel volume isopropanol was added and the solution was mixed. A QIAquick spin column was placed in a 2 ml collection tube. The samples were applied onto these columns and centrifuged for 1 min at 15,000 rpm. The flow-through was discarded. To remove all traces of agarose 0.5 ml buffer QG was added and the column centrifuged again for 1 min at 15,000 rpm. The column was washed with 0.75 ml buffer PE. After 2-5 min the column was centrifuged for 1 min at 15,000 rpm. The flow-through was discarded and the QIAquick column was centrifuged for an additional min to remove residual ethanol of the PE buffer. Then the column was placed into a fresh 1.5 ml Eppendorf tube. To elute DNA 30 µl buffer EB was transferred directly on the center of the column. After 1 min incubation, the column was centrifuged for 1 min at 15,000 rpm. Alternatively to the described method, the “QIAquick Gel Extraction Kit” of Qiagen (Cat.# 28704) was used and performed according to the instructions in the manual.

### **Ligation of DNA**

An insert of interest could be amplified by PCR or “restricted out” from a plasmid containing the insert. Prior to ligation DNA had to be purified using a “QIAquick PCR Purification Kit” or “QIAEX II Agarose Gel Extraction Kit”.

150 ng insert was ligated o/n at 14°C into 50 ng vector in a total volume of 10 µl containing 1 µl 10x ligation buffer, 1 µl vector (50 ng) and 1 µl T4 DNA ligase (3 U/µl). For highest efficacy the molar ratio between vector and insert should be between 1:1 and 1:3.

The ligation product was immediately used for transformation or stored at -20°C.



## Transformation of Bacteria

### Bacterial Strains

- JM109 High Efficiency Competent Cells with the genotype: *recA1, endA1, gryA96, thi, hsdR17 (r<sub>K</sub>-m<sub>K</sub>+), relA1, supE44, Δ(lac-proAB), [F', traD36, proAB, lac<sup>q</sup>ZΔM15]*  
> 10<sup>8</sup> cfu/μg (Promega, Cat.# L2001)
- JM110 Competent Cells with the genotype: *rpsL (Str<sup>r</sup>) thr leu thi-l lacY galK galT ara tonA tsx dam dcm supE44 Δ(lac-proAB) [F' traD36 proAB lac<sup>f</sup>ZΔM15]*  
> 5x10<sup>6</sup> cfu/μg (Stratagene, Cat.# 200239)

### Transformation of JM109

*E. coli* cells were thawed on ice.

2 μl ligation reaction was added to an aliquote of 50 μl competent cells and incubated 20 min on ice. Following a 45-50 sec heat shock at 42°C, cells were incubated for further 2 min on ice. Then 950 μl SOC medium (Invitrogen, Cat.# 15544-034) was added and the cells were incubated 1 h at 37°C with shaking (220 rpm). 100 μl of each transformation-culture were plated on agar plates containing the appropriate antibiotic for selection. The plates were incubated o/n at 37°C.

Positive clones were analysed by "Colony Screening (PCR)". The DNA of transformed cells was isolated by "Miniprep" and sequenced.

### Transformation of JM110

JM110 *E. coli* cells were used for obtaining plasmids which further needed to be cut with dam- or dcm-sensitive restriction enzymes.

*E. coli* cells were thawed on ice.

An aliquote of 100 μl of competent cells was mixed with 1.7 μl of β-mercaptoethanol, provided with the kit, and incubated for 10 min on ice, swirling gently every 2 min.

2 μl ligation reaction was added to competent cells and incubated 30 min on ice. Following a 45-50 sec heat shock at 42°C, cells were incubated for further 2 min on ice. Then 950 μl SOC medium (Invitrogen, Cat.# 15544-034) was added and the cells were incubated 1 h at 37°C with shaking (220 rpm). 100 μl transformation-culture was plated on agar plates containing the appropriate antibiotic for selection. The plates were incubated o/n at 37°C.

Positive clones were analysed by “Colony Screening (PCR)”. The DNA of transformed cells was isolated by “Miniprep” and sequenced.

## **Plasmid Preparations**

### **Miniprep**

For plasmid preparation, the “QIAprep Spin Miniprep Kit” of Qiagen (Cat.# 27106) was used. The protocol is designed for purification of up to 20 µg of high-copy plasmid DNA from 1-5 ml overnight cultures of *E. coli* in LB-medium.

*E. coli* cells were incubated o/n in 2.5 ml LB-amp medium at 37°C in an air-incubator at 225 rpm. The cell suspension was centrifuged for 30 sec at 6,000 rpm. Pelleted bacterial cells were resuspended in 250 µl buffer P1. 250 µl lysis buffer P2 was added and the tube was gently inverted 4-6 times. Then 350 µl buffer N3 was added and the tube was again gently inverted 4-6 times. After 10 min centrifugation at 15,000 rpm, the supernatant was applied to the QIAprep column and centrifuged for 1 min at 15,000 rpm. The flow-through was discarded and the plasmid DNA which was bound to the column matrix was washed once with 0.5 ml buffer PB and once with 0.75 ml buffer PE. Between washing steps, the columns were centrifuged and the flow-through was discarded. After washing steps the column was again centrifuged for 1 min to remove residual wash buffer. Then the QIAprep column was placed into a clean 1.5 ml tube and the DNA was eluted with 50 µl buffer EB (10 mM Tris-HCl, pH 8.5). After 1 min incubation, the column was centrifuged for 1 min.

The DNA-solutions were stored at -20°C.

### **Maxiprep**

For preparation of larger amounts of DNA, the “EndoFree Plasmid Maxi Kit” from Qiagen (Cat.# 12362) was used. The protocol is designed for purification of 500 µg of endotoxin-free plasmid DNA.

300 ml overnight bacteria culture was centrifuged for 30 min at 4°C at 6,000 rpm in a “Sorvall RC-5B Refrigerated Superspeed Centrifuge”.

The pellets were resuspended in 10 ml P1 buffer. Then 10 ml P2 buffer was added and the tube was gently mixed. After 5 min incubation at RT, 10 ml of chilled P3 buffer was added and the reaction mixture again gently mixed.

The lysate (but not the plunger) was transferred to the barrel of the QIAfilter Maxi cartridge, placed in a convenient tube and incubated at RT for 10 min.

The QIAfilter cartridge was then held over the previously equilibrated QIAGEN-tip and the cap was removed from the QIAfilter outlet nozzle. The Plunger was gently inserted to the QIAfilter Maxi cartridge to filter the cell lysate into a 50 ml tube. Then 2.5 ml endotoxin removal buffer ER was added to the filtered lysate, the sample mixed by inverting the tube about 10 times and incubated on ice for 30 min.

During incubation a QIAGEN-tip 500 was equilibrated by applying 10 ml buffer QBT and the column was allowed to empty by gravity flow.

Then the incubated filtrate was applied to the QIAGEN-tip and allowed to enter the resin by gravity flow. The QIAGEN-tip was then washed with 2 x 30 ml buffer QC. DNA was eluted with 15 ml buffer QN (into an endotoxin-free 30 ml Nalgene-tube). Plasmid DNA was precipitated with 10.5 ml isopropanol at RT and centrifuged at 11,000 rpm (Sorvall RC-5B, rotor HB-4 11,000 rpm) at 4°C for 30 min.

The pellet was briefly washed with 70 % ethanol and again centrifuged at 11,000 rpm at 4°C for 15 min. Finally, the pellet was air dried and DNA was dissolved in a suitable volume of buffer EB (10 mM Tris-HCl, pH 8.5).

### Determination of DNA/RNA Concentration

The concentration and purity of nucleic acids was determined by measuring the optical density (OD) at 260 nm and 280 nm in a SmartSpec 3000 spectrometer (Biorad). An OD<sub>260</sub> of 1 represents either 40 µg/ml RNA or ssDNA or 50 µg/ml dsDNA. The OD<sub>260</sub>/OD<sub>280</sub> ratio between 1.8 and 2 indicates high purity of nucleic acid. Contaminants that absorb at 280 nm (e.g. protein) will lower this ratio.

### DNA Sequencing

Sequencing of dsDNA was performed with “ABI PRISM Big Dye Terminator v3.1 Cycle Sequencing Kit” according to manufacturer guidelines provided with the kit.

The following reagents were combined:

<i>reagent</i>	<i>µl per reaction tube</i>
250-500 ng DNA diluted in aqua dest.	4.4
sequence primer (5 pmol/µl)	1.6
terminator ready reaction mix	4
<i>total volume</i>	<i>10</i>

The following amplification parameters were chosen in a “PE GeneAmp PCR System 2400” or “PE GeneAmp PCR System 9700”:

1 cycle:	1 min	96°C
28 cycles:	10 sec	96°C
	15 sec	50°C
	2 min	60°C
hold at:		4°C

Samples were transferred to the “in house sequencing lab”, where DNA sequencing was performed on an ABI-Prism 3100 System (Applied Biosystems).

Specific sequencing primers were chosen for each approach. As the maximal fragment length being analysed does not exceed 500-800 bp, analyses of longer sequences of interest were divided into 500 bp intersections.

Sequence data were edited and analysed with the software VectorNTI of Invitrogen.

### **Freezing of Bacteria**

800 µl of cultured bacteria suspension was mixed with 800 µl of sterile glycerol in a cryotube and mixed to ensure that the glycerol was homogenously dispensed.

The cultures were stored at -80°C.

## ***Cell Biology***

### **Cell Lines**

All used cell lines were grown in an atmosphere containing 5 % (v/v) CO<sub>2</sub> and 95 % relative humidity. All cell lines except HN5 and T47D Tet-on were obtained from ATCC and were propagated according to provider’s instructions.

#### **HN5**

HN5 is a human head and neck squamous cell carcinoma cell line which was originally obtained from Invitrogen, CA, USA.

For medium condition see chapter “Media and Buffers”.

#### **T47D Tet-on**

T47D Tet-on cell line (BD Pharmingen) stably expressing a tet-repressor, was propagated following provider’s instructions. “Tet System Approved Fetal Bovine Serum” from Clontech (Cat.# 631101) was used for cultivation of the tet-sensitive cell line. For induction, Doxycycline (Clontech, Cat# 631311) was used at a concentration of 2 µg/ml media.

### **Thawing and Freezing of Cells**

At least  $1 \cdot 10^6$  cells in excellent condition (derived from log growth phase) were centrifuged at 1,000 rpm for 2 min in a Megafuge 2.0R (Haereus). Afterwards the supernatant was removed. The pellet was resuspended gently in 1 ml of the pre-cooled freeze-medium "Cryo-SFM" (PromoCell, Cat.# C-29912) and transferred into a cryovial which was labelled with an ethanol-resistant marker. Then the vial was put into a freeze container (NALGENE™ 1°C Cryo Freezing Container) and transferred into a -80°C freezer, whereby the temperature drops 1°C per min avoiding ice crystal formation. If cells should be stored longer than 6 months, they should be transferred to liquid nitrogen afterwards.

For thawing, frozen cells were put immediately from dry ice into a 37°C water bath, until the freeze-medium thawed. When only a small lump of ice was left, the vial was removed from the water bath and sprayed briefly with 70 % ethanol to avoid contamination. The vial was opened in a laminar flow and the cells were immediately transferred to a T25 cell culture flask and resuspended with 5 ml of their respective growth medium. After 24 h, the cells were washed with 1x PBS and the medium was changed. After one week in culture, usually the cells are in a good condition and ready for experiments.

### **Propagation of Adherent Cells**

The cells were trypsinised when confluency of ~ 90 % was reached.

For this, the cell culture medium was removed and cells were washed with 1x PBS. Then 1 ml (T75 flask) or 2.5 ml (T175 flask) of Trypsin-EDTA solution ("Trypsin-EDTA (1x), liquid - 0.05 % trypsin" of Invitrogen, Cat.# 25300-054) was added and the flasks incubated at RT (or at 37°C) until the cells were detached.

The cells were "split" according to their density and growth rate. Fresh culture medium was added and dispensed into new culture flasks.

### **Determination of Cell Count**

For determination of cell count, cells were detached with Trypsin-EDTA solution as described above and the trypsinisation reaction stopped with the respective cell medium. A homogenised cell solution or dilution thereof was measured with the "Vi-CELL™ Cell Viability Analyzer" from Beckman Coulter.

### **Determination of Growth Curve**

For determination of cell growth, in 2D cell culture, a defined number of cells were seeded into a cell culture flask or plate or well and after a certain period of time trypsinised and the cell solution counted with the “Vi-CELL™ Cell Viability Analyzer” from Beckman Coulter. With enough time points a growth curve could be compiled in MS Excel.

For experiments in 3D cell culture systems with spheroids, the area of spheroids was determined on different days by using the software „AxioVision Rel.4.6“ from Carl Zeiss Imaging Solutions.

### **Transient Transfection of Plasmid DNA to Eukaryotic Cells**

For transient transfection of eukaryotic cells with plasmid DNA the “Lipofectamine 2000” reagent of Invitrogen (Cat.# 11668-019) was used.

The day before transfection, cells were trypsinised and cultivated at a confluency of ~ 70 % o/n. For transfection of cells in 6-well-cell culture plates, 200,000 cells were seeded and grown in 2 ml of the appropriate media for at least one day. 2 µg plasmid per reaction was diluted with 200 µl OptiMEM (Invitrogen, Cat.# 51985-026), and 5 µl Lipofectamine 2000 was diluted with 200 µl OptiMEM. After 15 min incubation at RT both solutions were combined and incubated for further 15 min at RT. The cells were washed once with PBS and then treated with the lipofectamine-plasmid solution for 4 h in the incubator. 4 h after transfection, media was changed to the respective cell medium.

Usually cells were incubated for 24-48 h in the incubator prior to testing for transgene expression.

### **Generation of Stable Cell Lines**

For the establishment of CLCA2 stably transfected inducible T47D Tet-on cell lines, or cell lines with distinct mutations in CLCA2, the ORF's of CLCA2 with an HA-tag at the C-terminal end and various mutated CLCA2-ORF's were cloned to the pTRE2pur vector of the “Tet-on Gene Expression System” of Clontech (Cat.# 630922) and transfected to the T47D Tet-on cell line.

In the Tet-on System, rtTA (reverse tetracycline-controlled transactivator) binds the TRE (Tet response element) and activates transcription only in the presence of

Doxycycline (a Tetracycline derivative), whereby in the used T47D Tet-on cell line, the appropriate regulatory protein is already stably expressed.

CLCA2-HA-expressing stable cell clones, having the puromycin resistance gene from the transfected vector pTRE2pur, were selected for at least 2 weeks with 0.5 µg/ml Puromycin (Sigma, Cat.# P9620) in cultivation medium. Approximately 100 cell clones were analysed for Doxycycline-dependent expression of CLCA2-HA by using an anti-HA-antibody in Western blot analyses with induced versus non-induced cell lysates, which were generated 48 h post induction.

Those clones with no expression in uninduced cell lysates, but distinct expression in induced cell lysates were used for further analysis.

### **Generation of Cell Lysates from Human Tumour Cells**

To generate lysates of adherent cells, the medium and the detached cells were removed. The remaining attached cells were washed once with PBS, and then 150 µl lysis buffer was added to each well of a 6-well-plate or 1 ml lysis buffer to cells which were grown in a 13.5 cm culture dish. The lysis buffer was pipetted up and down, until all cells were detached. Then the lysate was immediately put to the freezer and stored for at least 2 h at -20°C.

### **Inhibition of Post-Translational Modifications**

The glycosylation inhibitor Tunicamycin and isoprenylation-inhibitor Perillic acid were obtained from Sigma. The inhibitors were dissolved in DMSO and added directly to the cell culture medium at different concentrations. Final DMSO concentration in all samples was adjusted to 1 %. 48 h after treatment cells were harvested and protein lysates tested in Western blot analysis.

### **Proliferation Assay (Alamar Blue)**

1,000-5,000 cells in 100 µl medium were seeded per well of a 96-well-plate. Proliferation assays were performed by adding 100 µl of 20 % Alamar reagent (Invitrogen, Cat.# DAL1100) in medium into each well. After subsequent incubation at 37°C the measurements were performed in a standard microtiter well plate reader such as EnVision 2101 multi label reader (Perkin Elmer).

## siRNA Experiments

### siRNAs

siGENOME SMART pool (Dharmacon, Cat.# MQ-003813-01-0005, human CLCA2, NM\_006536, 5nmol x 4) containing a mixture of four designed siRNAs targeting CLCA2 mRNA was tested in different cell lines for efficient downregulation of the specific mRNA and protein levels. Afterwards the individual siRNAs, shown in Table 6 were tested individually.

<i>Name of siRNA</i>	<i>Sequence (5' → 3')</i>	<i>Dharmacon Cat.#</i>
siCLCA2-2	GGAAUCAUUUGCCUUAUUAAUU	D-003813-02
siCLCA2-4	GAUCGAAAGUUGCUGGUUUUU	D-003813-04
siCLCA2-5	UGACAAACCUUUCUACAUAAUU	D-003813-05
siCLCA2-8	GCUACAAGCUAUGAAAUAUU	D-003813-08

**Table 6. Sequences of commercial available (Dharmacon) siRNAs, which were used for CLCA2 knock-down experiments**

The most efficient siRNA oligonucleotides, siCLCA2-2 and siCLCA2-4, were used for further experiments.

Non-targeting siRNA “siCONTROL#1” (herein named siCTRL) of Dharmacon (Cat.# D-001210-0105) was also purchased and used as a control for normalisation.

### siRNA Transfection in 6-Well-Plates

For each siRNA transfection approximately 150,000 cells were seeded into each well of a 6-well-cell culture plate and cultured for 24 h to yield 40-50 % confluency.

siRNA duplexes were dissolved and diluted with siRNA buffer (Dharmacon, Cat.# B-002000-UB) and nuclease free water to a concentration of 20 µM.

Cells were transfected with siRNAs dependent on the cell line with the indicated amount of appropriate DharmaFECT™ reagent at a final concentration of 25 nM siRNA.

For this, 2.5 µl siRNA solution (20 µM) was diluted in 200 µl of a serum-free respective cell culture medium. In parallel, 4 µl DharmaFECT was diluted in 200 µl of the serum-free respective cell culture medium. Both solutions were incubated separately. After 5 min of incubation the solutions were combined and incubated at RT for further 20 min. Then 1.6 ml of the corresponding full cell culture medium (including serum) was added to 400 µl of the mixture to obtain 2 ml transfection medium. After washing the target cells once with PBS, the medium of the target cells



was replaced with 2 ml of the transfection medium. After 24 h of incubation, the transfection medium was discarded and 2 ml respective cell culture medium was added.

The cells were harvested 24-72 h after siRNA transfection and analysed via quantitative PCR or Western blot analysis.

#### **siRNA Transfection in 96-Well-Plates**

For performing an Alamar Blue Assay with siRNA-transfected cells, siRNA transfections were performed in 96-well-plates. Therefore 5,000 cell per well were seeded into each well and final siRNA concentrations ranging from 390 pM up to 100 nM were tested for optimal transfection. (In detail, the following concentrations were used: 390 pM, 780 pm, 1.56 nM, 3.13 nM, 6.25 nM, 12.5 nM, 25 nM, 50 nM, 100 nM) 100 µl transfection reagent was added to each well of a 96-well-plate.

If RNA was isolated from such an experiment, the “FastLane Cell cDNA Kit” from Qiagen (Cat.# 215011) was used following the instructions in the manual.

#### **DharmaFECT Reagents**

Table 7 lists all transfected cell lines used in this study and the respective DharmaFECT reagent, which was used for transfection.

<b><i>Cell Line</i></b>	<b><i>DharmaFECT</i></b>	<b><i>Dharmacon Cat.#</i></b>
HN5	4	T-2004
MDA-MB-453	1 or 2	T-2001 & T2002
T47D Tet-on	4	T-2004

**Table 7. Optimal transfection reagents (Dharmacon) for cell lines used in this study**

#### **Live-Cell High-Content Screening (HCS) with Cellomics ArrayScan®**

HCS Reader is an automated fluorescence microscopic imaging system designed for high content screening and high content analysis. The instrument features include optics by Carl Zeiss, broad white-light source, 12-bit cooled CCD camera, and controller software. All Cellomics instruments are designed to work with image analysis modules (BioApplications) that automatically convert images into numeric data that capture changes in cell size, shape, intensity, and other properties.

The following Standard Operating Procedures for cell cycle and apoptosis analysis (CCYAPO) have been applied:

### **Tissue Culture**

Cells of interest were grown in maxi plates (175 cm<sup>2</sup>) using EMEM medium supplemented with 10 % heat-inactivated fetal calf serum, 0.15 % NaHCO<sub>3</sub>, 1 % Na pyruvate solution, 1% NEAA (100x) and 2 mM L-Glutamine. Cultures were incubated at 37°C and 5 % CO<sub>2</sub> in a humidified atmosphere.

Cell were transfected according the standard protocol (see previous chapters).

### **Staining Procedure**

All liquid handling was performed with Cybiwell instruments.

Apoptosis staining was performed on the life cells by adding 50 µl/well medium containing 500 nM Mitotracker Red CMXRos (1mM stock in DMSO, Invitrogen M-7512) and 100 nM SytoxGreen (100 µM stock in DMSO; Invitrogen S-7020). Then the cells were kept in the incubator for 60 minutes. After incubation the cell layer was washed 2 times with 100 µl PBS. Then cells were fixed by adding 100 µl 3.7 % formaldehyde/ 0.1 % TX100 in PBS for 10 min at RT. The cell layer was washed 2 times with 100 µl PBS. The nuclei were stained with 5 µg/ml Hoechst 33342 (stock 10 mg/ml in PBS; Invitrogen H1399) for 60 min. Then the cell layer was washed 1 x with 100 µl 0.1 % Triton X100 in PBS and 2 x with 100 µl PBS. The wells were filled with 100 µl PBS and the plates sealed with an adhesive sheet.

The measurement was performed with Cellomics “ArrayScan® VTI Live” (Protocol: Morphology Analysis TV\_APO\_20x) as follows:

### **Settings**

- objective: 20x
- acquisition camera mode: standard
- filter XF93: DAPI, FITC and TRIC channels
- autofocus interval = 2
- 600 cells, max 30 fields/well
- max 5 sparse fields per well
- fixed exposure time, set to 25 % saturation for the negative controls
- fixed threshold - adjusted to the actual staining intensities
- SegmentationCh1 = 6
- background correction = 0
- NucSmoothFactorCh1 = 0

## Features

- ObjectTotalIntenCh1      Hoechst stain: DAPI channel
- ObjectAreaCh1
- ObjectVarIntenCh1
- TotalIntenCh2              Sytox stain: FITC channel
- TotalIntenCh3              MitoTracker: TRITC channel
- CellsPerField

Sytox intensities were generated by dividing – on the single cell level – the TotalIntenCh2 by TotalIntenCh1 values.

## Integrin-Mediated Cell Adhesion Assays

Integrin-mediated cell adhesion assays were performed by using „Beta Integrin-Mediated Cell Adhesion Array” (Chemicon, Cat.# ECM531) and „Alpha Integrin-Mediated Cell Adhesion Array” (Chemicon, Cat.# ECM530).

The „Alpha Integrin-Mediated Cell Adhesion Array“ uses mouse monoclonal antibodies, generated against human  $\alpha$ -integrins/subunits ( $\alpha 1$ ,  $\alpha 2$ ,  $\alpha 3$ ,  $\alpha 4$ ,  $\alpha 5$ ,  $\alpha V$  and  $\alpha V\beta 3$ ) and the „Beta Integrin-Mediated Cell Adhesion Array“ uses mouse monoclonal antibodies, generated against human  $\beta$ -integrins/subunits ( $\beta 1$ ,  $\beta 2$ ,  $\beta 3$ ,  $\beta 4$ ,  $\beta 6$ ,  $\alpha V\beta 5$ , and  $\alpha 5\beta 1$ ), which are immobilised onto a goat anti-mouse antibody coated microtiter plate. The plate is used to capture cells expressing these integrines on their cell surface. Cells were seeded onto the coated substrate and incubated. Unbound cells were washed away and adherent cells were fixed and stained. Relative cell attachment was determined using absorbance readings, measured in a standard microtiter well plate reader.

The assays were performed according to the assay instructions in the manual.

For cell suspension  $1.0 \times 10^6$  cells/ml were used.

## Human Tissue Samples

Human tissues were collected at the Institute of Pathology, Medical University of Vienna, Austria, following institutional guidelines. In addition, ten cases of cervical SCCs were obtained from Oridis Biomed.

### **3D-In Vitro Carcinoma Assay: Spheroids**

For investigation of CLCA2-expressing cell lines in a 3D model, cells were grown in the form of spheroids. To achieve growth in this tumour similar format, cells have to be cultivated with methylcellulose in wells of a 96-well-plate for suspension culture, where cells could not attach at the surface of the plate. When spheroids were formed, they were transferred to a gel, where growth in all directions is possible.

#### **Methylcellulose**

1.8 g methylcellulose (Sigma, Cat.# M-0512-100G, 4000 centipoises) was weighted into a 100 ml flask containing a magnetic stirrer and autoclaved (the methylcellulose powder is resistant to this procedure). The autoclaved methylcellulose was resolved in 100 ml sterile basal medium (using a magnetic stirrer) o/n at 4°C. After clearing by centrifugation at 5,000 g for 2 h at RT, a final stock solution was aliquoted, whereby only the clear highly viscous supernatant was used for the spheroid assay (about 90 - 95 % of the stock solution). For spheroid generation, 20 % of the stock solution and 80 % culture medium were used.

#### **Spheroid Formation**

Cells were trypsinised and counted. For one spheroid 250 cells were used, so 25,000 cells were isolated, centrifuged at 1,000 g for 3 min at RT and resuspended in 10 ml appropriate medium (containing serum and all needed “goodies” such as L-glutamine, Na-pyruvate etc.) with 20 % Methylcellulose stock solution. 100 µl cell suspension was added into each well of a U-shaped 96-well-plate for suspension culture from Greiner (Cat.# 650185). The cells were incubated for 48 h at 37°C in an atmosphere containing 5 % (v/v) CO<sub>2</sub> and 95 % relative humidity.

#### **Harvesting of Spheroids**

The spheroids were collected by removing 50-100 µl of the medium near the deepest point of the well of the U-shaped 96-well-plate with a 200 µl Gilson/Eppendorf pipette and collected into a 1.5 ml Eppendorf tube. The collected spheroids were centrifuged carefully at 100 g for 3 min at RT and the medium was removed with a pipette.

#### **Gel Pouring Device**

For growing spheroids in collagen gel, a gel pouring device is needed to keep the stability of the gel.

For this, silicon gaskets were cut out in quadratical (2 cm x 2 cm) pieces from silicon gasket (Biorad silicone gasket for gel dryers) and a hole (diameter 1.5 cm, with a hollow punch) was made in the middle. The gaskets were autoclaved (45 min, 120°C) before use. The supporting nylon mesh was taken of Becton Dickinson Filcons (100 µm mesh size, Cat.# 340611) and autoclaved (45 min, 120°C).

To be used as a form for 3D-spheroid-gels, the silicone gaskets were placed onto the lid of a 4 cm cell culture dish with a nylon mesh placed into the hole and incubated for 30 min at 37°C before use.

### **Collagen Gel Preparation**

For collagen gels, “Collagen I, Rat Tail Tendon” from BD Biosciences (Cat.# 354236) was used.

The following reagents (for 2 ml collagen gel mix) were put on ice and mixed carefully by pipetting up and down for about 10 times avoiding production of bubbles:

0.2 ml	10x PBS
0.9 ml	Methylcellulose (20 %) in desired culture medium
0.9 ml	Collagen I
23 µl	1M NaOH

180 µl of ice cold collagen gel mix was added to desired spheroids and mixed carefully by pipetting up and down for about 10 times without producing bubbles.

The fluid spheroid gel was then pipetted into the pre-warmed pouring device with mesh and immediately put back to incubator, where the collagen hardens over a period of 30 min. Then, with the help of a sterile foreceps the silicone foil was carefully remove and the collagen gel transferred into a 24-well-plate with the appropriate culture medium. Thereby the gel was only touched at the mesh supported border.

The 3D-spheroid-gel was incubated at 37°C and the growth monitored every day with the microscope.

### **Matrigel**

As alternative to collagen, spheroids were also grown in “Growth Factor Reduced Matrigel” of BD Biosciences (Cat.# 356231).

150 µl Matrigel was used for one gel. Silicon gaskets and the nylon mesh were not used, because Matrigel very quickly hardens; so it was sufficient to form a drop and transfer the gel pouring device immediately to the 37°C incubator.

**Probidium Iodide Staining**

To observe the status of apoptotic cells in spheroids within a spheroid-gel, probidium iodide was added directly to the media (ratio 1:4000). This treatment easily allows observation with a fluorescence-microscope utilising the appropriate filter, exhibiting apoptotic cells as red points.

**Measuring of Diameter and Volume of Spheroids**

Photographs of the spheroids were taken every two days after embedding spheroids into the gel, with the microscope. The area of the spheroids were determined with the software „AxioVision Rel.4.6“ from Carl Zeiss Imaging Solutions. Growth curves were calculated with MS Excel.

***Biochemistry*****Determination of Protein Concentration in Cell Lysates (Bradford Assay)**

To normalise the different protein concentration for quantitative analysis of Western blots, first the protein concentration of protein lysates were analysed in a Bradford assay.

Protein lysates were pre-cleared by centrifugation at 14,000 rpm for 10 min at 4°C. The amount of whole protein content was measured by a standard Bradford assay, purchased of Biorad (Cat.# 500-0006). The sample was measured in parallel to samples of a calibration curve, consisting of samples with defined amounts of BSA (0 / 1 / 5 / 7 / 10 / 15 µg/ml BSA). 5 µl of each protein sample was mixed with 1 ml 1x Bradford solution and incubated for 5 min at RT. The optical density of each sample was measured at a wavelength of 595 nm in a SmartSpec 3000 spectrophotometer. The gradient of the calibration curve was calculated and used to assess the protein concentration of the samples.

**SDS-PAGE**

All SDS-PAGE analyses were performed using pre-cast Criterion XT Bis-Tris, 4-12 % gradient gels, 18-well, 30 µl, acquired from Biorad (Cat.# 345-0124), using the Biorad gel chamber for Criterion gels.

Depending on different approaches, 50-100 µg total protein was used for SDS-PAGE analysis. The specified amount of protein was prepared with 5x SDS-LB and then

boiled at 95°C for 5 min. The sample was cooled for 1 min at ice and spun down prior loading onto the protein gel. For determination of size of proteins, as marker was used “PageRuler Prestained Protein Ladder” of Fermentas (Cat.# SM0671).

The electrophoresis was started at 100 V and subsequently elevated up to 140 V.

### **Western Blotting**

The transfer of electrophoretically separated proteins to Immuno-blot PVDF membranes (Biorad, Cat.# 162-0239) was performed by Semidry-blotting a TE 70 Semi-Dry Transfer Unit at 170 mA for 1 h per membrane.

The membrane was equilibrated for a few seconds in methanol (MeOH) prior use. For transfer the membrane and the gel were incubated and the filter papers soaked in 1x transfer buffer. After the transfer, the blots were blocked in blocking solution (TBS-T plus 5 % dried milk) for 1 h at RT and then incubated with the primary antibody diluted in blocking solution o/n at 4°C. The next day, the antibody dilution was discarded and the membrane was washed 3 x for 10 min with TBS-T. Then the membrane was incubated with the respective horse-radish-peroxidase-conjugated secondary antibody, diluted in blocking solution, for 1 h at RT. Afterwards the membrane was again washed 3 x for 10 min with TBS-T.

Detection of bound antibodies was performed by chemiluminescence, using “Amersham ECL Western blotting detection reagents” from GE Healthcare (Cat.# RPN2106) and exposing the membrane to a light-sensitive film (“Amersham Hyperfilm MP” of GE Healthcare, Cat.# RPN1675K) for an appropriate time in an exposure-cassette. The film was developed using a Curix developer.

### **Proteome Analyses with Proteome Profiler™ (R&D Systems)**

#### **MAPK-Array**

For analysing the phosphorylation status of all three major families of mitogen-activated protein kinases (MAPKs), the extracellular signal-regulated kinases (ERK1/2), c-Jun N-terminal kinases (JNK1-3), different p38 isoforms ( $\alpha/\beta/\delta/\gamma$ ), other intracellular kinases such as Akt, GSK-3 and p70 S6 kinases, the “Human Phospho-MAPK Array Kit” from R&D Systems (Cat.# ARY002) was used.

The principle of the assays is that capture and control antibodies have been spotted in duplicate on nitrocellulose membranes. Cell lysates are diluted and incubated with the Human Phospho-MAPK Array. After binding both, phosphorylated and non-

phosphorylated kinases, unbound material is washed away. A cocktail of phospho-site-specific biotinylated antibodies is then used to detect phosphorylated kinases via Streptavidin-HRP and chemiluminescence.

### **RTK-Array**

For analysing the relative levels of phosphorylation of 42 different receptor tyrosine kinases, the “Human Phospho-RTK Array Kit” from R&D Systems (Cat.# ARY001) was used.

The principle of the assays is that capture and control antibodies have been spotted in duplicate on nitrocellulose membranes. Cell lysates are diluted and incubated with the Human Phospho-RTK Array. After binding the extracellular domain of both, phosphorylated and non-phosphorylated RTKs, unbound material is washed away. A pan anti-phospho-tyrosine-antibody conjugated to horseradish peroxidase (HRP) is then used to detect phosphorylated tyrosines on activated receptors by chemiluminescence.

### **Immunohistochemistry**

An indirect immunoperoxidase assay was used to detect expression of CLCA2. 5 µm thick sections were cut and mounted on poly-(L-lysine)-coated slides. After de-paraffinisation and epitope retrieval with Proteinase K in TrisEDTA buffer pH 8.0 for 15 min at 37°C, the sections were blocked with 10 % normal goat serum. The primary antibody was applied for 1 h at RT followed by incubation with goat anti-rabbit horseradish peroxidase labelled polymer, Dako Envision System (Dako) for 30 min at RT. The final reaction product was visualised with DAB (0.06 % 3,3'-diaminobenzidine in PBS, 0.003 % H<sub>2</sub>O<sub>2</sub>) for 2-5 min. Then the slides were dehydrated in alcohol and counterstained with hematoxylin. The specificity of the staining was confirmed by pre-incubating the primary anti-peptide-antibody with the corresponding synthetic peptide for 2 h at RT at the final concentration of 25 µg/ml of antibody which resulted in no staining of the tumour cells.

### **Antibody Generation**

CLCA2 antibodies were generated by immunising rabbits with peptides corresponding to the amino acid sequence of CLCA2 (NH<sub>2</sub>-epitope-COOH).

Three rabbits were immunised with the following peptides: Table 8



<b><i>Rabbit No.</i></b>	<b><i>Amino Acid Pos. in CLCA2 Protein Sequence</i></b>	<b><i>Peptide Sequence</i></b>
1	K94 – N110 N179 – D199	KANNNSKIKQESYEKAN NDKPFYINGQNQIKVTRCSSD
2	E498 – T513 H690 – H708	ESTGENVKPHHQLKNT HVNHSPSISTPAHSIPGSH
3	T643 – L656	TVEPETGDPVTLRL

**Table 8. Peptides used for generation of antisera in rabbits**

The serum containing the anti-CLCA2-antibodies was affinity purified using the corresponding peptide coupled to a Sulfo-Link-Gel-column, using the SulfoLink Kit from Pierce (Cat.# 44895). The antiserum was eluted with 0.2 mol/l Glycine/HCl pH 2.7, 150 mmol/l NaCl. The fractions were tested in Western blotting analysis.

## ***In Silicio Analyses***

### **Statistical and Bioinformatic Analyses**

All mathematical calculations and graphics were performed with MS Excel and GraphPad Prism 4.0.

### **Sequence Alignment**

Sequence data were edited and analysed with the VectorNTI Software of Invitrogen.

### **Expression Profiling**

For expression analysis, box-and-whisker plots were generated as described [75;168]. The respective hybridisations were performed on Affymetrix Exon GeneChips. These microarrays are based on 25-mer oligonucleotides and allow the detection of more than 39,000 human transcripts, with probe sets of 11 oligonucleotides used per transcript.

Approximately 1 µg of total RNA was converted into DNA, which was fragmented and end-labeled. 5 µg of labelled target DNA was hybridised to the Affymetrix GeneChip-Human Exon 1.0 Array at 45°C for 16 h as recommended by the manufacturer (<http://www.affymetrix.com>). After hybridisation arrays were washed and scanned on a GCS3000Scanner (Affymetrix, Santa Clara, CA). Chip data were normalised with the statistical algorithm implemented in the Microarray Suite version 5.0 (Affymetrix).

The raw expression intensity for a given chip experiment is multiplied by a global scaling factor to allow comparisons between chips. This factor is calculated by removing the highest 2 % and the lowest 2 % of the values of the non-normalised expression values, and calculating the mean for the remaining values, as trimmed mean. One hundred divided by the trimmed mean gives the scaling factor, where 100 is the standard value used by GeneLogic. For oligonucleotide-specific background normalisation individual absent- and present-calls are calculated by comparing the absolute signal intensities for corresponding perfect-match and mismatch oligonucleotides.

## **Media and Buffers** (in alphabetical order)

### **Molecularbiology**

<u>1<sup>st</sup> Strand buffer, 5x:</u> (Invitrogen; Cat.# 18064-014)	250 mM 375 mM 15 mM	Tris-HCl (pH 8.3) KCl MgCl <sub>2</sub>
<u>Ammonium acetate, 7.5 M:</u>	57.86 g add 100 ml	NH <sub>4</sub> Ac H <sub>2</sub> O
<u>Ampicillin stock:</u>	50 mg/ml	Ampicillin in H <sub>2</sub> O filter through 0.22 µm sterile
<u>Blocking solution:</u> (for Western blot)	1 x 5 %	TBS-T buffer dried milk
<u>Buffer EB:</u> (Qiagen; Cat.# 27106 )	10 mM	Tris-HCl pH 8.5
<u>Buffer P1:</u> (Qiagen; Cat.# 27106 )	50 mM 10 mM 100 µg/ml	Tris-HCl (pH 8.0) EDTA RNaseA
<u>Buffer P2:</u> (Qiagen; Cat.# 27106 )	200 mM 1 %	NaOH SDS
<u>Buffer P3:</u> (Qiagen; Cat.# 27106 )	2.55 M	KAc (pH 4.8)

<u>Buffer QBT:</u> (Qiagen; Cat.# 12163 )	750 mM 50 mM 15 % (v/v) 0.15 % (v/v)	NaCl MOPS (pH 7.0) Isopropanol Triton X-100
<u>Buffer QC:</u> (Qiagen; Cat.# 12163 )	1 M 50 mM 15 % (v/v)	NaCl MOPS (pH 7.0) Isopropanol
<u>Buffer QF:</u> (Qiagen; Cat.# 12163 )	1,25 M 50 mM 15 % (v/v)	NaCl Tris-HCl (pH 8.5) Isopropanol
<u>DEPC-H<sub>2</sub>O:</u>	0.1 % (v/v)	DEPC in Millipore water; shake well autoclave the next day 20 min at 1.5 bar
<u>DNA loading buffer 6x:</u>	0.3 % 0.3 % 1 % 30 % 30 mM	Bromphenole Blue Xylene Cyanol SDS Glycerol EDTA
<u>Klenow 10x buffer:</u> (Promega; Cat.# M195A)	500 mM 100 mM 1 mM	Tris-HCl (pH 7.2) MgSO <sub>4</sub> DTT
<u>LB media:</u> (Lauria-Bertani Broth) (Biolab; Cat.# LBB30500)	10 g/l 5 g/l 10 g/l	Tryptone Yeast extract NaCl pH 7.5 (approx.)
<u>LB-Amp media:</u>	1000 ml 1 ml	LB media 1000x Ampicillin Stock
<u>LB-Amp plates:</u>	1000 ml 15 g 1 ml	LB media Bacto Agar ( <i>Difco</i> ) autoclave 20 min at 1.5 bar 1000x Ampicillin Stock (added at 55°C)
<u>Ligase buffer, 10x:</u> (Promega; Cat.# C126A, C126B )	300 mM 100 mM 100 mM 10 mM	Tris-HCl (pH 7.8) MgCl <sub>2</sub> DTT ATP
<u>PCR buffer, 10x:</u> (TaKaRa; Cat.# R001A )	100 mM 500 mM 15 mM	Tris-HCl (pH 8.3) KCl MgCl <sub>2</sub>

<u>PCR buffer, 10x:</u>	100 mM	Tris-HCl (pH 8.3)
<u>Mg<sup>2+</sup> free:</u>	500 mM	KCl
(TaKaRa; Cat.# R001AM)		
<u>SDS-loading buffer, 1x:</u>	50 mM	Tris-HCl (pH 6.8)
	100 mM	DTT or $\beta$ -Mercaptoethanol
	2 %	SDS
	0.1 %	Bromphenol Blue
	10 %	Glycerol
<u>SOC media:</u>	2 %	Tryptone
	0.5 %	Yeast extract
(Invitrogen; Cat.# 15544-034)		
	10 mM	NaCl
	2.5 mM	KCl
	10 mM	MgCl <sub>2</sub>
	10 mM	MgSO <sub>4</sub>
	20 mM	Glucose
<u>Sodium acetate, 3M:</u>	40.8g	NaAc·3H <sub>2</sub> O
	80 ml	H <sub>2</sub> O
		adjust with Acetic acid to pH 5.2
	add 100 ml	H <sub>2</sub> O
<u>TBE buffer, 10x:</u>	1 M	Tris
	0.9 M	Boric acid
(Invitrogen; Cat.# 15581-044)		
	0.01 M	EDTA
<u>TBS-T:</u>	20 mM	Tris-HCl
(Tris buffered saline	150 mM	NaCl
with 0.05 % Tween 20)	0.05 %	Tween 20
<u>TE:</u>	10 mM	Tris-HCl (pH 7.5 - 8)
	1 mM	EDTA
<u>Transfer buffer:</u>	20 mM	Tris-HCl
	66.6 mM	Glycine
	20 %	Methanol

## Cell Culture

<u>PBS, Dulbecco's (1x):</u>	0.2 g/l	KCl
	0.2 g/l	KH <sub>2</sub> PO <sub>4</sub>
(Gibco; Cat.# 14190-094)		
	8 g/l	NaCl
	1.15 g/l	Na <sub>2</sub> HPO <sub>4</sub>
		pH 7.2

<u>Lysis buffer for protein lysates:</u>	20 mM	Hepes, pH 7.3
	5 mM	EDTA
	2 mM	EGTA
	30 mM	Sodiumfluoride
	1 mM	Sodiumorthovanadate (Na <sub>3</sub> VO <sub>4</sub> )
	20mM	Sodiumpyrophosphate
	40 mM	b Glycerophosphate
	30 mM	Sodiumfluoride
	0.5 %	Triton X-100
1 Tab. / 50 ml buffer		Protease Inhibitor Cocktail, "complete, EDTA-free", Roche, Cat.# 04693132001
<u>Mammalian cell culture media for T47D Tet-on cell line:</u>	~450 ml	DMEM high glucose medium, with L-glutamine
	10 %	Fetal bovine serum, Tet System approved (Clontech, Cat.# 631101)
	5 ml	100x Hepes buffer
	2 ml	Geneticin (50mg/ml)
	5 ml	100x Sodium pyruvate
	0.5 ml	Bovine Insuline (10g/ml)
<u>Mammalian cell culture media for HN5 cell line:</u>	~450 ml	DMEM high glucose medium, with L-glutamine
	10 %	Fetal Bovine Serum
	5 ml	100x Hepes buffer
	5 ml	100x Sodium pyruvate
	5 ml	100x NEAA Mixture
<u>Mammalian cell culture media for MDA-MB-453 cell cine:</u>	450 ml	DMEM high glucose medium, with L-glutamine
	10 %	Fetal Bovine Serum (GIBCOBRL)

Reagents for cell culture media: (in alphabetical order)

- Bovine Insuline, 10 mg/ml insuline in 25 mM HEPES, pH 8.2, Sigma, Cat.# I0516
- DMEM high glucose medium, with L-glutamine, Lonza Group, Cat.# BE12-604F
- Doxycycline 5 g, Clontech, Cat.# 631311
- D-PBS (1x), Invitrogen, Cat.# 14190-094
- Fetal bovine serum, JRH Biosciences, Cat.# 12103-500M
- Geneticin selective antibiotic, Invitrogen, 50 mg/ml Cat.# 10131-019
- GlutaMAX-I supplement, 200 mM, Invitrogen, Cat.# 35050-038
- Hepes buffer 1M, Cambrex, Cat.# BE17-737E
- MEM medium, Invitrogen, Cat.# 21090-022
- MEM non essential amino acids solution (100x), Invitrogen, Cat.# 11140-035
- Puromycin, Sigma, Cat.# P9620
- RPMI 1640 medium w/GlutaMAX, Invitrogen, Cat.# 61870-036

- Sodium Pyruvate MEM 100 mM, Invitrogen, Cat.# 11360-039
- Tet system approved fetal bovine serum, Clontech, Cat.# 631101

## Primer

All oligo-deoxynucleotides were ordered from metabion GmbH. The crystals were dissolved in elution buffer EB (10 mM Tris-HCl, pH 8.5) to a concentration of 100 pmol/μl. Aliquotes of 5 pmol/μl were prepared.

## Cloning Primer

$T_m$  (in PCR buffer) =  $22 + 1,46 (2*(G+C)+A+T)$

Name	EBI-No.	Sequenz (5' → 3')
hCLCA2-EcoRI f	15911	ccggaattcatgacccaaaggagcattgc
hCLCA2-XhoI r	15912	ccgctcgagttataataattttgtccattctcttc
CLCA2-BamHI r	15957	cgggatcctaataattttgtccattctcttctgt
hCLCA2-NotI f	15958	ataagaatgcggccgccaccatgacccaaaggagcattgc

Table 9. Sequences of cloning primer

## Cloning Primer for *In Vitro* Site-Directed Mutagenesis of CLCA2

Primers were designed according provider's instructions, the melting temperature was calculated according provider's Website:

<http://www.stratagene.com/QPCR/tmCalc.aspx>

Mutation	Basepair Change	EBI-No.	Sequence of Primer (5' → 3')
C132A	TGT → GCC	17201 (f)	ccctacaatacagagggGCCggaaaagagggaaaatacattcattcac
		17202 (r)	gtgaaatgaatgtatttccctctttccGCCccctctgtattgtagg
C196A	TGT → GCC	- (f)	caaattaaagtgaacaggGCCtcattctgacatcacaggg
		- (r)	gcctgtgatgtcagatgaGCCcctgtcactttaattg
C206A	TGT → GCC	- (f)	cacaggcattttgtgGCCgaaaaaggtccttgcc
		- (r)	ggcaaggaccttttcGCCcacaataatgcctgtg
C211A	TGC → GCC	- (f)	gtgtgtgaaaaaggtcctGCCccccagaaaactg
		- (r)	cagtttcttggggGCCaggaccttttcacacac
C216A	TGT → GCC	- (f)	ggccttgcccccaagaaaacGCCattattagtaagc
		- (r)	gctactaataatGCCgtttcttgggggcaaggacc
N150A	AAC → GCC	16863 (f)	cctaatttctactgaatgatGCCttaacagctggctacggatcacg
		16864 (r)	cgtgatccgtagccagctgttaagGCatcattcagtaggaaattagg
N522A	AAC → GCC	16865 (f)	ggataatactgtgggcGCCgacactatgtttctagtacgtggc
		16866 (r)	gccacgtaactagaaacatagtgtcGCCgcccacagtattatcc
N822A	AAT → GCC	16867 (f)	gctattttagtaGCCacatcaagcgaaatcctcagcaagctggcatcaggg
		16868 (r)	ccctgatgccagcttctgaggatttcgctttgatgtGCCtactaaaatagc
C132S	TGT → TCC	17199 (f)	ccctacaatacagagggTCCggaaaagagggaaaatacattcattcac
		17200 (r)	gtgaaatgaatgtatttccctctttccGGaccctctgtattgtagg

H164C	CAT → TGC	17207 (f)	gaggccgagtggtttgtcTGCgaatgggcccacctc
		17208 (r)	gaggtgggcccattcGCAgacaaacactcggcctc
H164N	CAT → AAC	16968 (f)	gaggccgagtggtttgtcAaCgaatgggcccacctc
		16969 (r)	gaggtgggcccattcGtAgacaaacactcggcctc
H164Y	CAT → TAC	16970 (f)	gaggccgagtggtttgtcTaCgaatgggcccacctc
		16971 (r)	gaggtgggcccattcGtAgacaaacactcggcctc
E165D	GAA → GAC	17203 (f)	cgagtgtttgtccatgaCtgggcccacctccgttg
		17204 (r)	caacggaggtgggcccGtcatggacaaacactcg
E165Q	GAA → CAG	16966 (f)	cgagtgtttgtccatCaGtgggcccacctccgttg
		16967 (r)	caacggaggtgggcccCtGatggacaaacactcg
H168C	CAC → TGC	17209 (f)	catgaatgggccTGcctccgttggggtgtg
		17210 (r)	cacacccaacggagqCAGgcccattcatg
H168N	CAC → AAC	16972 (f)	catgaatgggccAacctccgttggggtgtg
		16973 (r)	cacacccaacggaggtTggcccattcatg
H168Y	CAC → TAC	16974 (f)	catgaatgggccTacctccgttggggtgtg
		16975 (r)	cacacccaacggaggtaggcccattcatg
N186A	AAT → GCC	17205 (f)	caatgacaaacctttctacataGCCgggcaaaatcaaattaaagtgacaaggtgttc
		17206 (r)	gaacacctgtcactttaattgtatttggcccGGCtatgtagaaaggtttgtcattg
G670A	GGA → GCC	17211 (f)	gctgatgttataaaaaatgatgGCCatttactcgaggtatttttctccttgcctgc
		17212 (r)	gcagcaaaggagaaaaaaatcacctcgagtaaataGGcatcatttttataacatcagc
I671A	ATT → GCC	17213 (f)	gctgatgttataaaaaatgatggaGCCtactcgaggtatttttctccttgcctgc
		17214 (r)	gcagcaaaggagaaaaaaatcacctcgagtaGGCtccatcatttttataacatcagc
I671L	ATT → CTG	17386 (f)	gctgatgttataaaaaatgatggaCtGtactcgaggtatttttctccttgcctgc
		17387 (r)	gcagcaaaggagaaaaaaatcacctcgagtaCaGtccatcatttttataacatcagc
Y672A	TAC → GCC	17215 (f)	gctgatgttataaaaaatgatggaattGCctcgaggtatttttctccttgcctgc
		17216 (r)	gcagcaaaggagaaaaaaatcacctcgagGCaattccatcatttttataacatcagc
Y672E	TAC → GAG	17380 (f)	gctgatgttataaaaaatgatggaattGaGtcgaggtatttttctccttgcctgc
		17381 (r)	gcagcaaaggagaaaaaaatcacctcgaCtCaattccatcatttttataacatcagc
Y672F	TAC → TTC	17384 (f)	gctgatgttataaaaaatgatggaattTctcgaggtatttttctccttgcctgc
		17385 (r)	gcagcaaaggagaaaaaaatcacctcgagAaaattccatcatttttataacatcagc
Y672K	TAC → AAG	17378 (f)	gctgatgttataaaaaatgatggaattAaGtcgaggtatttttctccttgcctgc
		17379 (r)	gcagcaaaggagaaaaaaatcacctcgaCtTaattccatcatttttataacatcagc
Y672Q	TAC → CAG	17382 (f)	gctgatgttataaaaaatgatggaattCaGtcgaggtatttttctccttgcctgc
		17383 (r)	gcagcaaaggagaaaaaaatcacctcgaCtGaattccatcatttttataacatcagc
S673A	TCG → GCC	17217 (f)	gctgatgttataaaaaatgatggaatttacGcCaggtatttttctccttgcctgc
		17218 (r)	gcagcaaaggagaaaaaaatcacctGgCgtaaattccatcatttttataacatcagc
R674A	AGG → GCC	17219 (f)	gatggaatttactcgGCCtatttttctccttgcctgcaaatggtagatatagc
		17220 (r)	gctatatctaccatttgcagcaaaggagaaaaaaataGGCcgagtaaattccatc
R674E	AGG → GAG	17027 (f)	gatggaatttactcgGAGtatttttctccttgcctgcaaatggtagatatagc
		17023 (r)	gctatatctaccatttgcagcaaaggagaaaaaaatacTCcgagtaaattccatc
R674F	AGG → TTC	17029 (f)	gatggaatttactcgTTCtatttttctccttgcctgcaaatggtagatatagc
		17030 (r)	caagctatatctaccatttgcagcaaaggagaaaaaaataGAACgagtaaattccatc
R674I	AGG → ATC	17025 (f)	gatggaatttactcgaTCtatttttctccttgcctgcaaatggtagatatagc
		17026 (r)	gctatatctaccatttgcagcaaaggagaaaaaaataGAtcgagtaaattccatc
R674K	AGG → AAG	17362 (f)	gatggaatttactcgaAGtatttttctccttgcctgcaaatggtagatatagc
		17363 (r)	gctatatctaccatttgcagcaaaggagaaaaaaatacTtcgagtaaattccatc
R674Q	AGG → CAG	17366 (f)	gatggaatttactcgaCaGtatttttctccttgcctgcaaatggtagatatagc
		17367 (r)	gctatatctaccatttgcagcaaaggagaaaaaaataCtGcgagtaaattccatc
R674S	AGG → TCC	16545 (f)	gatggaatttactcgaTCCtatttttctccttgcctgc
		16546 (r)	gcagcaaaggagaaaaaaataggacgagtaaattccatc
R674T	AGG → ACC	17368 (f)	gatggaatttactcgaACCtatttttctccttgcctgcaaatggtagatatagc
		17369 (r)	gctatatctaccatttgcagcaaaggagaaaaaaataGGacgagtaaattccatc

<b>R674Y</b>	AGG → TAC	17364 (f)	gatggaatttactcgTaCtatttttctccttgctgcaaattgtagatatagc
		17365 (r)	gctatatctaccatttcagcaaaggagaaaaataGtAcgagtaaattccatc
<b>Y675A</b>	TAT → GCC	17221 (f)	gatggaatttactcgaggGCCtttttctccttgctgcaaattgtagatatagc
		17222 (r)	gctatatctaccatttcagcaaaggagaaaaaGGCcctcgagtaaattccatc
<b>Y675E</b>	TAT → GAG	17372 (f)	gatggaatttactcgaggGaGtttttctccttgctgcaaattgtagatatagc
		17373 (r)	gctatatctaccatttcagcaaaggagaaaaaCtCcctcgagtaaattccatc
<b>Y675F</b>	TAT → TTC	17376 (f)	gatggaatttactcgaggTTCtttttctccttgctgcaaattgtagatatagc
		17377 (r)	gctatatctaccatttcagcaaaggagaaaaaGAacctcgagtaaattccatc
<b>Y675K</b>	TAT → AAG	17370 (f)	gatggaatttactcgaggAaGtttttctccttgctgcaaattgtagatatagc
		17371 (r)	gctatatctaccatttcagcaaaggagaaaaaCtTcctcgagtaaattccatc
<b>Y675Q</b>	TAT → CAG	17374 (f)	gatggaatttactcgaggCaGtttttctccttgctgcaaattgtagatatagc
		17375 (r)	gctatatctaccatttcagcaaaggagaaaaaCtGcctcgagtaaattccatc
<b>F676A</b>	TTT → GCC	17223 (f)	gatggaatttactcgagggtatGCCttctccttgctgcaaattgtagatatagc
		17224 (r)	gctatatctaccatttcagcaaaggagaaGGCatacctcgagtaaattccatc
<b>F676W</b>	TTT → TGG	17390 (f)	gatggaatttactcgagggtatGGttctccttgctgcaaattgtagatatagc
		17391 (r)	gctatatctaccatttcagcaaaggagaaCCaatacctcgagtaaattccatc
<b>F676Y</b>	TTT → TAC	17388 (f)	gatggaatttactcgagggtatACttctccttgctgcaaattgtagatatagc
		17389 (r)	gctatatctaccatttcagcaaaggagaaGTaatacctcgagtaaattccatc
<b>F677A</b>	TTC → GCC	17225 (f)	gatggaatttactcgagggtatttGCctccttgctgcaaattgtagatatagc
		17226 (r)	gctatatctaccatttcagcaaaggagGCaaaatacctcgagtaaattccatc
<b>S678A</b>	TCC → GCC	17227 (f)	gatggaatttactcgagggtatttttGcctttgctgcaaattgtagatatagc
		17228 (r)	gctatatctaccatttcagcaaaggCGaaaaatacctcgagtaaattccatc

Table 10. Sequences of mutagenesis primer

## Sequencing Primers

$T_m$  (in PCR buffer) =  $22 + 1,46 (2*(G+C)+A+T)$

Name	EBI-No.	Sequenz (5' → 3')
T7f	5567	taatacgactcactataggg
pUC/M13r	6298	caggaaacagctatgac
T3r	13174	attaaccctcactaaaggg
pCMV-Tag1-T3 f	7148	aataaccctcactaaaggg
pCMV-Tag1-T7 r	13432	gtaatacgactcactatagggc
pCMV6-XL4 f (VP1.5)	15909	ggactttccaaaatgtcg
pCMV6-XL4 r (XL39)	15910	attaggacaaggctgggtggg
pTRE2pur f	-	cgcttgagagacgccatcc
pTRE2pur r	-	cattctaaacaacaccctg
CLCA2do3	-	gcacatggagatgatccatacaccccta
CLCA2do4	-	gcaagtaccacaaccaagaagcacca
CLCA2do6	-	ggaacagctaagcctgggcactggact
CLCA2do7	15906	ggttacacagcaaacggaatattcaga
CLCA2do12	10071	gcacccaaaatgcaactgcatcaataatgt
CLCA2do13	10072	gtgatgatattagtgaccagcgaga
CLCA2up2	9626	cactttcgctcctcctcatttgcct
CLCA2up3	9657	cctgagctgactcggctaaagcccca
CLCA2up10	9778	gacatttcacctgtactttcaagct
CLCA2up12	9818	ggtgcttctgtgtgtgggtacttgca
CLCA2up13	9819	gattacatcccatgcacttctgaggct
CLCA2up19	-	gttatcattcagtaggaattagggtga
CLCA2up21	-	gcacatggagatgatccatacaccccta
hClCa2-check-rev	15849	gggagatattacgttctcacc



<b>8F5-check-rev</b>	15411	ggattcaatctcgtctcagc
<b>HA-check-rev</b>	15842	gcgtaatctggaacatcgatg
<b>c-myc-check-rev</b>	15843	gtcctcctctgagatcagc
<b>lumio-check-rev</b>	15844	caacagccaggacaacagg
<b>V5-check-rev</b>	15845	ggagagggttagggatagg
<b>6x-His-check-rev</b>	15846	agtgatggtgatggtgatgg

Table 11. Sequences of sequencing primer

## Oligomers

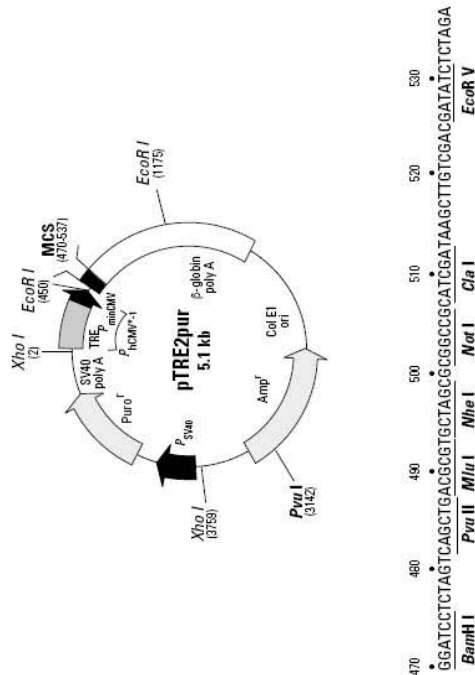
<b>Name</b>	<b>EBI-No.</b>	<b>Sequenz (5' → 3')</b>
<b>8F5-1</b>	15829	gatccggcaggggaaggttaaagctgagacgagattgaatccttagtgacccggggatatca
<b>8F5-2</b>	15830	agcttgatatccccgggtcactaaggattcaatctcgtctcagcttaacttcctgccg
<b>HA-1</b>	15831	gatcctacccatacgaatgtccagattacgcttagtgacccggggatatca
<b>HA-2</b>	15832	agcttgatatccccgggtcactaaggcgtaatctggaacatcgatgggtag
<b>c-myc-1</b>	15833	gatccgagcagaagctgatctcagaggaggacctgtagtacccggggatatca
<b>c-myc-2</b>	15834	agcttgatatccccgggtcactacaggtcctcctctgagatcagcttctgctcg
<b>V5-1</b>	15837	gatccgggaagcctatccctaaccctctcctcgggtctcgattctacgtagtacccggggatatca
<b>V5-2</b>	15838	agcttgatatccccgggtcactacgtagaatcgagaccgaggagagggttagggataggctcccg
<b>6xHis-1</b>	15839	gatcccatcaccatcaccatcactagtacccggggatatca
<b>6xHis-2</b>	15840	agcttgatatccccgggtcactagtatggtgatggtgatgg

Table 12. Sequences of oligomers

## Plasmids

### pTRE2pur Expression Vector

("Tet-on Gene Expression System" of Clontech, Cat.# 630922)



#### Location of Features

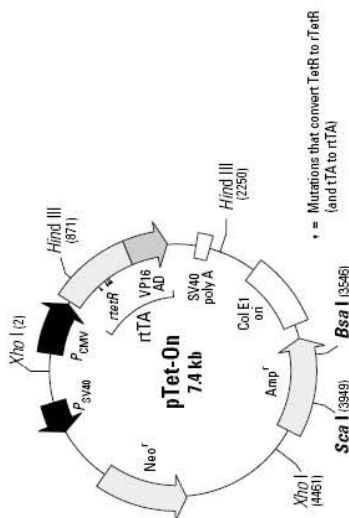
- Fragment containing  $P_{CMV}$ : 86–673
- reverse tetracycline-responsive transcriptional activator (rtTA): 774–1781
- Col E1 origin of replication: 2604–3247
- Ampicillin resistance gene:  $\beta$ -lactamase coding sequences: 4255–3395
- Fragment containing the SV40 poly A signal: 1797–2254
- Neomycin/kanamycin resistance gene: 6462–5668
- SV40 promoter ( $P_{SV40}$ ) controlling expression of neomycin/kanamycin resistance gene: 7125–6782.

#### Propagation in *E. coli*

- Suitable host strains: DH5 $\alpha$  and other general purpose strains.
- Selectable marker: plasmid confers resistance to ampicillin (50  $\mu$ g/ml) on *E. coli* hosts.
- *E. coli* replication origin: Col E1

#### References

1. Tet Expression Systems and Cell Lines (July 1996) *Clontech* **XI**(3):2–5.
2. Gossen, M. & Bujard, H. (1992) *Proc. Natl. Acad. Sci. USA* **89**:5547–5551.
3. Gossen, M., et al. (1995) *Science* **268**:1766–1769.
4. Heintzky, D., et al. (1994) *Mol. Cell. Biol.* **14**:1669–1679.



#### Location of Features

- Fragment containing  $P_{CMV}$ : 86–673
- reverse tetracycline-responsive transcriptional activator (rtTA): 774–1781
- Col E1 origin of replication: 2604–3247
- Ampicillin resistance gene:  $\beta$ -lactamase coding sequences: 4255–3395
- Fragment containing the SV40 poly A signal: 1797–2254
- Neomycin/kanamycin resistance gene: 6462–5668
- SV40 promoter ( $P_{SV40}$ ) controlling expression of neomycin/kanamycin resistance gene: 7125–6782.

#### Propagation in *E. coli*

- Suitable host strains: DH5 $\alpha$  and other general purpose strains.
- Selectable marker: plasmid confers resistance to ampicillin (50  $\mu$ g/ml) on *E. coli* hosts.
- *E. coli* replication origin: Col E1

#### References

1. Tet Expression Systems and Cell Lines (July 1996) *Clontech* **XI**(3):2–5.
2. Gossen, M. & Bujard, H. (1992) *Proc. Natl. Acad. Sci. USA* **89**:5547–5551.
3. Gossen, M., et al. (1995) *Science* **268**:1766–1769.
4. Heintzky, D., et al. (1994) *Mol. Cell. Biol.* **14**:1669–1679.

## pGEM-T Easy Vector (Promega, Cat.# A1380 )

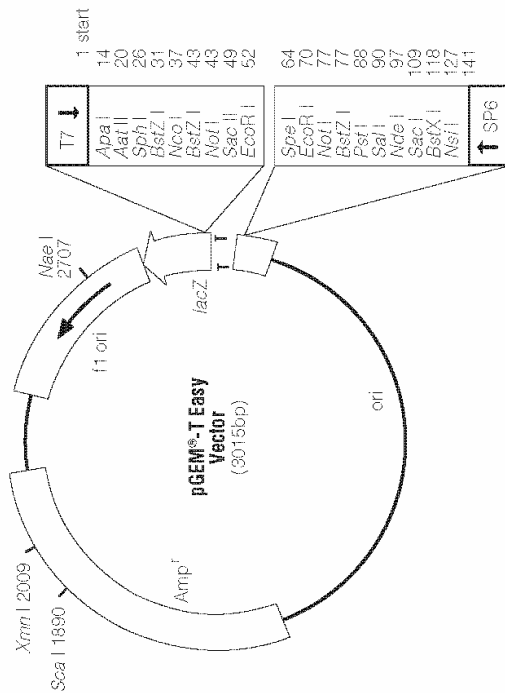


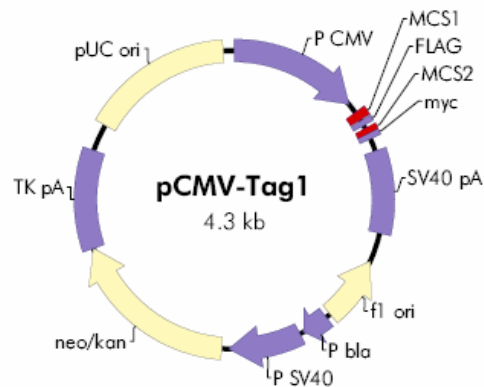
Figure 3. pGEM®-T Easy Vector circle map and sequence reference points.

### pGEM®-T Easy Vector Sequence reference points:

T7 RNA Polymerase transcription initiation site	1
SP6 RNA Polymerase transcription initiation site	141
T7 RNA Polymerase promoter (-17 to +3)	2999-3
SP6 RNA Polymerase promoter (-17 to +3)	139-158
multiple cloning region	10-128
<i>lacZ</i> start codon	180
<i>lac</i> operon sequences	2836-2996, 166-395
<i>lac</i> operator	200-216
β-lactamase coding region	1337-2197
phage f1 region	2380-2835
binding site of pUC/M13 Forward Sequencing Primer	2956-2972
binding site of pUC/M13 Reverse Sequencing Primer	176-192

## pCMV-Tag1 Expression Vector (Stratagene, Cat.# 211170)

CMV promoter 1-602  
multiple cloning site 1 651-692  
FLAG tag 699-722  
multiple cloning site 2 737-764  
c-myc tag 762-791  
SV40 polyA 852-1235  
f1 origin 1373-1679  
*bla* promoter 1704-1828  
SV40 promoter 1848-2186  
neomycin/kanamycin resistance ORF 2221-3012  
HSV-TK polyA 3013-3471  
pUC origin 3600-4267



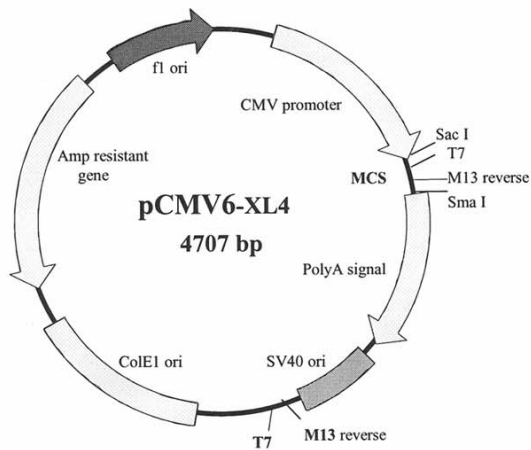
### pCMV-Tag 1 Multiple Cloning Site Region (sequence shown 620-840)

T3 promoter  
A ATT AAC CCT CAC TAA AGG GAA CAA AAG CTG GAG CTC CAC CGC GGT GGC GGC CGC TCT A...

...GC CCG GGC GGA TCC ACC ATG GAT TAC AAG GAT GAC GAC GAT AAG ATC TGA TCA GAT...  
FLAG tag  
M D Y K D D D D K I  
...ATC AAG CTT ATC GAT ACC GTC GAC CTC GAG CAG AAA CTC ATC TCT GAA GAG GAT CTG...  
myc tag  
E Q K L I S E E D L  
...TAGGTACCAGGTAAGTGTACCCAATTGCGCCCTATAGTGAGTCGTATTAC  
T7 promoter  
STOP

## Human Full-Length cDNA Clone of CLCA2 in pCMV6-XL4

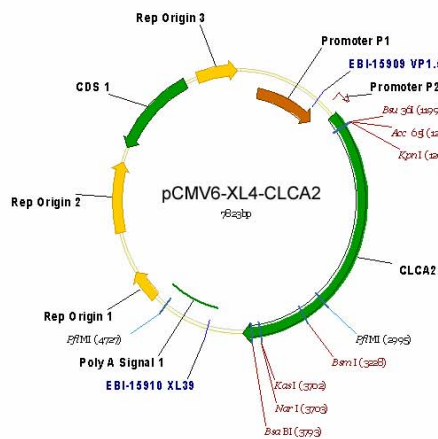
(Origene, Cat.# TC116023, Acc. NM\_006536: Human calcium-activated chloride channel, family member 2 (CLCA2))



The pCMV-XL4 vector is 4.7 kb in size, and the pCMV-XL5 and pCMV-XL6 vectors are 4.5 kb in size. All three vectors contain the same polylinker (*Sac* I to *Sma* I). The cDNA library inserts are directionally cloned between the *Eco* RI and *Sal* I sites. Note that the *Sal* I site is destroyed in the cloning process. The CMV promoter, which can be used to express the cloned cDNA, is followed by the hGH (human growth hormone) polyA signal located downstream of the insert. The ColE1 ori is the bacterial origin of replication, the SV40 ori allows for replication in mammalian cells and the f1 ori is the filamentous phage origin of replication, which allows for the recovery of single-stranded plasmids. Selection of the plasmid in *E. coli* is conferred by the ampicillin resistant gene.

T7 RNA polymerase can be used for generating transcripts of the cDNA by *in vitro* transcription. Apart from the T7 promoter site located within the polylinker sequence in the pCMV-XL4 vector, there is a second but opposing T7 site (with a one-base substitution on the 3' end) located between ColE1 ori and SV40 ori. Since a second T7 promoter site is present, the cDNA insert first has to be released from the vector, which may be accomplished by digesting with *Sac* I and *Sma* I, prior to the *in vitro* transcription reaction. The pCMV-XL5 vector does not have a second T7 promoter site, and the pCMV-XL6 vector has an SP6 promoter. Therefore, clones within the XL5 or XL6 vectors do not require prior excision.

The M13 primer sequence is represented twice within the pCMV6-XL4 and pCMV6-XL5 vector sequences with only a slight variation in bases between the two sites. Therefore, sequencing from the 3' end of cDNA inserts may not be performed using an M13 Reverse primer.



### Polylinker Sequence of pCMV6-XL4

```

T T T G G C A C C A A A A T C A A C G G G A C T T T C
A A A C C G T G G T T T T A G T T G C C C T G A A A C

C A A A A T G T C G T A A T A A C C C C G C C C C G T
G T T T T A C A G C A T T A T T G G G G C G G G G C A

T G A C G C A A A T G G G C G G T A G G C G T G T A C
A C T G C G T T T A C C C G C C A T C C G C A C A T G

G G T G G G A G G T C T A T A T A A G C A G A G C T C
C C A C C C T C C A G A T A T A T T C G T C T C G A G

Vector Primer 3
G T T T A G T G A A C C G T C A G A A T T T T G T A A
C A A A T C A C T T G G C A G T C T T A A A A C A T T

T7 Promoter Site
T A C G A C T C A C T A T A G G G C G C C G C G A A
A T G C T G A G T G A T A T C C C G C C G G C G C T T

EcoRI Bgl II Kpn I EcoRV Hind III
T T C A G A T C T G G T A C G G A T A T C A A G C T T
A A G T C T A G A C T A T G G C T A T A G T T C G A I A

G T C G A C T C T A G A T T G C G C C G C G G T C A
C A G C T G A G A T C T A A C G C C G C G C A G T

Sal I Xba I Not I Sma I
T A G C T G T T T C C T G A A C A T G T G A T C C C G
A T C G A C A A A G G A C T T G T A C A C T A G G G C

G G T G G C A T C C C T G T G A C C C C C C C A G
C C A C C G T A G G G A C A C T G G G G A G G G G T C

T G C C T C T C C T G G C C C T G G A A G T T G C C A
A C G G A G A G G A C C G G G A C C T T C A A C G G T

C T C C A G T G C C C A C C A G C C T T G T C C T A A
G A G G T C A C G G G T G G T C G G A A C A G G A T T
XL39 Reverse Vector Primer
T A A A A T T A A
A T T T T A A T T

```

## Antibodies

<b>Target Protein Name</b>	<b>Phospho-Site</b>	<b>Company</b>	<b>Cat. No.</b>
GAPDH (6C5)	pan	Abcam	ab8245
β-Actin	pan	Sigma	A5441
HA-Tag (6E2)	pan	Cell Signaling	2367
V5-Tag	pan	Invitrogen	R960-25
Integrin β4 (M126)	pan	Abcam	ab29042
PARP	pan	Cell Signalling	9542
Akt	S473	Cell Signaling	#9271
Akt	S308	Cell Signaling	#9275
Akt	Y326	Cell Signaling	#2968
Akt	pan	Cell Signaling	#9272
GSK-3beta	S9	Cell Signaling	#9336
PTEN	S380	Cell Signaling	#9551
PK1	S241	Cell Signaling	#3061
PK1	pan	Cell Signaling	#3062
PI3K	p85 Y458 / p55 Y199	Cell Signaling	#4228
FAK	Y861	Biosource	44-626G
iKalpha/beta	S176/180	Cell Signaling	#2697S
NF-KB p65	S536	Cell Signaling	#3031
NF-KB p65	pan	Cell Signaling	#3034
MEK 1/2	S217/221	Cell Signaling	#9121
p44/42 MAP Kinase	T202/Y204	Cell Signaling	#9101
p38 MAPK	T180/Y182	Cell Signaling	#9211
p90RSK	S380	Cell Signaling	#9341
RSK1	S221/S227	Biosource	44-924G
RSK1	S363/S369	Biosource	44-926G
Elk1	S383	Cell Signaling	#9181
Raf	S259	Cell Signaling	#9421
c-Raf	S338	Biosource	#9427
ERK 1 & 2	T185/Y187	Biosource	44-680G
Erk 1&2	pan	Biosource	44-654G
p70 S6 Kinase	T389	Cell Signaling	#9234S
p70 S6 Kinase	pan	Cell Signaling	#9202
mTOR	S2448	Cell Signaling	#2971
mTOR	S2481	Cell Signaling	#2974
4E-BP1	T37/46	Cell Signaling	#2855
4E-BP1	T70	Cell Signaling	#9455
4E-BP1	S65	Cell Signaling	#9451
FoxO1	S319	Cell Signaling	#2487
FoxO3a	S318/321	Cell Signaling	#9465
FoxO3a	S253	Cell Signaling	#9466
Stat1	Y701	Cell Signaling	#9171
Stat2	Y690	Cell Signaling	#4471
Stat3	Y705	Cell Signaling	#9131
Stat3	S727	Cell Signaling	#9134
Stat3	Y705	Cell Signaling	#9131
Stat5	Y694	Cell Signaling	#9351
Stat6	Y641	Cell Signaling	#9361
NPM/B23 (Nucleophosmin 1)	T234/T237	BioLegend	#619101
PKCe	pan	Biosource	AHO0743

<b>Target Protein Name</b>	<b>Phospho-Site</b>	<b>Company</b>	<b>Cat. No.</b>
p27	pan	novocastra	NCL-p27
Histon H3	S10	Upstate	#06-570
TSC2	T1462	Cell Signaling	#3611
TSC2	S1254	Cell Signaling	#3616
KI67	pan	Dako Cytomation	M7240
rabbit IgG-HRP conj.	pan	Sigma Aldrich	A8275
mouse IgG-HRP conj.	pan	Sigma Aldrich	A0168

**Table 13. Antibodies used for Western blots for this study**

## APPENDIX

### *Sequence of CLCA2*

#### DNA Sequence

Coding Sequence of human calcium-activated chloride channel, family member 2 (CLCA2) mRNA. ACCESSION NM\_006536:

```

atgacccaaa ggagcattgc aggtcctatt tgcaacctga agtttgtgac tctcctggtt      60
gccttaagtt cagaactccc attcctggga gctggagtac agcttcaaga caatgggtat      120
aatggattgc tcattgcaat taatcctcag gtacctgaga atcagaacct catctcaaac      180
attaaggaaa tgataactga agcttcattt tacctattta atgctaccaa gagaagagta      240
tttttcagaa atataaagat ttttaatacct gccacatgga aagctaataa taacagcaaa      300
ataaaacaag aatcatatga aaaggcaaat gtcatagtga ctgactggta tggggcacat      360
ggagatgata catacacctt acaatacaga ggggtgtggaa aagagggaaa atacattcat      420
ttcacaccta atttcctact gaatgataac ttaacagctg gctacggatc acgaggccga      480
gtgtttgtcc atgaatgggc ccacctccgt tggggtgtgt tcgatgagta taacaatgac      540
aaacctttct acataaatgg gcaaaatcaa attaaagtga caagggtgtc atctgacatc      600
acaggcattt ttgtgtgtga aaaaggctct tgccccaag aaaactgtat tattagtaag      660
ctttttaaag aaggatgcac ctttatctac aatagcacc aaatgcaac tgcataata      720
atgttcatgc aaagtttatc ttctgtgggt gaattttgta atgcaagtac ccacaaccaa      780
gaagcaccaa acctacagaa ccagatgtgc agcctcagaa gtgcatggga tgtaatcaca      840
gactctgctg actttcacca cagctttccc atgaatggga ctgagcttcc acctcctccc      900
acattctcgc ttgtacaggc tggtgacaaa gtggtctgtt tagtgctgga tgtgtccagc      960
aagatggcag aggctgacag actccttcaa ctacaacaag ccgcagaatt ttatttgatg     1020
cagattgttg aaattcatac cttcgtgggc attgccagtt tcgacagcaa aggagagatc     1080
agagcccagc tacaccaa ataacagcaat gatgatcgaa agttgctggg ttcatatctg     1140
cccaccactg tatcagctaa aacagacatc agcatttggt cagggcctaa gaaaggattt     1200
gaggtgggtg aaaaactgaa tggaaaagct tatggctctg tgatgatatt agtgaccagc     1260
ggagatgata agcttcttgg caattgctta cccactgtgc tcagcagtgg ttcaacaatt     1320
cactccattg ccctgggttc atctgcagcc ccaaatctgg aggaattatc acgtcttaca     1380
ggaggtttaa agttctttgt tccagatata tcaaactcca atagcatgat tgatgctttc     1440
agtagaattt cctctggaac tggagacatt ttccagcaac atattcagct tgaaagtaca     1500
ggtgaaaatg tcaaacctca ccatcaattg aaaaacacag tgactgtgga taatactgtg     1560
ggcaacgaca ctatgtttct agttacgtgg caggccagtg gtcctcctga gattatatta     1620

```

```

tttgatcctg atggacgaaa atactacaca aataatttta tcaccaatct aacttttcgg 1680
acagctagtc tttagattcc aggaacagct aagcctgggc actggactta caccctgaac 1740
aatacccatc attctctgca agccctgaaa gtgacagtga cctctcgcg cccaactca 1800
gctgtgcccc cagccactgt ggaagccttt gtggaaagag acagcctcca ttttctcat 1860
cctgtgatga tttatgcaa tgtgaaacag ggattttatc ccattcttaa tgccactgtc 1920
actgccacag ttgagccaga gactggagat cctgttacgc tgagactcct tgatgatgga 1980
gcagggtgctg atgttataaa aaatgatgga atttactcga ggtatttttt ctcctttgct 2040
gcaaatggta gatatagctt gaaagtgcac gtcaatcact ctcccagcat aagcacccca 2100
gccactcta ttccaggagg tcatgctatg tatgtaccag gttacacagc aaacggtaat 2160
attcagatga atgctccaag gaaatcagta ggcagaaatg aggaggagcg aaagtggggc 2220
tttagccgag tcagctcagg aggtcctttt tcagtgtctg gagttccagc tggcccccac 2280
cctgatgtgt ttccaccatg caaaattatt gacctggaag ctgtaaaagt agaagaggaa 2340
ttgaccctat cttggacagc acctggagaa gactttgatc agggccaggc tacaagctat 2400
gaaataagaa tgagtaaaag tctacagaat atccaagatg actttaacaa tgctatttta 2460
gtaaatacat caaagcgaaa tcctcagcaa gctggcatca gggagatatt tacgttctca 2520
cccaaattt ccacgaatgg acctgaacat cagccaaatg gagaaacaca tgaaagccac 2580
agaatttatg ttgcaatacg agcaatggat aggaactcct tacagtctgc tgtatctaac 2640
attgcccagg cgctctgtt tattcccccc aattctgatc ctgtacctgc cagagattat 2700
cttatattga aaggagtttt aacagcaatg ggtttgatag gaatcatttg ccttattata 2760
gttgtgacac atcatacttt aagcaggaaa aagagagcag acaagaaaga gaatggaaca 2820
aaattattat aa 2832

```

## Potein Sequence

Translation of human calcium-activated chloride channel, family member 2 (CLCA2)  
mRNA, ACCESSION NM\_006536:

Met Thr Gln Arg Ser Ile Ala Gly Pro Ile Cys Asn Leu Lys Phe Val  
1 5 10 15

Thr Leu Leu Val Ala Leu Ser Ser Glu Leu Pro Phe Leu Gly Ala Gly  
20 25 30

Val Gln Leu Gln Asp Asn Gly Tyr Asn Gly Leu Leu Ile Ala Ile Asn  
35 40 45

Pro Gln Val Pro Glu Asn Gln Asn Leu Ile Ser Asn Ile Lys Glu Met  
50 55 60

Ile Thr Glu Ala Ser Phe Tyr Leu Phe Asn Ala Thr Lys Arg Arg Val  
65 70 75 80



# APPENDIX

Phe Phe Arg Asn Ile Lys Ile Leu Ile Pro Ala Thr Trp Lys Ala Asn  
 85 90 95  
 Asn Asn Ser Lys Ile Lys Gln Glu Ser Tyr Glu Lys Ala Asn Val Ile  
 100 105 110  
 Val Thr Asp Trp Tyr Gly Ala His Gly Asp Asp Pro Tyr Thr Leu Gln  
 115 120 125  
 Tyr Arg Gly Cys Gly Lys Glu Gly Lys Tyr Ile His Phe Thr Pro Asn  
 130 135 140  
 Phe Leu Leu Asn Asp Asn Leu Thr Ala Gly Tyr Gly Ser Arg Gly Arg  
 145 150 155 160  
 Val Phe Val His Glu Trp Ala His Leu Arg Trp Gly Val Phe Asp Glu  
 165 170 175  
 Tyr Asn Asn Asp Lys Pro Phe Tyr Ile Asn Gly Gln Asn Gln Ile Lys  
 180 185 190  
 Val Thr Arg Cys Ser Ser Asp Ile Thr Gly Ile Phe Val Cys Glu Lys  
 195 200 205  
 Gly Pro Cys Pro Gln Glu Asn Cys Ile Ile Ser Lys Leu Phe Lys Glu  
 210 215 220  
 Gly Cys Thr Phe Ile Tyr Asn Ser Thr Gln Asn Ala Thr Ala Ser Ile  
 225 230 235 240  
 Met Phe Met Gln Ser Leu Ser Ser Val Val Glu Phe Cys Asn Ala Ser  
 245 250 255  
 Thr His Asn Gln Glu Ala Pro Asn Leu Gln Asn Gln Met Cys Ser Leu  
 260 265 270  
 Arg Ser Ala Trp Asp Val Ile Thr Asp Ser Ala Asp Phe His His Ser  
 275 280 285  
 Phe Pro Met Asn Gly Thr Glu Leu Pro Pro Pro Pro Thr Phe Ser Leu  
 290 295 300  
 Val Gln Ala Gly Asp Lys Val Val Cys Leu Val Leu Asp Val Ser Ser  
 305 310 315 320  
 Lys Met Ala Glu Ala Asp Arg Leu Leu Gln Leu Gln Gln Ala Ala Glu  
 325 330 335  
 Phe Tyr Leu Met Gln Ile Val Glu Ile His Thr Phe Val Gly Ile Ala  
 340 345 350  
 Ser Phe Asp Ser Lys Gly Glu Ile Arg Ala Gln Leu His Gln Ile Asn  
 355 360 365

# APPENDIX

Ser Asn Asp Asp Arg Lys Leu Leu Val Ser Tyr Leu Pro Thr Thr Val  
370 375 380

Ser Ala Lys Thr Asp Ile Ser Ile Cys Ser Gly Leu Lys Lys Gly Phe  
385 390 395 400

Glu Val Val Glu Lys Leu Asn Gly Lys Ala Tyr Gly Ser Val Met Ile  
405 410 415

Leu Val Thr Ser Gly Asp Asp Lys Leu Leu Gly Asn Cys Leu Pro Thr  
420 425 430

Val Leu Ser Ser Gly Ser Thr Ile His Ser Ile Ala Leu Gly Ser Ser  
435 440 445

Ala Ala Pro Asn Leu Glu Glu Leu Ser Arg Leu Thr Gly Gly Leu Lys  
450 455 460

Phe Phe Val Pro Asp Ile Ser Asn Ser Asn Ser Met Ile Asp Ala Phe  
465 470 475 480

Ser Arg Ile Ser Ser Gly Thr Gly Asp Ile Phe Gln Gln His Ile Gln  
485 490 495

Leu Glu Ser Thr Gly Glu Asn Val Lys Pro His His Gln Leu Lys Asn  
500 505 510

Thr Val Thr Val Asp Asn Thr Val Gly Asn Asp Thr Met Phe Leu Val  
515 520 525

Thr Trp Gln Ala Ser Gly Pro Pro Glu Ile Ile Leu Phe Asp Pro Asp  
530 535 540

Gly Arg Lys Tyr Tyr Thr Asn Asn Phe Ile Thr Asn Leu Thr Phe Arg  
545 550 555 560

Thr Ala Ser Leu Trp Ile Pro Gly Thr Ala Lys Pro Gly His Trp Thr  
565 570 575

Tyr Thr Leu Asn Asn Thr His His Ser Leu Gln Ala Leu Lys Val Thr  
580 585 590

Val Thr Ser Arg Ala Ser Asn Ser Ala Val Pro Pro Ala Thr Val Glu  
595 600 605

Ala Phe Val Glu Arg Asp Ser Leu His Phe Pro His Pro Val Met Ile  
610 615 620

Tyr Ala Asn Val Lys Gln Gly Phe Tyr Pro Ile Leu Asn Ala Thr Val  
625 630 635 640

Thr Ala Thr Val Glu Pro Glu Thr Gly Asp Pro Val Thr Leu Arg Leu  
645 650 655

# APPENDIX

Leu Asp Asp Gly Ala Gly Ala Asp Val Ile Lys Asn Asp Gly Ile Tyr  
 660 665 670  
 Ser Arg Tyr Phe Phe Ser Phe Ala Ala Asn Gly Arg Tyr Ser Leu Lys  
 675 680 685  
 Val His Val Asn His Ser Pro Ser Ile Ser Thr Pro Ala His Ser Ile  
 690 695 700  
 Pro Gly Ser His Ala Met Tyr Val Pro Gly Tyr Thr Ala Asn Gly Asn  
 705 710 715 720  
 Ile Gln Met Asn Ala Pro Arg Lys Ser Val Gly Arg Asn Glu Glu Glu  
 725 730 735  
 Arg Lys Trp Gly Phe Ser Arg Val Ser Ser Gly Gly Ser Phe Ser Val  
 740 745 750  
 Leu Gly Val Pro Ala Gly Pro His Pro Asp Val Phe Pro Pro Cys Lys  
 755 760 765  
 Ile Ile Asp Leu Glu Ala Val Lys Val Glu Glu Glu Leu Thr Leu Ser  
 770 775 780  
 Trp Thr Ala Pro Gly Glu Asp Phe Asp Gln Gly Gln Ala Thr Ser Tyr  
 785 790 795 800  
 Glu Ile Arg Met Ser Lys Ser Leu Gln Asn Ile Gln Asp Asp Phe Asn  
 805 810  
 Asn Ala Ile Leu Val Asn Thr Ser Lys Arg Asn Pro Gln Gln Ala Gly  
 820 825 830  
 Ile Arg Glu Ile Phe Thr Phe Ser Pro Gln Ile Ser Thr Asn Gly Pro  
 835 840 845  
 Glu His Gln Pro Asn Gly Glu Thr His Glu Ser His Arg Ile Tyr Val  
 850 855 860  
 Ala Ile Arg Ala Met Asp Arg Asn Ser Leu Gln Ser Ala Val Ser Asn  
 865 870 875 880  
 Ile Ala Gln Ala Pro Leu Phe Ile Pro Pro Asn Ser Asp Pro Val Pro  
 885 890 895  
 Ala Arg Asp Tyr Leu Ile Leu Lys Gly Val Leu Thr Ala Met Gly Leu  
 900 905 910  
 Ile Gly Ile Ile Cys Leu Ile Ile Val Val Thr His His Thr Leu Ser  
 915 920 925  
 Arg Lys Lys Arg Ala Asp Lys Lys Glu Asn Gly Thr Lys Leu Leu  
 930 935 940

## Abbreviations

°C	degree Celsius
µg	microgram
µl	microliter
µmol	micromole
14-3-3 sigma/ SDN	stratifin
2D	2 dimensional
3D	3 dimensional
4E-BP1	4E binding protein 1
AA	amino acid
AC	adenocarcinoma
Acc.	accession number
AFF4 (MCEF)	AF4/MR2 family member 4
Ala	Alanine
All	acute lymphocytic leukaemia
amp	Ampicillin
ASPM	Asp (abnormal spindle)-like, microcephaly associated (drosophila)
ATP	adenosine 5'-triphosphate
bp	base pair
BSA	bovine serum albumin
C10orf118	chromosome 10 open reading frame 118
Ca	carcinoma
Ca <sup>2+</sup>	calcium ion
CAM's	cell-cell adhesion molecules
cap	methyl-7-G(5')pppN - structure
CD8	cluster of differentiation
CDIPT	CDP-diacylglycerol-inositol 3-phosphatidyltransferase (phosphatidylinositol synthase)
CDK	cyclin-dependent kinase
cDNA	complementary DNA
cfu	colony forming unit
CHD6	chromodomain helicase DNA binding protein 6
chr1	Chromosome 1
CLCA	calcium-activated chloride channel
CMTX	Charcot-Marie-Tooth disease
CMV	cytomegalo virus
CN	copy number
ColonMucinCa	mucinous colon carcinoma
COPD	obstructive pulmonary disease
cpm	counts per minute
CTCL	cutaneous T cell lymphoma
Cys	Cysteine
DEPC	diethyl pyrocarbonate
DEPC-H <sub>2</sub> O	di-ethyl-propyl carbonate-treated H <sub>2</sub> O
DNA	deoxyribonucleic acid
dNTP	deoxyribonucleotides
Doxy	Doxycycline
DSC3	desmocollin 3
dsDNA	double strand DNA
DSG3	desmoglein 3
DTT	dithiothreitol
DTX2	deltex homolog 2 (drosophila)
E. coli	Escherichia coli

ECM	extracellular matrix
EDTA	ethylenediaminetetraacetic acid
EGF	epidermal growth factor
EGFR	epidermal growth factor receptor
eIF	eukaryotic initiation factor
EMCV	encephalomyocarditis virus
EMT	epithelial mesenchymal transition
EP300	E1A binding protein p300
ERBB2	erythroblastic leukemia viral oncogene homolog 2
ERK	extracellular signal-regulated kinase
EtBr	ethidiumbromide
FGF	fibroblast growth factor
g	gram
GAPDH	glyceraldehyde 3-phosphate dehydrogenase
GDP	guanosine 5'-diphosphate
GlioblastMultiform	glioblastoma multiforme
GPCR	G protein-coupled receptor
GTP	guanosine 5'-triphosphate
HA	hemagglutinin
HAV	hepatitis A virus
HCC	hepatocellular carcinoma
HCS	high-content screening
Her2	epidermal growth factor receptor 2
His	Histidine
HNF4A	hepatocyte nuclear factor 4 alpha
HNSCC	head and neck squamous cell carcinoma
HRV2	human rhinovirus type 2
IC <sub>50</sub>	half maximal inhibitory concentration
IGF-I R	insulin-like growth factor 1 receptor
IHC	immunohistochemistry
IL10	Interleukin 10
IL2	Interleukin 2
InfDuc	infiltrating ductal
InfLob	infiltrating lobular
IPA	Ingenuity Pathways Analysis
IQR	interquartile range
JNK	N-terminal kinase
K <sup>+</sup>	potassium ion
KAc	potassium acetate
kD	kilo Dalton
KPNA2	karyopherin alpha 2
KRT5	keratin 5
l	liter
LAD1/CD18	ladinin 1
LB	Lauria Bertani
LCC	large cell carcinomas
LCM	laser-capture-microdissected
LN	lymphnode
LNSCCMet	lymph node metastases of SCCs
LTBP1	latent transforming growth factor beta binding protein 1
Lys	Lysine
M	molar
MACF1	microtubule-actin crosslinking factor 1
Malig	malignant
MAPK	mitogen-activated protein kinase

---

Mel	melanoma
MEM	minimal essential medium
Met	metastasis
min	minute
ml	milliliter
MLL2	myeloid/lymphoid or mixed-lineage leukemia 2
mM	millimolar
MM	multiple myeloma
MOPS	4-morpholinepropanesulfonic acid
MRE11	meiotic recombination 11, <i>S. cerevisiae</i> , homolog of a MRE11A
mRNA	messenger RNA
myc	refers to the myc gene
Myc	refers to the Myc protein
NaAc	sodium acetate
NBS1	p95 protein of the MRE11/RAD50 complex
NEAA	non essential aminoacids
NED	no evidence of disease
ng	nanogram
NH <sub>4</sub> Ac	ammonium acetate
NPM	nucleophosmin
NSCLC	non-small cell lung cancer
nt	nucleotide
OD	optical density
ORF	open reading frame
P4HA2	prolyl-4 hydroxylase-2
p53	protein 53
PapillFollic	papillary and follicular
PARP	poly ADP-ribose polymerase
PBS	phosphate-buffered saline
PCR	polymerase chain reaction
PDGF	platelet-derived growth factor
PDK1	phosphoinositide dependent kinase 1
PERP	TP53 apoptosis effector
Phe	Phenylalanine
PI3K	phosphoinositide-3-kinase
PKP	plakophilin
pmol	picomole
POS	positive
PV	verified by pathologist
RAB38	member RAS oncogene family
RAD50	RAD50 homolog ( <i>S. cerevisiae</i> )
Rb	retinoblastoma
RCC	renal cell carcinoma
RE	restriction enzyme
RNA	ribonucleic acid
RNAse	ribonuclease
rpm	rotations per minute
RT	room temperature
RTK	receptor tyrosine kinase
RT-qPCR	quantative real-time PCR
RUTBC3	RUN and TBC1 domain containing 3
SATB1	special AT-rich sequence binding protein 1
SCC	squamous cell carcinoma
SCLC	small cell lung cancer
SDS	sodium dodecyl sulfate

sec	second
SFI1	spindle assembly associated (yeast)
siCTRL	non-targeting siRNA CONTROL#1 of Dharmacon
siRNA	small interfering RNA (also short interfering RNA or silencing RNA)
SMAD3	mothers against decapentaplegic homolog 3
SNP	single nucleotide polymorphism
Squam	squamous
ssDNA	single strand cDNA
STAT	signal transducer and activator of transcription
T reg	regulatory T cells
TCC	transitional cell carcinoma
Tet	Tetracycline
TGF	tumour growth factor
Tiss	tissue
Tm	melting temperature
TNF	tumour necrosis factor
TP53	tumour protein p53
TP53BP1	tumour protein p53 binding protein 1
TRIM29	tripartite motif-containing 29
TSC1	tuberous sclerosis complex 1
Tyr	Tyrosine
U	Unit
UNC84A	unc-84 homolog A (C. elegans)
UV	ultraviolet
VEGF	vascular endothelial growth factor
VP2	adeno-associated virus 2
vWA	von Willebrand factor type A
WHO	World Health Organization
wt	wild type
Zn <sup>2+</sup>	zinc ion

## REFERENCES

### Reference List

- (1) Amatschek S, Koenig U, Auer H, Steinlein P, Pacher M, Gruenfelder A, Dekan G, Vogl S, Kubista E, Heider KH, Stratowa C, Schreiber M, Sommergruber W. Tissue-wide expression profiling using cDNA subtraction and microarrays to identify tumor-specific genes. *Cancer Res* 2004; 64(3):844-856.
- (2) Konopitzky R, Konig U, Meyer RG, Sommergruber W, Wolfel T, Schweighoffer T. Identification of HLA-A\*0201-restricted T cell epitopes derived from the novel overexpressed tumor antigen calcium-activated chloride channel 2. *J Immunol* 2002; 169(1):540-547.
- (3) Fuller CM, Ji HL, Tousson A, Elble RC, Pauli BU, Benos DJ. Ca(2+)-activated Cl(-) channels: a newly emerging anion transport family. *Pflugers Arch* 2001; 443 Suppl 1:S107-S110.
- (4) Pauli BU, Abdel-Ghany M, Cheng HC, Gruber AD, Archibald HA, Elble RC. Molecular characteristics and functional diversity of CLCA family members. *Clin Exp Pharmacol Physiol* 2000; 27(11):901-905.
- (5) Jemal A, Siegel R, Ward E, Hao Y, Xu J, Murray T, Thun MJ. Cancer statistics, 2008. *CA Cancer J Clin* 2008; 58(2):71-96.
- (6) Ames BN. Identifying environmental chemicals causing mutations and cancer. *Science* 1979; 204(4393):587-593.
- (7) Schmutte C, Fishel R. Genomic instability: first step to carcinogenesis. *Anticancer Res* 1999; 19(6A):4665-4696.
- (8) Anderson J, Gordon A, McManus A, Shipley J, Pritchard-Jones K. Disruption of imprinted genes at chromosome region 11p15.5 in paediatric rhabdomyosarcoma. *Neoplasia* 1999; 1(4):340-348.
- (9) Herman JG, Baylin SB. Promoter-region hypermethylation and gene silencing in human cancer. *Curr Top Microbiol Immunol* 2000; 249:35-54.
- (10) Sigurdsson S, Bodvarsdottir SK, Anamthawat-Jonsson K, Steinarsdottir M, Jonasson JG, Ogmundsdottir HM, Eyfjord JE. p53 abnormality and chromosomal instability in the same breast tumor cells. *Cancer Genet Cytogenet* 2000; 121(2):150-155.
- (11) Brueckl WM, Jung A, Wein A, Brabletz T, Guenther K, Nusko G, Hahn EG. Microsatellite instability in colorectal adenomas: relevance and clinical importance. *Int J Colorectal Dis* 2000; 15(4):189-196.
- (12) Nowell PC. The clonal evolution of tumor cell populations. *Science* 1976; 194(4260):23-28.



- (13) Weinberg RA. Oncogenes, antioncogenes, and the molecular bases of multistep carcinogenesis. *Cancer Res* 1989; 49(14):3713-3721.
- (14) Vogelstein B, Kinzler KW. The multistep nature of cancer. *Trends Genet* 1993; 9(4):138-141.
- (15) Weinstein IB. Cancer. Addiction to oncogenes--the Achilles heal of cancer. *Science* 2002; 297(5578):63-64.
- (16) Hanahan D, Weinberg RA. The hallmarks of cancer. *Cell* 2000; 100(1):57-70.
- (17) Fedi P, Tronick SR, Aaronson SA. Growth factors in cancer medicine eds 1997.
- (18) Datto MB, Hu PP, Kowalik TF, Yingling J, Wang XF. The viral oncoprotein E1A blocks transforming growth factor beta-mediated induction of p21/WAF1/Cip1 and p15/INK4B. *Mol Cell Biol* 1997; 17(4):2030-2037.
- (19) Hannon GJ, Beach D. p15INK4B is a potential effector of TGF-beta-induced cell cycle arrest. *Nature* 1994; 371(6494):257-261.
- (20) Hahne M, Rimoldi D, Schroter M, Romero P, Schreier M, French LE, Schneider P, Bornand T, Fontana A, Lienard D, Cerottini J, Tschopp J. Melanoma cell expression of Fas(Apo-1/CD95) ligand: implications for tumor immune escape. *Science* 1996; 274(5291):1363-1366.
- (21) O'Connell J, O'Sullivan GC, Collins JK, Shanahan F. The Fas counterattack: Fas-mediated T cell killing by colon cancer cells expressing Fas ligand. *J Exp Med* 1996; 184(3):1075-1082.
- (22) Shay JW, Bacchetti S. A survey of telomerase activity in human cancer. *Eur J Cancer* 1997; 33(5):787-791.
- (23) Hanahan D, Folkman J. Patterns and emerging mechanisms of the angiogenic switch during tumorigenesis. *Cell* 1996; 86(3):353-364.
- (24) Aplin AE, Howe A, Alahari SK, Juliano RL. Signal transduction and signal modulation by cell adhesion receptors: the role of integrins, cadherins, immunoglobulin-cell adhesion molecules, and selectins. *Pharmacol Rev* 1998; 50(2):197-263.
- (25) Christofori G, Semb H. The role of the cell-adhesion molecule E-cadherin as a tumour-suppressor gene. *Trends Biochem Sci* 1999; 24(2):73-76.
- (26) Georgolios A, Batistatou A, Manolopoulos L, Charalabopoulos K. Role and expression patterns of E-cadherin in head and neck squamous cell carcinoma (HNSCC). *J Exp Clin Cancer Res* 2006; 25(1):5-14.
- (27) Eriksen JG, Steiniche T, Sogaard H, Overgaard J. Expression of integrins and E-cadherin in squamous cell carcinomas of the head and neck. *APMIS* 2004; 112(9):560-568.
- (28) Weinstein IB, Joe A. Oncogene addiction. *Cancer Res* 2008; 68(9):3077-3080.

- (29) Hubner A, Jaeschke A, Davis RJ. Oncogene addiction: role of signal attenuation. *Dev Cell* 2006; 11(6):752-754.
- (30) Paez JG, Janne PA, Lee JC, Tracy S, Greulich H, Gabriel S, Herman P, Kaye FJ, Lindeman N, Boggon TJ, Naoki K, Sasaki H, Fujii Y, Eck MJ, Sellers WR, Johnson BE, Meyerson M. EGFR mutations in lung cancer: correlation with clinical response to gefitinib therapy. *Science* 2004; 304(5676):1497-1500.
- (31) Zhang Z, Li M, Rayburn ER, Hill DL, Zhang R, Wang H. Oncogenes as novel targets for cancer therapy (part I): growth factors and protein tyrosine kinases. *Am J Pharmacogenomics* 2005; 5(3):173-190.
- (32) Nuber UA, Schafer S, Stehr S, Rackwitz HR, Franke WW. Patterns of desmocollin synthesis in human epithelia: immunolocalization of desmocollins 1 and 3 in special epithelia and in cultured cells. *Eur J Cell Biol* 1996; 71(1):1-13.
- (33) Bonifas JM, Bare JW, Lynch ED, Lebo RV, Epstein EH, Jr. Regional assignment of the human keratin 5 (KRT5) gene to chromosome 12q near D12S14 by PCR analysis of somatic cell hybrids and multicolor in situ hybridization. *Genomics* 1992; 13(2):452-454.
- (34) Mahoney MG, Simpson A, Aho S, Uitto J, Pulkkinen L. Interspecies conservation and differential expression of mouse desmoglein gene family. *Exp Dermatol* 2002; 11(2):115-125.
- (35) Heid HW, Schmidt A, Zimbelmann R, Schafer S, Winter-Simanowski S, Stumpp S, Keith M, Figge U, Schnolzer M, Franke WW. Cell type-specific desmosomal plaque proteins of the plakoglobin family: plakophilin 1 (band 6 protein). *Differentiation* 1994; 58(2):113-131.
- (36) Schmidt A, Langbein L, Pratzel S, Rode M, Rackwitz HR, Franke WW. Plakophilin 3--a novel cell-type-specific desmosomal plaque protein. *Differentiation* 1999; 64(5):291-306.
- (37) Ihrie RA, Marques MR, Nguyen BT, Horner JS, Papazoglu C, Bronson RT, Mills AA, Attardi LD. Perp is a p63-regulated gene essential for epithelial integrity. *Cell* 2005; 120(6):843-856.
- (38) Sanderson RD, Bernfield M. Molecular polymorphism of a cell surface proteoglycan: distinct structures on simple and stratified epithelia. *Proc Natl Acad Sci U S A* 1988; 85(24):9562-9566.
- (39) Johnson TM, Rowe DE, Nelson BR, Swanson NA. Squamous cell carcinoma of the skin (excluding lip and oral mucosa). *J Am Acad Dermatol* 1992; 26(3 Pt 2):467-484.
- (40) Christenson LJ, Borrowman TA, Vachon CM, Tollefson MM, Otley CC, Weaver AL, Roenigk RK. Incidence of basal cell and squamous cell carcinomas in a population younger than 40 years. *JAMA* 2005; 294(6):681-690.

- 
- (41) Tang CH, Chuang JY, Fong YC, Maa MC, Way TD, Hung CH. Bone-derived SDF-1 stimulates IL-6 release via CXCR4, ERK and NF-kappaB pathways and promotes osteoclastogenesis in human oral cancer cells. *Carcinogenesis* 2008; 29(8):1483-1492.
- (42) Rapidis AD, Vermorken JB, Bourhis J. Targeted therapies in head and neck cancer: past, present and future. *Rev Recent Clin Trials* 2008; 3(3):156-166.
- (43) Cunningham SA, Awayda MS, Bubien JK, Ismailov II, Arrate MP, Berdiev BK, Benos DJ, Fuller CM. Cloning of an epithelial chloride channel from bovine trachea. *J Biol Chem* 1995; 270(52):31016-31026.
- (44) Ran S, Benos DJ. Isolation and functional reconstitution of a 38-kDa chloride channel protein from bovine tracheal membranes. *J Biol Chem* 1991; 266(8):4782-4788.
- (45) Zhu DZ, Cheng CF, Pauli BU. Mediation of lung metastasis of murine melanomas by a lung-specific endothelial cell adhesion molecule. *Proc Natl Acad Sci U S A* 1991; 88(21):9568-9572.
- (46) Elble RC, Widom J, Gruber AD, Abdel-Ghany M, Levine R, Goodwin A, Cheng HC, Pauli BU. Cloning and characterization of lung-endothelial cell adhesion molecule-1 suggest it is an endothelial chloride channel. *J Biol Chem* 1997; 272(44):27853-27861.
- (47) Gandhi R, Elble RC, Gruber AD, Schreur KD, Ji HL, Fuller CM, Pauli BU. Molecular and functional characterization of a calcium-sensitive chloride channel from mouse lung. *J Biol Chem* 1998; 273(48):32096-32101.
- (48) Romio L, Musante L, Cinti R, Seri M, Moran O, Zegarra-Moran O, Galletta LJ. Characterization of a murine gene homologous to the bovine CaCC chloride channel. *Gene* 1999; 228(1-2):181-188.
- (49) Lee D, Ha S, Kho Y, Kim J, Cho K, Baik M, Choi Y. Induction of mouse Ca(2+)-sensitive chloride channel 2 gene during involution of mammary gland. *Biochem Biophys Res Commun* 1999; 264(3):933-937.
- (50) Komiya T, Tanigawa Y, Hirohashi S. Cloning and identification of the gene gob-5, which is expressed in intestinal goblet cells in mice. *Biochem Biophys Res Commun* 1999; 255(2):347-351.
- (51) Elble RC, Ji G, Nehrke K, DeBiasio J, Kingsley PD, Kotlikoff MI, Pauli BU. Molecular and functional characterization of a murine calcium-activated chloride channel expressed in smooth muscle. *J Biol Chem* 2002; 277(21):18586-18591.
- (52) Evans SR, Thoreson WB, Beck CL. Molecular and functional analyses of two new calcium-activated chloride channel family members from mouse eye and intestine. *J Biol Chem* 2004; 279(40):41792-41800.
- (53) Gruber AD, Elble RC, Ji HL, Schreur KD, Fuller CM, Pauli BU. Genomic cloning, molecular characterization, and functional analysis of human CLCA1,

- the first human member of the family of  $\text{Ca}^{2+}$ -activated  $\text{Cl}^-$  channel proteins. *Genomics* 1998; 54(2):200-214.
- (54) Agnel M, Verinat T, Culouscou JM. Identification of three novel members of the calcium-dependent chloride channel (CaCC) family predominantly expressed in the digestive tract and trachea. *FEBS Lett* 1999; 455(3):295-301.
- (55) Gruber AD, Schreur KD, Ji HL, Fuller CM, Pauli BU. Molecular cloning and transmembrane structure of hCLCA2 from human lung, trachea, and mammary gland. *Am J Physiol* 1999; 276(6 Pt 1):C1261-C1270.
- (56) Itoh R, Kawamoto S, Miyamoto Y, Kinoshita S, Okubo K. Isolation and characterization of a  $\text{Ca}^{2+}$ -activated chloride channel from human corneal epithelium. *Curr Eye Res* 2000; 21(6):918-925.
- (57) Gaspar KJ, Racette KJ, Gordon JR, Loewen ME, Forsyth GW. Cloning a chloride conductance mediator from the apical membrane of porcine ileal enterocytes. *Physiol Genomics* 2000; 3(2):101-111.
- (58) Yamazaki J, Okamura K, Ishibashi K, Kitamura K. Characterization of CLCA protein expressed in ductal cells of rat salivary glands. *Biochim Biophys Acta* 2005; 1715(2):132-144.
- (59) Jeong SM, Park HK, Yoon IS, Lee JH, Kim JH, Jang CG, Lee CJ, Nah SY. Cloning and expression of  $\text{Ca}^{2+}$ -activated chloride channel from rat brain. *Biochem Biophys Res Commun* 2005; 334(2):569-576.
- (60) Yoon IS, Jeong SM, Lee SN, Lee JH, Kim JH, Pyo MK, Lee JH, Lee BH, Choi SH, Rhim H, Choe H, Nah SY. Cloning and heterologous expression of a  $\text{Ca}^{2+}$ -activated chloride channel isoform from rat brain. *Biol Pharm Bull* 2006; 29(11):2168-2173.
- (61) Anton F, Leverkoehne I, Mundhenk L, Thoreson WB, Gruber AD. Overexpression of eCLCA1 in small airways of horses with recurrent airway obstruction. *J Histochem Cytochem* 2005; 53(8):1011-1021.
- (62) Loewen ME, Smith NK, Hamilton DL, Grahn BH, Forsyth GW. CLCA protein and chloride transport in canine retinal pigment epithelium. *Am J Physiol Cell Physiol* 2003; 285(5):C1314-C1321.
- (63) Gruber AD, Pauli BU. Clustering of the human CLCA gene family on the short arm of chromosome 1 (1p22-31). *Genome* 1999; 42(5):1030-1032.
- (64) Gruber AD, Pauli BU. Molecular cloning and biochemical characterization of a truncated, secreted member of the human family of  $\text{Ca}^{2+}$ -activated  $\text{Cl}^-$  channels. *Biochim Biophys Acta* 1999; 1444(3):418-423.
- (65) Pawlowski K, Lepisto M, Meinander N, Sivars U, Varga M, Wieslander E. Novel conserved hydrolase domain in the CLCA family of alleged calcium-activated chloride channels. *Proteins* 2006; 63(3):424-439.

- (66) Elble RC, Pauli BU. Tumor suppression by a proapoptotic calcium-activated chloride channel in mammary epithelium. *J Biol Chem* 2001; 276(44):40510-40517.
- (67) Elble RC, Walia V, Cheng HC, Connon CJ, Mundhenk L, Gruber AD, Pauli BU. The putative chloride channel hCLCA2 has a single C-terminal transmembrane segment. *J Biol Chem* 2006; 281(40):29448-29454.
- (68) Gruber AD, Pauli BU. Tumorigenicity of human breast cancer is associated with loss of the Ca<sup>2+</sup>-activated chloride channel CLCA2. *Cancer Res* 1999; 59(21):5488-5491.
- (69) Abdel-Ghany M, Cheng HC, Elble RC, Lin H, DiBiasio J, Pauli BU. The interacting binding domains of the beta(4) integrin and calcium-activated chloride channels (CLCAs) in metastasis. *J Biol Chem* 2003; 278(49):49406-49416.
- (70) Abdel-Ghany M, Cheng HC, Elble RC, Pauli BU. The breast cancer beta 4 integrin and endothelial human CLCA2 mediate lung metastasis. *J Biol Chem* 2001; 276(27):25438-25446.
- (71) Kumanovics A, Lindahl KF. G7c in the lung tumor susceptibility (Lts) region of the Mhc class III region encodes a von Willebrand factor type A domain protein. *Immunogenetics* 2001; 53(1):64-68.
- (72) Abdel-Ghany M, Cheng HC, Elble RC, Pauli BU. Focal adhesion kinase activated by beta(4) integrin ligation to mCLCA1 mediates early metastatic growth. *J Biol Chem* 2002; 277(37):34391-34400.
- (73) Goetz DJ, el Sabban ME, Hammer DA, Pauli BU. Lu-ECAM-1-mediated adhesion of melanoma cells to endothelium under conditions of flow. *Int J Cancer* 1996; 65(2):192-199.
- (74) Riker AI, Enkemann SA, Fodstad O, Liu S, Ren S, Morris C, Xi Y, Howell P, Metge B, Samant RS, Shevde LA, Li W, Eschrich S, Daud A, Ju J, Matta J. The gene expression profiles of primary and metastatic melanoma yields a transition point of tumor progression and metastasis. *BMC Med Genomics* 2008; 1:13.
- (75) Shen-Ong GL, Feng Y, Troyer DA. Expression profiling identifies a novel alpha-methylacyl-CoA racemase exon with fumarate hydratase homology. *Cancer Res* 2003; 63(12):3296-3301.
- (76) Tovey SM, Brown S, Doughty JC, Mallon EA, Cooke TG, Edwards J. Poor survival outcomes in HER2-positive breast cancer patients with low-grade, node-negative tumours. *Br J Cancer* 2009; 100(5):680-683.
- (77) Liu S, Chia SK, Mehl E, Leung S, Rajput A, Cheang MC, Nielsen TO. Progesterone receptor is a significant factor associated with clinical outcomes and effect of adjuvant tamoxifen therapy in breast cancer patients. *Breast Cancer Res Treat* 2009.

- (78) Hupe P, Stransky N, Thiery JP, Radvanyi F, Barillot E. Analysis of array CGH data: from signal ratio to gain and loss of DNA regions. *Bioinformatics* 2004; 20(18):3413-3422.
- (79) Glatt S, Halbauer D, Heindl S, Wernitznig A, Kozina D, Su KC, Puri C, Garin-Chesa P, Sommergruber W. hGPR87 contributes to viability of human tumor cells. *Int J Cancer* 2008; 122(9):2008-2016.
- (80) Chou PY, Fasman GD. Empirical predictions of protein conformation. *Annu Rev Biochem* 1978; 47:251-276.
- (81) Chou PY, Fasman GD. Prediction of the secondary structure of proteins from their amino acid sequence. *Adv Enzymol Relat Areas Mol Biol* 1978; 47:45-148.
- (82) Garnier J, Osguthorpe DJ, Robson B. Analysis of the accuracy and implications of simple methods for predicting the secondary structure of globular proteins. *J Mol Biol* 1978; 120(1):97-120.
- (83) Kyte J, Doolittle RF. A simple method for displaying the hydropathic character of a protein. *J Mol Biol* 1982; 157(1):105-132.
- (84) von Heijne G. On the hydrophobic nature of signal sequences. *Eur J Biochem* 1981; 116(2):419-422.
- (85) Engelman DM, Steitz TA, Goldman A. Identifying nonpolar transbilayer helices in amino acid sequences of membrane proteins. *Annu Rev Biophys Biophys Chem* 1986; 15:321-353.
- (86) Karplus PA, Schulz GE. Prediction of chain flexibility in proteins: a tool for the selection of peptide antigens. *Naturwissenschaften* 1985; 72:212-213.
- (87) Hopp TP, Woods KR. Prediction of protein antigenic determinants from amino acid sequences. *Proc Natl Acad Sci U S A* 1981; 78(6):3824-3828.
- (88) Parker JM, Guo D, Hodges RS. New hydrophilicity scale derived from high-performance liquid chromatography peptide retention data: correlation of predicted surface residues with antigenicity and X-ray-derived accessible sites. *Biochemistry* 1986; 25(19):5425-5432.
- (89) Thornton JM, Edwards MS, Taylor WR, Barlow DJ. Location of 'continuous' antigenic determinants in the protruding regions of proteins. *EMBO J* 1986; 5(2):409-413.
- (90) Welling GW, Weijer WJ, van der ZR, Welling-Wester S. Prediction of sequential antigenic regions in proteins. *FEBS Lett* 1985; 188(2):215-218.
- (91) Alix AJ. Predictive estimation of protein linear epitopes by using the program PEOPLE. *Vaccine* 1999; 18(3-4):311-314.
- (92) Jameson BA, Wolf H. The antigenic index: a novel algorithm for predicting antigenic determinants. *Comput Appl Biosci* 1988; 4(1):181-186.

- 
- (93) Bairoch A, Bucher P, Hofmann K. The PROSITE database, its status in 1997. *Nucleic Acids Res* 1997; 25(1):217-221.
- (94) Skern T, Neubauer C, Frasel L, Grundler P, Sommergruber W, Zorn M, Kuechler E, Blaas D. A neutralizing epitope on human rhinovirus type 2 includes amino acid residues between 153 and 164 of virus capsid protein VP2. *J Gen Virol* 1987; 68 ( Pt 2):315-323.
- (95) Devi L. Consensus sequence for processing of peptide precursors at monobasic sites. *FEBS Lett* 1991; 280(2):189-194.
- (96) Salisbury JL. Centrosomes: Sfi1p and centrin unravel a structural riddle. *Curr Biol* 2004; 14(1):R27-R29.
- (97) Naruke Y, Nakashima M, Suzuki K, Matsuu-Matsuyama M, Shichijo K, Kondo H, Sekine I. Alteration of p53-binding protein 1 expression during skin carcinogenesis: association with genomic instability. *Cancer Sci* 2008; 99(5):946-951.
- (98) Baba Y, Tsukuda M, Mochimatsu I, Furukawa S, Kagata H, Nagashima Y, Koshika S, Imoto M, Kato Y. Cytostatic effect of inostamycin, an inhibitor of cytidine 5'-diphosphate 1,2-diacyl-sn-glycerol (CDP-DG): inositol transferase, on oral squamous cell carcinoma cell lines. *Cell Biol Int* 2001; 25(7):613-620.
- (99) Rohatgi N, Matta A, Kaur J, Srivastava A, Ralhan R. Novel molecular targets of smokeless tobacco (khaini) in cell culture from oral hyperplasia. *Toxicology* 2006; 224(1-2):1-13.
- (100) Issaeva I, Zonis Y, Rozovskaia T, Orlovsky K, Croce CM, Nakamura T, Mazo A, Eisenbach L, Canaani E. Knockdown of ALR (MLL2) reveals ALR target genes and leads to alterations in cell adhesion and growth. *Mol Cell Biol* 2007; 27(5):1889-1903.
- (101) Bach C, Mueller D, Buhl S, Garcia-Cuellar MP, Slany RK. Alterations of the CxxC domain preclude oncogenic activation of mixed-lineage leukemia 2. *Oncogene* 2009; 28(6):815-823.
- (102) Robert I, Aussems M, Keutgens A, Zhang X, Hennuy B, Viatour P, Vanstraelen G, Merville MP, Chapelle JP, de Leval L, Lambert F, Dejardin E, Gothot A, Chariot A. Matrix Metalloproteinase-9 gene induction by a truncated oncogenic NF-kappaB2 protein involves the recruitment of MLL1 and MLL2 H3K4 histone methyltransferase complexes. *Oncogene* 2009.
- (103) Estable MC, Naghavi MH, Kato H, Xiao H, Qin J, Vahlne A, Roeder RG. MCEF, the newest member of the AF4 family of transcription factors involved in leukemia, is a positive transcription elongation factor-b-associated protein. *J Biomed Sci* 2002; 9(3):234-245.
- (104) Hasan S, Guttinger S, Muhlhauser P, Anderegg F, Burgler S, Kutay U. Nuclear envelope localization of human UNC84A does not require nuclear lamins. *FEBS Lett* 2006; 580(5):1263-1268.

- (105) Wilkin M, Tongngok P, Gensch N, Clemence S, Motoki M, Yamada K, Hori K, Taniguchi-Kanai M, Franklin E, Matsuno K, Baron M. *Drosophila* HOPS and AP-3 complex genes are required for a Deltex-regulated activation of notch in the endosomal trafficking pathway. *Dev Cell* 2008; 15(5):762-772.
- (106) Jennings MD, Blankley RT, Baron M, Golovanov AP, Avis JM. Specificity and autoregulation of Notch binding by tandem WW domains in suppressor of Deltex. *J Biol Chem* 2007; 282(39):29032-29042.
- (107) Han HJ, Russo J, Kohwi Y, Kohwi-Shigematsu T. SATB1 reprogrammes gene expression to promote breast tumour growth and metastasis. *Nature* 2008; 452(7184):187-193.
- (108) Ghosh AK, Varga J. The transcriptional coactivator and acetyltransferase p300 in fibroblast biology and fibrosis. *J Cell Physiol* 2007; 213(3):663-671.
- (109) Higashi T, Sasagawa T, Inoue M, Oka R, Shuangying L, Saijoh K. Overexpression of latent transforming growth factor-beta 1 (TGF-beta 1) binding protein 1 (LTBP-1) in association with TGF-beta 1 in ovarian carcinoma. *Jpn J Cancer Res* 2001; 92(5):506-515.
- (110) Chakraborty S, Mohiyuddin SM, Gopinath KS, Kumar A. Involvement of TSC genes and differential expression of other members of the mTOR signaling pathway in oral squamous cell carcinoma. *BMC Cancer* 2008; 8:163.
- (111) Maiuri MC, Tasdemir E, Ciriello A, Morselli E, Vicencio JM, Carnuccio R, Kroemer G. Control of autophagy by oncogenes and tumor suppressor genes. *Cell Death Differ* 2009; 16(1):87-93.
- (112) Chen HJ, Lin CM, Lin CS, Perez-Olle R, Leung CL, Liem RK. The role of microtubule actin cross-linking factor 1 (MACF1) in the Wnt signaling pathway. *Genes Dev* 2006; 20(14):1933-1945.
- (113) Lutz T, Stoger R, Nieto A. CHD6 is a DNA-dependent ATPase and localizes at nuclear sites of mRNA synthesis. *FEBS Lett* 2006; 580(25):5851-5857.
- (114) Katoh M, Katoh M. Characterization of RUSC1 and RUSC2 genes in silico. *Oncol Rep* 2004; 12(4):933-938.
- (115) Callebaut I, de Gunzburg J, Goud B, Mornon JP. RUN domains: a new family of domains involved in Ras-like GTPase signaling. *Trends Biochem Sci* 2001; 26(2):79-83.
- (116) Mackay A, Jones C, Dexter T, Silva RL, Bulmer K, Jones A, Simpson P, Harris RA, Jat PS, Neville AM, Reis LF, Lakhani SR, O'Hare MJ. cDNA microarray analysis of genes associated with ERBB2 (HER2/neu) overexpression in human mammary luminal epithelial cells. *Oncogene* 2003; 22(17):2680-2688.
- (117) Jarzab B, Wiench M, Fijarewicz K, Simek K, Jarzab M, Oczko-Wojciechowska M, Wloch J, Czarniecka A, Chmielik E, Lange D, Pawlaczek A, Szpak S, Gubala E, Swierniak A. Gene expression profile of papillary thyroid cancer: sources of variability and diagnostic implications. *Cancer Res* 2005; 65(4):1587-1597.



- (118) Lin SY, Pan HW, Liu SH, Jeng YM, Hu FC, Peng SY, Lai PL, Hsu HC. ASPM is a novel marker for vascular invasion, early recurrence, and poor prognosis of hepatocellular carcinoma. *Clin Cancer Res* 2008; 14(15):4814-4820.
- (119) Clark RA, Huang SJ, Murphy GF, Mollet IG, Hijnen D, Muthukuru M, Schanbacher CF, Edwards V, Miller DM, Kim JE, Lambert J, Kupper TS. Human squamous cell carcinomas evade the immune response by down-regulation of vascular E-selectin and recruitment of regulatory T cells. *J Exp Med* 2008; 205(10):2221-2234.
- (120) Di Fiore PP. Playing both sides: nucleophosmin between tumor suppression and oncogenesis. *J Cell Biol* 2008; 182(1):7-9.
- (121) Mishra BK, Purvish MP. Targeted Therapy in Oncology. *MJAFI* 2006; 62(2):169-173.
- (122) Nielsen DL, Andersson M, Kamby C. HER2-targeted therapy in breast cancer. Monoclonal antibodies and tyrosine kinase inhibitors. *Cancer Treat Rev* 2008.
- (123) Traxler P. Tyrosine kinases as targets in cancer therapy - successes and failures. *Expert Opin Ther Targets* 2003; 7(2):215-234.
- (124) Li D, Ambrogio L, Shimamura T, Kubo S, Takahashi M, Chirieac LR, Padera RF, Shapiro GI, Baum A, Himmelsbach F, Rettig WJ, Meyerson M, Solca F, Greulich H, Wong KK. BIBW2992, an irreversible EGFR/HER2 inhibitor highly effective in preclinical lung cancer models. *Oncogene* 2008; 27(34):4702-4711.
- (125) Schutze C, Dorfler A, Eicheler W, Zips D, Hering S, Solca F, Baumann M, Krause M. Combination of EGFR/HER2 tyrosine kinase inhibition by BIBW 2992 and BIBW 2669 with irradiation in FaDu human squamous cell carcinoma. *Strahlenther Onkol* 2007; 183(5):256-264.
- (126) Minkovsky N, Berezov A. BIBW-2992, a dual receptor tyrosine kinase inhibitor for the treatment of solid tumors. *Curr Opin Investig Drugs* 2008; 9(12):1336-1346.
- (127) Rath O, Himmeler A, Baum A, Sommergruber W, Beug H, Metz T. c-Myc is required for transformation of FDC-P1 cells by EGFRvIII. *FEBS Lett* 2007; 581(13):2549-2556.
- (128) Pourgholami MH, Morris DL. Inhibitors of vascular endothelial growth factor in cancer. *Cardiovasc Hematol Agents Med Chem* 2008; 6(4):343-347.
- (129) Hilberg F, Roth GJ, Krssak M, Kautschitsch S, Sommergruber W, Tontsch-Grunt U, Garin-Chesa P, Bader G, Zoephel A, Quant J, Heckel A, Rettig WJ. BIBF 1120: triple angiokinase inhibitor with sustained receptor blockade and good antitumor efficacy. *Cancer Res* 2008; 68(12):4774-4782.
- (130) Richardson CJ, Gao Q, Mitsopoulous C, Zvelebil M, Pearl LH, Pearl FM. MoKCa database--mutations of kinases in cancer. *Nucleic Acids Res* 2009; 37(Database issue):D824-D831.

- (131) Shapiro GI. Cyclin-dependent kinase pathways as targets for cancer treatment. *J Clin Oncol* 2006; 24(11):1770-1783.
- (132) Steegmaier M, Hoffmann M, Baum A, Lenart P, Petronczki M, Krssak M, Gurtler U, Garin-Chesa P, Lieb S, Quant J, Grauert M, Adolf GR, Kraut N, Peters JM, Rettig WJ. BI 2536, a potent and selective inhibitor of polo-like kinase 1, inhibits tumor growth in vivo. *Curr Biol* 2007; 17(4):316-322.
- (133) Bennett MK, Kirk CJ. Development of proteasome inhibitors in oncology and autoimmune diseases. *Curr Opin Drug Discov Devel* 2008; 11(5):616-625.
- (134) Sahin M, Sahin E, Gumuslu S. Cyclooxygenase-2 in Cancer and Angiogenesis. *Angiology* 2008.
- (135) Abbott RG, Forrest S, Pienta KJ. Simulating the hallmarks of cancer. *Artif Life* 2006; 12(4):617-634.
- (136) Garber K. New insights into oncogene addiction found. *J Natl Cancer Inst* 2007; 99(4):264-5, 269.
- (137) Sharma SV, Settleman J. Oncogene addiction: setting the stage for molecularly targeted cancer therapy. *Genes Dev* 2007; 21(24):3214-3231.
- (138) Felsher DW. Oncogene addiction versus oncogene amnesia: perhaps more than just a bad habit? *Cancer Res* 2008; 68(9):3081-3086.
- (139) Weinstein IB, Joe AK. Mechanisms of disease: Oncogene addiction--a rationale for molecular targeting in cancer therapy. *Nat Clin Pract Oncol* 2006; 3(8):448-457.
- (140) Verkman AS, Hara-Chikuma M, Papadopoulos MC. Aquaporins--new players in cancer biology. *J Mol Med* 2008; 86(5):523-529.
- (141) Prevarskaya N, Zhang L, Barritt G. TRP channels in cancer. *Biochim Biophys Acta* 2007; 1772(8):937-946.
- (142) Matthews CP, Colburn NH, Young MR. AP-1 a target for cancer prevention. *Curr Cancer Drug Targets* 2007; 7(4):317-324.
- (143) Myatt SS, Lam EW. The emerging roles of forkhead box (Fox) proteins in cancer. *Nat Rev Cancer* 2007; 7(11):847-859.
- (144) McCarthy PL, Mercer FC, Savicky MW, Carter BA, Paterno GD, Gillespie LL. Changes in subcellular localisation of MI-ER1 alpha, a novel oestrogen receptor-alpha interacting protein, is associated with breast cancer progression. *Br J Cancer* 2008; 99(4):639-646.
- (145) Caldwell GM, Jones CE, Soon Y, Warrack R, Morton DG, Matthews GM. Reorganisation of Wnt-response pathways in colorectal tumorigenesis. *Br J Cancer* 2008; 98(8):1437-1442.

- (146) Arcangeli A, Crociani O, Lastraioli E, Masi A, Pillozzi S, Becchetti A. Targeting ion channels in cancer: a novel frontier in antineoplastic therapy. *Curr Med Chem* 2009; 16(1):66-93.
- (147) Kim BJ, Park EJ, Lee JH, Jeon JH, Kim SJ, So I. Suppression of transient receptor potential melastatin 7 channel induces cell death in gastric cancer. *Cancer Sci* 2008; 99(12):2502-2509.
- (148) Mao J, Chen L, Xu B, Wang L, Wang W, Li M, Zheng M, Li H, Guo J, Li W, Jacob TJ, Wang L. Volume-activated chloride channels contribute to cell-cycle-dependent regulation of HeLa cell migration. *Biochem Pharmacol* 2009; 77(2):159-168.
- (149) Heo JH, Seo HN, Choe YJ, Kim S, Oh CR, Kim YD, Rhim H, Choo DJ, Kim J, Lee JY. T-type  $\text{Ca}^{2+}$  channel blockers suppress the growth of human cancer cells. *Bioorg Med Chem Lett* 2008; 18(14):3899-3901.
- (150) Cianfrocca M, Goldstein LJ. Prognostic and predictive factors in early-stage breast cancer. *Oncologist* 2004; 9(6):606-616.
- (151) Wennmalm K, Calza S, Ploner A, Hall P, Bjohle J, Klaar S, Smeds J, Pawitan Y, Bergh J. Gene expression in 16q is associated with survival and differs between Sorlie breast cancer subtypes. *Genes Chromosomes Cancer* 2007; 46(1):87-97.
- (152) Bergamaschi A, Tagliabue E, Sorlie T, Naume B, Triulzi T, Orlandi R, Russnes HG, Nesland JM, Tammi R, Auvinen P, Kosma VM, Menard S, Borresen-Dale AL. Extracellular matrix signature identifies breast cancer subgroups with different clinical outcome. *J Pathol* 2008; 214(3):357-367.
- (153) Doupnik CA. GPCR-Kir channel signaling complexes: defining rules of engagement. *J Recept Signal Transduct Res* 2008; 28(1-2):83-91.
- (154) Franco R, Ciruela F, Casado V, Cortes A, Canela EI, Mallol J, Agnati LF, Ferre S, Fuxe K, Lluís C. Partners for adenosine A1 receptors. *J Mol Neurosci* 2005; 26(2-3):221-232.
- (155) Sommergruber W, Casari G, Fessler F, Seipelt J, Skern T. The 2A proteinase of human rhinovirus is a zinc containing enzyme. *Virology* 1994; 204(2):815-818.
- (156) Keil B. Specificity of Proteolysis. Springer-Verlag Berlin Heidelberg New York 1992.
- (157) Xie J, Shen Z, Li KC, Danthi N. Tumor angiogenic endothelial cell targeting by a novel integrin-targeted nanoparticle. *Int J Nanomedicine* 2007; 2(3):479-485.
- (158) Whittaker CA, Hynes RO. Distribution and evolution of von Willebrand/integrin A domains: widely dispersed domains with roles in cell adhesion and elsewhere. *Mol Biol Cell* 2002; 13(10):3369-3387.
- (159) Dolznig H, Rupp C, Puri C, Sommergruber W, Garin-Chesa P. Development of a novel *in vitro* 3D-collagen gel co-culture system, which recapitulates

- tumor-stroma interaction. Jahrestagung der Deutschen Gesellschaft für Pathologie, Berlin 2008; 92.
- (160) Hwang-Verslues WW, Sladek FM. Nuclear receptor hepatocyte nuclear factor 4alpha1 competes with oncoprotein c-Myc for control of the p21/WAF1 promoter. *Mol Endocrinol* 2008; 22(1):78-90.
  - (161) Teng SC, Wu KJ, Tseng SF, Wong CW, Kao L. Importin KPNA2, NBS1, DNA repair and tumorigenesis. *J Mol Histol* 2006; 37(5-7):293-299.
  - (162) Gluz O, Wild P, Meiler R, Diallo-Danebrock R, Ting E, Mohrmann S, Schuett G, Dahl E, Fuchs T, Herr A, Gaumann A, Frick M, Poremba C, Nitz UA, Hartmann A. Nuclear karyopherin alpha2 expression predicts poor survival in patients with advanced breast cancer irrespective of treatment intensity. *Int J Cancer* 2008; 123(6):1433-1438.
  - (163) Sato F, Abraham JM, Yin J, Kan T, Ito T, Mori Y, Hamilton JP, Jin Z, Cheng Y, Paun B, Berki AT, Wang S, Shimada Y, Meltzer SJ. Polo-like kinase and survivin are esophageal tumor-specific promoters. *Biochem Biophys Res Commun* 2006; 342(2):465-471.
  - (164) Yu Z, Weinberger PM, Sasaki C, Egleston BL, Speier WF, Haffty B, Kowalski D, Camp R, Rimm D, Vairaktaris E, Burtneess B, Psyrris A. Phosphorylation of Akt (Ser473) predicts poor clinical outcome in oropharyngeal squamous cell cancer. *Cancer Epidemiol Biomarkers Prev* 2007; 16(3):553-558.
  - (165) Kasid U, Pfeifer A, Brennan T, Beckett M, Weichselbaum RR, Dritschilo A, Mark GE. Effect of antisense c-raf-1 on tumorigenicity and radiation sensitivity of a human squamous carcinoma. *Science* 1989; 243(4896):1354-1356.
  - (166) Zhang Q, Thomas SM, Xi S, Smithgall TE, Siegfried JM, Kamens J, Gooding WE, Grandis JR. SRC family kinases mediate epidermal growth factor receptor ligand cleavage, proliferation, and invasion of head and neck cancer cells. *Cancer Res* 2004; 64(17):6166-6173.
  - (167) Sheikh Ali MA, Gunduz M, Nagatsuka H, Gunduz E, Cengiz B, Fukushima K, Beder LB, Demircan K, Fujii M, Yamanaka N, Shimizu K, Grenman R, Nagai N. Expression and mutation analysis of epidermal growth factor receptor in head and neck squamous cell carcinoma. *Cancer Sci* 2008; 99(8):1589-1594.
  - (168) Dolznig H, Schweifer N, Puri C, Kraut N, Rettig WJ, Kerjaschki D, Garin-Chesa P. Characterization of cancer stroma markers: in silico analysis of an mRNA expression database for fibroblast activation protein and endosialin. *Cancer Immun* 2005; 5:10.

# CURRICULUM VITAE

## PERSONAL DATA

Name: **Mag.rer.nat. Daniela Kozina**  
 Date of birth: 22.04.77 (Vienna)  
 Citizenship: Austria  
 Address: 1080 Vienna  
 E-Mail-Address: daniela.kozina@redlpatent.com



## EDUCATION AND WORK EXPERIENCE

- 10/2008 – present **Patent Attorney Trainee (Patentanwaltsanwärter)** at REDL Life Science Patent Attorneys, Vienna
- 02/2008 – 09/2008 **Patent Manager** at f-star Biotechnologische Forschungs- u. Entwicklungsges.m.b.H, Vienna
- 11/2004 – 01/2008 **PhD-Thesis** at the University of Vienna, Dep. for Anthropology, performed at Boehringer Ingelheim Austria, Vienna  
**Title of Thesis:** „Functional Characterisation of Calcium-activated Chloride Channel 2 (hCLCA2) in Human Tumour Cells“  
**Publication:** „Glatt S, Halbauer D, Heindl S, Wernitznig A, Kozina D, Su KC, Puri C, Garin-Chesa P, Sommergruber W. hGPR87 contributes to viability of human tumor cells. Int J Cancer 2008; 122(9):2008-2016.“
- 09/2002 – 03/2004 **Diploma work** at Boehringer Ingelheim Austria, Vienna  
**Titel of Thesis:** „The 5'-UTR of Laminin B1 Comprises an IRES-Region Enabeling Cap-Independent Translation“  
**Publication:** „Petz M, Kozina D, Huber H, Siwiec T, Seipelt J, Sommergruber W, Mikulits W. The leader region of Laminin B1 mRNA confers cap-independent translation; Nucleic Acids Res. 2007;35(8):2473-82. Epub 2007 Mar 29.“

- 10/1996 – 10/2004      **Study of Biology** at the the University of Vienna  
Branch of Study: Anthropology with optional subjects in Molecular
- 09/1991 – 06/1996      **HTL for Chemical Industry**, Department for Biochemistry  
Rosensteingasse, Vienna

#### STUDENT JOBS

- 10/2000 – 04/2001      Temporary personnel at Boehringer Ingelheim Austria, Vienna  
Department: R&D NCE Lead Discovery; Group: Dr. Sommergruber
- 1998 – 2000              Summer student at Boehringer Ingelheim Austria, Vienna  
Department: R&D NCE Lead Discovery
- 1993 – 1997              Summer student at ESW Consulting Wruss in the laboratory for  
environmental analytics

#### CONFERENCES

- 11/2004                  Poster Presentation „GENAU Evaluation Conference“, Vienna  
Titel: „Artificial oncogenic transformation of human primary  
fibroblasts“
- 01/2004                  Poster Presentation „First International Symposium of the Austrian  
Proteomics Platform“, Seefeld, Tirol  
Titel: „Cap-independent Translation of Tumor-specific Transcripts“
- 10/2003                  Poster-Presentation „GENAU Evaluation Conference“, Vienna  
Titel: „Cap-independent Translation of Tumor-specific Transcripts“  
Award for best Poster